Joint University Program for Air Transportation Research - 1981

*Proceedings of a conference
held at NASA Headquarters
Washington, D.C.
December 11, 1981*

NASA

NASA Conference Publica

Joint University Program for Air Transportation Research - 1981

Proceedings of a conference
held at NASA Headquarters
Washington, D.C.
December 11, 1981

NASA

National Aeronautics
and Space Administration

Scientific and Technical
Information Branch

1982

PREFACE

The Joint University Program for Air Transportation Research is a coordinated set of three grants sponsored by NASA Langley Research Center, one each with Massachusetts Institute of Technology (NGL-22-009-640), Ohio University (NGR-36-009-017), and Princeton University (NGL-31-001-252), to support the training of students for the air transportation system. These grants, initiated in 1971, encourage the development of innovative curriculums and support the establishment of graduate and undergraduate research assistantships and internships.

An important feature of this program is the quarterly review, one held at each of the schools and the fourth at a NASA facility. This latter review for 1981 was conducted at NASA Headquarters in Washington, D.C., December 11, 1981. At these reviews the program participants, both graduate and undergraduate, have an opportunity to present their research activities to their peers, professors, and invited guests from government and industry.

This conference publication represents the second in a series of yearly summaries of the activities of the program. (The 1980 summary appears in NASA CP-2176.) The majority of the material is the efforts of the students supported by the grants. Because of the ongoing nature of some of the work, certain graphics (notably photographs) are not of high quality; however, it was decided to publish the best material available, and if the reader's interest is sufficient, the appropriate advisor can be contacted for more recent and complete data.

Three types of contributions are included. Completed works are represented by the full technical papers. Research previously published in the open literature, for example, theses or journal articles, is presented in an annotated bibliography. Status reports of ongoing research are represented by copies of viewgraphs augmented with a brief descriptive text.

Use of trade names or names of manufacturers in this report does not constitute an official endorsement of such products or manufacturers, either expressed or implied, by the National Aeronautics and Space Administration.

CONTENTS

PRINCETON UNIVERSITY

Massachusetts
Institute
of
Technology

INVESTIGATION OF AIR TRANSPORTATION TECHNOLOGY AT MASSACHUSETTS

INSTITUTE OF TECHNOLOGY, 1981

Professor Robert W. Simpson
Director, Flight Transportation Laboratory
Massachusetts Institute of Technology
Cambridge, Massachusetts 02139

SUMMARY OF RESEARCH

There have been three areas of research sponsored by the Joint University Program at MIT during the past year: 1) Dynamic Scheduling of Runway Operations at a Major Airport; 2) General Aviation Electronic Flight Displays - (P-POD); 3) Prevention of Airframe Icing with Microwaves. There are three faculty responsible for supervising student research in the program; Robert Simpson, Antonio Elias, and Walter Hollister.

1.   DYNAMIC SCHEDULING OF RUNWAY OPERATIONS

In past years, an ATC simulation facility called TASIM (Terminal Area Simulation) was developed to provide a tool for investigating human factors problems associated with automated decision making in ATC. The current research goals are associated with demonstrating in real time the potential reductions in delay from the introduction of dynamic scheduling of landing and takeoff operations for a system of runways at a major airport. This potential was first indicated by Dear's research (ref. 1).

In the past year two decision-making modules have been designed. The "Traffic Scheduler" module has been successfully coded and tested in the Boston scenario for a single runway with landings and takeoffs. A schedule of runway operations is displayed on an auxiliary CTID (Controller Traffic Information Display), and can be seen to change dynamically as real time arrivals and departures enter the system. On the controller's "radar" display, the current FAA ARTS III display is augmented to show "boxes" for landing arrivals along the extended runway centerline. These landing boxes show the desired position of landing aircraft for its landing schedule. A second module "Flight Path Generation" has been designed but is not yet tested successfully. It generates a sequence of commands of altitude, heading, and speed for landing aircraft such that they will be vectored into their box. Further modules associated with conformance and hazard monitoring have yet to be designed, and the problems of man-machine interactions with this automated "decision support" software which arise from incorporating controller "override" capability (so that he remains in command of the computer system) and from operational problems (such as changing runways) have not yet been addressed. There is an annotated slide presentation by John Pararas in this publication.

2. GENERAL AVIATION ELECTRONIC FLIGHT DISPLAYS (P-POD)

This research is focused on the interface between the pilot and the display systems of his aircraft. We are interested in the information handling processes and consequent pilot workloads encountered in flying IFR in today's and future ATC systems. In the past year, a low cost digital electronic flight display has been assembled using microprocessor components commercially available to the home computer hobbyist. This display is called P-POD (Programmable Pilot-Oriented Display) and is described in a conference paper by Professor Antonio Elias. There are two research projects currently underway using P-POD. The first is described by James Littlefield in an annotated slide presentation given at the conference. Its goals are to create an operational "long range" RNAV display by interfacing P-POD to a commercially available Loran-C receiver. This will be tested on the bench, and in flight test. The second project has interfaced P-POD to a table-top general aviation cockpit simulator to create a novel electronic flight director display which provides rate of crosstrack deviation to the general aviation pilot. The display has other proposed projects concerned with LNAV approaches to a runway and the development of an "Electronic Kneepad" for flight management activities of the IFR pilot. These are described briefly by Elias in his paper.

3. PREVENTION OF AIRFRAME ICING WITH MICROWAVES

John Hansman describes his research into the possibilities for using microwave energy to preheat supercooled water droplets before they reach an airfoil. This consists of some theoretical work on droplet movement and flattening due to accelerations due to the flow around the airfoil. The droplet shape is important in determining the optimal frequency for the microwave and whether there is sufficient time to heat the droplets at speeds typical of general aviation aircraft. There is also an experimental portion of the research in a rain-fog section of a 1 foot by 1 foot wind tunnel at MIT. This is aimed at a proof of principal experiment with a prototype system mounted on an airfoil section in the tunnel where measurements can be made of microwave power requirements and droplet temperatures.

REFERENCE

1. Dear, Roger D.: The Dynamic Scheduling of Aircraft in the Near Terminal Area. Flight Transportation Report R76-9, Dept. of Aeronautics and Astronautics, Massachusetts Institute of Technology, Cambridge, Mass., Sept. 1976.

MASSACHUSETTS INSTITUTE OF TECHNOLOGY

ANNOTATED BIBLIOGRAPHY, 1980-81

Pararas, John: Man Vehicle Systems Research Facility: Functional
    Specification of the ATC Subsystem. Flight Transportation Laboratory
    Report R80-13, Department of Aeronautics and Astronautics, MIT,
    December 1980.

This document establishes the functional and operational specifications
for the ATC subsystem of the Manned Vehicle Systems Research Facility to be built
at NASA Ames Research Center. The ATC subsystem will provide a realistic ATC en-
vironment for two transport cockpit simulators. Fuel mission, high fidelity simu-
lation of extended flights in both today's and future ATC systems is required. The
ATC subsystem design recommended consists of three audio/visual controller
stations and a corresponding three pseudo-pilot stations with a voice disguiser
capable of representing several different pilot voices. The ATC subsystem makes
use of software developed for TASIM under the Joint University Program.

Natarajan, Krishman: Use of Loran-C for General Aviation Aircraft
    Navigation. Flight Transportation Laboratory Report R81-2,
    February 1981.

This report describes an extensive evaluation of Loran-C for use by
general aviation. Flight, ground, and antenna tests were done. Flight tests
measured the accuracy and the ability to make approaches. Receiver reliability
and susceptibility to atmospheric noise were also studied. Ground tests looked
into grid stability and grid warpage. Antenna tests were done to evaluate three
antenna configurations -- ADF, vertical whip, and trailing wire antennas.

The measured accuracy met FAA AC 90-45A requirements for all phases of
flight. Loran-C was found to be satisfactory for approaches with AC 90-45A
specifications. Reliability was 99.7%, and the receiver was insensitive to
atmospheric noise. The time difference grid was stable in the long run.
Antenna tests showed the ADF and vertical whip antennas to be suitable for
airborne use.

It is concluded that Loran-C is suitable for navigation as an alternative
to VHF RNAV. This navigation system is suitable for use in general aviation
aircraft.

DYNAMIC SCHEDULING
OF RUNWAY OPERATIONS

John Pararas

MIT, Flight Transportation Laboratory

RESEARCH OBJECTIVES

—Demonstrate the feasibility of automated ATM/C
  decision making in the terminal area

      — Develop prototype algorithms for automation
  functions

          — Runway Scheduling

          — Flight Plan Generator

Terminal Area Geometry

Due to the airway structure of the enroute airspace, landing aircraft tend to enter the terminal area airspace at specific points called entry fixes. Nominal approach routes (the dashed lines) define typical paths leading from the entry fixes to the runway threshold(s). Similarly, nominal departure routes (dotted lines) define typical paths for departing aircraft.

Whenever a new arrival enters the terminal area, its preferred time of arrival at the runway is estimated based on the entry fix and the associated nominal approach path. For departures the preferred time of arrival at the runway is determined using an estimate of the taxiing time. The nominal sequence of operations at the runway is determined based on the preferred times of arrival at the runway of all aircraft currently in the system. This sequence is perturbed to optimize the runway utilization for the given traffic, thus producing the optimal schedule of operations. Given the latter, 4-dimensional flight plans are generated for all aircraft.

ENTRY POINT
TIME TO RUNWAY
(3:12)

SPEEDMARKER

DEPARTURES

ENTRY POINT
TIME TO RUNWAY
(3:57)

RUNWAY

ENTRY POINT
TIME TO RUNWAY
(4:38)

DEPARTURES

DEPARTURES

ENTRY POINT
TIME TO RUNWAY
(8:12)
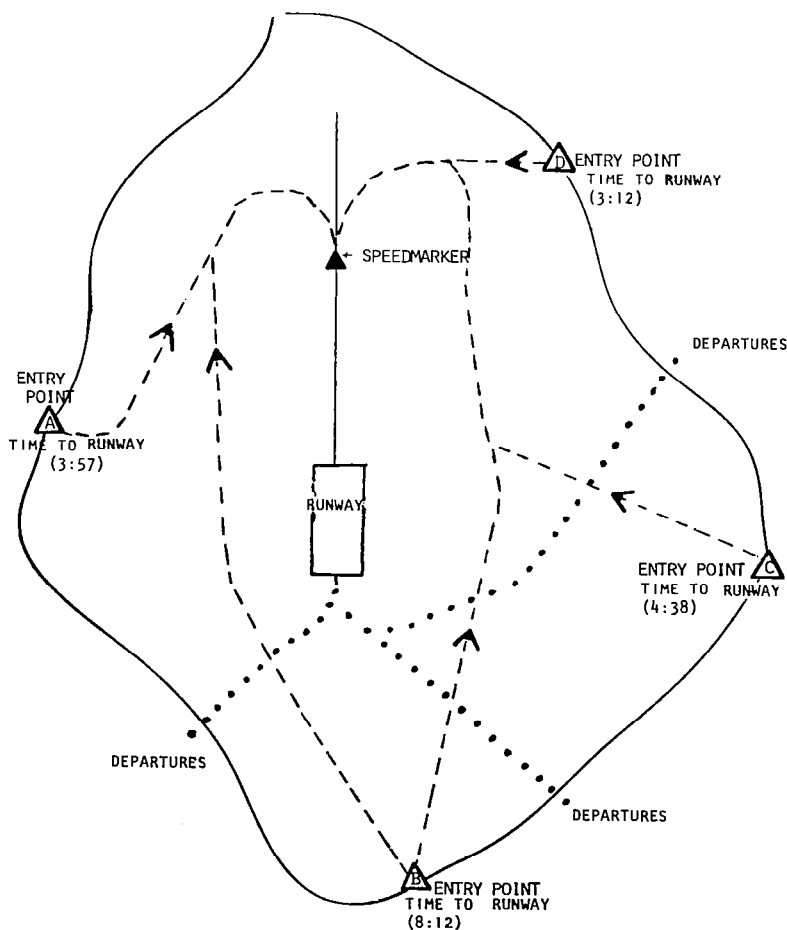
Schematic Diagram of the Terminal Area ATM/C System

The air-to-ground data acquisition (surveillance) system provides position information on all aircraft in the system. Nominal flight plans are generated for new entries and provided to the runway scheduler which updates the optimal schedule of operations at the runway(s). The traffic flight plan generator updates the flight plans according to the new schedule. The decision process is now complete until a new aircraft enters the system.

The command processor is responsible for the timely dispatch of commands to the air traffic controller. This is done through the traffic display. The commands can also be transferred directly to the pilot via an air-to-ground digital data link if one is available. The commands are such that will keep the aircraft in conformance with their flight plans. The traffic display provides the controller with a situation display of all the traffic in the system and allows him to communicate with the remaining system through "display requests".

The conformance monitor compares actual and desired aircraft positions and generates an alert when the discrepancy detected exceeds prespecified limits for some aircraft. This in general will cause a new flight plan to be generated for this (and possibly other) aircraft. The hazard monitor compares separations of short term projections of aircraft positions and generates an alert when violations of ATC separations are imminent. Again such an alert will require new flight plans to be generated but first avoidance paths are generated for the aircraft in hazard.
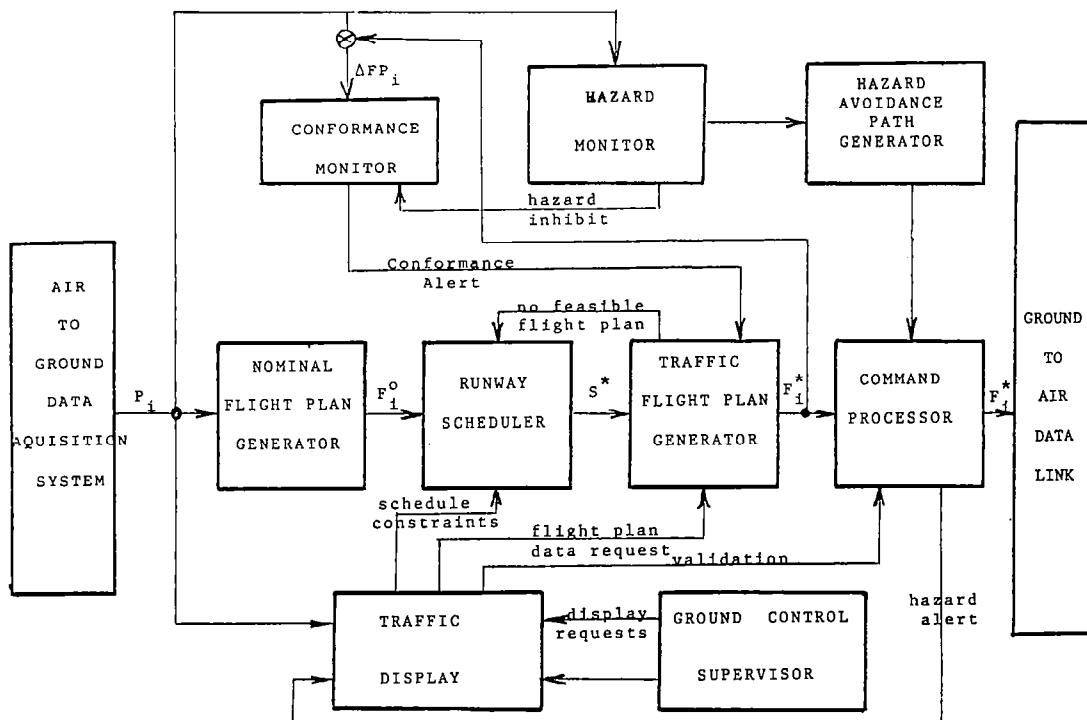
Final Vector Controller Display

This display is designed to facilitate precise delivery of landing aircraft at the outer marker without automated flight plan and command generation. Each box corresponds to the landing aircraft having the same number in the landing sequence. The boxes are moving along the runway centerline extension at the landing speed of the corresponding aircraft. The distance from the threshold is such that the aircraft reaches the runway at its scheduled landing time. Given the current and the landing speeds of the aircraft we can determine the relative bearing between the aircraft and its box such that if the aircraft then turns to intercept the ILS it will intercept the box before it reaches the outer marker. The wands shown are the pictorial representation of the appropriate relative bearing. The controller needs to approximately time the aircraft so that it will be within the final vectoring area when it is touched by the wand of its box. At that time the turn to intercept the ILS should be given.

11
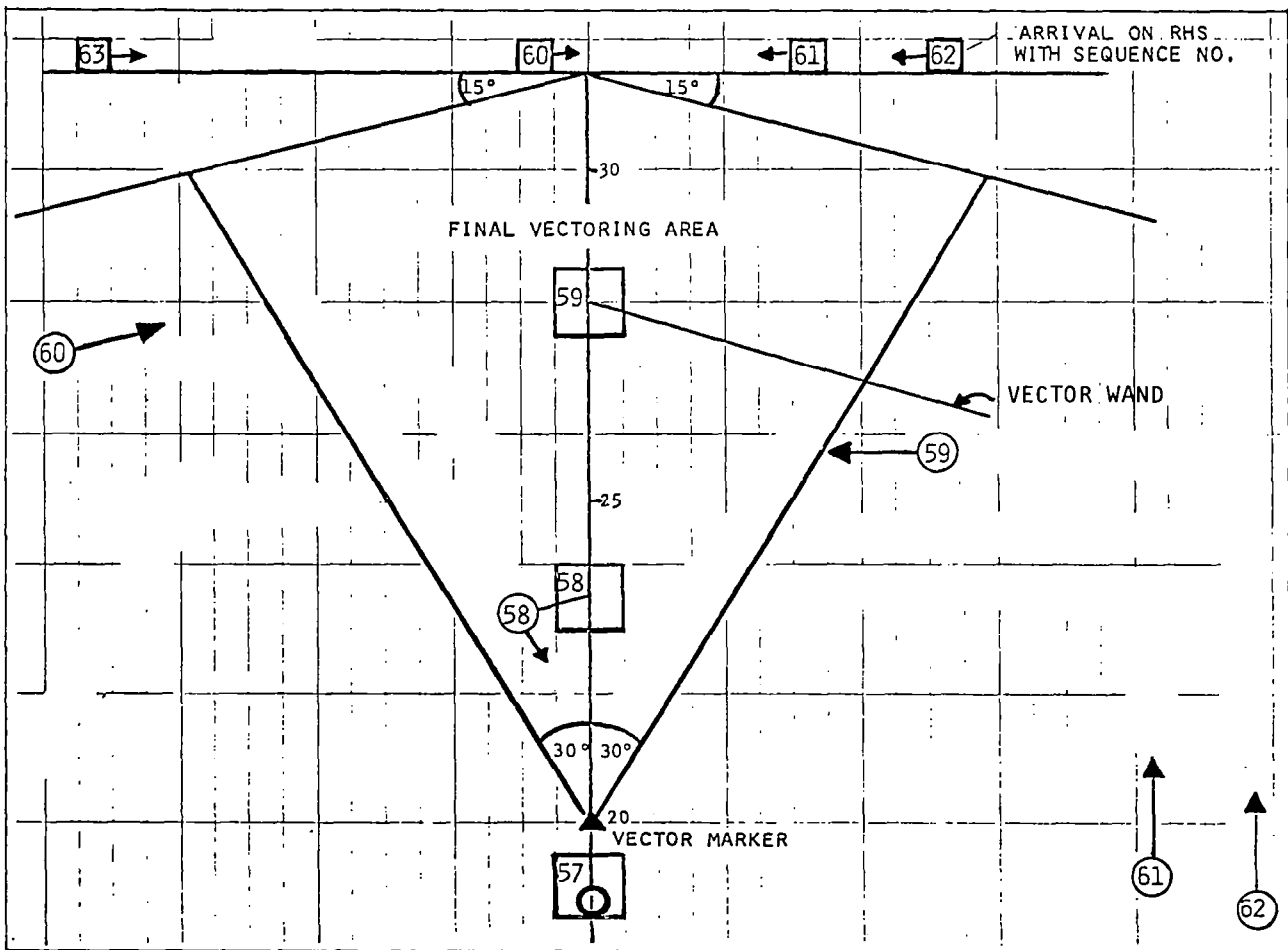
A major portion of the work has been consumed in creating TASIM (Terminal Area Simulation). It is a flexible research simulator for ATC problems involving automated decision making for ATC, but can be useful to many researchers interested in ATC problems. It forms the basis for the ATC subsystem to be built for the MVRSF (Manned Vehicle Research Simulation Facility) at NASA Ames Research Center, and is of interest to the FAA Technical Center at Atlantic City.

At present the simulation can be operated by a human controller through the keyboard in a scenario of the Boston Logan terminal area. The automated runway scheduler based on the CPS (Constrained Position Shifting) method of Dear has been coded and operates successfully with the display scheme shown for the Final Vectoring. The automated Flight Plan generator has been designed but is not yet operational. The Command Processor is operational and passes controller-generated commands directly to each target aircraft. There are two controller displays. The ATC or PVD display is a reproduction of the current ARTS III display (with the Final Vectoring display augmentation). There is also an auxiliary CTID (Controller Traffic Information Display) which displays the dynamically changing schedule for runway operations, some simulation statistics, and has message areas, command preview areas, etc., for controller interaction.

1. TASIM INTERACTIVE SIMULATION

2. SOFTWARE

- ## RUNWAY SCHEDULER
  - CPS

- ## TRAFFIC PLAN GENERATOR
  - TERMINAL AREA NETWORK
  - design of the algorithm
- ## COMMAND PROCESSOR
  - CONTROLLER INPUTS
  - TRAFFIC PLAN GENERATOR INPUTS

- ## DISPLAYS
  - ATC DISPLAY (PVD)
  - CTID

```
┌─────────────────────────────────────────────────────────────────┐
│ ─ ─ ─ ─ ─ ─ ─ ─ ─ ─ ─ ─ ─ ─ ─ ─ ─ ─ ─ ─ ─ ─ ─ ─ ─ ─ ─ ─ ─ ─ ─   │
│                                                                   │
│                                                                   │
│              SCHEDULE  INFORMATION  AREA                          │
│                                                                   │
│                                                                   │
├───────────────────────────────────────────────────────────────────┤
│                                                                   │
│              SIMULATION  STATISTICS  AREA                         │
│                                                                   │
├───────────────────────────────────────────────────────────────────┤
│                                                                   │
│              ATC  INFORMATION  &  MESSAGE  AREA                   │
│                                                                   │
│              COMMAND  PREVIEW  AREA                               │
│                                                                   │
├───────────────────────────────────────────────────────────────────┤
│              CONTROLLER  INPUT  PREVIEW  AREA                     │
│                   COMPUTER  RESPONSE  AREA                        │
└─────────────────────────────────────────────────────────────────┘
```
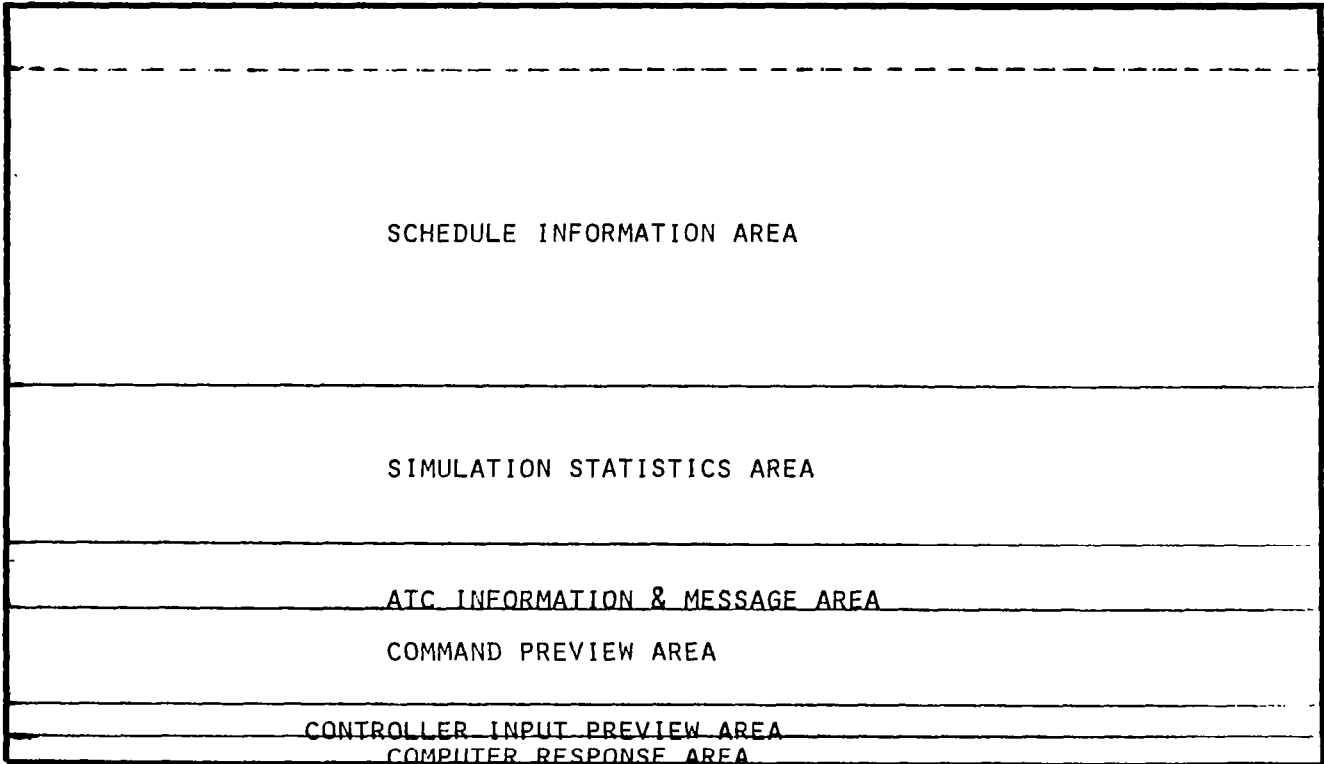
CONTROLLER TABULAR INFORMATION DISPLAY
                 (CTID)

13

PPOD PROGRAMMABLE PILOT-ORIENTED DISPLAY

Antonio L. Elias
Assistant Professor
Flight Transportation Laboratory
Massachusetts Institute of Technology
Cambridge, MA   02139

SUMMARY

A general-purpose low cost research microprocessor system for General Aviation has been developed at MIT under the sponsorship of the Joint University Program. This system is intended to be the vehicle for individual research efforts in low cost airborne hardware and software as well as advanced microprocessor based navigation systems and techniques. During 1981, two such research projects were undertaken, yielding results in the areas of micro hardware/software design, cost and performance, and pilot/computer interface. Five new projects are being developed for 1982, including a new approach to low-cost flight software reliability and a time-difference based Loran approach procedure that eliminates the need for propagation corrections and latitude/longitude transformations.

INTRODUCTION

Before the advent of microprocessors, the design of navigation systems was strongly influenced by the lack of convenient computational capabilities. This lack, combined with the need to minimize pilot workload, led to "direct readout" systems such as VOR/DME, where the signal scheme itself directly yields navigation information in easy to use format, e.g. rho-theta. Similarly, systems which required any significant amount of "post-processing", such as Loran, were deemed unsuitable for aeronautical use, unless a crewmember was dedicated to the navigation task.

Microprocessors make available so much computational capability that this traditional limitation no longer exists, thus opening up important new possibilities in the design and use of avionic systems. However, this technology has evolved in such a way that the principal costs involved in the use of microprocessors in avionic systems are not the cost of the processors itself, but of the environment required to support the digital processing functions, namely:

1) The development (non-recurring) cost of flight software

2) The certification of the digital hardware and software (also non-recurring)

3) Repetitive design of the discrete (i.e. non-LSI) hardware, e.g. busses, cards, interfaces, etc. (mainly a recurrent cost)

These high non-recurrent and recurrent costs appear to have driven the avionics industry to a very specific technological and marketing niche, namely the high cost, high performance devices used on executive aircraft. Thus we find units such as the Garrett AirResearch 2000 navigator, with both high performance and high price. Ironically, most of these aircraft operate with two crewmembers so that, in spite of the increased complexity of the aircraft, the resulting workload may be lower than the typical single-pilot IFR situation on a simpler but less equipped aircraft. It is precisely this situation that could benefit the most from workload-reducing microprocessor based avionics.

If this segment of the General Aviation community is to receive the benefits of microprocessor-based systems, ways must be found to make the low-cost market attractive to industry. The first step is to demonstrate that microprocessor avionics can be produced at a low unit cost without the risk of committing to very large production runs. Only after this has been demonstrated is industry likely to embark on larger production run projects with larger non-recurrent costs.

We believe that there may be major cost-reduction demonstration opportunities on each of the cost areas mentioned before, in particular:

1)   Improved software techniques, which may reduce both the development and the certification costs of embedded software

2)   The use of standard ("off the shelf") modules for commonly-used functions, such as power supply, data busses, interfaces, memory, processors systems, display drivers, etc.

3)   Multifunctionality; that is, the use of a single digital processor to perform a number of avionic functions, rather than embedding individual microprocessors on each avionics box (1)

---

(1) Distributed processing, that is, the use of individual processors for each function, may be the best design when other factors, such as performance and reliability, dominate over cost.

OVERVIEW OF PPOD PROJECT

The motivation for developing PPOD was to make available to researchers a low-cost general-purpose tool with which to investigate the areas mentioned above. The result is a three-processor system (main, I/O, display) using standard hardware and software, which can be configured (both from the hardware and the software point of view) for a wide range of operations and uses. The intent is that individual research projects be undertaken using this system, in order to try out novel digital avionics ideas while at the same time accumulating the experience of using and developing low-cost hardware and software.

The PPOD hardware consists of an S-100 box (including the motherboard and ground power supply), a single-board Z-80 processor (including serial I/O, disk controller and EPROM burner), 64K of dynamic memory, 32K of ROM space, a high-resolution monochrome raster display (using its own Z-80), and a slave processor (also a Z-80) with DMA capability, 24 bits of parallel I/O and small amounts of RAM and ROM.

The emphasis of all of these sub-projects will be the reduction of single-pilot IFR workload, with the secondary goal of reducing the physical complexity of cockpit instrumentation.

SPECIFIC RESEARCH ISSUES: SOFTWARE

Although ultimately it will be up to industry to develop the actual designs for low-cost microprocessor based avionics, some of the research that may demonstrate the viability of doing so may be best carried out from the detachment of a non-commercial research organization, such as NASA or the Universities; in commercial avionics development, marketing and timing reasons may prevent the kind of general-application research that PPOD is intended to support.

In the software areas, three specific issues are addressed:

1) The use of high-order languages

2) The use of resident-based (as opposed to host-based) development systems

3) The development of standard software functions

Use of high-order languages

Large-scale aerospace processors, such as the IBM AP101, have modern high-order language support (e.g. HAL), whereas microprocessor flight software is commonly done in assembler code. One of the reasons for this situation is the large investment required to develop a high-order language environment (up to $1M for the HAL system).

On the other hand, the explosion of the personal computer market has resulted in the development of a number of modern high-order language systems (Pascal, PL1, Forth, C, etc.) for microprocessors. Naturally but unfortunately, most of them are geared towards non-real time applications, and require disk drives for program operation. We would like to identify exactly the shortcomings of these systems, and what has to be added or modified to make them suitable for flight software use.

Finally, we would like to quantify the cost benefits of high-order languages in the GA avionics environment, in particular the tradeoffs between the reduction in software cost, the increase in memory needs, and the reduction in processing efficiency for significantly different languages and systems.

Alternative development systems

There are three possible approaches to developing microprocessor software, listed here in order of increasing procurement cost:

1) The use of an existing time-sharing system to edit, compile, link and, under certain circumstances, execute (by simulation) the flight code, or, alternatively, download it to the target machine for execution and checkout

2) The use of the target microprocessor itself both for development and checkout

3) The use of a specially-configured micro or minicomputer system geared towards software development (a "Development System")

Traditionally, embedded microprocessor software has been developed by the first and last methods, sometimes in combination. Use of the target machine for software development is another technique that has come of age with the explosion of the

personal computer industry. Each of the methods has advantages and disadvantages; with PPOD, we can experiment with the first two methods (the use of a Development System being beyond the reasonable reach of the project's budgetary expectations).

Standard software libraries

The last software research issue addressed is the use of standard functions in flight software, that is, the identification of functions that are general enough, and common enough so as to warrant the development of "library" modules to reduce subsequent software development/certification costs. Of particular interest is the human interface/display area, where a standardization of protocols and/or formats could also result in uniform user procedures across different designs.

SPECIFIC RESEARCH ISSUES: HARDWARE

In the hardware side, we will identify the hardware functions that are required, and relate these functions with board-level modules that are either currently available, or should be made available as "off the shelf" components for GA avionics use.

It should be noted that the purpose is <u>not</u> to determine the suitability or unsuitability of <u>existing</u> components for GA avionics use, but rather to identify the functions required, and to quantify the benefits that would accrue from the availability of such standard components. As a consequence of this research, we hope to identify opportunities for GA-oriented industry standards for busses, hardware interfaces, etc. that could be an incentive for production of standard boards.

Finally, in the systems design area, we hope to identify and quantify the acquisition, maintenance, and operating cost reductions that would accrue from integrating, rather than distributing, the processing functions.

Status of project

As of December 1981, the following milestones had been achieved:

1) A hardware configuration was selected, procured and assembled.

2) The hardware has been interfaced with a ground-based simulator for testing and development purposes.

3) An operating system environment for the various high-order languages has been selected and procured, including elements of a resident software development system (e.g. compilers, assembler, linker, full-screen editor, etc.)

4) The first high-order language system (PL1) has been procured.

5) Two pilot projects have been started, and are yielding initial research results.

Hardware configuration

The "S-100" family of hardware components was selected for P-POD; the main basis for this selection was the large number of board-level components available for this family, including processors, memory, device controllers and I/O, ROM, video displays, voice I/O, etc. The bus used in this family (and from which the name derives) is not without its faults, particularly in the area of noise immunity, bandwidth, and signal path architecture. On the other hand, it is a flexible design whose noise performance has been improved with active termination and heavy-duty construction, and whose signal definition faults have been at least partially remedied by an IEEE standard definition (IEEE 696) of the bus.

The initial configuration consisted of a Teletek FDC-1 single-board processor, a Measurement Systems and Controls (MSC) 64K dynamic memory board, a Digital Research Computers 32K selectable-address ROM board, and a Scion Corp. Microangelo display board.

The FDC-1 board includes, in addition to the Z-80 chip, two serial ports, floppy controller, 2K of ROM, and an EPROM burner. This board is used both for software development (using the CP/M floppy-based operating system) and for actual execution of the flight code. The Microangelo display board is a medium-resolution (512x480) monochrome bit-mapped raster display with a dedicated Z-80 processor, 8K of ROM and 2K of RAM (in addition to the screen RAM). Communication between the main processor board and the display board is by buffered interrupt driven physical I/O.

Earlier into the first project (Loran-C pilot interface) it was determined that the amount of I/O that could be accomplished by the main processor board was limited, and therefore a Teletek I2 board was procured. This board, which is produced commercially as an Intelligent Interface for devices such as Winchester hard disks (and therefore geared towards the OEM market), consists of a Z-80 processor, 2K of RAM, 2K of ROM, and the bus support circuitry required to interface with the bus owner (the Z-80 on the FDC-1) by a combination of vectored interrupts and Direct Memory Access.

These boards are contained in a California Computer Systems motherboard and card cage, which includes an unregulated heavy-duty 115 volts power supply to feed the series regulators on each of the boards. For flight use, the power supply is fed AC from a 300 watt static inverter.

PROJECT #1: VOR/RNAV-LIKE INTERFACE FOR LORAN-C

The first project initiated under P-POD was a display system that would allow a pilot to use a Loran-C receiver as a rho-theta navigation device similar to a VORDME/RNAV system. The motivation for this project was the observation that pilots prefer the rho-theta presentation of information to almost any other type of presentation, including maps. Whether this preference is due to the considerable experience that pilots have with the VOR system, or whether the popularity of the VOR system is due to its rho-theta presentation, is subject for debate.

In any case, the advantages of Loran (low equipment cost, wide area coverage) could be combined with the ease of use of VORDME by a device that would store names and geographical locations of VORTAC's. The aircraft latitude and longitude, as determined by Loran, is then converted to great-circle bearing and distance to a VORTAC selected by the pilot, and presented in a form vaguely resembling the familiar CDI and DME range window. In addition, the system allows the pilot to define (in-flight or before the flight) waypoints using either latitude and longitude or offsets from existing waypoints, and to assign three-letter identifiers to these new waypoints.

To test this concept, P-POD was interfaced to an existing commercial receiver (a Digital Marine Northstar 6000). However, one of the factors that was considered in selecting this as the first P-POD project was the expected availability of low-cost Loran-C receiver boards, such as the Ohio University unit. The display produced, the definitions of the navigation terms used,

and the commands available to the user are summarized in Figures 1, 2 and 3.

The system has been tested both on the bench and on a moving vehicle. Flight tests during late summer of 1981 were hampered by power supply and antenna problems. Flight tests with a new DC power supply, retractable downwards-pointing whip antenna, and improved keyboard will begin this spring. A preliminary result of some interest is the figures for utilization of high-order language (PL1) versus assembler code, summarized in Figure 4. In essence, it is estimated that the use of PL1 reduced programming time by a factor of 7 (1000 lines of code vs. 7000 lines of code), while the program memory required increased by 40% (14,000 bytes vs. 10,000 bytes).

Of some concern is the total amount of memory used by the applications code (some 7700 bytes), considering that the total address space of these machines is only 64K bytes, and that the operating system takes some 6500 bytes out of them. On the other hand, one-third of this code is made up of pilot input handling and display routines that could be shared by other functions. Also, the system incorporates a large number of ""features" not all of which may be considered "indispensable".

A major obstacle encountered during development of this code was that the PL1 system subroutines do not initialize storage memory, because they expect its contents to be initialized from diskette as part of the program load. When the code is resident in ROM, however, there is no program load, and thus no initialization of storage memory. A system was developed to simulate this function at a cost of 25% of the storage memory required by systems programs (application programs were coded so that they perform their own initialization). In spite of this fix, it was concluded that any high-order language system that is to be useful for GA avionics use must either explicitly initialize memory storage itself, or at least separate storage memory into two areas, one of which requires initialization and thus must be "replicated" in ROM.

Code for this project was developed both with the resident system and the time-sharing system. On the basis of this experience we conclude that:

1) The resident system is superior to the time-sharing system for developing I/O (including user interface and display) code, and for final code integration, due to its "closeness" to the target machine.

2) The time-sharing system can be extremely useful for development and coding of algorithm-intensive functions (i.e. math-intensive), due to its faster compilation turnaround and its more powerful mathematical debugging capabilities (debugging can be performed at the PL1 level).

3) The time-sharing system is superior for maintaining and preprocessing data bases (e.g. VORTAC identifiers and positions).

PROJECT #2: RATE-ESTIMATING ILS DISPLAY

Flight Directors are devices that combine navigation and attitude information (including rate information) and generate an attitude command that is displayed on the same instrument that displays attitude. By suitable generation of the command attitude, the pilot workload required to fly a high-performance aircraft (requiring substantial command lead compensation) can be greatly reduced.

On the other hand, Flight Directors are expensive devices, because they require attitude and attitude rate (and, sometimes, control surfaces position) information, and because the computation and display devices are electromechanical in nature.

General aviation aircraft usually exhibit benign dynamics(1) which make full Flight Directors somewhat of an unnecessary luxury. The dynamics of lateral control during ILS precision approaches, however, do involve a significant amount of pilot workload due to the piloting strategy required by the low-gain, low rate information localizer display. The data processing and display capabilities of a P-POD like device in the cockpit could be used to generate a rate-aided display, maybe not as sophisticated as a Flight Director, but at essentially zero marginal cost given the ILS receiver and the P-POD display.

For that cost to be indeed "zero", the display must not require the attitude and attitude rate data (and the corresponding

---

(1) Under the sponsorship of this same NASA Joint University Program, Princeton is examining the dynamic and handling features of GA aircraft that make them more or less suitable for single-pilot IFR.

electro-mechanical instruments) that the true Flight Director requires.(1)

This project attempts to produce a simple display, using ILS localizer information and digital filtering techniques to estimate lateral deviation rate. This rate information is then presented to the pilot in the form of a rotating CDI needle, very much like the one used in the Loran-C display.

The specific research issues addressed by this project are:

1) Adequacy of 8-bit processor throughput for fast repetition rate processes

2) Adequacy of bit-mapped displays for fast update rate control oriented (as opposed to navigation oriented) displays

3) Adaptability of interface subroutines developed for one project (Loran-C) for other projects

This project was developed and tested using a desktop simulator (ATC-610) of a Piper Cherokee Arrow single-engine retractable. A PDP-11/10 was used to extract simulator X-Y position and synthesize ILS localizer information from it. This localizer "signal" was then fed to P-POD, which then generated the display. Flight tests will begin as soon as a navigation receiver is procured for this purpose.

One of the results obtained so far is that bit-mapped displays, such as the one used by P-POD, complicate the display design process because they "erase" the background over which a symbol is written, unless special precautions are taken to "save" the background information. In essence, three approaches are possible:

1) Design the display itself so that symbols do not overlap; this was the approach taken on the Loran-C display. In the case of the Localizer, this led to awkward displays.

2) Save the pixels that are over-written by a symbol and restore them at the time the symbol is erased

---

(1) At most, a low cost single axis fluidic rate gyro may be required.

for re-positioning. This requires complex graphics
primitives and additional memory.

3) Write the moving symbols by complementing, rather
than 1-ing the pixels; erase the symbol by
re-complementing, thus restoring the background sym-
bol. Does not require complex code or memory, but
two overlapping symbols have blank pixels at their
common locations.

All three techniques will be explored during the coming year.

PROPOSED NEW PROJECTS

A number of projects, all using the P-POD hardware and software,
and all contributing towards the ultimate goal of identifying
cost-reducing techniques, have been identified and will be
started as resources become available. Some of these projects
are:

1) The possible use of redundancy to improve the
cost/reliability ratio of flight software
("Layered-redundant coding")

2) A Loran-C non-precision approach procedure based on
Time Differences, not on latitude and longitude of
runways

3) An "electronic kneepad" that would make available
flight information to the pilot in a dynamic fash-
ion, as well as perform flight-plan following compu-
tations (using pilot inputs, not direct navigation
information)

4) An R/Nav device using a single, digitally-tunable,
fast-locking DME and a large VORTAC
position/frequency catalog to achieve country wide
"hands-off" navigation

5) The use of voice I/O to augment/supplement the above
functions

The first two projects require some elaboration:

There are two approaches to reliability in avionics hardware:
producing hardware that is essentially very reliable, and using

less reliable hardware in redundant numbers, with the appropriate error detection and correction protocols. Two excellent examples of these approaches are the Apollo Guidance Computer, a single unit with MTBF's in excess of 20,000 hrs, and the Shuttle Orbiter Main Computer Complex, using four identical units with MTBF's of less than 1000 hours. Economic considerations dictate which approach is the most cost-effective for a particular situation.

Software reliability can only be achieved by the first (or "brute force") method, since two copies of the same software are guaranteed to have the same identical bugs; as opposed to hardware, there is no distinction between the design and the fabrication stages, and thus there are no advantages to redundant copies of the same code.

If, however, identical functional specifications for software are given to different software designers (i.e. coders), then there will be no correlation between the bugs in one version of the software and another. Such "truly redundant" software then has to be executed in an environment that recognizes differences in their outputs, and takes appropriate action in case of disagreement, much in the same way as redundant hardware.

The cost of producing two independent codes for the same function is, indeed, twice that of producing a single version.(1) However, that cost may very well be much less than that of testing and inspecting the single version to achieve the same degree of confidence that would result from the redundant execution. Also, any deficiencies in the specifications themselves will show up on both versions, requiring either duplicate specifications (hence the term "layered software redundancy"), or the use of conventional brute force reliability techniques for all higher level software and specifications.

To our knowledge, this approach has never been tried. In order to evaluate its potential, an experience base must be developed, including cost and performance statistics. We propose to use the P-POD project, and the sub-projects developed under it, as a test bench for the redundant coding concept. Selected functions will be double-coded by different individuals (using different languages, if possible) from the same specifications. The Operating System environment will be modified to handle the double-calling of the subroutines, comparing their outputs, and taking appropriate action when disagreement is detected. Finally, selected equivalent functions will be subject to the conventional testing

---

(1) The apparent duplication of execution cost may be reduced by alternating codes during successive "passes", where this is possible.

and inspection approach, and records kept of the performance and cost of both approaches.

The Time-difference based Loran approach procedure tries to cope with a major objection to the use of Loran-C for non-precision approaches: the use of corrections for signal propagation anomalies.

Due to variations in the propagation characteristics of the terrain between a Loran station and a receiver position, the "electric" grid of hyperbolas of constant time-differences is "distorted" with respect to the "geometric" grid of constant distance-difference hyperbolas. This difference can be of the order of half a microsecond in time difference, or 150 meters in position. On the other hand, it is contended that these differences are repeatable within 0.1 microseconds, or some 15 meters, leading to the suggestion that correction terms be used to achieve 15 meter type performance. This suggestion is viewed with concern by certification authorities because it may lead to blunders (if entered manually) or complex secular changes (similar to magnetic variation, but infinitely more complex). To make matters worse, there is disagreement on the procedures that must be used to convert time differences to latitude and longitude, and differences in the navigated position of different types of Loran receivers have been traced to differences in the mathematical generation of the geometric grid.

The proposed technique is to base the navigation solution for the approach entirely on time-differences, i.e. navigate on the electric, rather than the geometric grid. In this procedure, the "Loran approach" is based on five parameters: two time differences at each end of the runway, and the distance between these points, namely the runway length.(1) The benefits of this technique are twofold: a reduction of the complications (and potential errors) resulting from the use of propagation corrections and various lat-lon conversion schemes, and a reduction of the complexity of the navigation computations required during approach, which can lead to faster display update rates.

---

(1) Additionally, some <u>approximate</u> information about the location of the airport with respect to the stations may be used to improve the linearity of the approximations involved, particularly at airports situated close to a Loran station; but in any case the navigation solution guides to <u>time-differences</u>, not to a point in lat and lon.

"Current waypoint"   Local magnetic course   Current magnetic
   area   to current waypoint   groundtrack

WP#	DIST	RAD	CRS	6S	TRK	TTG
3	69.3	133.1	312.8	135	311	15.2

312

to/from indicator (to position)

linear displacement markers
(programmable scale factor)

CDI (shows both lateral
   deviation and CRS - TRK)

WPNT DISPLAY:		-- OFFSET --		
WP#	OFF	DIST	BRNG	DES.RAD.
3	BOS	12.8	278	133

Definition of waypoint #3

ENTER COMMAND:

>

Command line area   Error message area

Figure 1.   Loran-C navigator commands.

CURRENT A/C POSITION

GROUND TRACK

"COURSE" (TO WAYPOINT)

"COURSE DEVIATION"

RANGE

"CURRENT
RADIAL"

GREAT CIRCLE ARCS

OTHER DEFINITIONS

"DESIRED RADIAL"

"WAYPOINT" -- same as RNAV (#1, #2, etc.)

"NAMED WAYPOINT" -- a number of pre-stored

   points, identified by a three-letter

   code.   Mostly VOR's, may be airports,

   NDB's, etc.

"CURRENT WAYPOINT"

LOCAL MAGNETIC NORTH
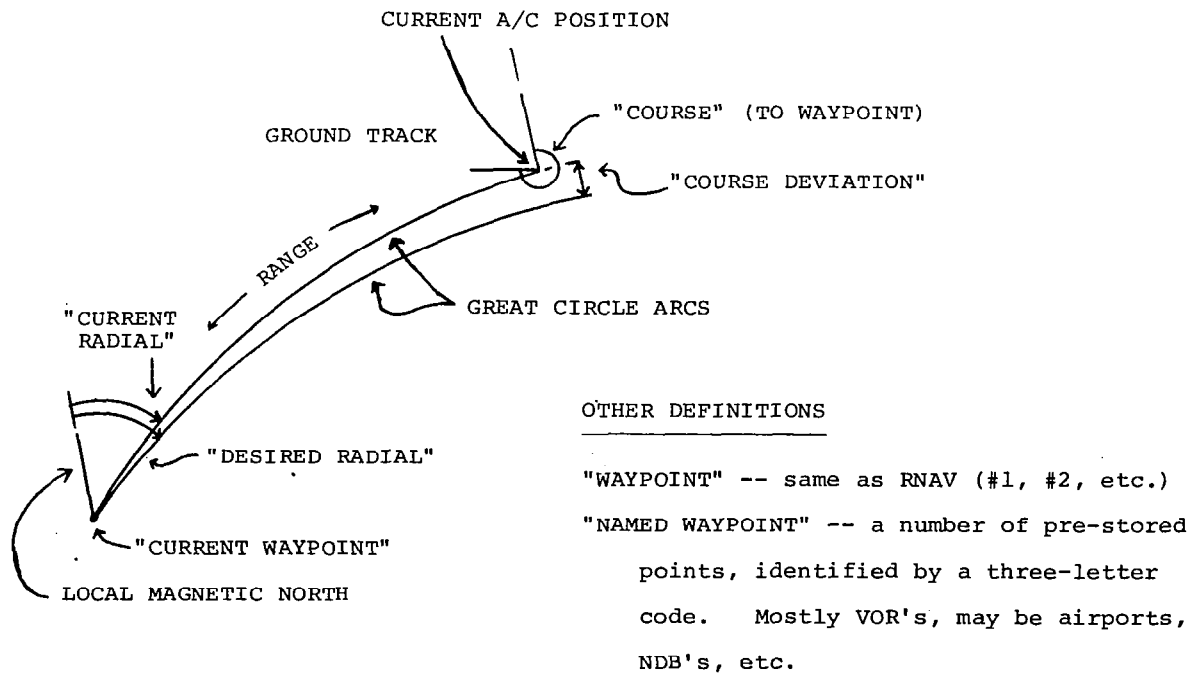
Figure 2.   Enroute Loran navigation - geometry and definitions.

```
E  --  enter new waypoint in waypoint list

I  --  insert new waypoint in waypoint list

D  --  delete a waypoint

A  --  advance the "current waypoint" to the next
       waypoint in the list

B  --  back up the "current waypoint" to the previous
       waypoint in the list

S  --  show  a waypoint (from the waypoint list) in
       the waypoint display area

T  --  set CDI tracking to the "TO" position

F  --  set CDI tracking to the "FROM" position

R  --  set desired tracking radial to/from a waypoint
```

Figure 3.   Summary of Loran-C navigator commands.

PROGRAM MEMORY

ITEM	SOURCE LINES	CODE (BYTES)	
PL1 CODE	706	7177	(10 BYTES/LINE)
ASSEMBLER CODE	365	511	(1.4 BYTES/LINE)
SYSTEM CODE:	-	6522	
TOTAL PROGRAM MEMORY:		14210	

ESTIMATED SAVINGS AND PENALTIES

(PL1 VS. ASSEMBLER)

- MEMORY PENALTY: 4000 BYTES (10000 VS 14000)

- SOURCE CODE SAVINGS: 6000 LINES (1000 VS 7000)

Figure 4.   Core and memory usage summary - enroute Loran navigation
            pilot interface software.

THE P-POD PROJECT: PROGRESS REPORT

James A. Littlefield

MIT, Flight Transportation Laboratory

P-POD PROJECT: PROGRESS REPORT

The programmable pilot oriented display (P-POD) is a multiprocessor based flight information processing and display unit. Most of the work to date has been directed toward optimizing communication protocols between the three Z-80 processors inside P-POD. As described in a previous report, one processor (P0) is dedicated to IO control, data buffering, and formatting; a second processor (P1) is reserved for coordinate transformations and supervision of the other two Z-80's; the third unit (P2) is dedicated solely to display generation.

At the last quarterly meeting of the Tri-University program a description of the interface between the video processor, P2, and the main processor, P1, was given. Subsequent reliability testing led to significant revisions in both hardware and software. Figure 1 illustrates the cycle of data flow between P1 and P2. Should a failure (either hardware or software timing) occur at any point in the data transmission cycle, the process will hang indefinitely, resulting in cessation of display generation and an overflow of the P1/P2 command buffer. While running diagnostic routines to exercise the P1/P2 interface at maximum speed an intermittent failure was observed. A careful check of possible noise sources or race conditions in the hardware diagramed in figure 2 did not reveal the source of this failure. Possible software timing problems were also fully investigated. Due to the sporadic nature of this failure it was not possible to isolate its source; however, all test results point to a portion of the status generation circuit on the video board as the error source.

To eliminate the effects of this type of failure a performance monitor routine is now being used to detect these occasional failures and correct for them. This software correction for hardware failure was deemed prudent for two reasons; detailed debugging of the video board would be very time-consuming with the available documentation; these failures are serious and might be induced by external noise sources. At present,

the real time clock on board P1 is used to trigger execution of a routine
which observes the history of interface operation over the previous second.
Based on the setting of a flag and contents of a status byte, the data
transmission cycle between P1/P2 is either allowed to continue normal
operation or is re-initialized and restarted when an error condition is
detected.

One of the advantages of a software reliability monitor is that it
will correct for any temporary operational failure in the interface (i.e.,
power line spike, missed interrupt, software timing error, EMI).
In addition the assembly coded monitor routine occupies less than 41 bytes.
The performance check routine runs every second in the current implementation.
Since all commands to the graphics processor, P2, are buffered, no bytes are
lost due to momentary hardware failures of the type observed. Command
buffer contents are preserved until the transmission cycle is restarted by
error detection code. An additional function of the performance monitor
is accumulation of a total error count indicating the number of failures
detected and corrected since system startup. Presently failure rates of
approximately $6/(3 \times 10^5)$ bytes are being observed.

Loran data processing has been the second major area of work during
the past quarter. Two 8-bit latches have been connected to the Loran
receiver data bus. Whenever new data is latched into these buffers a
mode 1 Z-80 interrupt is sent to P0. P0 multiplexes the 16 bits of data
onto its own 8 bit IO port by cycling the tri-state enable lines of the
octal latches. Once Loran data has entered the P0 memory map it is
processed by the control program outlined in figure 3.

The Northstar 6000 receiver is capable of transmitting digital data
to four external devices (D0-D3). Data for each of these devices is
multiplexed onto the same data bus. IUSER3, the P0 control program,
decodes 2 of the four available devices. D1 data consists of TD's for
the first and second slaves in the selected chain. D2 data is composed
of TD's, SNR's, ECD's, mode numbers, and latitude/longitude for all
stations in the chain. D1 data is available once every 2 seconds.

D2 data is available about every 2.7 seconds. IUSER3 will observe both D1, D2 data and transmit either or both to P1 via a DMA operation. IUSER3 can also be configured to select the best data source; if the first and second slaves have high enough SNR's, then D1 data is preferred since it is available more often. SNR's are determined by observing the D2 data stream at all times. Should first or second slave SNR's fall below a programmed threshold value, the D2 data stream will be sent to P1. Whenever data is transferred to P1 memory, the first byte of the transmit buffer contains a tag indicating the contents of that buffer (D1, D2 data).

Use of the additional IO processor frees the P1 processor from several tasks. The PO control program formats each data frame and does length checking to ensure that each frame is complete. Thus P1 is assured of having a valid position fix before attempting coordinate conversion.

Objectives for the next quarter are completion of the interface between the PO control program and the existing PL/1 Loran data processing code which was demonstrated at Ohio University. Successful flight testing of this configuration will be followed by some execution speed tests to more fully document the performance of the interprocessor communications package. Final documentation will complete my thesis work. The interprocessor communications package will provide subsequent users of PPOD with a modular operating environment which will ease adaptation to a wide range of experimental goals.
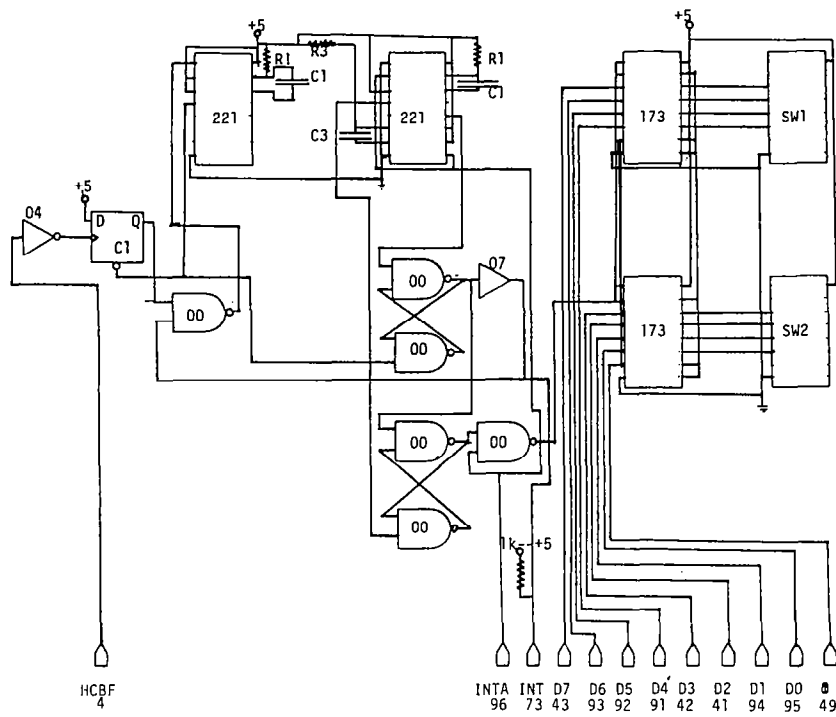
Figure 1.   Interrupt jammer rev. 2.
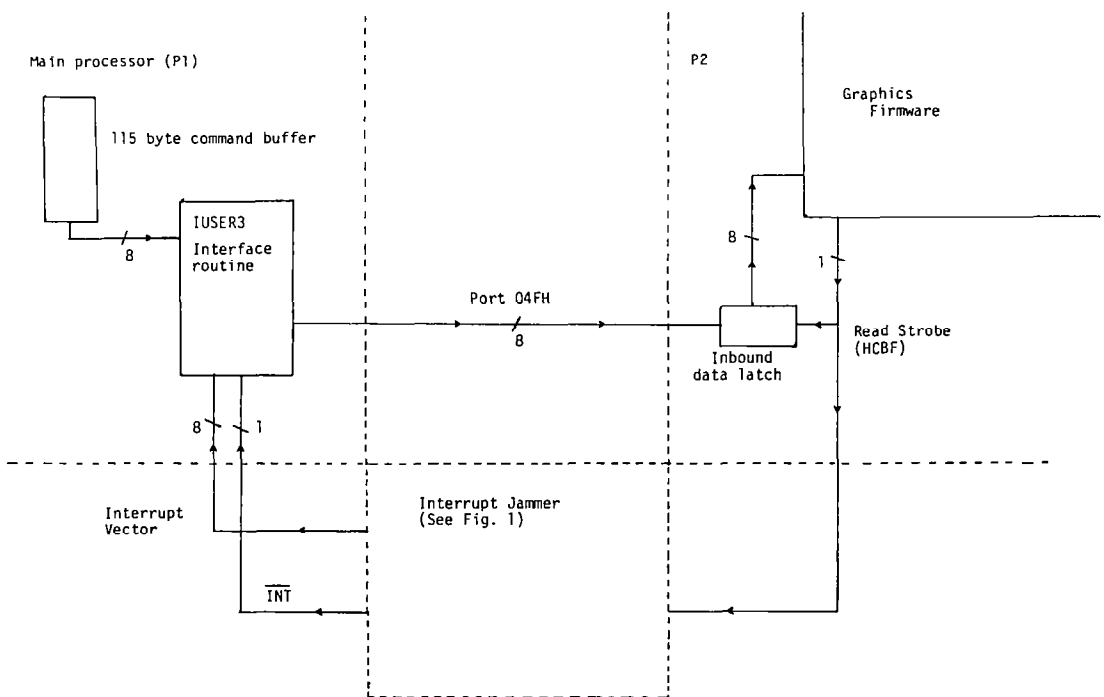
Figure 2.   P1/P2 communication data flow.
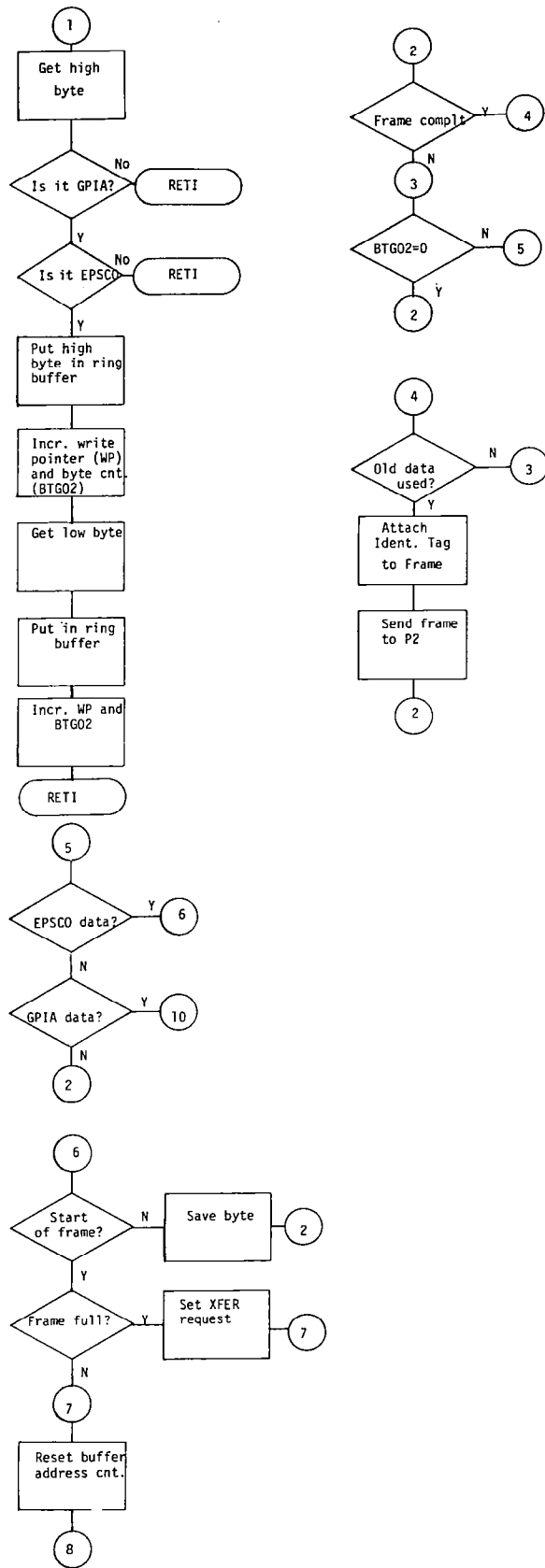
Figure 3.   1USER3 flowchart.
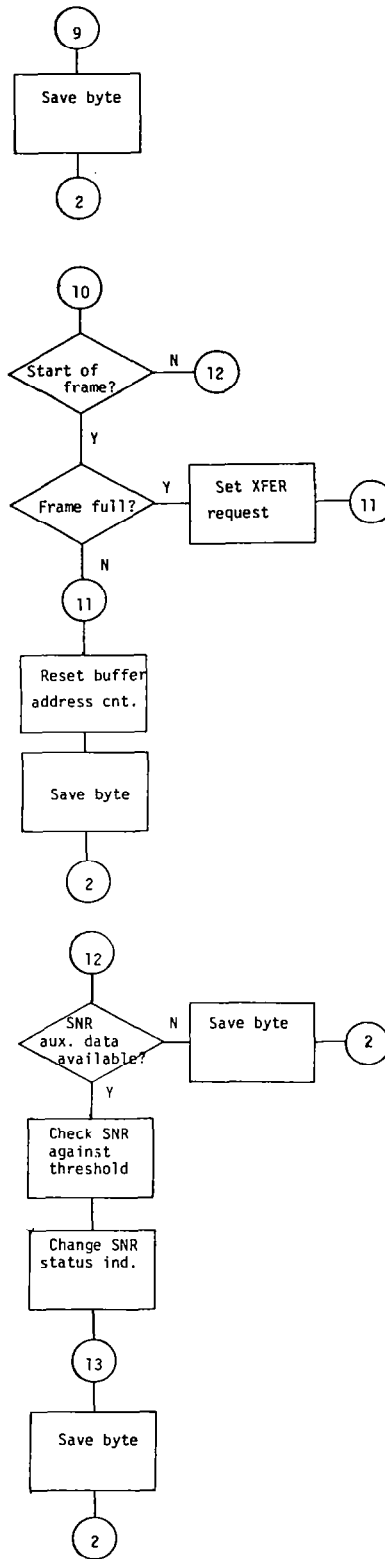
Figure 3. (Concluded).

MICROWAVE ICE PREVENTION

R. John Hansman, Jr.

and

Walter Hollister

MIT, Flight Transportation Laboratory

RESEARCH ON ANTI-ICING BY MICROWAVE HEATING OF SUPERCOOLED WATER DROPLETS

The study of the novel concept of using microwave energy to provide aircraft ice protection, specifically an anti-icing system, and the feasibility of such a system is the aim of this research. In a microwave anti-icing system impinging supercooled water droplets are heated to above freezing by the resonant absorption of microwave energy located upstream of the airfoil. This process is inherently more efficient than existing anti-icing devices due to the saving of the latent heat of fusion (a substantial 334 joules/gm (80 cal/gm)) and the fact that only the droplets are heated, thereby reducing convective losses to the air.

Efficiency improvements of factors of 10 or 20 are, in principle, possible. This would make anti-icing feasible in applications where less desirable de-icing devices are now used. The light weight and low aerodynamic drag of microwave systems are also desirable characteristics.

In studying the microwave anti-ice concept three major issues became obvious:

1. Is there sufficient time to heat the supercooled water droplets? (i.e., will it work?)

2. What efficiencies are realistically possible?

3. What are the applications problems? (i.e., cost, high frequency, interference, runback, etc.)

The work to date has been focused on the first two questions.

The question of droplet heating time has been approached on both a theoretical and experimental basis. The theoretical work has resulted in a model for the heating of a droplet as it approaches an airfoil. The model has undergone several levels of refinement and is manifest in a computer code which calculates droplet trajectories and temperatures. At present, the model includes the following

effects or assumptions:

    Rayleigh-Gans absorption

    Inviscid airflow around body

    Electromagnetic field (can be varied -- normally exponential radial, $\cos^2$ angular behavior)

    Droplet trajectories -- iterative solution of equations of motion from reference 1

    Increased heating due to:

        droplets slowing before impact

        increased absorption from flattening due to pressure gradients

    Polarization and near field effects

    Evaporative and convective losses

    Max. electric field limited by gaseous breakdown

The code is 75% complete and when completed should provide detailed design and efficiency data. Hand calculations of droplet heating including the above effects indicate that there is clearly time to heat the droplets if the microwave frequency is sufficiently high. Pending completion of the code calculations the operating frequency is expected to be between 10 GHz and 30 GHz.

One effect which is considered important but was not included in the above computer simulation due to a lack of a quantative model is the increase in droplet absorption as it passes through the ice-water phase transition. An increase in absorption is expected at the phase transition due to the nonspherical shapes of freezing and melting droplets.

The theoretical work described above is being supprted by an experimental program. The predictions of droplet trajectories and droplet flattening are being compared with wind tunnel investigations of droplet flow around cylindrical and airfoil shapes. Velocity and flattening information are obtained from fast strobe photography and fixed "time of flight" photography in a rain-fog section of the MIT

1 ft by 1 ft tunnel. In addition an experiment is being set up to quantify droplet absorption through the ice-water phase transition. This sensitive measurement is made by observing the change in Q (Q = power stored/power dissipated) of a resonant cavity which contains melting or freezing water droplets. For more details of the experimental or theoretical work to date, see figures 1 through 17, which were presented at the NASA Joint University Air Transportation Research Conference.

With the completion of the computer simulation of droplet heating and its experimental verification the question of whether there is sufficient heating time will be answered, and we are therefore prepared to begin the next phase of the work. This phase consists of two parallel tasks.

(1) Proof of principal experiment, consisting of the design of a microwave anti-icing system using the above analysis. The system will be mounted on an airfoil section and tested in the wind tunnel. The system can be tested both at room temperature and at icing temperatures (the winter operation of MIT 1 x 1 tunnel is adequate for this purpose). Measurements can be made of microwave power drain and of droplet temperature. The temperature measurement can be made in situ by using advanced fiberoptic thermometry which allows an unperturbing measurement of temperature even in the presence of microwave fields.

(2) Completion of droplet heating work by measuring absorption during the ice-water phase transition described earlier. This work should provide some insight into both the "mixed phase" icing conditions about which there is only limited information and the phenomenon of the "bright band".

REFERENCE

1. Bergrun, Norman R.: A Method for Numerically Calculating the Area and Distribution of Water Impingement on the Leading Edge of an Airfoil in a Cloud. NACA TN 1397, 1947.

```
              CLOUD DROPLETS (FAR 25)      FREEZING RAIN

    T              0 → -20°C                 0 → -5°C

    LWC            0 → 1 gm/m³               0 → 3 gm/m³

    D             10 → 40 μm                 1 → 5 mm
```

Generally below 10,000 ft in localized layers and zones

PROBLEM BECAUSE OF:

```
        weight                    ice-ingestion
        drag                      antenna
        flutter (anti-ice)
```

CURRENT TECHNIQUES

```
        boots                 hot air
        electrothermal        liquid-glycol or alcohol,   TKS
```

Figure 1. The general parameters of the icing problem and
           the current techniques used to deal with it.

1. Ice prevention -- use resonant absorption properties
    of water
                A. Anti-Ice (Preheat Droplets)
                B. De-Ice (Melt Ice)

2. The possibility of using radar to remotely detect
    and avoid icing zones was first proposed by
    David Atlas in 1954 J. Met. Vol. 11, p. 309. While
    his concept was based on a ground weather radar,
    advances in "on board" radar capability along
    with certain scattering characteristics of droplets
    at the ice-water phase transition (to be discussed)
    may make remote detection feasible.   Requires
    vertical scan.

Figure 2. Several concepts of using radiation for ice protection or remote
           detection. The idea of remotely detecting icing zones by air or ground
           radar is intriguing and was spawned by meteorological radar observations
           of a highly-reflecting "bright-band" at the melting layer in precipitation.
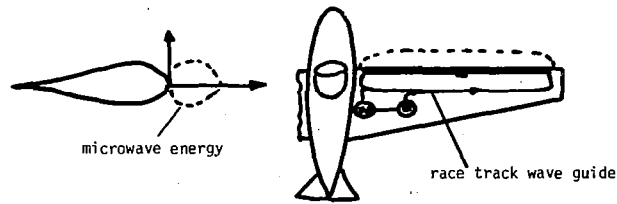
This scheme operates in two modes: anti-ice or de-ice

ANTI-ICE

Droplets are preheated to above freezing before impact

Power requirements estimated (V = 200 mph, 20 μm droplets)

Wing   40 watts/linear foot

Prop or Rotor   25 watts/linear foot (Goodrich "Hot Prop",
        200 watts/linear foot)

DE-ICE (Magenheim)

Ice on surface waveguide causes the effective thickness of the dielectric to increase which causes the wave to be more tightly bound. The high fields which result cause heating at the ice-dielectric interface, thus unbinding the ice from the surface.

Figure 3. One possible scheme for using radiation for ice prevention, primarily anti-icing. First-order conceptual scheme employing surface waveguides.

(1)   Only water heated -- low convective losses

(2)   Saves latent heat

$$L_{iw} = 80 \frac{cal}{gm} \qquad L_{wv} = 600 \frac{cal}{gm}$$

(3)   Only draws power when liquid water present
       (i.e., serves as its own detector)

(4)   Aerodynamically clean

(5)   Low maintenance

(6)   High power microwave technology on a strong
       growth trend

Figure 4. Several potential advantages of a microwave anti-icing system.

44

RATIO OF ENERGY REQUIRED
TO HEAT WATER COMPARED T:
THE ENERGY REQUIRED TO HEAT
AND MELT ICE

$L_{i,w}$=334 joules/gm. (80 cal/gm)

C_w=4.19 joules/gm ^oC (1 cal/gm ^oC)

ΔT (^oC)
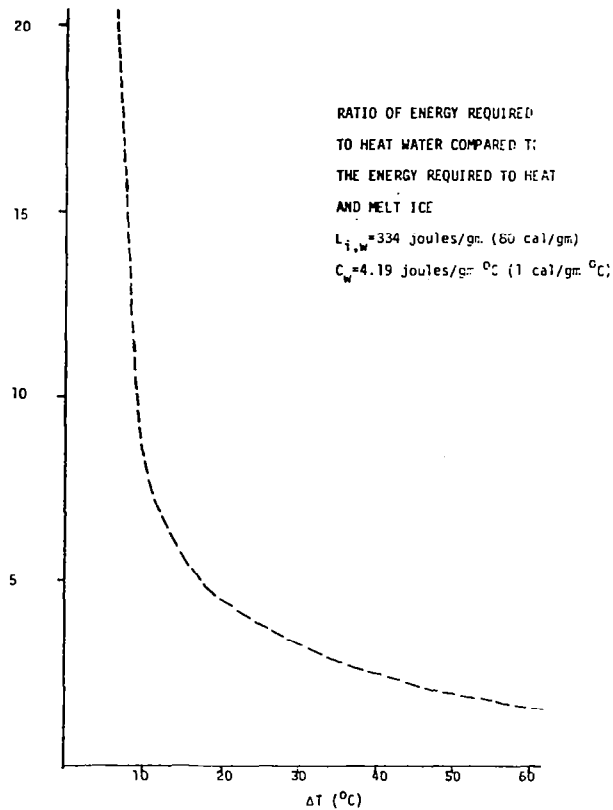
Figure 5. Efficiency improvement gained by avoiding the loss of the latent heat of fusion at the ice-water phase transition (80 ml/gm). Note that a similar but greater effect occurs with the latent heat of evaporation (600 cal/gm).

1. Is there sufficient time to heat the droplets? i.e., what are the absorption properties of the impinging droplets?

2. How well can the RF energy be focussed determines effectively
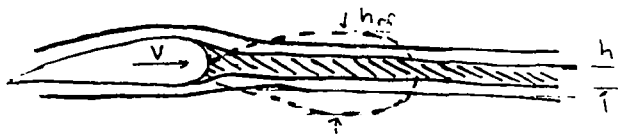
efficiency goes as h_i/h_{rf} implies shorter wavelength desirable

$$h_i \sim 1 \text{ cm}$$

3. Runback refreeze problems

4. Applications problems (i.e., cost, HFI etc)

While all the above are important, the most germaine is #1.

Figure 6. Major questions which must be addressed in order to determine the feasibility and operating frequency of a microwave anti-ice system.
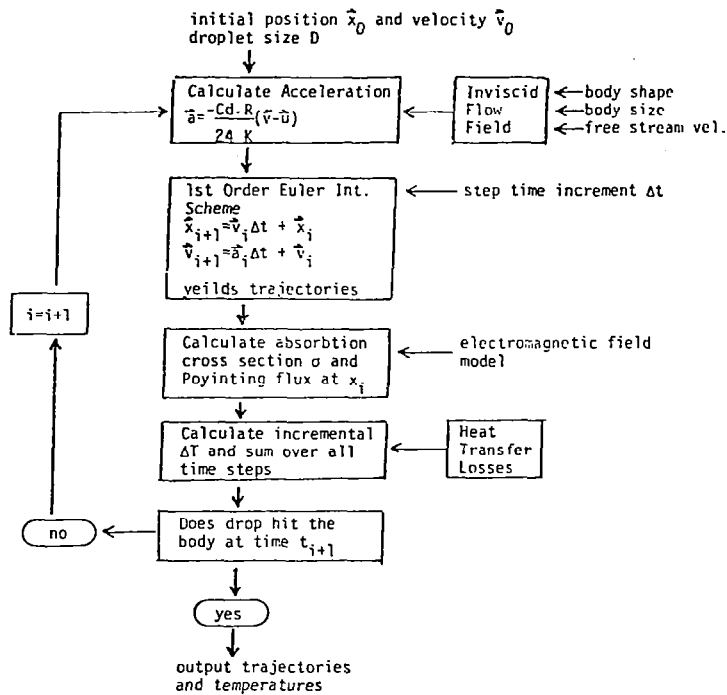
Figure 7. Flow chart for a computer simulation of droplet trajectories and heating. This code has been written to help address the questions of droplet heating time and efficiency. The absorption cross section includes Rayleigh or Mie absorption, with pressure-induced shape effects, polarization, and phase effects included. Equation of motion is from reference 1.
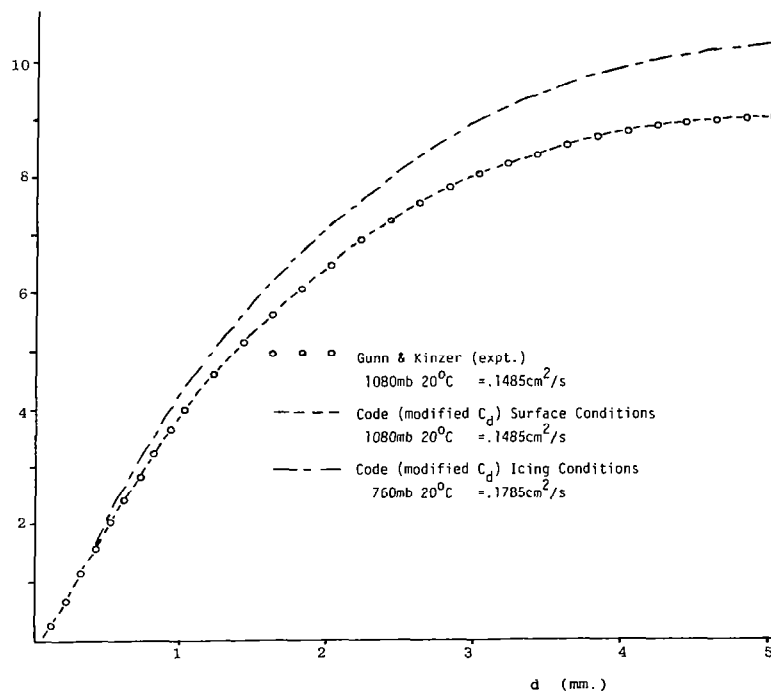
Figure 8. Computer-calculated trajectories are checked by computing the terminal fall velocity of drops (m/sec) versus droplet diameter (mm). With the drag coefficients modified to include droplet flattening the code is in good agreement with established experimental data.
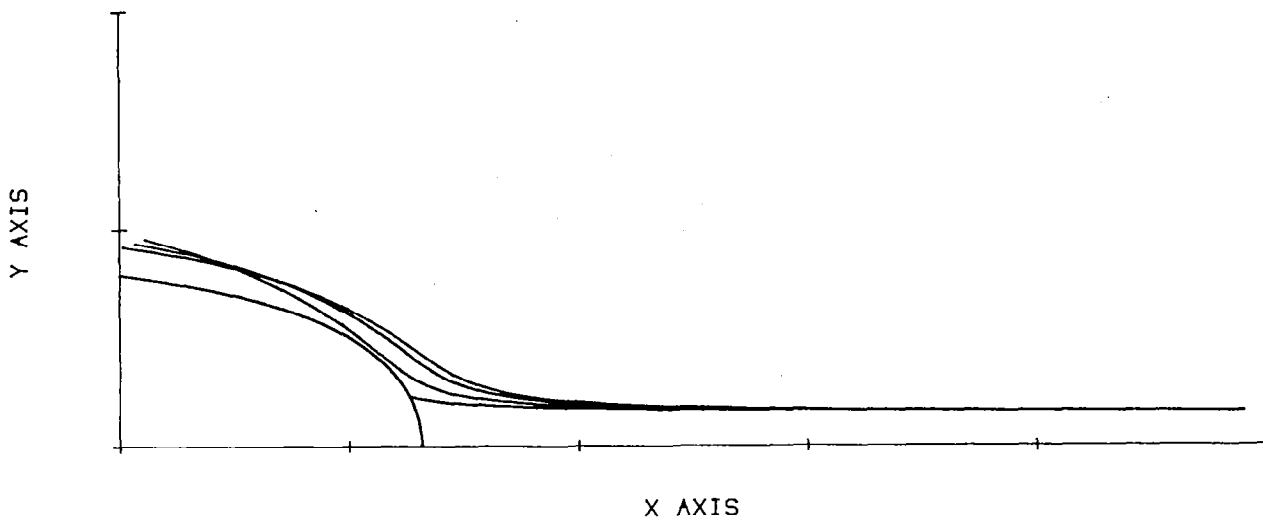
Figure 9.   Droplet trajectories near half body.   Droplets of four
   different sizes, 5, 10, 20, and 40 µm, approach a "half-body"
   airfoil.   The smaller droplets are accelerated around the body
   while the larger droplets impact.   The effect of the increasing
   catch efficiency with droplet size is discussed in figures 10
   and 11.
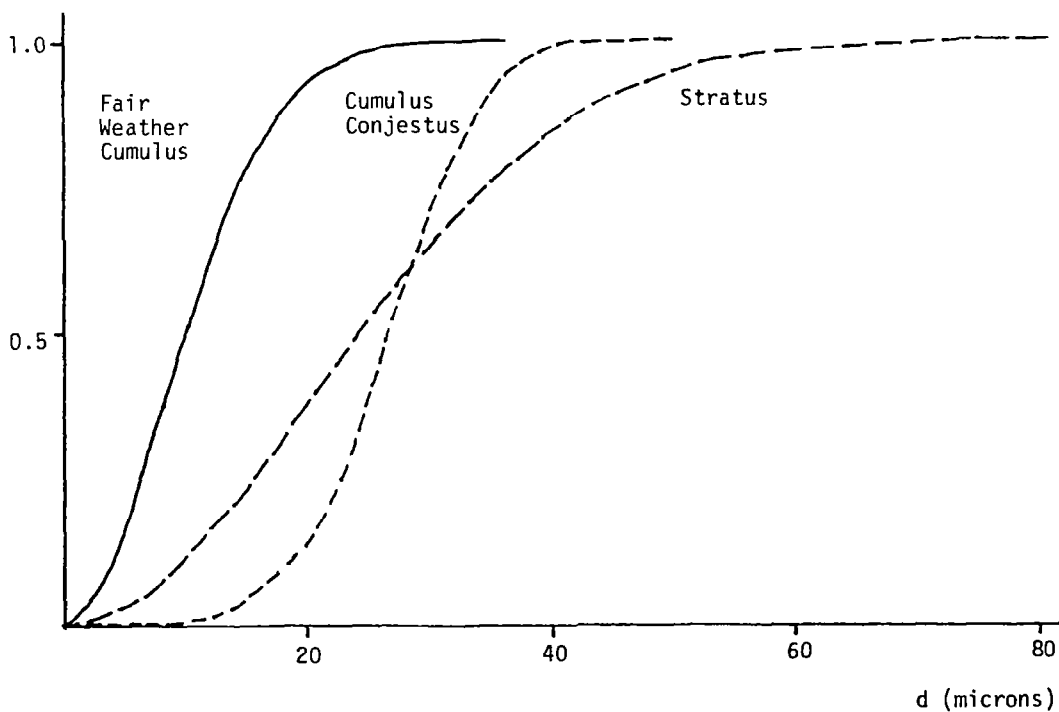
Figure 10.   Fraction of liquid water with diameter smaller than d,
   showing typical droplet size distributions in several different
   types of clouds.

KHRGIAN-MAZAN DISTRIBUTION (Arb. Units)

--- 1. Drop size in cloud average diameter
        20 microns.

--- 2. Impinging mass distribution.

d (microns)
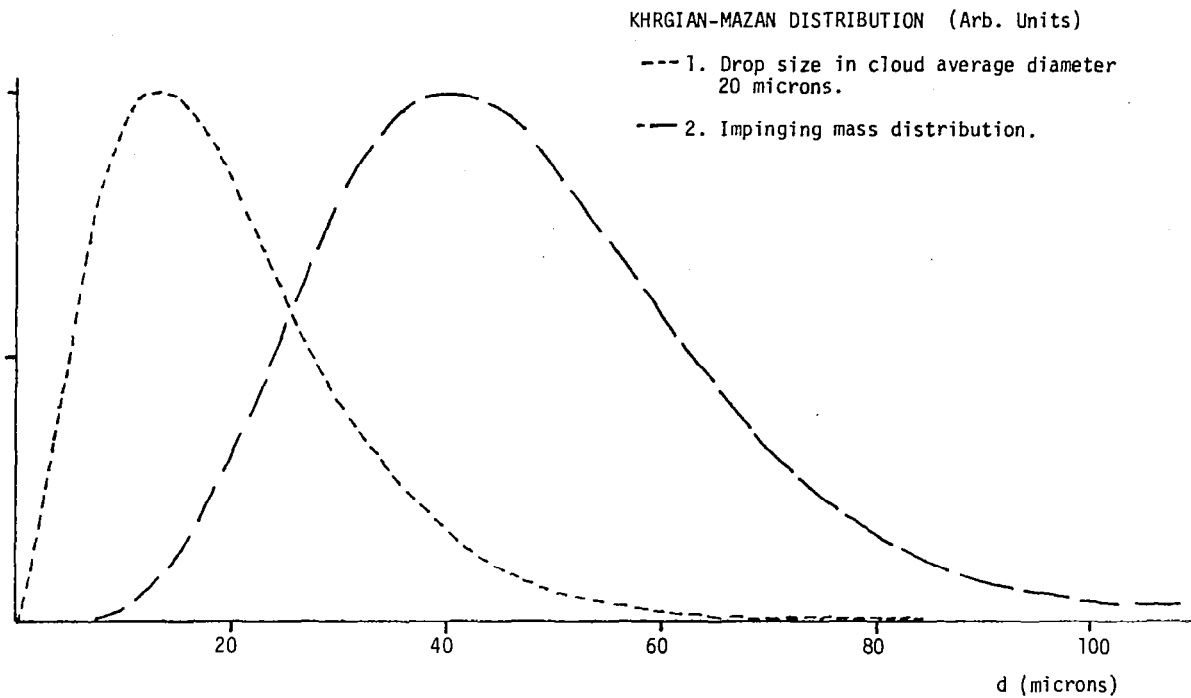
Figure 11. Illustration of the effect of the larger droplets being caught more efficiently by the airfoil. The larger droplets contribute appreciably more to the icing mass than the more prevalent smaller droplets.

Current anti-ice systems evaporate all water

$$L_{WV} = 600 \text{ cal/gm} \qquad C_W = 1 \text{ cal/gm K}$$

Preliminary heat transfer calculations over wet wing show factor of 10 to 20 improvement over evaporative systems

HEAT LOSS FROM WET WING

ambient temp. -20°C

V = 136 mph
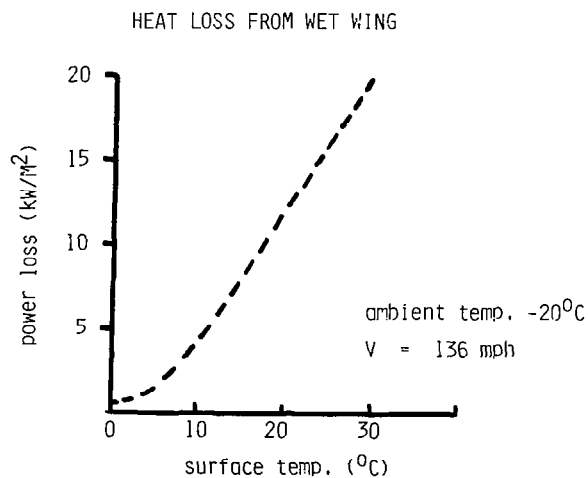
surface temp. (°C)

Figure 12. Some preliminary calculations of heat loss during runback. It is clear that the coolest feasible surface temperature is the most desirable for an electrical system, as opposed to the 20° to 30°C temperatures used in hot air systems.

48
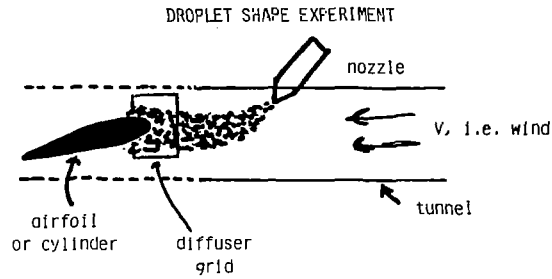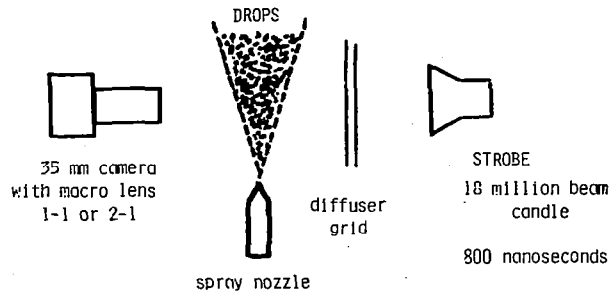
Figure 13. Photographic setup used to attempt to validate the computer simulation of droplet flattening and trajectories.
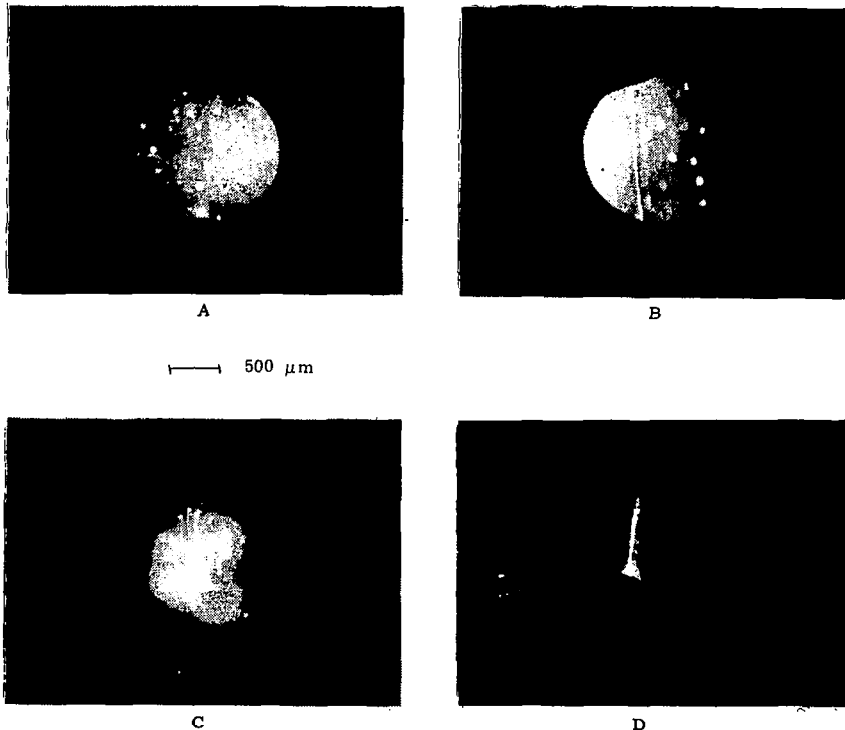
Figure 14. Photographs taken on the stagnation streamline of a 4.4" diameter cylinder with a free-stream velocity of 60 mph.
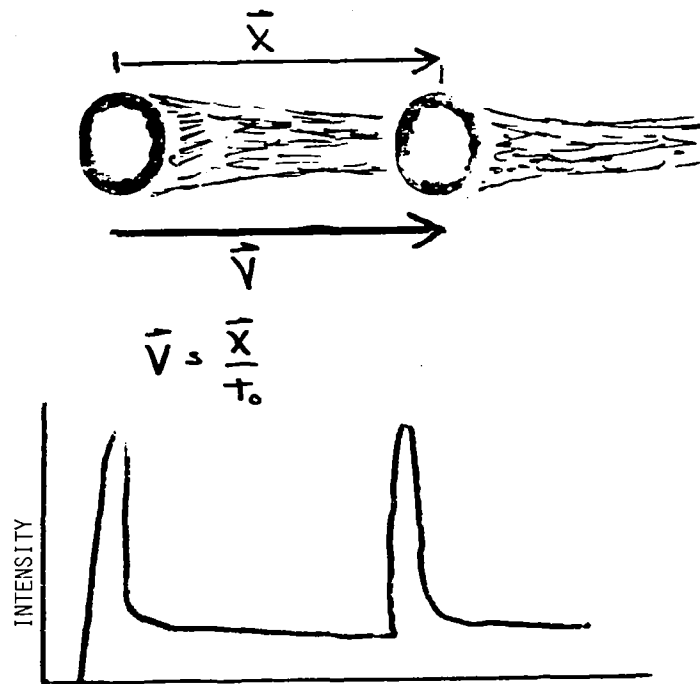
Figure 15. Droplet velocity measurement by double strobe photography.
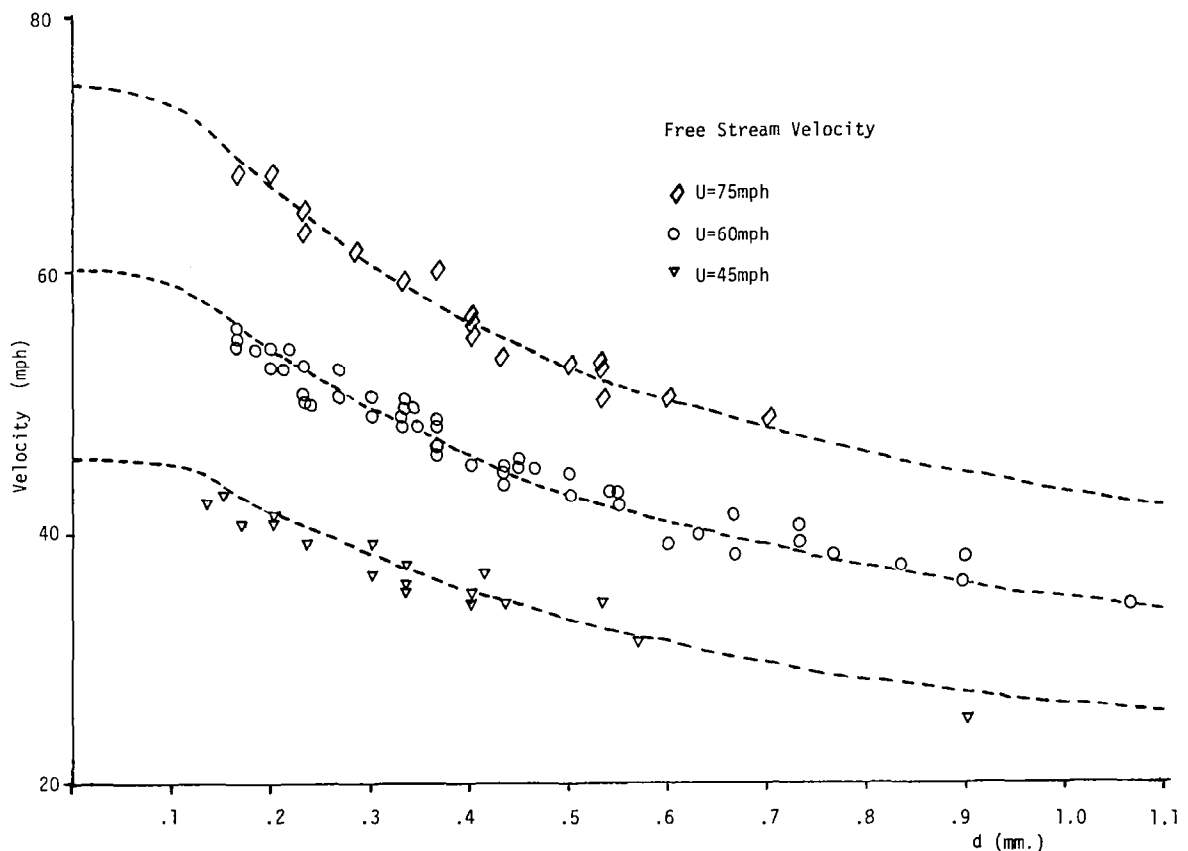
Figure 16. Plot of velocity along tunnel axis (1.25 m downstream of injection site) versus droplet diameter for droplets injected into an unobstructed tunnel. These velocity measurements were made by the technique described previously and are in good agreement with the computer simulation values (dashed lines).
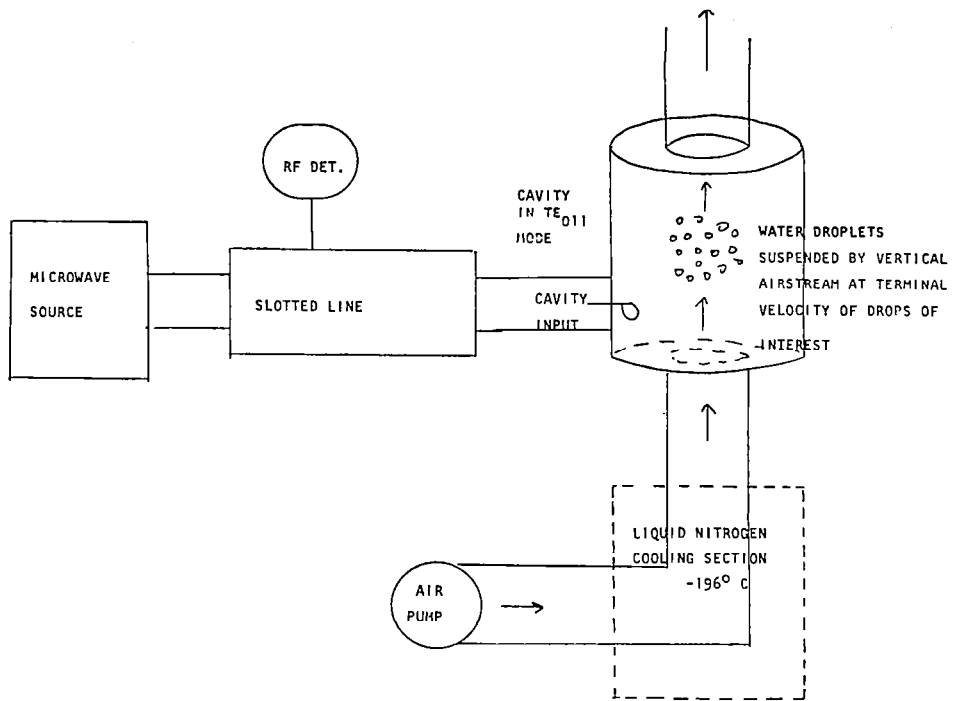
Figure 17. Schematic of phase-change absorption experiment
   being done to quantify absorption of droplets as they
   pass through ice-water phase transition.

Ohio
University

INVESTIGATION OF AIR TRANSPORTATION TECHNOLOGY

AT OHIO UNIVERSITY, 1981

Professor Richard H. McFarland
Avionics Engineering Center
Department of Electrical Engineering
Ohio University
Athens, Ohio 45701

INTRODUCTORY REMARKS

Loran-C has had much of its development motivated by military and marine applications. The increased availability of Loran signals in the United States has encouraged consideration of Loran for airborne applications and has motivated a somewhat similar evaluation and approach as was performed by Ohio University several years ago in this NASA-supported joint university program then using Omega navigation.

The low-frequency band because of its relatively high noise contamination, requires high-quality signal processing to obtain effective signal-to-noise ratios which permit good reliability in position determination consistent with airborne applications. To this end Ohio University has investigated techniques for deriving air-navigation quality information from Loran-C. A part of this objective has been to produce the navigation data in as efficient and cost-effective a manner as possible. Specifically, the volume, weight and power requirements of the equipment are to be compatible with light airplane flown in the general aviation environment.

The Lilley-McCall paper describes the effort which led to a prototype Loran-C receiver which was designed, built and flight tested as a part of this year's work effort. Two undergraduate students, two graduate students and two staff supervisors worked on this project for over a year. The final results have been to produce a receiver which, for demonstrations, operates with a master-dependent, single chain tracking three stations.

The Burhans paper which follows reveals the development of the RF circuitry. During the evolution of this receiver prototype, students in particular have also obtained rich experiences in microprocessor applications, software development, fabrication techniques and final proofing of concepts by measurements of navigation performance in flight on board a Piper Cherokee and a Douglas DC-3.

The use of a navigation receiver during flight leads to consideration of several ancillary aspects of the navigation equipment itself. One consideration is the development of a more intuitively satisfying and useful reference coordinate frame. The hyperbolic geometries inherent in the Loran time-difference system are not easily used by pilots; consequently, a

coordinate conversion is highly desirable. One approach to a coordinate conversion uses an on-board microprocessor for producing the convenient and common polar coordinate geometries available with contemporary VORTAC navigation.

Finally, and with work in progress, the concern is with the human interface. Display of the navigation information in a manner which is consistent with the general aviation cockpit environment and in a form which is convenient and conducive for interpretation by the pilot is the goal. Completion of the display work described by Novacki will mean that the project has been involved with a totality of aspects of the Loran-C airborne equipment ranging from conceptualizing and design to flight testing. Further movement along this line will take place with colleagues at MIT obtaining data on performance and pilot usage of the equipment.

Following also are a bibliography of reports and presentations of reports completed during 1981 on the tasks integral to the Loran airborne receiver developed at Ohio University.

The reports referred to as OU NASA TM-XX in the papers and in the annotated bibliography are the work of Ohio University and should not be confused with the NASA TM series of reports, which are represented by five-digit numbers (NASA TM-XXXXX). Research done at Ohio University under the Joint University Program is supported by NASA and reported in the OU NASA TM-XX series. These reports may be obtained from the University directly.

FIRST TECHNICAL AREA - OMEGA NAVIGATION

DEVELOP TECHNOLOGY TO MAKE OMEGA SUITABLE FOR GENERAL AVIATION

- RF CIRCUIT DESIGN

- SIGNAL PROCESSING

- RECEIVER DESIGN

- FLIGHT EVALUATION

IDENTIFY FUNDAMENTAL PROBLEMS AFFECTING GENERAL AVIATION

- NOISE FACTORS

- GEOMETRIES

- PROPAGATION FACTORS

- ACCURACY REQUIREMENTS

SECOND TECHNICAL AREA - LORAN-C

DEVELOP TECHNOLOGY MAKING LORAN-C APPLICABLE TO GENERAL AVIATION

- RF CIRCUITS

- AGC

- ENVELOPE DETECTION

- PROTOTYPE RECEIVER

INVESTIGATIONS OF NOISE EFFECTS
        PHASE-LOCK TRACKING LOOPS

APPLICATIONS OF MICROPROCESSOR TECHNIQUES TO LORAN-C

COORDINATE CONVERSIONS

DISPLAY INTERFACE

BENEFITS

TECHNOLOGY PRODUCT - 82 TECHNICAL MEMORANDUMS

STUDENT PRODUCT - OVER 31 GRADUATES
   (BSEE, MS AND PHD LEVELS)

STUDENT IMPROVEMENT IN THE LAB AND CLASSROOM

INDUSTRY BENEFITS - TECHNICAL INFORMATION PROVIDED TO MORE THAN
   100 CONTACTS. EXAMPLES ITT, LITTON, TELEDYNE,
   MAGNAVOX, ROCKWELL

ANNOTATED BIBLIOGRAPHY

OU NASA TM Number

1   SIMULTANEOUS PAIR OMEGA RECEIVER
           Ralph W. Burhans, August 4, 1972.

           A new concept of OMEGA receiver operation is presented. The
           simultaneous comparison of 13.6 and 10.2 KHz in a single time
           slot results in 3.4 KHz, 10.2 KHz, and phantom 40.8 KHz dif-
           ference pair lanes. Direct lane count without intermediate
           storage or sequential feedback loops is possible. Small boat
           receivers using low cost recorders such as a Rustrak might be
           possible at $300 market prices. Completely digital readout
           devices for general aviation use could become $500 instru-
           ments. Even with restricted lane pair use this could provide
           low cost navigation aids for over half of the U.S.A. and all
           of the coastal areas including most of the Great Lakes.

2   SIMPLE BAND PASS FILTERS
           Ralph W. Burhans, December 28, 1972.

           A single power source operational amplifier provides tunable-
           high Q band pass resonators of possible utility for OMEGA VLF
           receiver input processors and other audio frequency applica-
           tions.

3   LOW BIT SINE WAVE APPROXIMATIONS FOR AUDIO SIGNAL SOURCES
           Ralph W. Burhans, January 1973.

           Special purpose sine wave sources are easily obtained using
           digital counting-decoder-filter methods with second harmonic
           distortion less than 1%. Good frequency stability and reason-
           able variety in choice of output frequency result when the
           input clock signal is derived from a crystal oscillator
           through programmable divider chains. The resulting sine wave
           output would be suitable for applications such as the 90 and
           150 Hz modulation frequencies of ILS transmitters, as well as
           other limited range audio frequency use.

4   SIMPLIFIED OMEGA RECEIVERS
           Ralph W. Burhans, March 1974.

           Circuit details are presented for a low cost OMEGA receiver
           being developed for general aviation use. Some novel pro-
           cessing methods, not used in commercial systems, have been
           demonstrated in experimental bench processors. An airborne
           model is being designed.

5   BINARY PHASE LOCK LOOPS FOR SIMPLIFIED OMEGA RECEIVERS
           Ralph W. Burhans, March 1974.

           A sample binary phase lock loop is proposed for periodically
           correcting OMEGA receiver internal clocks. The circuit is
           particularly simple to implement and provides a means of
           generating long range 3.4 KHz difference frequency lanes from
           simultaneous pair measurements.

6   PHASE LOCK LOOP SYNTHESIZER FOR OMEGA REFERENCE FREQUENCIES
Kent A. Chamberlin, April 1974.

An OMEGA reference frequency of 4080 KHz is provided by a
single loop VCXO circuit driven from an atomic clock or stable
crystal standard. The circuit is used to provide OMEGA
frequencies for direct ranging, differential correction moni-
toring, or as a laboratory source for calibrating OMEGA
receivers.

7   SIMULTANEOUS MASTER-SLAVE OMEGA PAIRS
Ralph W. Burhans, April 1974.

Master-Slave sequence ordering of the OMEGA system is
suggested as a method of improving the pair geometry for low
cost receiver user benefit. The sequence change will not
affect present sophisticated processor users other than to
require new labels for some pair combinations, but may require
worldwide transmitter operators to slightly alter their long
range synchronizing techniques.

8   SELECTED BIBLIOGRAPHY OF OMEGA, VLF AND LF TECHNIQUES APPLIED
TO AIRCRAFT NAVIGATION SYSTEMS
NASA Project Staff, August 1974.

A bibliography of references collected during the first three
years of the NASA Tri-University Program in Air Transportation
Systems.

9   LOW-COST OMEGA NAVIGATION RECEIVER
Robert W. Lilley, October 1974.

The status of Ohio University's efforts towards specifying a
low-cost Omega receiver is reviewed at the onset of the
fourth-year program under the NASA Tri-University Program in
Air Transportation Systems.

10   BINARY PROCESSING CONCEPTS FOR OMEGA RECEIVERS
Robert W. Lilley, November 1974.

Preprint of paper presented at the Second Omega Symposium,
sponsored by the Institute of Navigation, Washington, D.C.,
November 7, 1974.

11   THE MEMORY-AIDED DIGITAL PHASE-LOCKED LOOP
Kent A. Chamberlin, November 1974.

Preprint of paper presented at the Second Omega Symposium,
sponsored by the Institute of Navigation, Washington, D.C.,
November 7, 1974.

12   OMEGA FLIGHT-TEST DATA REDUCTION SEQUENCE
Robert W. Lilley, November 1974.

A series of FORTRAN computer programs for preparation and summary of flight-test data obtained from the Ohio University Omega Receiver.

13   FLIGHT EVALUATION: OHIO UNIVERSITY OMEGA RECEIVER BASE
Kent A. Chamberlin, R. W. Lilley, and Richard J. Salter, November 1974.

A description is given of the data-collection flight, round-trip from Athens, Ohio to Langley Field, Virginia, during which Omega data was collected on machine-readable media for use in the Tri-University Program in Air Transportation.

14   COMPUTER PROGRAM CORDET
R. A. Palkovic, November 1974.

A simulation tool is described for use in the design and analysis of digital phase-locked loops, with specific application to the DPLL in the Ohio University Omega receiver base.

15   A SIMULATION ANALYSIS OF PHASE PROCESSING CIRCUITRY IN THE OHIO UNIVERSITY OMEGA RECEIVER PROTOTYPE (Master's Thesis)
R. A. Palkovic, June 1975 (CR-132707).

A first-order digital phase-lock loop is modeled on the computer. Loop response to signal phase in noise is evaluated. Optimum integration time is determined. Phase jitter in a frequency synthesizer used as the local oscillator is quantified, and design is optimized. Design rules for use of synchronous rate multipliers are presented. Overall system response is discussed.

16   GANGED SERIES POTENTIOMETER MIXER NETWORKS
Ralph W. Burhans, December 1974.

A ganged potentiometer with a single linear section and two opposite log tapered sections is rediscovered for providing a simple series resistor control element for mixing of audio frequency signals. An application is for bench evaluation of detector signal-to-noise ratios with Omega receivers.

17   COMMON ANTENNA PREAMPLIFIER-ISOLATOR FOR VLF-LF RECEIVERS
Ralph W. Burhans, July 1975.

An improved high impedance preamplifier circuit provides outputs to drive an Omega-VLF receiver and an ADF-LF receiver from a common antenna such as the ADF sense antenna on general aviation aircraft. The preamplifier has been evaluated with fixed ground station receivers and is anticipated for use in the second generation prototype Ohio University Omega receiver design.

18   LOW COST, HIGH-PERFORMANCE, VLF RECEIVER FRONT-END
Ralph W. Burhans, September 1975.

A VLF receiver front-end has been designed using standard
linear integrated circuits. The basic methods have been
evaluated extensively on the Omega 10.2 KHz channel but are
readily adaptable to any other VLF frequency in the 10.2 KHz
to 20 KHz region. Applications for the modules exist in
position location, time-frequency measurements, and signal
propagation. The set provides control gates, zero crossing
signals, and analog outputs to interface with any type of
digital logic, microprocessor, or analog signal processor.

19   DIGITAL CORRELATION DETECTOR FOR LOW-COST OMEGA NAVIGATION
Kent A. Chamberlin, February 1976 (CR-144956) (Master's Thesis)

This report describes the background information on the
research that led to the development of the memory-aided
phase-locked loop (MAPLL) which is an all-digital correlation
device that is capable of determining the phase of extremely
noisy fixed-frequency signals. This design is of special
interest for Omega or other phase sensitive VLF navigation
purposes since it is relatively inexpensive, maintenance-free,
and can operate in a time-multiplexed fashion.

20   THE MINI-O, A DIGITAL SUPERHET, OR A TRULY LOW-COST OMEGA
NAVIGATION RECEIVER
Ralph W. Burhans, November 1975. (CR-144923)

A quartz tuning fork filter circuit and some unique CMOS clock
logic methods provide a very simple OMEGA-VLF receiver with
true hyperbolic station pair phase difference outputs. An
experimental system has been implemented on a single battery-
operated circuit board requiring only an external antenna
preamplifier and LOP output recorder. A bench evaluation and
preliminary navigation tests indicate the technique is viable
and can provide very low-cost OMEGA measurement systems. The
method is promising for marine use with small boats in the
present form, but might be implemented in conjunction with
digital microprocessors for airborne navigation aids.

21   FLIGHT TEST OF 4-HZ AND 30-HZ OMEGA RECEIVER FRONT-END
Lee Wright, February 1976.

A test flight in DC-3 aircraft was conducted to evaluate the
performance of a 4-Hz ultra-narrowband, Omega receiver front-
end compared to a more conventional 30-Hz bandwidth receiver.
Results indicate that the 4-Hz front-end has superior signal-
to-noise performance. Other interesting results obtained
during the test flight were recordings of the sunset noise
effects on amplitude, and the attenuation of signal levels
when flying through clouds.

22   POSSIBLE METHODS FOR USSR-VLF NAVIGATION RECEIVERS
         Ralph W. Burhans, March 1976.

         A brief study of the USSR-VLF navigation system indicates that
         very low-cost digital techniques might be applied to receiver
         systems. The transmitted signal format is of interest for
         application to other VLF systems in the future. Some possible
         circuits for simplified receiver processors are presented.

23   A PROPOSED MICROCOMPUTER IMPLEMENTATION OF AN OMEGA NAVIGATION
         PROCESSOR
         John D. Abel, March 1976.

         Documentation of current status of research pertaining to a
         microprocessor-based Omega navigation processor to be used in
         conjunction with the Ohio University Avionics Engineering
         Center Omega sensor processor is presented.

24   IMPROVEMENTS FOR OMEGA RF PREAMPLIFIERS
         Lee Wright, April 1976

         An Omega preamplifier with no phase shift over the ADF band
         but with bandpass filtering and gain at the Omega-VLF band has
         been designed, built, and tested. This is expected to be use-
         ful principally in planned work at MIT and Princeton involving
         the use of the Ohio University Omega Sensor Processor
         Receiver.

25   NARROW BAND BINARY PHASE LOCKED LOOPS
         Ralph W. Burhans, April 1976.

         Very high Q digital filtering circuits for audio frequencies
         in the range of 1 Hz to 15 KHz are implemented in simple CMOS
         hardware using a binary local reference clock frequency. The
         circuits have application to VLF navigation receivers and
         other narrow band audio range tracking problems.

26   SIMULATION ANALYSIS OF A MICROCOMPUTER-BASED LOW-COST OMEGA
         NAVIGATION SYSTEM
         Robert W. Lilley and Richard J. Salter, Jr., May 1976.

         Preprint of paper presented at the Bicentennial National
         Symposium of the Institute of Navigation, Warminster,
         Pennsylvania, April 28, 1976.

27   AUTOMATIC NOISE LIMITER-BLANKER
         Ralph. W. Burhans, May 1976.

         Modifications of an audio noise limiter circuit, used in WW II
         era radio communications receivers, provides a noise limiter-
         blanker for narrow bandwidth low-level audio signals. The
         method has been evaluated for noise blanking with OMEGA-VLF
         navigation receivers but is adaptable to more general audio
         frequency processing systems.

28   SMALL AIRCRAFT FLIGHT EVALUATION OF RUSTRAK CHART RECORDER
Richard J. Salter, Jr. and Robert W. Lilley, May 1976.

In support of the NASA Omega Prototype Receiver project, three
short flight evaluations of the RUSTRAK chart recorder were
flown.

29   DIGITAL TIME SLOT DISPLAY FOR OMEGA RECEIVER
Ralph E. Smith, July 1976.

Variations of circuits to display the Omega sequence letters
A through H have been designed, breadboarded, and tested.
One of these is suggested as an alternative station display
method for the Ohio University Omega sensor processor systems.

30   LOW-COST MECHANICAL FILTERS FOR OMEGA RECEIVERS
R. W. Burhans, June 1976.

A set of mechanical filter assemblies has been obtained for
possible use in the RF front-end of an OMEGA navigation
receiver. The resonators provide very narrow bandwidth per-
formance with good skirt selectivity in a simple two-stage
circuit. It is recommended that these filters be used in a
complete receiver system for long-term evaluation on reception
of low-level OMEGA signals.

31   A MEMORY-MAPPED OUTPUT INTERFACE: OMEGA NAVIGATION OUTPUT
DATA FROM THE JOLT (TM) MICROCOMPUTER
R. W. Lilley, August 1976.

A hardware interface which allows both digital and analog data
output from the JOLT microcomputer is described in context with
the Ohio University software-based Omega Navigation Receiver.

32   A MICROPROCESSOR INTERFACE FOR THE OHIO UNIVERSITY PROTOTYPE
OMEGA NAVIGATION RECEIVER
R. W. Lilley, August 1976.

A hardware interface is described which allows a microcomputer
to obtain data and interrupt signals from the Ohio University
Omega Receiver Prototype.

33   TEST PROGRAM FOR 4-K MEMORY CARD, JOLT MICROPROCESSOR
R. W. Lilley, August 1976.

A memory test program is described for use with the JOLT
micro-computer memory board used in development of the Ohio
University Omega navigation receiver.

34   A MICROCOMPUTER-BASED LOW-COST OMEGA NAVIGATION SYSTEM
R. W. Lilley and R. J. Salter, Jr., August 1976.

Preprint of paper presented at the First Annual Meeting,
International Omega Association, Arlington, Virginia,
July 27-29, 1976

35   MINI-O, SIMPLE OMEGA RECEIVER HARDWARE FOR USER EDUCATION
            R. W. Burhans, August 1976.

            Preprint of paper presented at the First Annual Meeting,
            International Omega Association, Arlington, Virginia,
            July 27-29, 1976.

36   OPERATING INSTRUCTIONS: KENNEDY TEST FIXTURE
            Donald P. Seyler, September 1976.

            A unit for testing the integrity of data and control circuits
            of the Kennedy 1600/360 Incremental Tape Recorders is
            described.

37   OPERATING INSTRUCTIONS: MEMODYNE/KENNEDY INTERFACE UNIT
            Donald P. Seyler, January 1977.

            A unit for transcribing incremental data from magnetic
            cassette tapes to magnetic reel-to-reel tapes is described.
            This includes integral testing for validity of data.

38   KIM-1 INTERFACE ADAPTER TO 3-WIRE TELETYPE SYSTEMS
            R. W. Burhans, August 1976.

            This brief technical note has been submitted to the KIM-1
            microcomputer group publication, KIM User Notes. It is of
            interest to others who have 3-wire ASR-33 teletype systems in
            using microcomputer hardware with the Ohio University
            Prototype Omega Sensor Receivers.

39   OMEGA DISTRIBUTION AMPLIFIER WITH FOUR CHANNEL INDEPENDENT
            LEVEL CONTROL
            Donald P. Seyler, September 1976.

            A portable unit for distributing a single small signal source
            to a maximum of four loads, with independent source level
            control for each load, is described.

40   MEASURING CLOCK OFFSETS FOR MINI-O WITH KIM-1
            R. W. Burhans, September 1976.

            The previous MINI-O Omega receiver system required adjustment
            of the local clock to a low offset for proper operation.
            Single station tracking loop software provides an easy way of
            determining the offset prior to experimental navigation tests.
            A second order software tracking loop is suggested to elimi-
            nate the local clock error problem.

41-Mod 1   IMPROVED ANALOG OUTPUT CIRCUITS FOR OHIO UNIVERSITY PROTOTYPE
            OMEGA NAVIGATION RECEIVERS
            Lee Wright, October 1976.

            A minor hardware change is described which provides a more
            accurate analog output from the Ohio University Omega Prototype
            Receivers.

42   DIURNAL MEASUREMENTS WITH PROTOTYPE CMOS OMEGA RECEIVERS
            R. W. Burhans, November 1976.

            The Ohio University Prototype CMOS Omega Sensor Processor is
            capable of receiving all eight Omega channels on 10.2 KHz.
            Diurnal recordings of selected station pairs made during the
            period October-November 1976 demonstrate the receiver perfor-
            mance and illustrate limitations for navigation using diurnal
            corrections.

43   DEMONSTRATION PROGRAM FOR OMEGA RECEIVER PROTOTYPE MICRO-
            COMPUTER DATA PROCESSING
            R. W. Lilley, November 1976.

            Using the prototype Omega receiver developed for the NASA
            Joint University Program plus a digital interface to a
            commercial microcomputer, a software routine to demonstrate
            receiver operation is described.

44   AN ASSEMBLER FOR THE MOS TECHNOLOGY 6502 MICROPROCESSOR AS
            IMPLEMENTED IN JOLT (TM) AND KIM-1 (TM)
            Robert W. Lilley, November 1976.

            The 6502 Assembler implemented at Ohio University for support
            of microprocessor program development in the Tri-University
            Program is described.

45   INTERACTIVE OMEGA PROPAGATION CORRECTIONS
            Robert W. Lilley, January 1977.

            An implementation of Coast Guard computer programs for Omega
            propagation corrections is described.

46   ANALYSIS OF A FIRST ORDER PHASE LOCKED LOOP IN THE PRESENCE OF
            GAUSSIAN NOISE
            Paul R. Blasche, March 1977.

            A first-order digital phase-locked loop is analyzed by appli-
            cation of a Markov chain model. Steady-state loop error pro-
            abilities, phase standard deviation and mean loop transient
            times are determined for various input signal-to-noise ratios.
            In addition, results for direct loop simulation are presented
            for comparison.

47   A MICROCOMPUTER-BASED LOW-COST OMEGA SENSOR PROCESSOR
            Richard J. Salter, Jr., February 1977, Master's Thesis.

48   MINI-L LORAN-C RECEIVER
            R. W. Burhans, March 1977.

            A low-cost prototype Loran-C receiver front-end has been
            designed and bench-tested. This receiver concept provides
            outputs to interface with a microcomputer system. The devel-
            opment of sensor and navigation software for use with the Mini-
            L system is underway.

49   SIMULATION OF DIGITAL PHASE-LOCKED LOOPS
Paul R. Blasche, April 1977.

This technical memorandum deals with development of simulation equations for first- and second-order digital phase-locked loops. In addition, examples of loop simulation are given to determine loop performance with respect to several loop parameters.

50   A KEYBOARD INTERFACE FOR THE JOLT MICROPROCESSOR
Lee Wright, May 1977.

The Ohio University Microprocessor Navigation Receiver Base utilizes the JOLT(TM) microcomputer. This keyboard interface is designed to allow data input without use of a teleprinter.

51   A FOUR DIGIT MEMORY-MAPPED DISPLAY
Ralph E. Smith, May 1977.

An interface board has been fabricated for the Ohio University Microcomputer-Based Navigation Receiver to display data from the microprocessor.

52   INTERACTIVE LORAN-C-TO-GEOGRAPHIC AND GEOGRAPHIC-TO-LORAN-C COMPUTATION
Lynn M. Piecuch and Robert W. Lilley, August 1977.

An implementation of Naval Oceanographic Office computer software for Loran-C is presented.

53   CIRCUIT METHODS FOR VLF ANTENNA COUPLERS
R. W. Burhans, September 1977.

A summary of E-field antenna preamplifiers developed during the course of the NASA Tri-University Program studies on VLF methods for general aviation is presented. The circuit techniques provide useful alternative methods for Loran-Omega receiver system designers.

54   LORAN-C DIGITAL WORD GENERATOR FOR USE WITH A KIM-1 MICRO-PROCESSOR SYSTEM
James D. Nickum, December 1977.

The digital word generator used with Mini-L front end to develop a Loran sensor processor at Ohio University is described.

55   MICROPROCESSOR-TO-SYSTEM/370 INTERFACE
Robert W. Lilley, February 1978.

A hardware interface is described which allows direct memory load of a microprocessor from the host System/370 computer, eliminating paper tape handling.

56   STAND-ALONE DEVELOPMENT SYSTEM USING A KIM-1 MICROCOMPUTER
        MODULE
        James Nickum, March 1978.

        Documentation of the stand-alone microprocessor development
        system used in the navigation sensor processor research at
        Ohio University is described.

57   A LOW-COST LORAN-C ENVELOPE PROCESSOR (The Mini-L Loran-C
        Receiver)
        R. W. Burhans, April 1978.

        A reprint of published article on the Mini-L Loran-C receiver
        front-end is presented. Complete circuit details are given
        with a basic introduction to Loran-C navigation and time-
        frequency standard uses. The Mini-L concept is of particular
        interest to the low-budget experimenter as an RF signal inter-
        face for more sophisticated end use.

58   A VIDEO DISPLAY INTERFACE FOR THE LORAN-C NAVIGATION RECEIVER
        DEVELOPMENT SYSTEM
        Joseph P. Fischer and Robert W. Lilley, May 1978.

        A character-mode video unit is described which allows micro-
        processor-controlled display of program and navigation data
        with a small investment in logic.

59   COMPUTING LORAN TIME DIFFERENCES WITH AN HP-25 HAND
        CALCULATOR
        Edwin D. Jones, August 1978.

        Accurate Loran-C time differences can be calculated from
        known transmitter and receiver positions using the program
        described.

60   PHASE-LOCKED TRACKING LOOPS FOR LORAN-C
        R. W. Burhans, August 1978.

        Two, portable, battery-operated Loran-C receivers have been
        fabricated to evaluate simple envelope detector methods with
        hybrid analog-digital phase-locked loop sensor processors.
        The receivers are being used to evaluate Loran-C in general
        aviation applications. Complete circuit details are given
        for the experimental sensor and readout system.

61   LORAN-C FLIGHT TEST SOFTWARE
        James D. Nickum, August 1978.

        Described is the software package developed for the KIM-1
        Micro-System and the Mini-L PLL receiver to simplify taking
        flight test data at Ohio University.

62   PREAMPLIFIER NOISE IN VLF RECEIVERS
          R. W. Burhans, September 1978.

          Rapid methods of estimating antenna preamplifier noise contri-
          bution to receiver performance are presented for JFET or CMOS
          transistors. An improved CMOS preamplifier circuit is
          suggested.

63   LORAN-C TIME DIFFERENCE CALCULATIONS
          Joseph P. Fischer, October 1978.

          A simplified approach to calculate Loran-C time differences
          from a given geographic location is presented.

64   INITIAL FLIGHT TEST OF A LORAN-C RECEIVER/DATA COLLECTION
          SYSTEM
          Joseph P. Fischer and James D. Nickum, November 1978.

          Described are the flight test results of a Loran-C navigation
          receiver/data collection system designed at Ohio University.

65   ACTIVE ANTENNA FOR THE VLF TO HF OBSERVER
          R. W. Burhans, February 1979.

          This report is a prepublication manuscript submitted to one of
          the contemporary electronics magazines as part of a series on
          VLF-LF signal reception problems. The report presents a sim-
          ple and low-cost method of fabricating an active antenna pre-
          amplifier system covering the range of 10 KHz to 10 MHz, for
          use with tunable communications receivers. The same type of
          preamplifier system can be used with airborne VLF navigation
          receivers.

66   ANALYSIS AND DESIGN OF A SECOND-ORDER DIGITAL PHASE-LOCKED
          LOOP
          Paul R. Blasche, March 1979.

          A second-order digital phase-locked loop is analyzed by
          application of a Markov chain model with alternatives.
          Steady-state loop error statistics and mean transient time
          are determined for various loop parameters. In addition, a
          hardware digital phase-locked loop was constructed and tested
          to demonstrate the applicability of the Markov chain mode.

67   LORAN-C FLIGHT DATA BASE
          Robert W. Lilley, February 1979.

          A large file of Loran-C data to be used in receiver design
          and testing is documented.

68   RESULTS OF THE SECOND FLIGHT TEST OF THE LORAN-C RECEIVER/
          DATA COLLECTION SYSTEM
          Joseph P. Fischer, March 1979.

          Reported are the results of a second flight test of the

Loran-C system under development at Ohio University using a
variation of the techniques used for the first flight test.

69   DIGITAL PHASE-LOCKED LOOP DEVELOPMENT AND APPLICATION TO
        LORAN-C
        Daryl L. McCall, September 1979.

        A digital phase-locked loop has been developed and implemented
        for use in a low-cost Loran-C receiver. This paper documents
        the DPLL design and application to Loran-C.

70   ACTIVE ANTENNA COUPLER FOR VLF
        R. W. Burhans, November 1979.

        A reprint of a paper published in the "Ham Radio Magazine",
        Volume 12, Number 10, October 1979, is presented. The circuit
        designs are applicable to a variety of VLF-HF active antenna
        receiving systems including Omega and Loran-C for airborne and
        marine users.

71   EXPERIMENTAL LOOP ANTENNAS FOR 60 KHz to 200 KHz
        R. W. Burhans, December 1979.

        A series of loop antennas have been fabricated and evaluated
        for possible use with Loran-C and other VLF to LF band
        receivers. A companion low noise and very high gain pream-
        plifier circuit has been devised to operate the loop antennas
        remote from the receiver. Further work is suggested on the
        multiple loop antenna systems to provide omni-directional
        coverage and reduce E-field noise pickup in navigation or
        communications systems.

72   DATA REDUCTION SOFTWARE FOR LORAN-C FLIGHT TEST EVALUATION
        Joseph P. Fischer, December 1979.

        This paper describes a set of programs written for use on
        Ohio University's 370 computer for reducing and analyzing
        flight test data.

73   LORAN DIGITAL PHASE-LOCKED LOOP AND RF FRONT-END SYSTEM ERROR
        ANALYSIS
        Daryl L. McCall, December 1979.

        Various experiments have been performed to determine the
        system error of the DPLLs and RF front-end currently being
        used in a Loran receiver prototype. This paper documents
        those experiments and their results.

74   RESULTS OF A LORAN-C FLIGHT TEST USING AN ABSOLUTE DATA
        REFERENCE
        Joseph P. Fischer, January 1980.

        The results of a flight test using the Loran-C receiver and
        data collection system developed at Ohio University are
        described in this paper. An absolute data reference was

provided by the Lincoln Laboratories DABS (Discrete Address
Beacon System) facility.

75   ANALYSIS OF FIRST AND SECOND ORDER BINARY QUANTIZED DIGITAL
      PHASE-LOCKED LOOPS FOR IDEAL AND WHITE GAUSSIAN NOISE INPUTS
      Paul R. Blasche, March 1980. (Dissertation)

      Specific configurations of first and second order all digital
      phase-locked loops are analyzed for both ideal and additive
      white gaussian noise inputs. In addition, a design for a
      hardware digital phase-locked loop capable of either first
      or second order operation is presented along with appropriate
      experimental data obtained from testing of the hardware loop.
      All parameters chosen for the analysis and the design of the
      digital phase-locked loop are consistent with an application
      to an Omega navigation receiver although neither the analysis
      nor the design is limited to this application.

76   DC-TO-DC POWER SUPPLY FOR LIGHT AIRCRAFT FLIGHT TESTING
      Stephen R. Yost, December 1980.

      A DC-to-DC power supply has been designed and fabricated to
      operate the prototype Loran-C receiver and data collection
      system currently in use at Ohio University. The supply is
      designed to operate from an aircraft electrical system.

77   BI-DIRECTIONAL COMMUNICATION INTERFACE FOR MICROPROCESSOR-TO-
      SYSTEM/370
      Joseph P. Fischer, January 1981.

      Described is a hardware and software interface to allow two-
      way communication between a microprocessor system and the IBM
      System/370.

78   LORAN-C PLOTTING PROGRAM FOR PLOTTING LINES OF POSITION ON
      STANDARD CHARTS
      James P. Roman, February 1981.

      The Loran-C plotting program was designed to plot Loran-C
      lines of position on any standard chart and is used in the
      data-collection system currently in use at Ohio University
      Avionics Engineering Center.

79   AUTOMATIC GAIN CONTROL
      James P. Roman, March 1981.

      An automatic gain control has been designed and fabricated to
      operate with the Loran-C prototype receiver and data-
      collection system currently in use at Ohio University.

80   A LORAN-C PROTOTYPE NAVIGATION RECEIVER FOR GENERAL AVIATION
      Robert W. Lilley and Daryl L. McCall, August 1981.

      The design, fabrication and evaluation of a prototype Loran-C
      receiver is described. Hardware is complete and microcom-
      puter programming continues for addition of area-navigation

capability. The receiver is an envelope-processor, offering simplicity of RF processor circuitry.

81   COMMUTATED AUTOMATIC GAIN CONTROL SYSTEM
      Stephen R. Yost, November 1981

      A commutated AGC system for the Ohio University prototype
      Loran-C receiver is described. The circuit design, fabrication, and test results are presented in this paper.

82   A PROTOTYPE INTERFACE UNIT FOR MICROPROCESSOR-BASED NAVIGATION
      SYSTEM
      Stanley M. Novacki III, November 1981

      A command entry and display device designed to allow convenient operation of the Loran-C receiver-processor is described.

TECHNICAL MEMORANDUM OU NASA 77

BI-DIRECTIONAL COMMUNICATION INTERFACE

FOR MICROPROCESSOR-TO-SYSTEM/370

Described is a hardware and software interface
to allow two-way communication between a
microprocessor system and the IBM System/370

Joseph P. Fischer

Avionics Engineering Center
Department of Electrical Engineering
Ohio University
Athens, Ohio 45701

I. INTRODUCTION

This paper documents the design and operation of a bi-directional communication interface between a microcomputer and the IBM System/370. The hardware unit inter-connects a modem to interface to the S/370, the microcomputer with an EIA I/O port, and a terminal for sending and receiving data from either the microcomputer or the S/370. Also described is the software necessary for the two-way interface. This interface has been designed so that no modifications need to be made to the terminal, modem, or microcomputer. This unit is designed to upgrade a uni-directional interface already in use [1]

II. INTERFACE DESCRIPTION: HARDWARE

Figure 1 shows the paths of signals between the microcomputer, the modem, and the terminal. The hardware interface consists of a four-pole, three-position switch and cables and plugs to connect the switch box to the other devices. All signals are assumed to be RS-232C (EIA standard).

In switch position 1, the microcomputer is connected directly to the terminal; all communications are between these two only. The modem is isolated in this position and it is not necessary to have it connected if no communication to the S/370 is desired. In position 2, the serial out from the keyboard is routed to the modem for communicating to the S/370. The serial out from the modem goes to the terminal and the serial in of the microcomputer. In this position, it is possible to send commands and receive responses from the S/370, while the microcomputer reads the data sent by the S/370. Thus it is possible to load a program into the microcomputer by displaying the object file on terminal. It is necessary to switch to position 1 and issue the microcomputer load command prior to typing the file. Position 3 on the switch box connects the serial out from the modem to the terminal and to the serial in on the microcomputer. In addition, the serial out from the microcomputer is sent to the modem. Here, the microcomputer communicates directly with the S/370, the terminal always displays the response sent by the S/370. With proper positioning of the half-duplex/ full-duplex switches on the terminal and modem, the responses from the microcomputer may also be displayed. Note that the serial-out from the terminal is isolated, thus it may be necessary to start a program on the microcomputer by pressing the NMI (non-maskable interrupt) switch on the switch box.

Table 1 lists the connection used on the terminal and modem. Connections for RS-232C are made through 25-pin D-connectors. Data terminal equipment (DTE) devices are supplied with a male (DB-25P) connector while data communication equipment (DCE) devices are supplied with a female (DB-25S) connector. Figure 2 shows the detailed routing of connections from the connectors on the terminal and modem through the switch box.

III.   INTERFACE DESCRIPTION: SOFTWARE

Full utilization of the bi-directional interface requires a set of programs to be run simultaneously on the microcomputer and the S/370. Figure 3 shows a block diagram of how the programs would operate for a typical application. Some points to be considered in writing the interface software are:

a.   Most microcomputers store character data internally as ASCII.

b.   Serial communications between devices are generally in ASCII format.

c.   The I/O routines for the S/370 expect to receive ASCII which is then converted to EBCDIC, which the S/370 uses for internal storage of character data .

d.   The Conversational Monitor System (CMS) portion of the VM/370 operating system is line-oriented, i.e., no system action is taken until a carriage return (hex OD) is received .

e.   The S/370 issues a prompt when ready for another line.

A typical application for which this interface has been used is transmitting data collected by the microcomputer on a cassette tape to the S/370, where it is stored on a disk file for further processing. The sequence of events is as follows: the data to be transmitted is stored in a buffer in the microcomputer's memory. Generally, 80 characters comprise one line. Note that one byte consists of two four-bit hexadecimal numbers, each of which is converted to ASCII. Thus if 80 characters are to be sent, the buffer is 40 bytes long. After 80 characters are sent, a carriage return (hex OD) is sent. The S/370 does the ASCII-to-EBCDIC conversion and places the EBCDIC characters in a user buffer in the S/370 memory. When the S/370 is ready to receive another line, it sends a series of control characters. The microcomputer reads and recognizes these control characters as the prompt signal to send another line. The sequence of control characters currently sent by S/370 is shown in Figure 4.

Appendix A gives a listing of a MOS Technology 6502 microcomputer program (intended to be run using the 'Super-Jolt' micro unit) for reading 40 bytes of data from a Memodyne digital cassette tape unit and sending these to the S/370. The data to be sent are packed BCD numbers; i.e., one BCD digit occupies four bits, two BCD numbers are contained in one byte. Each BCD digit is sent as ASCII by the 'output byte' routine in the microcomputer monitor program (at address 72B1 (hex) in the Super-Jolt (TM) monitor). A carriage return is sent at the end of the line with a call to the WRT routine at address 72C6 (hex).

Program lines 1 to 78 are initialization steps used for the Memodyne interface hardware and to position the tape properly. Lines 79 to 91 constitute the main part of the program which builds up the 40-byte buffer then sends the buffer to the S/370. This part loops continuously whether or not any data is received. The operator should monitor the operation to stop the program when all the data has been transmitted. Subroutine READ is called to read a byte from the tape unit. Subroutine W370 sends the 40-character buffer to the S/370, sends a carriage return, then looks for a period (hex 2E) followed by a DC-1 (hex 11). If this sequence is not done, the S/370 issues a read-error message. When these two characters are received, control is passed back to the main program sequence.

Subroutine RDT is a modification of the RDT routine at address 72E9 in the Jolt monitor. Most serial-read routines on microcomputers are full-duplex; as each bit is received, it is echoed back out to the sending device. However, the S/370 can receive half-duplex only. Thus it is necessary to change the interface method through the modem or to re-write the read routine so that the received bits are not echoed by the microcomputer. This is the purpose of having a separate read routine. If this is not done, read-errors result. The program presented here is shown to illustrate one application of the bi-directional interface. Other uses on other micro-computers would still use the same basic philosophy.

The companion program that is run on the S/370 is shown in Appendix B. This program is written in IBM 360/370 assembler language [2] using standard CMS I/O routines. Again this program illustrates the application of sending data to the S/370 for storage on a disk file.

The data is read 80 bytes at a time, each BCD character in its ASCII format. Each character read is stripped of the upper four-digit mask and is repacked. This is done by the translate instruction at line 88 and the PACK instruction at line 90. Since one record produces only 40 packed BCD digits, two lines are read before one 80-byte record is written to the file. A blank line or an incomplete line is filled to the end with zeros. Each time a record is written, a counter is incremented which is printed at the end of program execution.

IV.   INTERFACE OPERATION

The example of transmitting data from the microcomputer to the S/370 will be continued here to show how the interface may be operated. After the interface is properly connected, power should be applied to all units. At this point it is usually necessary to load the microcomputer with a program stored on a disk file. Thus the switch box should be set to position 2 and the appropriate CMS LOGON procedure performed. When the microprocessor object code is ready for transmittal (through editing, assembling, simulating, etc.) the switch box should be set to position 1, the microcomputer reset button pushed, and a carriage return or other appropriate

key to reset the microcomputer typed. Then issue the proper command to set the microcomputer for loading hexadecimal data over its serial lines. The switch box is then set back to position 2 and the appropriate command is issued to the S/370 to load the microcomputer with the object file. Next, the unit is switched back to position 1 to verify correct loading, initialize any memory locations and set up the NMI vector address to the start of the program. Now the switch box is placed in position 2 and the program to receive the data is started and then the unit is set to position 3 and the NMI button pressed.

As operation commences, the prompting period and any other responses from the S/370 will be displayed on the terminal. Depending on the setting of the half-duplex/full-duplex switches on the terminal and modem, data sent by the microcomputer will also be displayed on the terminal.

When the operation is finished, the unit may be set to position 2 to stop the S/370 program then position 1 to stop the microcomputer program.

V.   SUMMARY

A discussion was presented here of an interface unit and software procedures to allow two-way communication between a microcomputer and a central computer. This can be used for two-way data transmission, control and other applications where bi-directional communications are necessary. As an aid to setting up the software for other computer systems, ASCII [3] and EBCDIC [4] tables are given in Tables 2 and 3.

VI.   REFERENCES

[1]   Lilley, Robert W., Microprocessor-to-System/370 Interface, OU NASA TM-55 (Revised), Avionics Engineering Center, Department of Electrical Engineering, Ohio University, April, 1978.

[2]   OS/VS - DOS/VS - VM/370 Assembler Language, GC33-4010-4, International Business Machines Corporation, February, 1975.

[3]   Deem, Bill R., Kenneth Muchow, and Anthony Zeppa, "Digital Computer Circuits and Concepts", Reston Publishing Company, Inc., Reston Virginia, 1974, pg. 56.

[4]   IBM System/370 Principles of Operation, GA22-7000-5, International Business Machines Corporation, August 1976, pg. 288.

	DTE			DCE	
P GND	1		———————————	1	Protective Ground
S OUT	2		——————————→	2	Serial Output
S IN	3	←———————————		3	Serial Input
RTS	4		——————————→	4	Request to Send
CTS	5	←———————————		5	Clear To Send
DSR	6	←———————————		6	Data Set Ready
S GND	7		———————————	7	Signal Ground
RLSD	8	←———————————		8	Received Line Signal Detect
DTR	20		——————————→	20	Data Terminal Ready
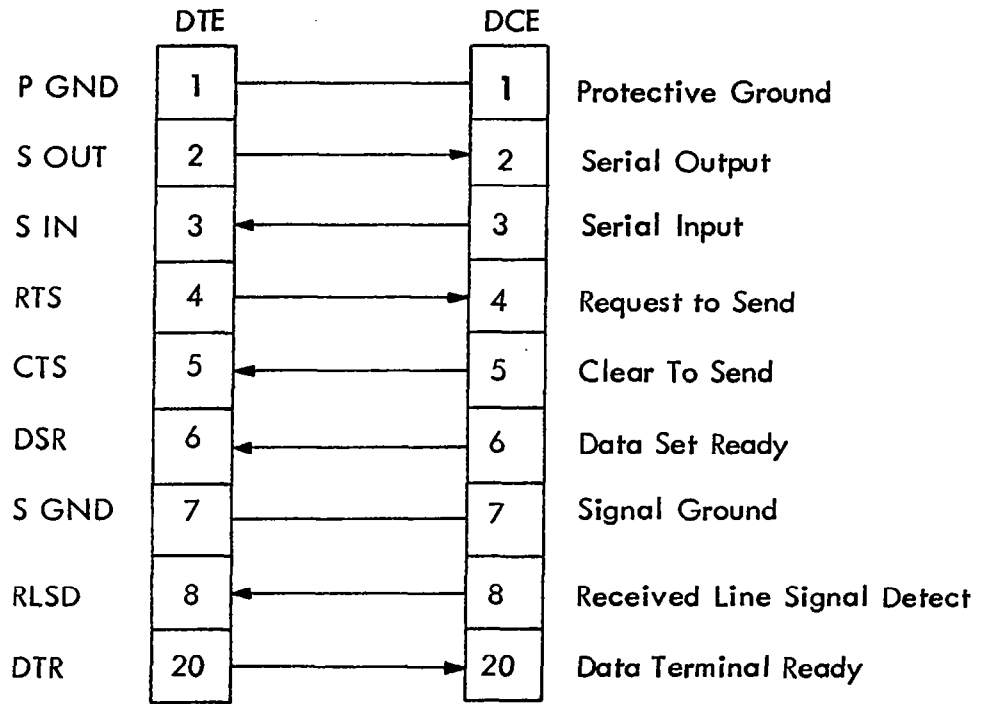
Table 1. RS-232C Connections.

	000	001	010	011	100	101	110	111
0000	NULL	① DC_0	b	0	@	P		
0001	SOM	DC_1	!	1	A	Q		
0010	EOA	DC_2	"	2	B	R		
0011	EOM	DC_3	#	3	C	S		
0100	EOT	DC_4 (stop)	$	4	D	T		
0101	WRU	ERR	%	5	E	U		
0110	RU	SYNC	&	6	F	V		
0111	BELL	LEM	'	7	G	W	Unassigned	
1000	FE_0	S_0	(	8	H	X		
1001	HT / SK	S_1	)	9	I	Y		
1010	LF	S_2	*	:	J	Z		
1011	V_{TAB}	S_3	+	;	K	[		
1100	FF	S_4	(comma) ,	<	L	\		ACK
1101	CR	S_5	—	=	M	]		②
1110	SO	S_6	.	>	N	↑		ESC
1111	SI	S_7	/	?	O	←		DEL

Example: | 100 | 0001 | = A

b_7 ———————— b_1

The abbreviations used in the figure mean:

NULL	Null Idle	CR	Carriage return
SOM	Start of message	SO	Shift out
EOA	End of address	SI	Shift in
EOM	End of message	DC_0	Device control ①
			Reserved for data
			Link escape
EOT	End of transmission	DC_1 - DC_3	Device control
WRU	"Who are you?"	ERR	Error
RU	"Are you . . . . ?"	SYNC	Synchronous idle
BELL	Audible signal	LEM	Logical end of media
FE	Format effector	SO_0 - SO_7	Separator (information)
HT	Horizontal tabulation		Word separator (blank,
			normally non-printing)
SK	Skip (punched card)	ACK	Acknowledge
LF	Line feed	②	Unassigned control
V/TAB	Vertical tabulation	ESC	Escape
FF	Form feed	DEL	Delete Idle

Table 2.   ASCII Table.

Table 3. EBCDIC Table.

The table below uses the following column identification (First Hexadecimal Digit 0–F), with Bit Positions 0,1 (00 / 01 / 10 / 11) and Bit Positions 2,3 (00 / 01 / 10 / 11). Rows are identified by Bit Positions 4,5,6,7 and Second Hexadecimal Digit (0–F).

Bit 4-7 / Hex	0	1	2	3	4	5	6	7	8	9	A	B	C	D	E	F
0000 0	NUL	DLE	DS		SP	&	-						{	}	\	0
0001 1	SOH	DC1	SOS				/		a	j	~		A	J		1
0010 2	STX	DC2	FS	SYN					b	k	s		B	K	S	2
0011 3	ETX	TM							c	l	t		C	L	T	3
0100 4	PF	RES	BYP	PN					d	m	u		D	M	U	4
0101 5	HT	NL	LF	RS					e	n	v		E	N	V	5
0110 6	LC	BS	ETB	UC					f	o	w		F	O	W	6
0111 7	DEL	IL	ESC	EOT					g	p	x		G	P	X	7
1000 8	GE	CAN							h	q	y		H	Q	Y	8
1001 9	RLF	EM						`	i	r	z		I	R	Z	9
1010 A	SMM	CC	SM		¢	!	|	:						,		|
1011 B	VT	CU1	CU2	CU3	.	$	,	#						.		
1100 C	FF	IFS		DC4	<	*	%	@					ʃ		⅃	
1101 D	CR	IGS	ENQ	NAK	(	)	_	'								
1110 E	SO	IRS	ACK		+	;	>	=							Ψ	
1111 F	SI	IUS	BEL	SUB	'	¬	?	"								EO

Card Hole Patterns
① 12-0-9-8-1	⑤ No Punches	⑨ 12-0	⑬ 0-1
② 12-11-9-8-1	⑥ 12	⑩ 11-0	⑭ 11-0-9-1
③ 11-0-9-8-1	⑦ 11	⑪ 0-8-2	⑮ 12-11
④ 12-11-0-9-8-1	⑧ 12-11-0	⑫ 0	

Control Character Representations

ACK	Acknowledge	EOT	End of Transmission	PF	Punch Off
BEL	Bell	ESC	Escape	PN	Punch On
BS	Backspace	ETB	End of Transmission Block	RES	Restore
BYP	Bypass	ETX	End of Text	RLF	Reverse Line Feed
CAN	Cancel	FF	Form Feed	RS	Reader Stop
CC	Cursor Control	FS	Field Separator	SI	Shift In
CR	Carriage Return	GE	Graphic Escape	SM	Set Mode
CU1	Customer Use 1	HT	Horizontal Tab	SMM	Start of Manual Message
CU2	Customer Use 2	IFS	Interchange File Separator	SO	Shift Out
CU3	Customer Use 3	IGS	Interchange Group Separator	SOH	Start of Heading
DC1	Device Control 1	IL	Idle	SOS	Start of Significance
DC2	Device Control 2	IRS	Interchange Record Separator	SP	Space
DC4	Device Control 4	IUS	Interchange Unit Separator	STX	Start of Text
DEL	Delete	LC	Lower Case	SUB	Substitute
DLE	Data Link Escape	LF	Line Feed	SYN	Synchronous Idle
DS	Digit Select	NAK	Negative Acknowledgr	TM	Tape Mark
EM	End of Medium	NL	New Line	UC	Upper Case
ENQ	Enquiry	NUL	Null	VT	Vertical Tab
EO	Eight Ones				

Special Graphic Characters

¢	Cent Sign	>	Greater-than Sign
.	Period, Decimal Point	?	Question Mark
<	Less-than Sign	`	Grave Accent
(	Left Parenthesis	:	Colon
+	Plus Sign	#	Number Sign
|	Logical OR	@	At Sign
&	Ampersand	'	Prime, Apostrophe
!	Exclamation Point	=	Equal Sign
$	Dollar Sign	"	Quotation Mark
*	Asterisk	~	Tilde
)	Right Parenthesis	{	Opening Brace
;	Semicolon	ʃ	Hook
¬	Logical NOT	Ψ	Fork
-	Minus Sign, Hyphen	}	Closing Brace
/	Slash	\	Reverse Slant
|	Vertical Line	⅃	Chair
,	Comma	|	Long Vertical Mark
%	Percent		
_	Underscore		

Note: Switches Shown in Position 1.

Figure 1. Signal Routing For Bi-Directional Interface.
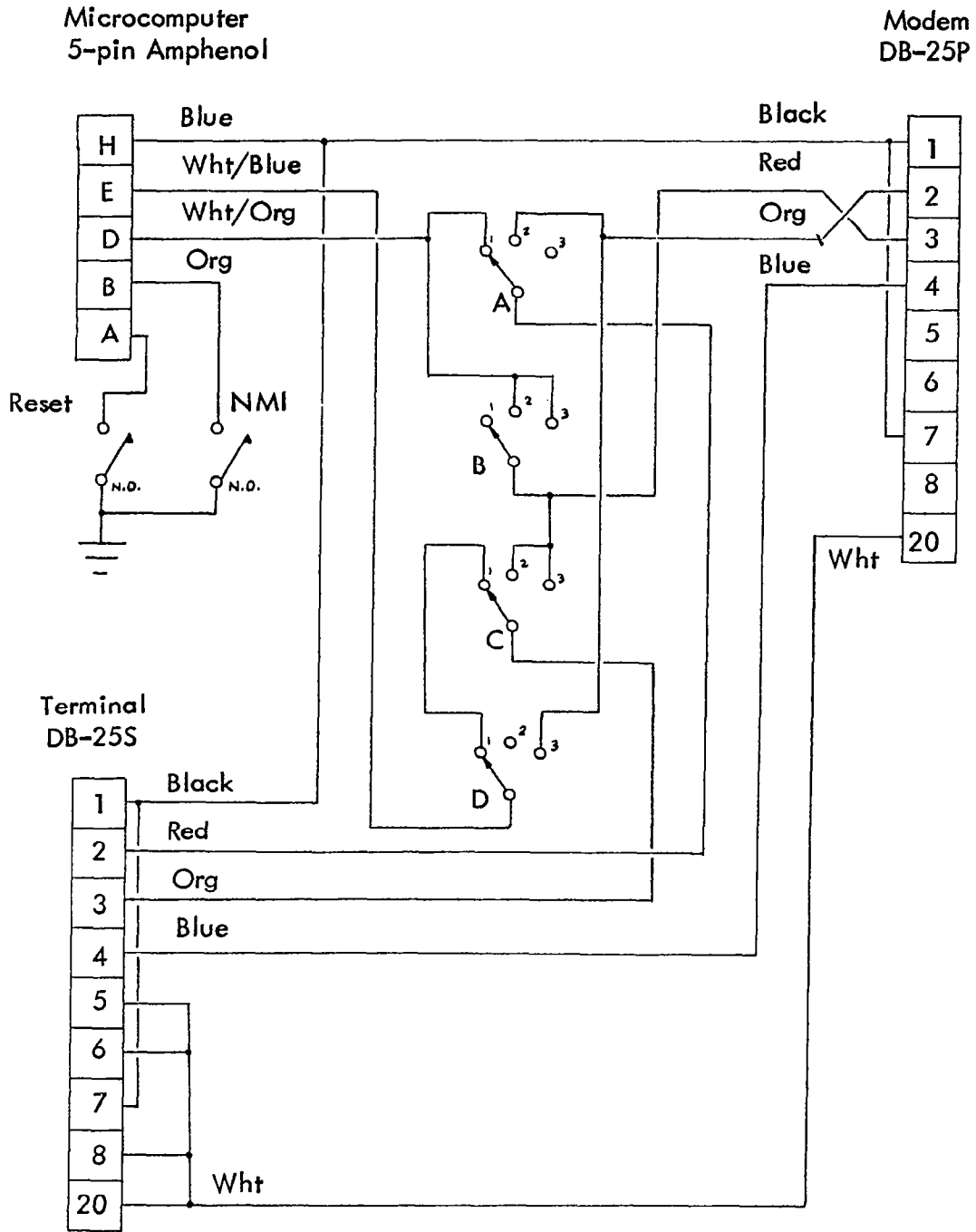
Figure 2. Interface Wiring Diagram.
(REVISED)

MICROCOMPUTER

```
┌─────────────────┐
│     Place       │
│   Characters    │
│    in Line      │
│    Buffer       │
└─────────────────┘
         │
         ▼
┌─────────────────┐
│     Get a       │
│   Character     │
└─────────────────┘
         │
         ▼
┌─────────────────┐
│   Translate     │
│   Each Digit    │
│    to ASCII     │
└─────────────────┘
         │
         ▼
┌─────────────────┐
│   Convert to    │
│    Serial;      │
│   Send Over     │
│   EEIA Lines    │
└─────────────────┘
         │
         ▼
┌─────────────────┐
│   Send 'CR'     │
│    at End       │
│    of Line      │
└─────────────────┘
         │
         ▼
┌─────────────────┐
│  Read Return    │
│   Codes from    │
│     S/370       │
└─────────────────┘
         │
         ▼
┌─────────────────┐
│   Loop Until    │
│ Period and DC1  │
│   Recognized    │
└─────────────────┘
         │
         ▼
┌─────────────────┐
│    Process      │
│  Another Line   │
└─────────────────┘
```

S/370

```
┌─────────────────┐
│   Read Line     │
│    Sent by      │
│     Micro       │
└─────────────────┘
         │
         ▼
┌─────────────────┐
│   Take Each     │
│  Byte, Remove   │
│   ASCII Zones   │
└─────────────────┘
         │
         ▼
┌─────────────────┐
│ Pack Two Digits │
│  Together to    │
│  Form One Byte  │
└─────────────────┘
         │
         ▼
┌─────────────────┐
│  Store Packed   │
│    Bytes in     │
│  Output Buffer  │
└─────────────────┘
         │
         ▼
┌─────────────────┐
│  Store Buffer   │
│  on Disk File   │
└─────────────────┘
         │
         ▼
┌─────────────────┐
│    Process      │
│    Another      │
│     Line        │
└─────────────────┘
```

Figure 3. Control Program Flow Charts.

```
┌─────────────────────┐                          ┌─────────────────────┐
│      Sent by        │                          │      Sent by        │
│   Microcomputer     │                          │       S/370         │
└─────────────────────┘                          └─────────────────────┘

┌─────────────────────┐
│  Carriage Return    │
│    hex 'ØD'         │
└─────────────────────┘
```
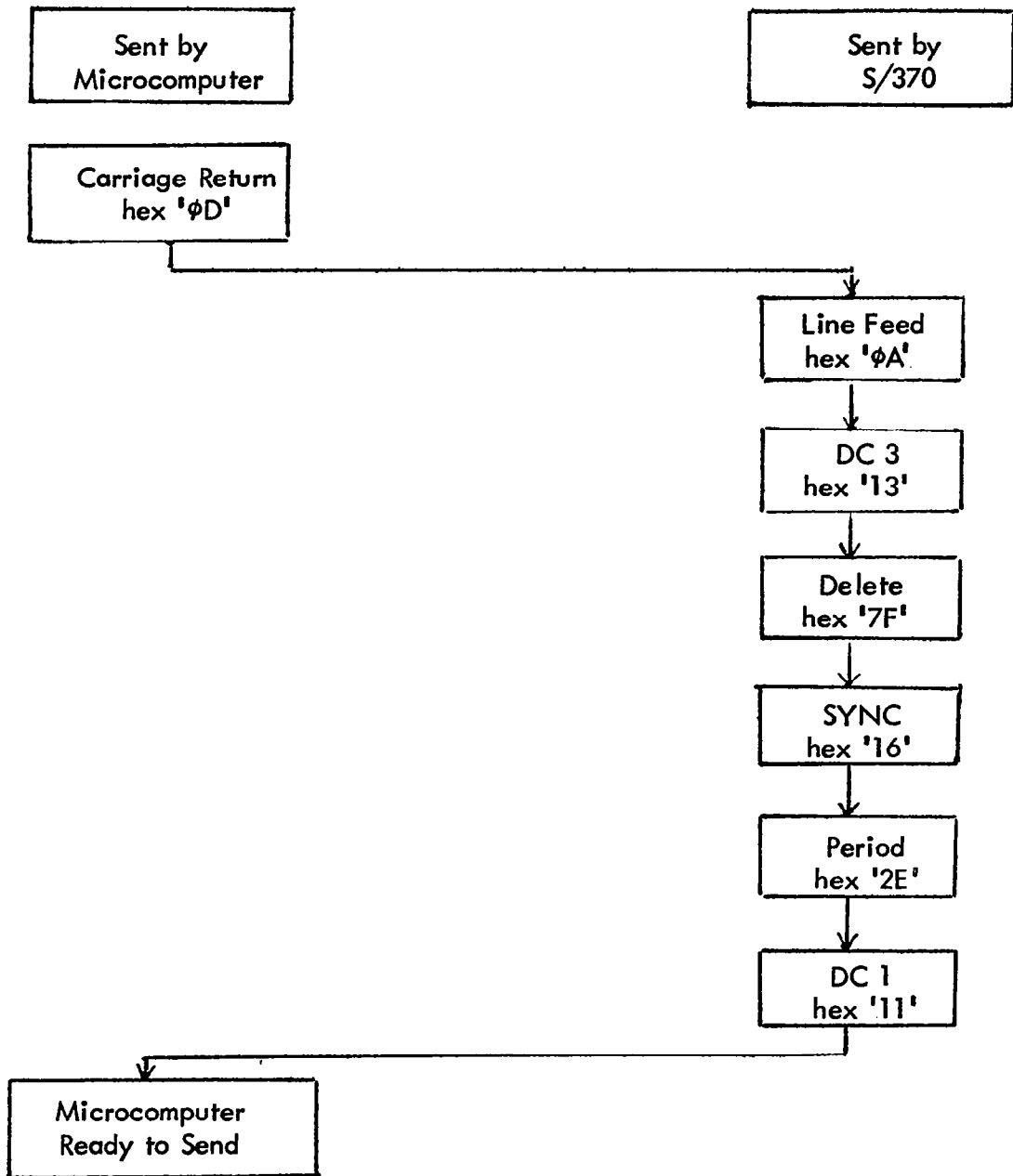
Figure 4. Control Characters Sent by S/370 After
Receiving Carriage Return.

APPENDIX A.   Program Listing for Microcomputer Control Program

FILE: UNLOAD   S6502   A   OHIO UNIVERSITY AVIONICS ENGINEERING CENTER

```
************************************************************************  UNL00010
*                                                                     *  UNL00020
*      THIS PROGRAM IS DESIGNED FOR RUNNING ON THE JOLT/MEMODYNE      *  UNL00030
*      SYSTEM FOR RECOVERING DATA STORED ON THE DIGITAL TAPE.         *  UNL00040
*      THE DATA IS READ IN 40 BYTES AT A TIME AND STORED IN A         *  UNL00050
*      BUFFER. THEN THE BUFFER IS SENT TO THE S/370 OVER THE JOLT'S   *  UNL00060
*      SERIAL LINES. WITH ASCII CONVERSION, 80 BYTES ARE ACTUALLY     *  UNL00070
*      SENT OVER THE SERIAL LINES.                                    *  UNL00080
*                                                                     *  UNL00090
*         J.P. FISCHER          08/1980                               *  UNL00100
*                                                                     *  UNL00110
************************************************************************  UNL00120
*                                                                        UNL00130
*                                                                        UNL00140
PIAA    EQU $4000    ADDRESS OF PIA SIDE A                                UNL00150
PIAB    EQU $4002    ADDRESS OF PIA SIDE B                                UNL00160
WRT     EQU $72C6    JOLT WRITE DATA TO SERIAL OUT LINE                   UNL00170
WROB    EQU $72B1                                                         UNL00180
MPB     EQU $6E02    PIA B FOR SERIAL I/O WORK                            UNL00190
MCLK1T  EQU $6E04    PIA TIMER                                            UNL00200
MCLKRD  EQU $6E04    SAME AS ABOVE                                        UNL00210
MCLK1F  EQU $6E05    SOME MORE TIMER STUFF                                UNL00220
MAJCRT  EQU $EA      UPPER 8 BITS OF BAUD RATE                            UNL00230
MINCRT  EQU $EB      LOWER 8 BITS OF BAUD RATE                            UNL00240
TAPESY  EQU %00000010 PATTERN FOR TAPE SYNC CHECK                        UNL00250
BOT     EQU %00000100 PATTERN FOR BOT/EOT CHECK                          UNL00260
LF      EQU %00010000 PATTERN FOR LOAD FOWARD FUNCTION                   UNL00270
REW2    EQU %00100000 PATTERN FOR REWIND OPERATION                       UNL00280
START   EQU %10000000 PATTERN FOR INITIATING START                      UNL00290
*                                                                        UNL00300
        ORG 0                                                            UNL00310
XTEMP   BSS 1        TEMPORARY FOR X                                      UNL00320
YTEMP   BSS 1        TEMPORARY FOR Y                                      UNL00330
BUFFER  BSS 40                                                           UNL00340
*                                                                        UNL00350
*                                                                        UNL00360
        ORG $200                                                         UNL00370
        JSR INIT     SET UP PIA FOR MEMODYNE                             UNL00380
        LDA PIAB     PREPARE TO CHECK BOT                                UNL00390
        AND =BOT     SEE IF ON LEADER                                    UNL00400
        BNE NOTBOT   IF NOT, THEN OK                                     UNL00410
        LDA PIAB     GET SIDE B                                          UNL00420
        EOR =LF      CLEAR LCAD FOWARD BIT                               UNL00430
        ORA =START   SET START BIT HIGH                                  UNL00440
        STA PIAB     AND STORE TO LOAC FOWARD                            UNL00450
BTLOOP  LDA PIAB     GET STATUS                                          UNL00460
        AND =BOT     SEE IF STILL ON LEADER                              UNL00470
        BEQ BTLOOP   CONTINUE TESTING UNTIL OFF                          UNL00480
        LDA PIAB                                                         UNL00490
        ORA =LF      SET LOAD FOWARD HIGH                                UNL00500
        STA PIAB     AND REPLACE                                         UNL00510
LDLOOP  LDA PIAB                                                         UNL00520
        AND =BOT     NOW LOOP UNTIL AT READY POINT                       UNL00530
        BNE LDLOOP   KEEP GOING UNTIL ON HOLE                            UNL00540
        LDA PIAB                                                         UNL00550
```

```
            EOR =LF       SET LOAD FOWARD IOW TO MOVE                UNL00560
            STA PIAB      OFF OF HOLE                                UNL00570
TLOOP   LDA PIAB                                                     UNL00580
            AND =BOT                                                 UNL00590
            BEQ TLOOP                                                UNL00600
            LDX =$80      TIMER ROUTINE                              UNL00610
TIMXT   DEX                                                          UNL00620
            BNE TIMXT     KEEP LOOPING UNTIL OUT                     UNL00630
            ORA =LF       NOW RETURN LOAD FOWARD                     UNL00640
            STA PIAB      HIGH, SHOULD BE OFF OF HOLE                UNL00650
NOTBOT  LDA =0        CLEAR ACCUM. AND SET                           UNL00660
            STA PIAA+1                                               UNL00670
            STA PIAB+1                                               UNL00680
            LDA =$F8                                                 UNL00690
            STA PIAB                                                 UNL00700
            LDA =0                                                   UNL00710
            STA PIAA                                                 UNL00720
            LDA =$FF                                                 UNL00730
            STA PIAB+1                                               UNL00740
            STA PIAA+1                                               UNL00750
            LDA PIAB                                                 UNL00760
            AND =%11110111                                           UNL00770
            STA PIAB                                                 UNL00780
*                                                                    UNL00790
*               NOW INITIALIZE THE 370 AND START                    UNL00800
*               SENDING DATA.                                        UNL00810
*                                                                    UNL00820
LFLDS   LDX =0        READ 40 CHARACTERS FROM TAPE                   UNL00830
L80     JSR READ      GET A BYTE FROM RECORDER                       UNL00840
            STA BUFFER,X  SAVE IN OUTPUT BUFFER                      UNL00850
            INX           DO ANOTHER ONE                             UNL00860
            CPX =40       DONE 40 BYTES YET?                         UNL00870
            BNE L80       IF NOT, DO AGAIN                           UNL00880
            LDY =40       SEND THESE 40                              UNL00890
            JSR W370      SEND TO SYSTEM                             UNL00900
            JMP LFLDS                                                UNL00910
*                                                                    UNL00920
*               INITIALIZATION FOR PIA                              UNL00930
*                                                                    UNL00940
INIT    LDX =0                                                       UNL00950
            STX PIAA+1                                               UNL00960
            STX PIAB+1                                               UNL00970
            STX PIAA                                                 UNL00980
            LDA =$B8                                                 UNL00990
            STA PIAB                                                 UNL01000
            LDA =$FF                                                 UNL01010
            STA PIAA+1                                               UNL01020
            STA PIAB+1                                               UNL01030
            LDA =0                                                   UNL01040
            ORA =LF                                                  UNL01050
            ORA =REW2                                                UNL01060
            STA PIAB                                                 UNL01070
            RTS                                                      UNL01080
*                                                                    UNL01090
*                                                                    UNL01100
```

```
*********************************************************************   UNL01110
*                                                                  *   UNL01120
*        THIS IS THE READING PORTION CF THE PROGRAM TO RECOVER     *   UNL01130
*        DATA FROM THE RECORDER AND PLACE IN THE MICROCOMPUTER'S   *   UNL01140
*        MEMORY.                                                   *   UNL01150
*                                                                  *   UNL01160
*********************************************************************   UNL01170
*                                                                      UNL01180
*                                                                      UNL01190
READ      LDA PIAB                                                     UNL01200
          ORA =START   SET START HIGH                                  UNL01210
          STA PIAB                                                     UNL01220
RDLP      LDA PIAB                                                     UNL01230
          AND =TAPESY WAIT UNTIL SYNC IS HIGH                          UNL01240
          BEQ RDLP                                                     UNL01250
          LDA PIAB                                                     UNL01260
          EOR =START   SET START LOW AGAIN                             UNL01270
          STA PIAB                                                     UNL01280
INLP1     LDA PIAB                                                     UNL01290
          AND =TAPESY WAIT UNTIL SYNC IS LOW                           UNL01300
          BNE INLP1                                                    UNL01310
          LDA PIAA     GET THE DATA FROM RECORDER                      UNL01320
          RTS                                                          UNL01330
*                                                                      UNL01340
*                                                                      UNL01350
*********************************************************************   UNL01360
*                                                                  *   UNL01370
*        THIS SUBROUTINE OUTPUTS A LINE OF CHARACTERS TO THE S/370. *   UNL01380
*        THE ADDRESS OF THE BUFFER IS IN PAGE ZERO AND IS          *   UNL01390
*        INDEXED BY THE X-REGESTER.  THE LENGTH OF THE BUFFER      *   UNL01400
*        TO BE SENT IS CONTAINED IN THE Y-REGESTER.  AFTER THE     *   UNL01410
*        BUFFER IS SENT, A 'CR' IS SENT THEN THE PROGRAM WAITS     *   UNL01420
*        FOR THE CONTROL CHARACTERS BETWEEN THE 'CR' AND PERIOD    *   UNL01430
*        TO BE SENT BACK, THEN WAITS FOR THE CONTROL              *   UNL01440
*        CHARACTER AFTER THE PERIOD INDICATING THE S/370           *   UNL01450
*        IS IN THE READ STATE.                                     *   UNL01460
*                                                                  *   UNL01470
*********************************************************************   UNL01480
*                                                                      UNL01490
W370      LDX =0       POINT TO FIRST CHARACTER                        UNL01500
          STX XTEMP    ZERO X-TEMP SPACE                               UNL01510
          STY YTEMP    SAVE LENGTH                                     UNL01520
WLOOP     LDX XTEMP    GET POINTER                                     UNL01530
          LDA BUFFER,X GET A CHARACTER                                 UNL01540
          JSR WROB     SEND IT                                         UNL01550
          INC XTEMP    X+1                                             UNL01560
          DEC YTEMP    LESS ONE CHARACTER                              UNL01570
          BNE WLOOP    GO AGAIN IF NOT DONE                            UNL01580
          LDA =$D      CARRIAGE RETURN                                 UNL01590
          JSR WRT      TELL 370 THIS IS END-OF-LINE                    UNL01600
SCANP     JSR RDT      READ JUNK FROM SYSTEM                           UNL01610
          CMP =$2E     PERIOD                                          UNL01620
          BNE SCANP                                                    UNL01630
          JSR RDT      LOOK FOR                                        UNL01640
          CMP =$11     DC1                                             UNL01650
```

```
        BNE SCANP                                           UNL01660
        RTS             RETURN TO CALLER                    UNL01670
*                                                           UNL01680
*                                                           UNL01690
**********************************************************  UNL01700
*                                                        *  UNL01710
*       HIGH SPEED REWIND.                               *  UNL01720
*                                                        *  UNL01730
**********************************************************  UNL01740
*                                                           UNL01750
        JSR INIT                                            UNL01760
        LDA =$B8                                            UNL01770
        STA PIAB                                            UNL01780
        LDA =LF                                             UNL01790
        STA PIAB                                            UNL01800
        ORA =REW2                                           UNL01810
        STA PIAB                                            UNL01820
        BRK                                                 UNL01830
*                                                           UNL01840
*                                                           UNL01850
**********************************************************  UNL01860
*                                                        *  UNL01870
*       MODIFIED JOLT READ ROUTINE.                      *  UNL01880
*       THIS ROUTINE IS IDENTICAL TO THE ORIGINAL 'RDT' ROUTINE *  UNL01890
*       AT ADDRESS $72E9, BUT THIS ROUTINE OPERATES IN HALF- *  UNL01900
*       DUPLEX RATHER THAN FULL-DUPLEX MODE.             *  UNL01910
*                                                        *  UNL01920
**********************************************************  UNL01930
*                                                           UNL01940
RDT     LDX =8                                              UNL01950
*                                                           UNL01960
RDT1    LDA MPB         WAIT FOR START BIT                  UNL01970
        LSR A                                               UNL01980
        BCC RDT1                                            UNL01990
*                                                           UNL02000
        JSR DLY1                                            UNL02010
*                                                           UNL02020
RDT2    JSR DLY2                                            UNL02030
        LDA MPB         CY = NEXT BIT                       UNL02040
        LSR A                                               UNL02050
*                                                           UNL02060
        PHP             SAVE BIT                            UNL02070
        TYA             Y CONTAINS CHAR BEING FORMED        UNL02080
        LSR A                                               UNL02090
        PLP             RECALL BIT                          UNL02100
        BCC RDT4                                            UNL02110
        ORA =$80        ADD IN NEXT BIT                     UNL02120
RDT4    TAY                                                 UNL02130
        DEX                                                 UNL02140
        BNE RDT2        LOOP FOR 8 BITS                     UNL02150
        EOR =$FF        COMPLEMENT DATA                     UNL02160
        AND =$7F        CLEAR PARITY                        UNL02170
        JSR DLY2                                            UNL02180
        CLC                                                 UNL02190
*                                                           UNL02200
```

```
DLY2    JSR DLY1                                                         UNL02210
*                                                                        UNL02220
DLY1    PHA           SAVE FLAGS AND A                                   UNL02230
        PHP                                                              UNL02240
        TXA                                                              UNL02250
        PHA           SAVE X                                             UNL02260
        LDX MAJCRT                                                       UNL02270
        LDA MINCRT                                                       UNL02280
*                                                                        UNL02290
        STA MCLK1T                                                       UNL02300
DL3     LDA MCLK1F                                                       UNL02310
        BPL DL3                                                          UNL02320
        DEX                                                              UNL02330
        PHP                                                              UNL02340
        LDA MCLKRD    RESET TIMER INT FLAG                               UNL02350
        PLP                                                              UNL02360
        BPL DL3                                                          UNL02370
*                                                                        UNL02380
        PLA                                                              UNL02390
        TAX                                                              UNL02400
        PLP                                                              UNL02410
        PLA                                                              UNL02420
        RTS                                                              UNL02430
*                                                                        UNL02440
*                                                                        UNL02450
        ORG $FFFA                                                        UNL02460
        HEX 00,02                                                        UNL02470
*                                                                        UNL02480
        END                                                              UNL02490
```

FILE: UNLOAD$S ASSEMBLE A   OHIO UNIVERSITY AVIONICS ENGINEERING CENTE

```
          TITLE 'UNLOAD$S:  READS RECORDS FROM MEMODYNE/MICROCOMPUTER IN*UNL0001J
                TERFACE AND STORES ON DISK.'                          UNL00020
          PRINT NOGEN                                                 UNL0003U
          SPACE                                                       UNL00040
*******************************************************************   UNL00050
*                                                                 *   UNL00060
*         THIS PROGRAM IS DESIGNED TO BE RUN ON THE S/370 IN CON- *·UNL00070
*         JUCTION WITH THE MICRO 'UNLOAD' PROGRAM AND THE MEMODYNE/*   UNL0008J
*         MICROCOMPUTER HARDWARE INTERFACE.  RECORDS READ FROM    *   UNL00090
*         TAPE BE THE MICRO ARE SENT TO THE 370 IN ASCII, CP THEN  *  UNL00100
*         TRANSLATES THESE TO EBCDIC WHICH MUST BE TRANSLATED     *   UNL0011J
*         BACK TO HEX BY THIS PROGRAM.  80 BYTES ARE SENT AT A    *   UNL00120
*         TIME (40 EQUIVALENT HEX CHARACTERS) AND 80 HEX CHARACTERS *  UNL00130
*         ARE STORED ON THE DISK FILE.                            *   UNL00140
*                                                                 *   UNL00150
*         J. P. FISCHER       08/1980                             *   UNL00160
*                                                                 *   UNL00170
*******************************************************************   UNL00180
          SPACE 2                                                     UNL00190
UNLOAD$S  START X'E000'                                               UNL00200
          USING UNLOAD$S,12                                           UNL00210
          MVI   FLAGS,0          CLEAR ALL FLAG BITS                  UNL00220
          LA    1,8(,1)          POINT TO FILE NAME FIELD             UNL00230
          LR    2,1              SAVE PLIST ADDRESS                   UNL00240
          CLI   0(1),X'FF'       BLANK ?                              UNL00250
          BE    NOID             IF SO, ERROR                         UNL00260
          LA    1,8(,1)                                               UNL00270
          CLI   0(1),X'FF'       NO FILETYPE?                         UNL00280
          BE    NOID             IF NOT, ERROR                        UNL00290
          MVC   FILEID+8(16),0(2)    MOVE PARTIAL ID                  UNL00300
          LA    1,8(,1)                                               UNL00310
          CLI   0(1),X'FF'       NO FILEMODE                          UNL00320
          BE    NOMODE           IF NOT SUBSTITUTE 'A'                UNL00330
          MVC   FILEID+24(2),16(2)   MOVE IN NEW MODE                 UNL00340
          B     CHECK            CONTINUE                             UNL00350
NOMODE    MVI   FILEID+24,C'A'   MOVE IN 'A'                          UNL00360
          MVI   FILEID+25,C' '                                        UNL00370
          SPACE                                                       UNL00380
CHECK     LA    1,8(,1)          MOVE POINTER UP SOME MORE            UNL00390
          CLI   0(1),X'FF'       SEE IF ANYTHING THERE                UNL00400
          BE    CHECK1           IF NOT, CONTINUE                     UNL00410
          CLI   0(1),C'('        SEE IF OPTION                        UNL00420
          BNE   PARMERR          IF NOT, BAD PARM                     UNL00430
          LA    1,8(,1)          NEXT FIELD                           UNL00440
          CLI   0(1),X'FF'       SEE IF BLANK                         UNL00450
          BE    CHECK1                                                UNL00460
          CLC   0(8,1),OPTREP    SEE IF REPLACE OPTION                UNL00470
          BNE   BADOPT           IF NOT, CONTINUE                     UNL0048J
          OI    FLAGS,1          SET REPLACE BIT                      UNL00490
          SPACE                                                       UNL00500
CHECK1    TM    FLAGS,1          SEE IF REPLACE IN EFFECT             UNL0051J
          BZ    OPENF            IF NOT,GO ON                         UNL00520
          FSERASE FSCB=FILEID                                         UNL00530
OPENF     FSOPEN FSCB=FILEID     OPEN FOR WRITING                     UNL0054J
          CL    15,F36           SEE IF INVALID DISK                  UNL00550
```

90

```
          BE      INVDISK                                            UNL00560
          SPACE 2                                                    UNL00570
*****************************************************************    UNL00580
*                                                             *      UNL00590
*            THIS PART OF THE PROGRAM CAUSES A TERMINAL       *      UNL00600
*            READ TO GET THE ASCII CHARACTERS, THEN TRANSLATES *     UNL00610
*            THEM TO HEX AND STORES ON DISK.                  *      UNL00620
*                                                             *      UNL00630
*****************************************************************    UNL00640
          SPACE                                                      UNL00650
          SLR     4,4                                                UNL00660
          SLR     7,7            CLEAR RECORD COUNTER                 UNL00670
          LA      2,WBUF         WRITE BUFFER ADDRESS                 UNL00680
          LA      4,8            LOOP INCREMENT                       UNL00690
          L       5,IBUF80       END OF LOOP                          UNL00700
RDLOOP    LA      3,IBUF         READ BUFFER ADDRESS                  UNL00710
          RDTERM  IBUF           GET A RECORD                         UNL00720
          LTR     0,0            SEE IF NULL LINE                     UNL00730
          BZ      DONE           GO IF IT IS                          UNL00740
          WAITT                  WAIT FOR I/O                         UNL00750
          TR      IBUF(80),TRTBL CHANGE TO HEX                        UNL00760
STRIPZ    MVC     TEMP(8),0(3)   GET 8 ZONED BYTES                    UNL00770
          PACK    TEMP1(5),TEMP(9)    REMOVE THE ZONES                UNL00780
          MVC     0(4,2),TEMP1   PUT PACKED CHARS. IN OUT BUFFER      UNL00790
          LA      2,4(2)         NEXT POSITION IN OUTPUT BUFFER       UNL00800
          BXLE    3,4,STRIPZ     CONTINUE UNTIL WHOLE RECORD DONE     UNL00810
          SPACE                                                      UNL00820
          RDTERM  IBUF           GET ANOTHER 80 CHARS.                UNL00830
          LTR     0,0            SEE IF NULL LINE                     UNL00840
          BZ      DONE1          GO IF IT IS                          UNL00850
          WAITT                  WAIT FOR I/O                         UNL00860
          LA      3,IBUF         RE-INITIALIZE POINTER                UNL00870
          TR      IBUF(80),TRTBL                                      UNL00880
Z1        MVC     TEMP(8),0(3)   GET 8 BYTES                          UNL00890
          PACK    TEMP1(5),TEMP(9)    REMOVE ZONES                    UNL00900
          MVC     0(4,2),TEMP1   PUT IN OUT BUFFER                    UNL00910
          LA      2,4(2)         NEXT LOCATION                        UNL00920
          BXLE    3,4,Z1         DO 80 BYTES                          UNL00930
          LA      2,WBUF         REINTIALIZE WRITE POINTER            UNL00940
          FSWRITE FSCB=FILEID    SEND TO DISK                         UNL00950
          LTR     15,15          SEE IF ERROR                         UNL00960
          BNZ     WRTERR         GO IF THERE IS                       UNL00970
          LA      7,1(7)         ADD ONE TO RECORD COUNT              UNL00980
          B       RDLOOP         PROCESS SOME MORE                    UNL00990
          SPACE                                                      UNL01000
DONE1     MVI     WBUF+40,0      PREPARE TO CLEAR                     UNL01010
          MVC     WBUF+41(39),WBUF+40 REMAINING FIELD                 UNL01020
          FSWRITE FSCB=FILEID                                         UNL01030
          LTR     15,15                                               UNL01040
          BNZ     WRTERR                                              UNL01050
          LA      7,1(7)         ADD ONE TO RECORD COUNT              UNL01060
          SPACE                                                      UNL01070
*****************************************************************    UNL01080
*                                                             *      UNL01090
*            NOW CLOSE THE FILE.                              *      UNL01100
```

```
*                                                                    *  UNL0111J
*****************************************************************************  UNL01120
          SPACE                                                      UNL01130
DONE      FSCLOSE FSCB=FILEID   CLOSE THE FILE                       UNL01140
          LINEDIT TEXT='..... RECORDS WRITTEN TO FILE.',             *UNL01150
                SUB=(DEC,(7)),DOT=NO,RENT=NO                         UNL0116U
          SLR    15,15          CLEAR RETURN CODE                    UNL01170
          BR     14             GO TO CMS                            UNL0118J
          EJECT                                                      UNL01190
NOID      LINEDIT TEXT='DMSULD054E INCOMPLETE FILEID SPECIFIED.',    *UNL01200
                DISP=ERRMSG,DOT=NO,RENT=NO                           UNL01210
          LA     15,24          RETURN CODE                          UNL01220
          BR     14             BACK TO CMS                          UNL01230
          SPACE                                                      UNL01240
INVDISK   LR     2,15           SAVE RETURN CODE                     UNL0125U
          LINEDIT TEXT='DMSULD069E DISK ''..'' NOT ACCESSED.',       *UNL01260
                SUB=(CHARA,FILEID+24),DISP=ERRMSG,DOT=NO,RENT=NO     UNL0127J
          LR     15,2           GET RETURN CODE                      UNL0128J
          BR     14             BACK TO CMS                          UNL0129J
          SPACE                                                      UNL01300
WRTERR    LR     2,15           SAVE RETURN CODE                     UNL01310
          LINEDIT TEXT='DMSULD105S ERROR ''..'' WRITING FILE ''......... *UNL01320
                ......... ..'' ON DISK.',SUB=(DEC,(2),CHARA,FILEID+8,CHAR*UNL01330
                A,FILEID+16,CHARA,FILEID+24),DISP=ERRMSG,           *UNL01340
                DOT=NO,RENT=NO                                       UNL01350
          LA     15,100         RETURN CODE                          UNL01360
          BR     14             BACK TO CMS                          UNL01370
          SPACE                                                      UNL01380
PARMERR   LR     2,1            SAVE PARM ADDRESS                    UNL0139J
          LINEDIT TEXT='DMSULD070E INVALID PARAMETER ''.........''', *UNL01400
                SUB=(CHARA,(2)),DISP=ERRMSG,DOT=NO,RENT=NO           UNL0141J
          LA     15,24          RETURN CODE                          UNL01420
          BR     14             BACK TO CMS                          UNL01430
          SPACE                                                      UNL01440
BADOPT    LR     2,1            SAVE OPTION ADDRESS                  UNL01450
          LINEDIT TEXT='DMSULD003E INVALID OPTION ''.........''',    *UNL01460
                SUB=(CHARA,(2)),DISP=ERRMSG,DOT=NO,RENT=NO           UNL01470
          LA     15,24          RETURN CODE                          UNL01480
          BR     14             BACK TO CMS                          UNL01490
          EJECT                                                      UNL01500
          DS     0D                                                  UNL01510
F36       DC     F'36'                                               UNL01520
IBUF80    DC     AL4(IBUF+79)                                        UNL01530
OPTREP    DC     CL8'REP'                                            UNL01540
FILEID    FSCB   '* * *',BUFFER=WBUF,BSIZE=80                        UNL0155J
TEMP      DS     XL8                                                 UNL0156U
          DC     C'1'                                                UNL01570
TEMP1     DS     XL5                                                 UNL0158J
FLAGS     DS     XL1                                                 UNL01590
WBUF      DS     XL80                                                UNL01600
IBUF      DS     XL132                                               UNL01610
TBL       DC     X'00'                                               UNL01620
          ORG    TBL+8*16                                            UNL01630
          DC     XL16'00FAFBFCFDFEFFF0F0F0F0F0F0F0F0'                UNL01640
          ORG    TBL+11*16                                           UNL01650
          DC     XL16'F0F1F2F3F4F5F6F7F8F9F0F0F0F0F0F0'              UNL01660
TRTBL     EQU    TBL-X'40'                                           UNL01670
          END    UNLOAD$S                                            UNL01680
```

LORAN-C PLOTTING PROGRAM FOR PLOTTING LINES

OF POSITION ON STANDARD CHARTS

The Loran-C plotting program was designed to plot Loran-C lines of position on any standard chart and is used in the data-collection system currently in use at Ohio University Avionics Engineering Center.

James P. Roman

Avionics Engineering Center
Department of Electrical Engineering
Ohio University
Athens, Ohio 45701

I.   INTRODUCTION

The NASA Tri-University program at Ohio University is currently involved in the development of a low-cost Loran-C navigation receiver for use in general aviation aircraft. This paper describes a set of programs designed to be run on the IBM System/370 computer at Ohio University. These programs are used to plot Loran-C lines of position (LOP) on any common map or standard aviation sectional chart. The Loran-C plotting program JRPLOT FORTRAN uses a standard Calcomp-compatible plotting subroutine package for the Hewlett-Packard 7203A graphic plotter.

This paper gives a general description of the features of the Loran-C plotting program. This program involves a simple add/subtract method to calculate the LOP. Refer to Figure 1. Included is a description on how to use the program and some methods of operation.

II.   FEATURES OF THE LORAN-C PLOTTING PROGRAM

The program will accommodate any scale of map desired. (Note: the larger the scale of the map the more distortion will occur.) The program was designed for standard aviation sectional charts; any larger scale than 1:500,000 is not recommended.

Plotting may be done on any size chart within the limitations of the Hewlett-Packard 7203A graphic plotter (10" high by 15" wide).

Four station pairs are calculated in the program's execution where, for the 9960 chain: (Master) control for W, X, Y, and Z is Seneca, NY 42° 42' 50.6"N and 76° 49' 33.9"W

Block address 1 is the W-pair
Caribou, ME 46° 48' 27.2"N and 67° 55' 37.7"W

Block address 2 is the X-pair
Nantucket, MA 41° 15' 11.9"N and 69° 58' 39.1"W

Block address 3 is the Y-pair
Carolina Beach, NC 34° 03' 46.0"N and 77° 54' 46.8"W

and block address 4 is the Z-pair
Dana, IN 39° 51' 07.5"N and 87° 29' 12.1"W

For best results only plot two LOP sets on a single chart.

The time difference for each line of position is placed to the top or side of the chart, depending on the angle of the LOP, along with the station pair identifier.

III. ACCURACY

There are two sources of error in the system. Although the latitude/longitude conversion subprogram takes into account the curvature of the earth, the plotting routine is purely linear, therefore, the larger the scale of the chart the greater the percentage of error. The error for large scale sectionals is approximately ± 10 μsec. The error for small scale geographic survey charts is ± 5 μ sec. The other source of error is in measurement of the parameters listed below. These errors can be reduced by methods listed in Section IV depending on the accuracy the programmer wishes to achieve.

IV. EXECUTION

1. The center point of the chart must be measured as accurately as possible. Then, the latitude and longitude must be taken from that point. The proper form for entering into the computer is:

integer degrees   integer minutes   floating point seconds

$\#\#\#_{space}\#\#_{space}\#\#.\#$

2. Then measure the number of inches per degree of latitude and measure the number of inches per degree of longitude. See Figure 2.

3. Then enter the increment that the lines of position should be spaced apart.

Recommended increments are:

50.0 for standard sectional charts

2.0 for geographic survey charts.

4. Enter the actual dimensions of the chart to be plotted (see Figure 2). The chart should be no larger than 11 x 15 inches and no smaller than 5 x 5 inches. These are the practical limitations of the Hewlett-Packard 7203A plotter. When the program is finished executing, the chains will be located as follows:

Block Address	Station Pair
1	W
2	X
3	Y
4	Z

It is recommended to plot all four chains on a blank sheet of paper the same size as the chart.

V.   IMPROVING ACCURACY

This procedure should be necessary only when there is a need for extreme accuracy. To make the Loran-C plotting program more accurate, three time difference positions are needed before execution of the program: the time difference of the center point, the time differences for a point left of center, and the time differences for a point right of center.   Then it is a simple matter to align the grid with the known time-difference positions. By adding or subtracting from the latitude position of the center point, the grid will shift north or south respectively.   By adding or subtracting from the longitude center point position, the grid will shift west or east respectively.   Another method of adjusting the grid would be to add or subtract from the inches per degree parameters.   Then the grid may be expanded or contracted respectively.

VI.   SUMMARY

The Loran-C plotting program is a system of plotting routines and conversion subprograms.   The program is designed to accommodate a wide range of mapping needs. The program may be easily modified to meet the specific needs of the current experiment.

VII.   ACKNOWLEDGEMENTS

The subprogram TDPOS is a program written by Joseph P. Fischer of the Ohio University Avionics Engineering Center.   The program was originally written for use in Loran-C data reduction.   The subprogram TDS is a modification of a program also written by Mr. Fischer.   This work is supported by the National Aeronautics and Space Administration.

VIII.   BIBLIOGRAPHY

Loran-C User Handbook, United States Coast Guard, May 1980.
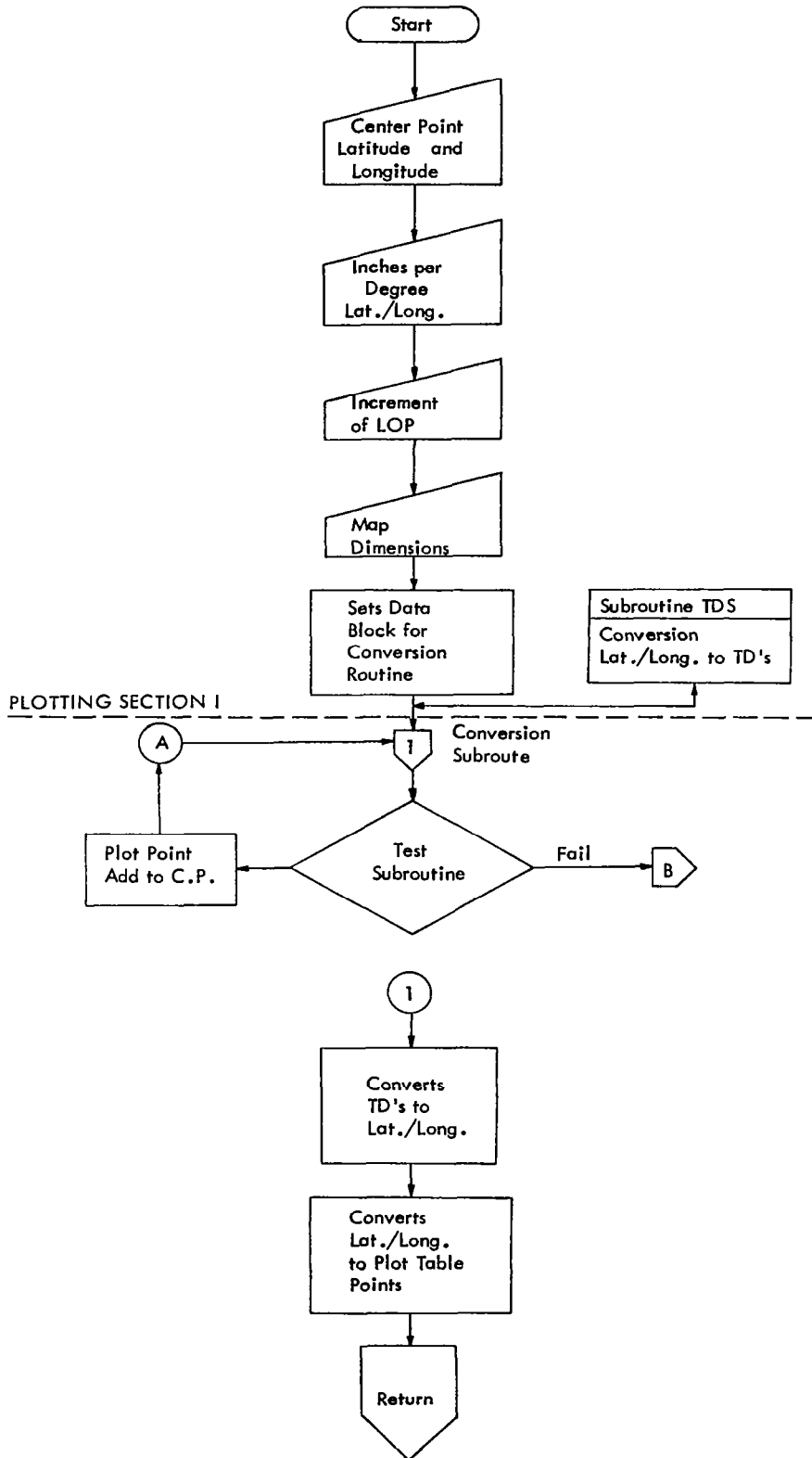
Figure 1. Flow Chart.
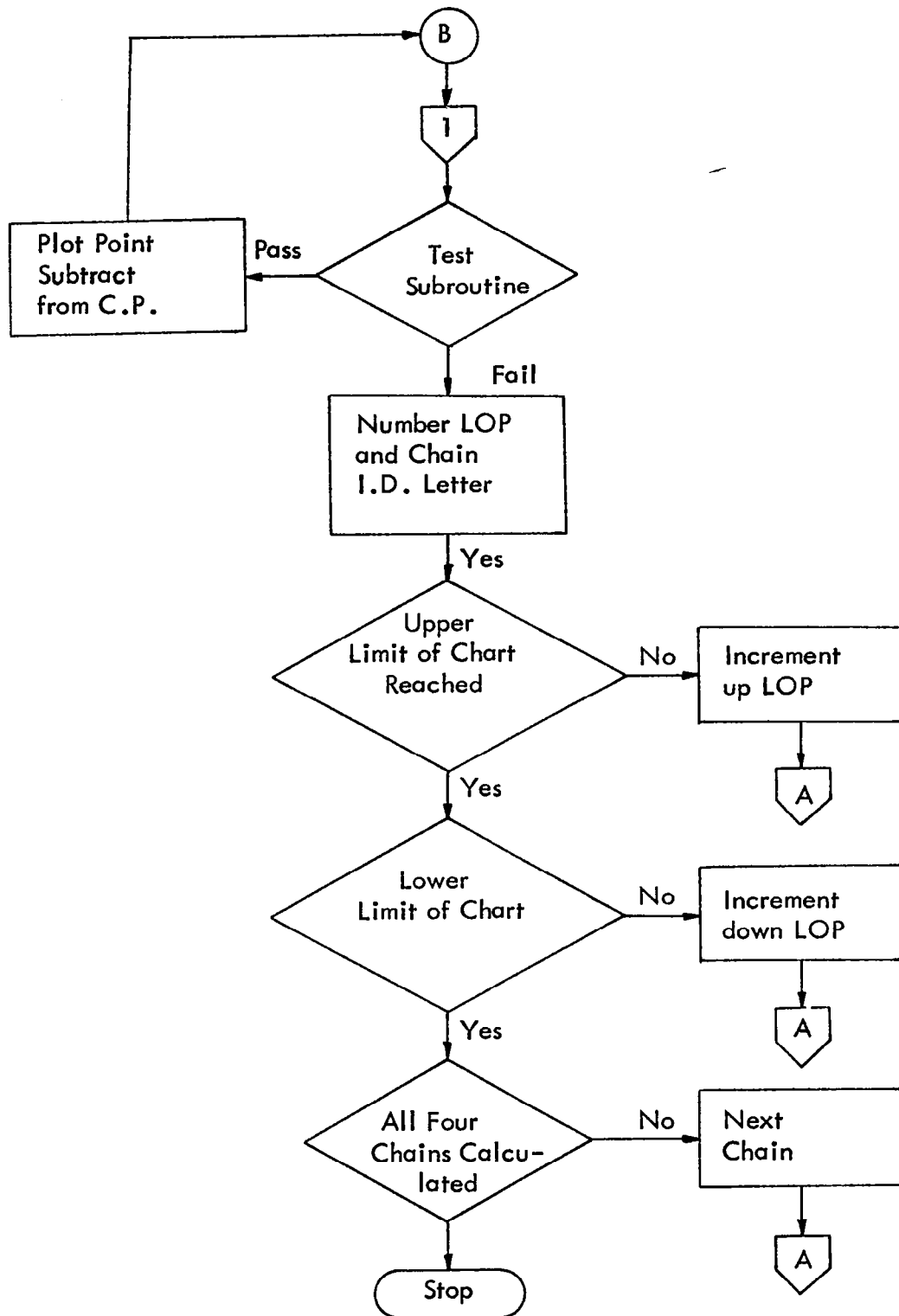
Figure 1. (Continued).
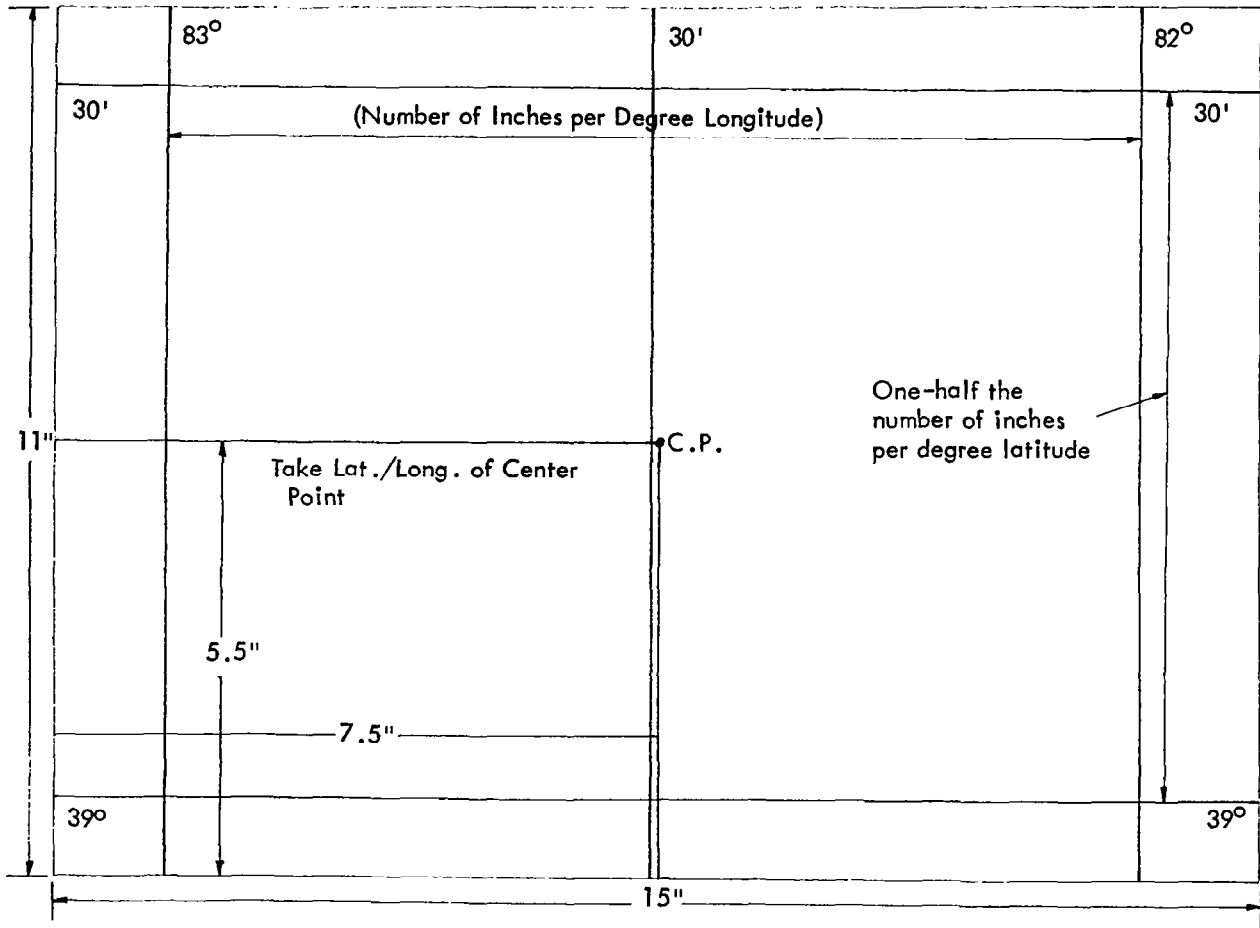
Figure 2. Sample Chart for Measurements.

FILE: JRPLOT   FORTRAN C   OHIO UNIVERSITY AVIONICS ENGINEERING CENTER

```
CCCCCCCCCCCCCC PLOTTING LORAN-C CURVES ON SECTIONAL CHARTS CCCCCCC     JRP00010
      DIMENSION TD(4),TH(4),ORPOS(2),POS(2)                            JRP00020
      DIMENSION IBCD(2),X2(2,200),Y2(2,200)                           JRP00030
      DIMENSION BUF(1)                                                JRP00040
      REAL*8 PHIR,GAMR                                                JRP00050
      COMMON PHIR,GAMR                                                JRP00060
      COMMON/CHAIND/DEL(2),A5,A6,AD(8),DM(8),CS(8)                    JRP00070
CCCCCCCCCCCCCCCCCCCCCCCCCCC INPUT SECTION CCCCCCCCCCCCCCCCCCCCCCCCCCCCCCCCCJRP00080
      WRITE(6,11)                                                     JRP00090
11    FORMAT('+','ENTER LATITUDE OF CENTER POINT FORM ### ## ##.# ')  JRP00100
      READ(5,4)IDEG,MIN,SEC                                           JRP00110
      WRITE(6,12)                                                     JRP00120
12    FORMAT(' ','ENTER LONGITUDE OF CENTER POINT')                   JRP00130
      READ(5,4)IDEG1,MIN1,SEC1                                        JRP00140
4     FORMAT(I3,1X,I2,1X,F3.1)                                        JRP00150
      WRITE(6,13)                                                     JRP00160
13    FORMAT(' ','ENTER NUMBER OF INCHES PER DEGREE LATITUDE')        JRP00170
      READ(5,5)A                                                      JRP00180
      WRITE(6,14)                                                     JRP00190
14    FORMAT(' ','ENTER NUMBER OF INCHES PER DEGREE LONGITUDE')       JRP00200
      READ(5,5)B                                                      JRP00210
5     FORMAT(F7.4)                                                    JRP00220
      WRITE(6,15)                                                     JRP00230
15 .  FORMAT('+','INPUT INCREMENT BETWEEN L.O.P..')                   JRP00240
      READ(5,5)XINC                                                   JRP00250
      XINC2=XINC                                                      JRP00260
      IF(XINC.GT.10.0)XINC2=10.0                                      JRP00270
      B=B*(-1.0)                                                      JRP00280
      YIP=IDEG+(MIN+SEC/60.0)/60.0                                    JRP00290
      XIP1=IDEG1+(MIN1+SEC1/60.0)/60.0                                JRP00300
      CALL PLOTS(BUF,1,11)                                            JRP00310
CCCCCCCCCCCCCCCCCCCC MAP DIMENSIONS CCCCCCCCCCCCCCCCCCCCCCCCCCCCCCCCCCCCCCCJRP00320
      WRITE(6,1)                                                      JRP00330
1     FORMAT('+','ENTER HORIZONTAL DIMENSION')                        JRP00340
      READ(5,2)XLAT                                                   JRP00350
2     FORMAT(F6.2)                                                    JRP00360
      WRITE(6,3)                                                      JRP00370
3     FORMAT('+','ENTER VERTICAL DIMENSION')                          JRP00380
      READ(5,2)XLONG                                                  JRP00390
      XLAT=XLAT-0.375                                                 JRP00400
      XLONG=XLONG-1.0                                                 JRP00410
      PHIR=(IDEG+(MIN+SEC/60.)/60.)*3.14159265/180.                   JRP00420
      GAMR=(IDEG1+(MIN1+SEC1/60.)/60.)*3.14159265/180.               JRP00430
      YCP=XLAT/2.0                                                    JRP00440
      XCP1=XLONG/2.0                                                  JRP00450
CCCCCCCCCCCCCCCCCCCCCCCCCCCCCCCCCCCCCCCCCCCCCCCCCCCCCCCCCCCCCCCCCCCCCCCCCCCJRP00460
CCCCCCCCCCCCCCCCCCCCCCC CONVERSION TO TIME DIFF. CCCCCCCCCCCCCCCCCCCCCCCCCC JRP00470
      CALL TDS(TD)                                                    JRP00480
      ORPOS(1)=IDEG+(MIN+SEC/60.)/60.                                 JRP00490
      ORPOS(2)=IDEG1+(MIN1+SEC1/60.)/60.                             JRP00500
      WRITE(6,10)IDEG,MIN,SEC,IDEG1,MIN1,SEC1                         JRP00510
10    FORMAT(' ','LATITUDE= ',I2,' ',I2,' ',F5.2,'LONGITUDE=',I2     JRP00520
     >,' ',I2,' ',F5.2)                                               JRP00530
      IF(A.GT.20.0)GOTO 45                                            JRP00540
      DO 40 K=1,4,1                                                   JRP00550
```

```
         K1=TD(K)/10                                              JRP00560
         K1=K1*10                                                 JRP00570
         C=TD(K)-K1                                               JRP00580
         IF(C-5.0)20,30,30                                        JRP00590
20       TD(K)=TD(K)-C                                            JRP00600
         GOTO 40                                                  JRP00610
30       TD(K)=TD(K)+(10.0-C)                                     JRP00620
40       CONTINUE                                                 JRP00630
45       WRITE(6,50)(TD(K),K=1,4)                                 JRP00640
50       FORMAT(' ','TDS=',4F15.2)                                JRP00650
         DO 2999 I7=1,5,1                                         JRP00660
CCCCCCCCCCCCCCCCCCCCCCCCCCCCCCCCCCCCCCCCCCCCCCCCCCCCCCCCCCCCCCCC  JRP00670
CCCCCCCCCCCCCCCCCCCCC DATA ALLOCATION CCCCCCCCCCCCCCCCCCCCCCCCCCCCCJRP00680
         IF(I7.GE.5)GOTO 3000                                     JRP00690
         J7=0                                                     JRP00700
         IF(I7-2)90,100,110                                       JRP00710
90       I=1                                                      JRP00720
         J=2                                                      JRP00730
         I2=1                                                     JRP00740
         J2=2                                                     JRP00750
         CALL DATAWX                                              JRP00760
         GOTO 130                                                 JRP00770
100      I=2                                                      JRP00780
         J=1                                                      JRP00790
         I2=2                                                     JRP00800
         J2=1                                                     JRP00810
         CALL DATAWX                                              JRP00820
         GOTO 130                                                 JRP00830
110      IF(I7.EQ.4)GOTO 120                                      JRP00840
         I=3                                                      JRP00850
         J=2                                                      JRP00860
         I2=2                                                     JRP00870
         J2=1                                                     JRP00880
         CALL DATAXY                                              JRP00890
         GOTO 130                                                 JRP00900
120      I=4                                                      JRP00910
         J=3                                                      JRP00920
         I2=2                                                     JRP00930
         J2=1                                                     JRP00940
         CALL DATAYZ                                              JRP00950
130      IF(DRPOS(2).GT.76.0)CALL NEWDAT(I7,I,I2,J,J2)            JRP00960
         IC=0                                                     JRP00970
         IB=0                                                     JRP00980
         TH(I2)=TD(I)                                             JRP00990
         TH(J2)=TD(J)                                             JRP01000
         IPEN=3                                                   JRP01010
CCCCCCCCCCCCCCCCCCCCCCCCCCCCCCCCCCCCCCCCCCCCCCCCCCCCCCCCCCCCCCCCCCCJRP01020
CCCCCCCCCCCCCCCCCCCCCCCCCCCCCC PLOTTING SECTION 1 CCCCCCCCCCCCCCCCCCJRP01030
140      CALL CONVER(TH,POS,DRPOS,IERROR,YCP,XCP1,YIP,XIP1,X,Y,B,A) JRP01040
         IC=IC+1                                                  JRP01050
         Y2(1,IC)=Y                                               JRP01060
         X2(1,IC)=X                                               JRP01070
         I3=0                                                     JRP01080
         CALL TEST(XLAT,XLONG,X,Y,I3,IERROR)                      JRP01090
         IF(I3.GE.1)GOTO 160                                      JRP01100
```

101

```
        CALL PLOT(X,Y,IPEN)                                              JRP01110
        TH(J2)=TH(J2)+XINC2                                              JRP01120
        IPEN=2                                                          JRP01130
150     IF(I3-1)140,900,900                                             JRP01140
CCCCCCCCCCCCCCCCCCCCCCCCCCCCC PLOTTING SECTION 2 CCCCCCCCCCCCCCCCCCCCCCCCCCCCCCCCCCCCJRP01150
900     I3=0                                                            JRP01160
        DPPOS(1)=IDEG+(MIN+SEC/60.0)/60.0                               JRP01170
        DPPOS(2)=IDEG1+(MIN1+SEC1/60.0)/60.0                            JRP01180
        TH(J2)=TD(J)                                                    JRP01190
        IPEN=3                                                          JRP01200
        GOTO 915                                                        JPP01210
910     TH(J2)=TH(J2)-XINC2                                             JRP01220
915     CALL CONVER(TH,POS,DPPOS,IEPROP,YCP,YCP1,YIP,XIP1,X,Y,B,A)      JRP01230
        IB=IB+1                                                         JRP01240
        Y2(2,IB)=Y                                                      JRP01250
        X2(2,IB)=X                                                      IRP01260
        I3=0                                                            JPP01270
        CALL TEST(XLAT,XLONG,X,Y,I3,IEPROP)                             JRP01280
        IF(I3.GE.1)GOTO 930                                             JRP01290
        CALL PLOT(X,Y,IPEN)                                             JRP01300
        IPEN=2                                                          JRP01310
930     IF(I3-1)910,1000,1000                                           JRP01320
CCCCCCCCCCCCCCCCCCCCCCCCCCCCCCCCCCCCCCCCCCCCCCCCCCCCCCCCCCCCCCCCCCCCCCCCCCCCCCJRP01330
CCCCCCCCCCCCCCCCCCCCCCCCCCC NUMBERING SECTION CCCCCCCCCCCCCCCCCCCCCCCCCCCCCCCJRP01340
1000    HEIGHT=0.1                                                      JPP01350
        IF(IC.LT.20)GOTO 1005                                           JRP01360
        GOTO 1006                                                       JRP01370
1005    DELTAX=X2(2,(IB/2))-X2(2,(IB/3))                                JRP01380
        DELTAY=Y2(2,(IB/2))-Y2(2,(IB/3))                                JRP01390
        IP=2                                                            JRP01400
        GOTO 1007                                                       JRP01410
1006    DELTAX=X2(1,(IC/2))-X2(1,(IC/3))                                JRP01420
        DELTAY=Y2(1,(IC/2))-Y2(1,(IC/3))                                JRP01430
        IP=1                                                            JRP01440
1007    ANGLE=ATAN2(DELTAY,DELTAX)                                      JRP01450
        ANGLE=ABS((ANGLE*180.)/3.14159265)                             JRP01460
        IF(((ANGLE.LE.45.).OR.(ANGLE.GE.315.)).OR.((ANGLE.GE.135.)      JRP01470
       >.AND.(ANGLE.LE.225.)))IPOS1=1                                   JRP01480
        IF(((ANGLE.GT.45.).AND.(ANGLE.LT.135.)).OR.((ANGLE.GT.225.)     JRP01490
       >.AND.(ANGLE.LT.315.)))IPOS1=2                                   JRP01500
1008    NPLACE=0                                                        JRP01510
        ANGLE=1.0                                                       JRP01520
        NCHAR=0                                                         JRP01530
        FNUM=TH(I2)                                                     JRP01540
        IBCD(1)=101+I7                                                  JRP01550
        IF(IPOS1-2)1020,1011,1011                                       JRP01560
1011    XDOWN=1.0                                                       JRP01570
        CALL NUMBER(X2(1,IC),(XLAT-XDOWN),HEIGHT,FNUM,ANGLE,NPLACE)     JRP01580
        CALL SYMBOL((X2(1,IC)+0.2),(XLAT-(XDOWN-0.2)),HEIGHT,IBCD(1),ANGLEJRP01590
       >,NCHAR)                                                         JRP01600
        GOTO 1030                                                       JRP01610
1020    CALL NUMBER(0.2,Y2(2,IB),HEIGHT,FNUM,ANGLE,NPLACE)             JRP01620
        CALL SYMBOL(0.8,Y2(2,IB),HEIGHT,IBCD(1),ANGLE,NCHAR)           JRP01630
1030    IC=0                                                            JRP01640
        IB=0                                                            JRP01650
```

```
        IF(J7.EQ.1)GOTO 2010                                              JRP01660
CCCCCCCCCCCCCCCCCCCCCCCCCCCCCCCCCCCCCCCCCCCCCCCCCCCCCCCCCCCCCCCCCCCCCCCCCCCJRP01670
CCCCCCCCCCCCCCCCCCCCCCCCCCC INCREMENT UP CCCCCCCCCCCCCCCCCCCCCCCCCCCCCCCCCCC JRP01680
1010    TH(I2)=TH(I2)+XINC                                                JRP01690
        TH(J2)=TD(J)                                                      JRP01700
        IPEN=3                                                            JRP01710
        CALL CONVER(TH,POS,DRPOS,IERROR,YCP,XCP1,YIP,XIP1,X,Y,B,A)        JRP01720
        I3=0                                                              JRP01730
        CALL TEST(XLAT,XLONG,X,Y,I3,IERROR)                              JRP01740
        IF(I3-1)140,2000,2000                                            JRP01750
CCCCCCCCCCCCCCCCCCCCCCCCCCCCCCC INCREMENT DOWN CCCCCCCCCCCCCCCCCCCCCCCCCCCCC JRP01760
2000    TH(I2)=TD(I)                                                      JRP01770
        J7=1                                                              JRP01780
        I3=0                                                              JRP01790
2010    TH(I2)=TH(I2)-XINC                                                JRP01800
        TH(J2)=TD(J)                                                      JRP01810
        IPEN=3                                                            JRP01820
        CALL CONVER(TH,POS,DRPOS,IERROR,YCP,XCP1,YIP,XIP1,X,Y,B,A)        JRP01830
        I3=0                                                              JRP01840
        CALL TEST(XLAT,XLONG,X,Y,I3,IERROR)            .                 JRP01850
        IF(I3-1)140,2999,2999                                            JRP01860
CCCCCCCCCCCCCCCCCCCCCCCCCCCCCCCCCCCCCCCCCCCCCCCCCCCCCCCCCCCCCCCCCCCCCCCCCCCJRP01870
2999    CALL PLOT(0.0,0.0,-3)                                            JRP01880
3000    CALL PLOT(0.0,0.0,999)                                           JRP01890
        STOP                                                              JRP01900
        END                                                              JRP01910
        SUBROUTINE TDS(TD)                                               JRP01920
CCCCCCCCCCCCCCCCCCCCCCCCC DATA FOR TIME DIFF. CONVERSION CCCCCCCCCCCCCCCCCCCJRP01930
        DIMENSION TD(4)                                                   JRP01940
        REAL*8 PHIM,GAMM,PHIW,GAMW,PHIX,GAMX,PHIY,GAMY,PHIZ,GAMZ          JRP01950
        DATA PHIM,GAMM/0.7455002761,1.340870724/                         JRP01960
        DATA PHIW,GAMW/0.8169491590,1.185559303/                         JRP01970
        DATA PHIX,GAMX/0.7200063971,1.221345098/                         JRP01980
        DATA PHIY,GAMY/0.5945057338,1.359840319/                         JRP01990
        DATA PHIZ,GAMZ/0.6955476439,1.526928009/                         JRP02000
        DATA CDRW/1.379724E4/                                            JRP02010
        DATA CDRX/2.696991E4/                                            JRP02020
        DATA CDRY/4.222161E4/                                            JRP02030
        DATA CDRZ/5.716205E4/                                            JRP02040
        TDM=ARC(PHIM,GAMM)                                               JRP02050
        TD(1)=CDRW+ARC(PHIW,GAMW)-TDM                                     JRP02060
        TD(2)=CDRX+ARC(PHIX,GAMX)-TDM                                     JRP02070
        TD(3)=CDRY+ARC(PHIY,GAMY)-TDM                                     JRP02080
        TD(4)=CDRZ+ARC(PHIZ,GAMZ)-TDM                                     JRP02090
        RETURN                                                            JRP02100
CCCCCCCCCCCCCCCCCCCCCCCCCCCCCCCCCCCCCCCCCCCCCCCCCCCCCCCCCCCCCCCCCCCCCCCCCCCJRP02110
CCCCCCCCCCCCCCCCCCCCCCCCC TESTING ROUTINE CCCCCCCCCCCCCCCCCCCCCCCCCCCCCCCCCCJRP02120
        END                                                              JRP02130
        SUBROUTINE TEST(XLAT,XLONG,X,Y,I3,IERROR)                        JRP02140
        IF(Y.GE.(XLAT-1.5))I3=1                                          JRP02150
        IF(Y.LE.1.375)I3=1                                               JRP02160
        IF(X.GE.(XLONG-1.0))I3=1                                         JRP02170
        IF(X.LE.1.5)I3=1                                                 JRP02180
        IF(IERROR.EQ.-1)I3=2                                             JRP02190
        RETURN                                                            JRP02200
```

```
CCCCCCCCCCCCCCCCCCCCCCCCCCCCCCCCCCCCCCCCCCCCCCCCCCCCCCCCCCCCCCCCCCCCCCJRP02210
CCCCCCCCCCCCCCCCCCCCCCCCCCC DATA FOR LAT. , LONG CONVERSION CCCCCCCCCCCJRP02220
           END                                                       JRP02230
           SUBROUTINE DATAWX                                         JRP02240
           COMMON/CHAIND/DEL(2),A5,A6,AD(8),DM(8),CS(8)              JRP02250
           DEL(1)=11.0E3                                             JRP02260
           DEL(2)=25.0E3                                             JRP02270
           A5=2.1275406E4                                            JRP02280
           A6=2.1203281E4                                            JRP02290
           AD(1)=42.0                                                JRP02300
           AD(2)=76.0                                                JRP02310
           AD(3)=46.0                                                JRP02320
           AD(4)=67.0                                                JRP02330
           AD(5)=42.0                                                JRP02340
           AD(6)=76.0                                                JRP02350
           AD(7)=41.0                                                JRP02360
           AD(8)=69.0                                                JRP02370
           DM(1)=42.0                                                JRP02380
           DM(2)=49.0                                                JRP02390
           DM(3)=49.0                                                JRP02400
           DM(4)=55.0                                                JRP02410
           DM(5)=42.0                                                JRP02420
           DM(6)=49.0                                                JRP02430
           DM(7)=15.0                                                JRP02440
           DM(8)=58.0                                                JRP02450
           CS(1)=50.47                                               JRP02460
           CS(2)=34.44                                               JRP02470
           CS(3)=27.86                                               JRP02480
           CS(4)=39.16                                               JRP02490
           CS(5)=50.47                                               JRP02500
           CS(6)=34.44                                               JRP02510
           CS(7)=11.98                                               JRP02520
           CS(8)=40.51                                               JRP02530
           RETURN                                                    JRP02540
           END                                                       JRP02550
           SUBROUTINE DATAXY                                         JRP02560
           COMMON/CHAIND/DEL(2),A5,A6,AD(8),DM(8),CS(8)              JRP02570
           DEL(1)=25.0E3                                             JRP02580
           DEL(2)=39.0E3                                             JRP02590
           A5=2.128260E4                                             JRP02600
           A6=2.121045E4                                             JRP02610
           AD(1)=42.0                                                JRP02620
           AD(2)=76.0                                                JRP02630
           AD(3)=41.0                                                JRP02640
           AD(4)=69.0                                                JRP02650
           AD(5)=42.0                                                JRP02660
           AD(6)=76.0                                                JRP02670
           AD(7)=34.0                                                JRP02680
           AD(8)=77.0                                                JRP02690
           DM(1)=42.0                                                JRP02700
           DM(2)=49.0                                                JRP02710
           DM(3)=15.0                                                JRP02720
           DM(4)=58.0                                                JRP02730
           DM(5)=42.0                                                JRP02740
           DM(6)=49.0                                                JRP02750
```

```
        DM(7)=3.0                                              JRP02760
        DM(8)=54.0                                             JRP02770
        CS(1)=50.47                                            JRP02780
        CS(2)=34.44                                            JRP02790
        CS(3)=11.98                                            JRP02800
        CS(4)=40.51                                            JRP02810
        CS(5)=50.47                                            JRP02820
        CS(6)=33.44                                            JRP02830
        CS(7)=45.61                                            JRP02840
        CS(8)=47.20                                            JRP02850
        RETURN                                                 JRP02860
        END                                                    JRP02870
        SUBROUTINE DATAY7                                      JRP02880
        COMMON/CHAIND/DEL(2),A5,A6,AD(8),DM(8),CS(8)           JRP02890
        DEL(1)=39.0E3                                          JRP02900
        DEL(2)=54.0E3                                          JRP02910
        A5=2.129260E4                                          JRP02920
        A6=2.121045E4                                          JRP02930
        AD(1)=42.0                                             JRP02940
        AD(2)=76.0                                             JRP02950
        AD(3)=34.0                                             JRP02960
        AD(4)=77.0                                             JRP02970
        AD(5)=42.0                                             JRP02980
        AD(6)=76.0                                             JRP02990
        AD(7)=39.0                                             JRP03000
        AD(8)=87.0                                             JRP03010
        DM(1)=42.0                                             JRP03020
        DM(2)=49.0                                             JRP03030
        DM(3)=03.0                                             JRP03040
        DM(4)=54.0                                             JRP03050
        DM(5)=42.0                                             JRP03060
        DM(6)=49.0                                             JRP03070
        DM(7)=51.0                                             JRP03080
        DM(8)=29.0                                             JRP03090
        CS(1)=50.47                                            JRP03100
        CS(2)=34.44                                            JRP03110
        CS(3)=45.96                                            JRP03120
        CS(4)=46.76                                            JRP03130
        CS(5)=50.47                                            JRP03140
        CS(6)=34.44                                            JRP03150
        CS(7)=07.46                                            JRP03160
        CS(8)=12.14                                            JRP03170
        RETURN                                                 JRP03180
        END                                                    JRP03190
        SUBROUTINE NEWDAT(I7,I,I2,J,J2)                        JRP03200
        COMMON/CHAIND/DEL(2),A5,A6,AD(8),DM(8),CS(8)           JRP03210
        IF(I7-2)10,20,30                                       JRP03220
10      I=1                                                    JRP03230
        J=2                                                    JRP03240
        I2=1                                                   JRP03250
        J2=2                                                   JRP03260
        CALL DATAWX                                            JRP03270
        GOTO40                                                 JRP03280
20      I=2                                                    JRP03290
        J=3                                                    JRP03300
```

105

```
        I2=1                                                            JRP03310
        J2=2                                                            JRP03320
        CALL DATAXY                                                     JRP03330
        GOTO 40                                                         JRP03340
30      IF(I7.EQ.4)GOTO 35                                              JRP03350
        I=3                                                             JRP03360
        J=4                                                             JRP03370
        I2=1                                                            JRP03380
        J2=2                                                            JRP03390
        CALL DATAYZ                                                     JRP03400
        GOTO 40                                                         JRP03410
35      I=4                                                             JRP03420
        J=3                                                             JRP03430
        I2=2                                                            JRP03440
        J2=1                                                            JRP03450
        CALL DATAYZ                                                     JRP03460
40      RETURN                                                          JRP03470
CCCCCCCCCCCCCCCCCCCCCCCCCCCCCCCCCCCCCCCCCCCCCCCCCCCCCCCCCCCCCCCCCCCCCCCCJRP03480
CCCCCCCCCCCCCCCCCCCCC CONVERSION ROUTINE CCCCCCCCCCCCCCCCCCCCCCCCCCCCCCCCJRP03490
        END                                                             JRP03500
        SUBROUTINE CONVER(TH,POS,DRPOS,IERROR,YCP,XCP1,YIP,XIP1,X,Y,B,A) JRP03510
        DIMENSION TH(4),POS(2),DRPOS(2)                                 JRP03520
        CALL TOPOS(TH,POS,DRPOS,IERROR)                                 JRP03530
        DO 10 K=1,2,1                                                   JRP03540
10      DRPOS(K)=POS(K)                                                 JRP03550
        X=((POS(2)-XIP1)*B)+XCP1                                        JRP03560
        Y=((POS(1)-YIP)*A)+YCP                                          JRP03570
20      RETURN                                                          JRP03580
CCCCCCCCCCCCCCCCCCCCCCCCCCCCCCCCCCCCCCCCCCCCCCCCCCCCCCCCCCCCCCCCCCCCCCCCJRP03590
        END                                                             JRP03600
```

APPENDIX B. Listing of TDPOS Program

```
      SUBROUTINE TDPOS(TH,POS,DRPOS,IERROR)                          TDP00010
      DIMENSION IQSV(2),QSV(2),ANG(8),AD(8),OM(8),CS(8),POS(2),ZIWD(2),FTDP00020
     :WM(2),DEL(2),IDR(2),DRD(2),DRM(2),TH(2),A(11),B(11),C(11),D(11),E(TDP00030
     :11),CC(11),TM(2),BLEM(2),BEDEL(2),RADR(2),BETA(2),OMG(2),TWD(2),IDTDP00040
     :PO(2),DRPOS(2)                                                  TDP00050
C  -                                                                 TDP00060
      DATA A1/24.0305/,A2/-0.40758/,A3/3.46776E-3/,B1/0.510483/,B2/-0.01TDP00070
     :1402/,B3/0.001760/,RD/1.745329E-2/,RM/2.908882E-4/,RS/4.848137E-6/TDP00080
     :,PI/3.141592/,A4/2.996912E2/                                    TDP00090
C  -                                                                 TDP00100
      COMMON/CHAIND/DEL,A5,A6,AD,OM,CS                               TDP00110
C  -                                                                 TDP00120
C  - BEGIN TIME DIFFERENCE TO POSITION CONVERSION.                  TDP00130
C  -                                                                 TDP00140
      DO 1 I=1,2                                                     TDP00150
      IDRD(I)=DRPOS(I)                                               TDP00160
      DRD(I)=IDRD(I)                                                 TDP00170
    1 DRM(I)=(DRPOS(I)-DRD(I))*60.0                                  TDP00180
      IERROR=1                                                       TDP00190
      A10=(A5*A5-A6*A6)/(A5*A5)                                      TDP00200
      A14=1.0-A6/A5                                                  TDP00210
      A50=(1.0+A14+A14*A14)                                          TDP00220
      A51=(A50-1.0)                                                  TDP00230
      A52=(A14*A14)/2.0                                              TDP00240
      A53=-A51/2.0                                                   TDP00250
      A54=(A14*A14)/16.0                                             TDP00260
      A55=(A14*A14)/8.0                                              TDP00270
      A56=A14*A14                                                    TDP00280
      A57=A56*1.25                                                   TDP00290
      A58=A56/4.0                                                    TDP00300
      DO 128 K=1,8                                                   TDP00310
      IF(AD(K))124,126,126                                           TDP00320
  124 ANG(K)=RD*AD(K)-RM*OM(K)-RS*CS(K)                              TDP00330
      GO TO 128                                                      TDP00340
  126 ANG(K)=RD*AD(K)+RM*OM(K)+RS*CS(K)                              TDP00350
  128 CONTINUE                                                       TDP00360
      A12=(ANG(1)-ANG(5)+ANG(2)-ANG(6))                             TDP00370
      A12=ABS(A12)                                                   TDP00380
      IF(A12-0.00001)7,7,8                                          TDP00390
    7 A11=-1.0                                                       TDP00400
      GO TO 9                                                        TDP00410
    8 A11=1.0                                                        TDP00420
C  -                                                                 TDP00430
C  - APPROXIMATE POSITIONS AND STATION COORDINATES.                 TDP00440
C  -                                                                 TDP00450
    9 E(1)=ANG(1)                                                    TDP00460
      E(2)=ANG(2)                                                    TDP00470
      CC(1)=ANG(3)                                                   TDP00480
      CC(2)=ANG(4)                                                   TDP00490
      E(3)=SIN(E(1))                                                 TDP00500
      E(4)=COS(E(1))                                                 TDP00510
      E(5)=E(3)/E(4)                                                 TDP00520
      E(8)=(E(5))*(1.0-A14)                                          TDP00530
      A62=ATAN(E(8))                                                 TDP00540
      E(6)=SIN(A62)                                                  TDP00550
```

```
        F(7)=COS(A62)                                  TOP00560
        CC(3)=SIN(CC(1))                               TOP00570
        CC(4)=COS(CC(1))                               TOP00580
        CC(5)=CC(3)/CC(4)                              TOP00590
        CC(8)=(CC(5))*(1.0-A14)                        TOP00600
        A62=ATAN(CC(8))                                TOP00610
        CC(6)=SIN(A62)                                 TOP00620
        CC(7)=COS(A62)                                 TOP00630
        I=1                                            TOP00640
        GO TO 500                                      TOP00650
   15   F(9)=A35                                       TOP00660
        F(10)=A46                                      TOP00670
        F(11)=A47                                      TOP00680
        DO 17 J=1,11                                   TOP00690
        A(J)=F(J)                                      TOP00700
   17   B(J)=CC(J)                                     TOP00710
        F(1)=ANG(5)                                    TOP00720
        F(2)=ANG(6)                                    TOP00730
        CC(1)=ANG(7)                                   TOP00740
        CC(2)=ANG(8)                                   TOP00750
        F(3)=SIN(F(1))                                 TOP00760
        F(4)=COS(F(1))                                 TOP00770
        F(5)=F(3)/F(4)                                 TOP00780
        F(8)=(F(5))*(1.0-A14)                          TOP00790
        A62=ATAN(F(8))                                 TOP00800
        F(6)=SIN(A62)                                  TOP00810
        F(7)=COS(A62)                                  TOP00820
        CC(3)=SIN(CC(1))                               TOP00830
        CC(4)=COS(CC(1))                               TOP00840
        CC(5)=CC(3)/CC(4)                              TOP00850
        CC(8)=(CC(5))*(1.0-A14)                        TOP00860
        A62=ATAN(CC(8))                                TOP00870
        CC(6)=SIN(A62)                                 TOP00880
        CC(7)=COS(A62)                                 TOP00890
        I=2                                            TOP00900
        GO TO 500                                      TOP00910
   19   F(9)=A35                                       TOP00920
        F(10)=A46                                      TOP00930
        F(11)=A47                                      TOP00940
        DO 21 J=1,11                                   TOP00950
        C(J)=F(J)                                      TOP00960
   21   D(J)=CC(J)                                     TOP00970
        TM(1)=A(10)+A(11)                              TOP00980
        TM(2)=C(10)+C(11)                              TOP00990
        DO 45 M=1,2                                    TOP01000
        BETA(M)=TM(M)                                  TOP01010
        BEDEL(M)=BETA(M)+DEL(M)                        TOP01020
   45   ALEM(M)=BETA(M)+BEDEL(M)                       TOP01030
        IOSV(1)=99999                                  TOP01040
        IOSV(2)=99999                                  TOP01050
        ITER=0                                         TOP01060
   82   SDR=DRD(1)+DRM(1)+DRD(2)+DRM(2)                TOP01070
        IF(SDR)83,84,83                                TOP01080
   83   DO 30 K=1,2                                    TOP01090
        IF(DRD(K))32,34,34                             TOP01100
```

```
32  RADR(K)=RD*DRD(K)-RM*DRM(K)                                    TOPO1110
    GO TO 30                                                       TOPO1120
34  RADR(K)=RD*DRD(K)+RM*DRM(K)                                    TOPO1130
30  CONTINUE                                                       TOPO1140
    F(1)=RADR(1)                                                   TOPO1150
    F(2)=RADR(2)                                                   TOPO1160
    A28=-1.0                                                       TOPO1170
94  F(3)=SIN(F(1))                                                 TOPO1180
    F(4)=COS(F(1))                                                 TOPO1190
    F(5)=F(3)/F(4)                                                 TOPO1200
    F(8)=(F(5))*(1.0-A14)                                          TOPO1210
    A62=ATAN(F(8))                                                 TOPO1220
    F(6)=SIN(A62)                                                  TOPO1230
    F(7)=COS(A62)                                                  TOPO1240
    DO 86 J=1,8                                                    TOPO1250
86  CC(J)=D(J)                                                     TOPO1260
    I=3                                                            TOPO1270
    GO TO 500                                                      TOPO1280
90  C1=A35                                                         TOPO1290
    C2=A44                                                         TOPO1300
    C3=A45                                                         TOPO1310
    C101=A47                                                       TOPO1320
    DO 92 J=1,8                                                    TOPO1330
92  CC(J)=C(J)                                                     TOPO1340
    I=4                                                            TOPO1350
    GO TO 500                                                      TOPO1360
95  C4=A35                                                         TOPO1370
    C5=A44                                                         TOPO1380
    C6=A45                                                         TOPO1390
    C104=A47                                                       TOPO1400
    DO 50 J=1,8                                                    TOPO1410
50  CC(J)=B(J)                                                     TOPO1420
    I=5                                                            TOPO1430
    GO TO 500                                                      TOPO1440
55  C7=A35                                                         TOPO1450
    C8=A44                                                         TOPO1460
    C9=A45                                                         TOPO1470
    C107=A47                                                       TOPO1480
    IF(A11)52,90,53                                                TOPO1490
53  C10=C7                                                         TOPO1500
    C11=C8                                                         TOPO1510
    C12=C9                                                         TOPO1520
    C110=C107                                                      TOPO1530
    DO 63 J=1,8                                                    TOPO1540
63  CC(J)=A(J)                                                     TOPO1550
    I=6                                                            TOPO1560
    GO TO 500                                                      TOPO1570
65  C7=A35                                                         TOPO1580
    C8=A44                                                         TOPO1590
    C9=A45                                                         TOPO1600
    C107=A47                                                       TOPO1610
    C13=TH(2)-C(10)-C(11)-C101+C104-DEL(2)                         TOPO1620
    C17=C13*A4                                                     TOPO1630
    C18=TH(1)-A(10)-A(11)-C110+C107-DEL(1)                         TOPO1640
    C22=C18*A4                                                     TOPO1650
```

```
      DO 4840 M=1,2                                                     TOP02210
      W=OMG(M)/RD                                                       TOP02220
      IWD(M)=W                                                          TOP02230
      FWD=IWD(M)                                                        TOP02240
      DWD=W-FWD                                                         TOP02250
      EWM=DWD*60.0                                                      TOP02260
      FWM(M)=ABS(EWM)                                                   TOP02270
      IF(FWM(M)-59.9995)4840,4810,4810                                 TOP02280
 4810 FWM(M)=0.0                                                       TOP02290
      IF(IWD(M))4820,4830,4830                                         TOP02300
 4820 IWD(M)=IWD(M)-1                                                  TOP02310
      GO TO 4840                                                       TOP02320
 4830 IWD(M)=IWD(M)+1                                                  TOP02330
 4840 CONTINUE                                                         TOP02340
      GO TO 900                                                        TOP02350
C -                                                                    TOP02360
C - CALCULATION OF INVERSE VARIABLES.                                 TOP02370
C -                                                                    TOP02380
  500 A59=-CC(2)                                                       TOP02390
      A60=-F(2)                                                        TOP02400
      C35=A59-A60                                                      TOP02410
      C36=ABS(C35)                                                     TOP02420
      IF(C36-PI)501,502,502                                           TOP02430
  502 A16=2.0*PI-C36                                                  TOP02440
      GO TO 505                                                       TOP02450
  501 A16=C36                                                         TOP02460
  505 IF(A16)506,507,506                                             TOP02470
  507 A16=0.00000005                                                 TOP02480
  506 A17=SIN(A16)                                                   TOP02490
      A18=COS(A16)                                                   TOP02500
      A19=F(6)*CC(6)                                                 TOP02510
      A20=F(7)*CC(7)                                                 TOP02520
      A21=A19+A20*A18                                                TOP02530
      A22=((A17*CC(7))**2+(CC(6)*F(7)-F(6)*CC(7)*A18)**2)**0.5        TOP02540
      A23=(A20*A17)/A22                                              TOP02550
      A24=1.0-A23*A23                                                TOP02560
      A25=ARSIN(A22)                                                 TOP02570
      A26=A25*A25                                                    TOP02580
      A27=1.0/A22                                                    TOP02590
      A28=A21/A22                                                    TOP02600
      A29=A24*A24                                                    TOP02610
      A30=(A50*A25)+A19*(A51*A22-A52*A26*A27)                        TOP02620
      A31=A24*(A53*A25+A53*A22*A21+A52*A26*A28)                      TOP02630
      A32=A19*A19*(-A52*A21*A22)                                     TOP02640
      A33=A29*(A54*A25+A54*A21*A22-A52*A26*A28-A55*A22*(A21**3))      TOP02650
      A34=A19*A24*(A52*A26*A27+A52*A22*A21*A21)                      TOP02660
      A35=(A30+A31+A32+A33+A34)*A6*A4                                TOP02670
      A36=(A51*A25)+A19*(-A52*A22-A14*A14*A26*A27)                   TOP02680
      A37=A24*(-A57*A25+A58*A22*A21+A14*A14*A24*A28)                 TOP02690
      A38=(A36+A37)*A23+A16                                          TOP02700
      A39=SIN(A38)                                                   TOP02710
      A40=COS(A38)                                                   TOP02720
      A41=(CC(6)*F(7)-A40*F(6)*CC(7))/(A39*CC(7))                    TOP02730
      IF(A41)510,509,510                                             TOP02740
  509 A41=0.00000005                                                 TOP02750
```

110

```
          C23=C1-C17                                              TOP01660
          C24=C4                                                  TOP01670
          C25=C7+C22                                              TOP01680
          C26=C10                                                 TOP01690
          C27=((C2-C5)*(C25-C26)+(C23-C24)*(C11-C8))             TOP01700
          C29=((C2-C5)*(C12-C9)+(C3-C6)*(C8-C11))               TOP01710
          C30=C27/C29                                             TOP01720
          C28=(C23-C24+C30*(C3-C6))/(C5-C2)                      TOP01730
          GO TO 130                                               TOP01740
   52     C13=TH(2)-C(10)-C(11)-C101+C104-DEL(2)                 TOP01750
          C17=C13*A4                                              TOP01760
          C18=TH(1)-A(10)-A(11)-C107+C104-DEL(1)                 TOP01770
          C22=C18*A4                                              TOP01780
          C23=C1-C17                                              TOP01790
          C24=C4                                                  TOP01800
          C25=C7-C22                                              TOP01810
          C27=(C2*(C25-C24)+C23*(C5-C8)+C8*C24-C5*C25)          TOP01820
          C29=(C2*(C6-C9)+C3*(C8-C5)+C5*C9-C8*C6)               TOP01830
          C30=C27/C29                                             TOP01840
          C28=(C23-C24+C30*(C3-C6))/(C5-C2)                      TOP01850
  130     C31=(A5*A4*(1.0-A10))/(1.0-A10*F(3)*F(3))**1.5        TOP01860
          C32=(A5*A4)/(1.0-A10*F(3)*F(3))**0.5                  TOP01870
          C33=(C30/C31)                                          TOP01880
          C34=(-C28/(C32*F(4)))                                 TOP01890
          F(1)=F(1)+C33                                          TOP01900
          F(2)=F(2)+C34                                          TOP01910
          IF(A28)132,99,134                                     TOP01920
  132     A29=1.0                                                TOP01930
          GO TO 84                                               TOP01940
C -                                                              TOP01950
C - CONVERSION DONE, RETURN TO DISTANCE-BEARING ROUTINE.        TOP01960
C -                                                              TOP01970
  200     IF(IOSV(1).NE.IWD(1))GO TO 7713                       TOP01980
          IF(IOSV(2).NE.IWD(2))GO TO 7713                       TOP01990
          IF(ABS(QSV(1)-FWM(1)).GT.0.1)GO TO 7713               TOP02000
          IF(ABS(QSV(2)-FWM(2)).GT.0.1)GO TO 7713               TOP02010
          IDR(1)=IDR(1)*10                                       TOP02020
          DO 839 I=1,2                                           TOP02030
          ZIWD(I)=IWD(I)                                         TOP02040
  839     POS(I)=ZIWD(I)+FWM(I)/60.0                            TOP02050
          RETURN                                                 TOP02060
C -                                                              TOP02070
C - CONTINUE ITERATIONS.                                        TOP02080
C -                                                              TOP02090
 7713     DO 7712 M=1,2                                          TOP02100
          DRD(M)=0.0                                             TOP02110
          DRM(M)=0.0                                             TOP02120
          OSV(M)=FWM(M)                                          TOP02130
 7712     IQSV(M)=IWD(M)                                        TOP02140
          ITER=ITER+1                                            TOP02150
          IF(ITER.LT.100)GO TO 82                               TOP02160
          IERROR=-1                                              TOP02170
          RETURN                                                 TOP02180
  134     OMG(1)=F(1)                                           TOP02190
          OMG(2)=F(2)                                           TOP02200
```

111

```
  510  A42=1.0/A41                                              TOPO2760
       A43=ATAN(A42)                                            TOPO2770
       IF(C35)515,514,514                                       TOPO2780
  514  IF(C35-PI)511,512,512                                    TOPO2790
  511  IF(A41)520,521,521                                       TOPO2800
  520  A43=PI+A43                                               TOPO2810
       GO TO 521                                                TOPO2820
  512  IF(A41)517,518,518                                       TOPO2830
  515  IF(C35+PI)511,511,516                                    TOPO2840
  516  IF(A41)517,518,518                                       TOPO2850
  517  A43=PI-A43                                               TOPO2860
       GO TO 521                                                TOPO2870
  518  A43=2.0*PI-A43                                           TOPO2880
  521  A43=A43+PI                                               TOPO2890
       A43=A43-2.0*PI                                           TOPO2900
       IF(A43)522,523,523                                       TOPO2910
  522  A43=A43+2.0*PI                                           TOPO2920
  523  A44=SIN(A43)                                             TOPO2930
       A45=COS(A43)                                             TOPO2940
       A46=A35/1609.344                                         TOPO2950
       IF(A46-100.0)525,526,526                                 TOPO2960
  525  A47=B1/A46+B2+B3*A46                                     TOPO2970
       GO TO 527                                                TOPO2980
  526  A47=A1/A46+A2+A3*A46                                     TOPO2990
  527  A46=A35/A4                                               TOPO3000
       GO TO(15,19,90,95,55,65),I                               TOPO3010
   99  RETURN                                                   TOPO3020
       END                                                      TOPO3030
```

112

STANDARD AVIATION SECTIONAL

114
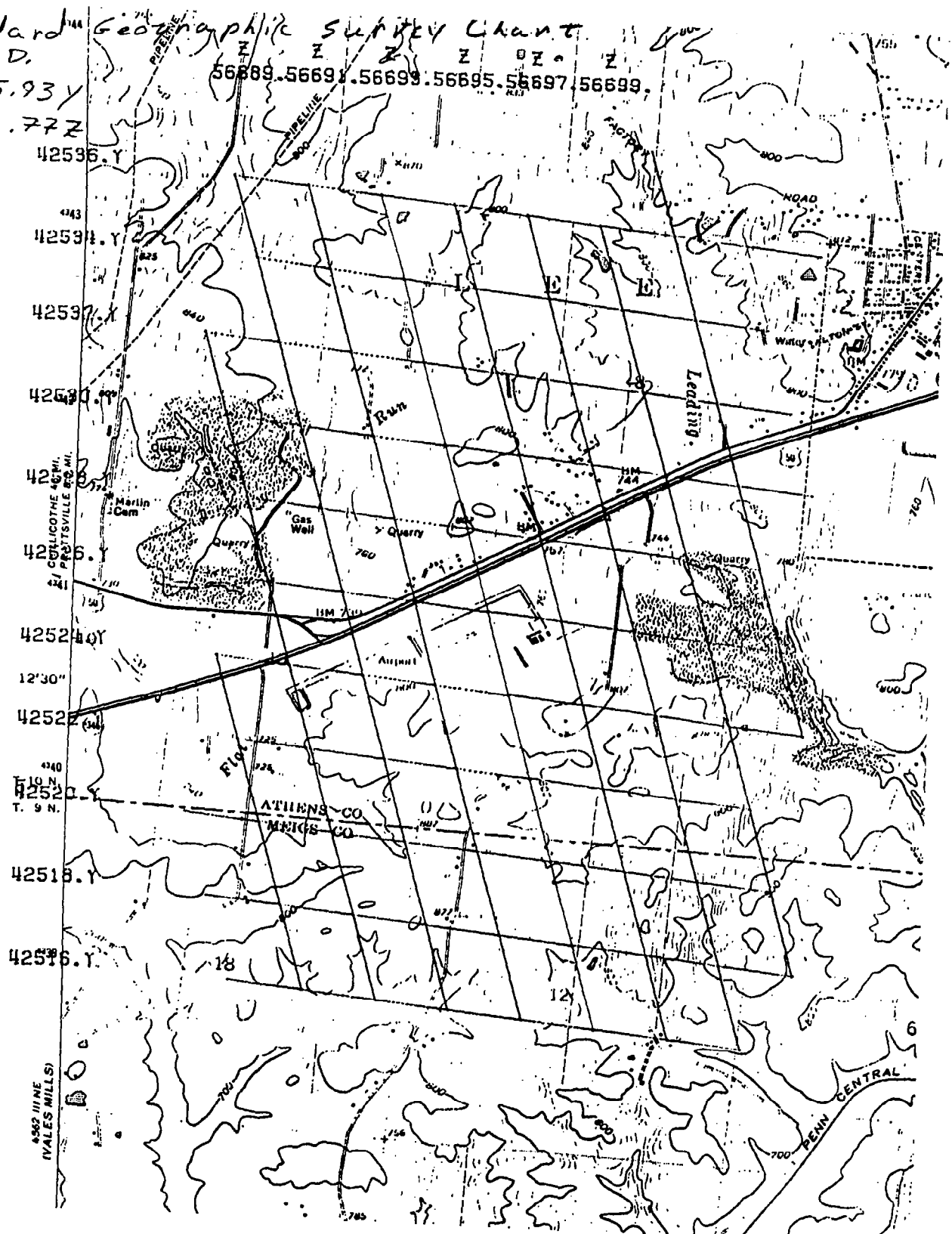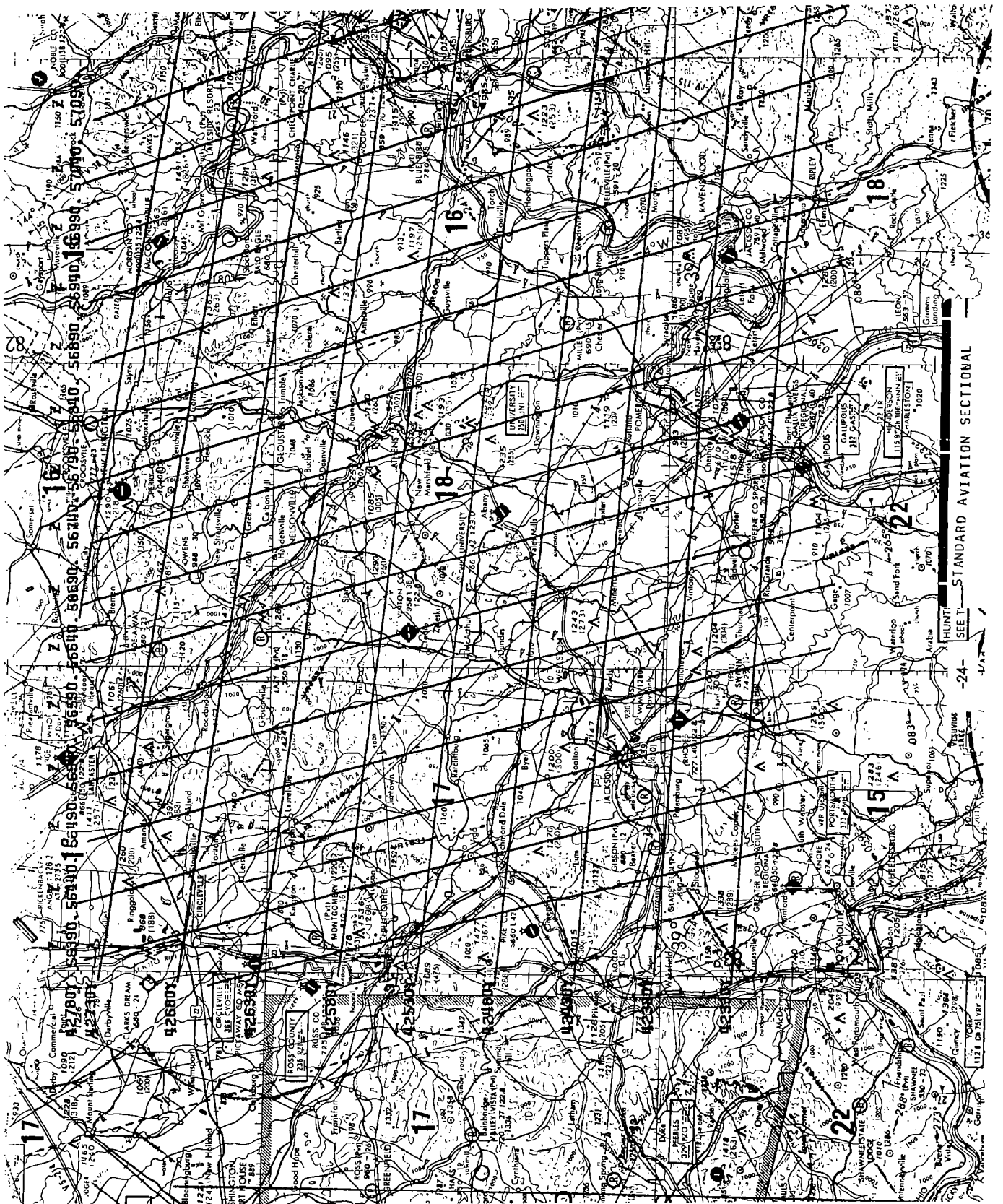
TECHNICAL MEMORANDUM OU NASA 79

AUTOMATIC GAIN CONTROL

An automatic gain control has been designed and fabricated to operate with the Loran-C prototype receiver and data collection system currently in use at Ohio University.

James P. Roman

Avionics Engineering Center
Department of Electrical Engineering
Ohio University
Athens, Ohio 45701

I. INTRODUCTION

The NASA Tri-University program at Ohio University is currently involved in the development of a low-cost Loran-C receiver for use in general aviation aircraft. An automatic gain control (AGC) has been designed and built to operate with the prototype Loran-C receiver.

Since there are such extreme distances between Loran stations, the signal strengths coming into the user are at different magnitudes. It is advantageous to have the signal magnitudes equal; therefore, the automatic gain control was designed for the front end of the prototype Loran-C receiver.

II. CIRCUIT DESCRIPTION

The automatic gain control is a three-transistor circuit (see Figure 1) which requires a constant D.C. voltage of 8 volts. Tests conclude that this value may be in the range of 4 to 12 V without change in circuit performance. Transistors Q_1 and Q_2 are cascaded to pass and amplify the input signal. The gain of Q_1 and Q_2 is controlled by Q_3 which itself is controlled by an external AGC voltage between 0 and 8 volts D.C. The integrated circuit used is an RCA CA3028A, an 8-pin chip, which is a differential cascode amplifier designed for use in communications operating at frequencies from D.C. to 120 MHz. The integrated circuit has been balanced for AGC capabilities, and has a wide operating current range. The maximum input current at pins 1 and 5 is 0.1 mA. The absolute maximum dissipation at $T_a \leq 85°$ C is 450 mW. At $T_a > 85°$ C the integrated circuit is derated linearly 5 mW/° C. The ambient temperature for operation is -55° C to +125° C and -65° C to +150° C for storage.

III. TEST RESULTS

1. Gain Vs. Frequency and Phase Angle Vs. Frequency (Figure 2)

The frequency response and phase angle is measured with the input signal voltage held constant at 50 mV, and is an average of all AGC voltages from 1 V to 8 V. The band width of the automatic gain control is 20 KHz to 2 MHz, with a standard deviation of no greater than ± 0.4 dB. The phase angle increases linearly at frequencies between 70 KHz to 120 KHz, from 0° to +21.6° respectively.

2. Gain Vs. AGC Voltage (Figure 3)

This test was performed at a constant frequency of 105.4 KHz and a constant input signal voltage of 50 mV. The gain is approximately -26 dB from 0 to +2.5 volts, between 1 and 2.5 volts the gain increases rapidly from -22 dB to +2.5 dB, between 3 and 8 volts the gain increases from 2.5 dB to 25 dB. Distortion and gain compression occurs at 8.4 volts AGC and loss of gain occurs at AGC voltages greater than 12 volts.

116

3. Gain Vs. Signal Voltage (Figure 4)

This test was performed at a constant frequency of 100 KHz and is an average of AGC voltages from 3 to 8 volts. The operating recommended input voltages are between 5mV and 75 mV. In this range there was a constant gain with a standard deviation of only ± 0.109 dB.

4. Power Dissipation and Circuit Resistance

This test was performed at a frequency of 100 KHz with an input signal voltage of 50 mV. The circuit draws 50 mA constant current. The D.C. power dissipation was 59 mW (Max. $P_{D.C.}$ dissipation 450 mW). A.C. current at pins 1 and 5 is approximately 61.21 μ A at 100 KHz. The A.C. power dissipation is approximately 3.035×10^{-6} watts with a power factor of .9 leading calculated error for A.C. power is 4.1%.

Circuit Resistance
Input Resistance $R_i' = 140 \ \Omega$
Output Resistance $R_o' = 740 \ \Omega$

IV. SUMMARY

The automatic gain control was designed specifically to operate with the prototype Loran-C receiver and data collection system. The use of the automatic gain control is intended to eliminate error which occurs when signals are received at different magnitudes.

V. ACKNOWLEDGEMENTS

VI. BIBLIOGRAPHY

"R.C.A. Integrated Circuits", R.C.A. Solid State, Somerville, New Jersey, Pub. 1976.
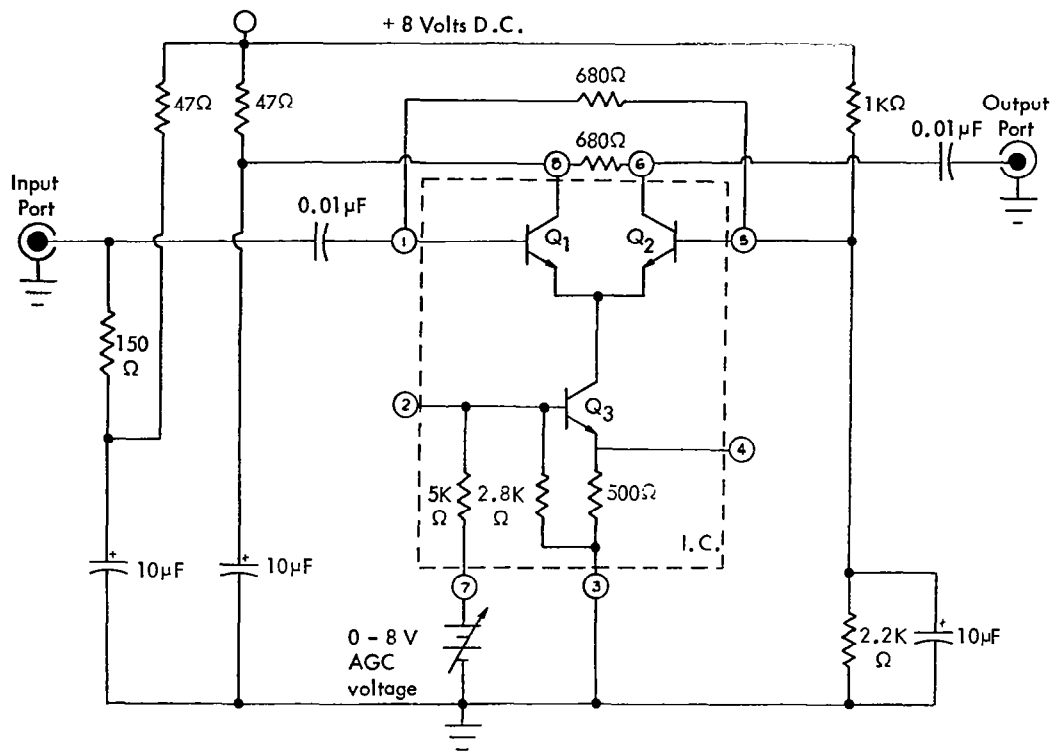
Figure 1. Automatic Gain Control Circuit.
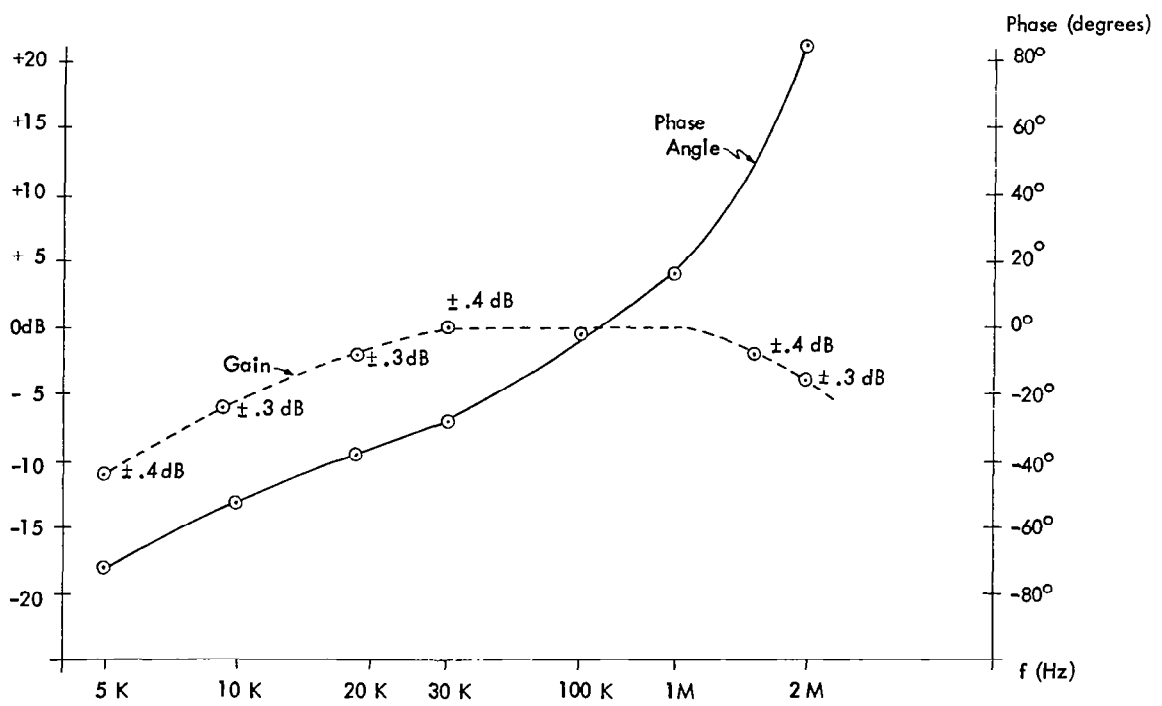
Figure 2. Phase Angle Vs. Frequency.

Gain (dB)

Gain Compression
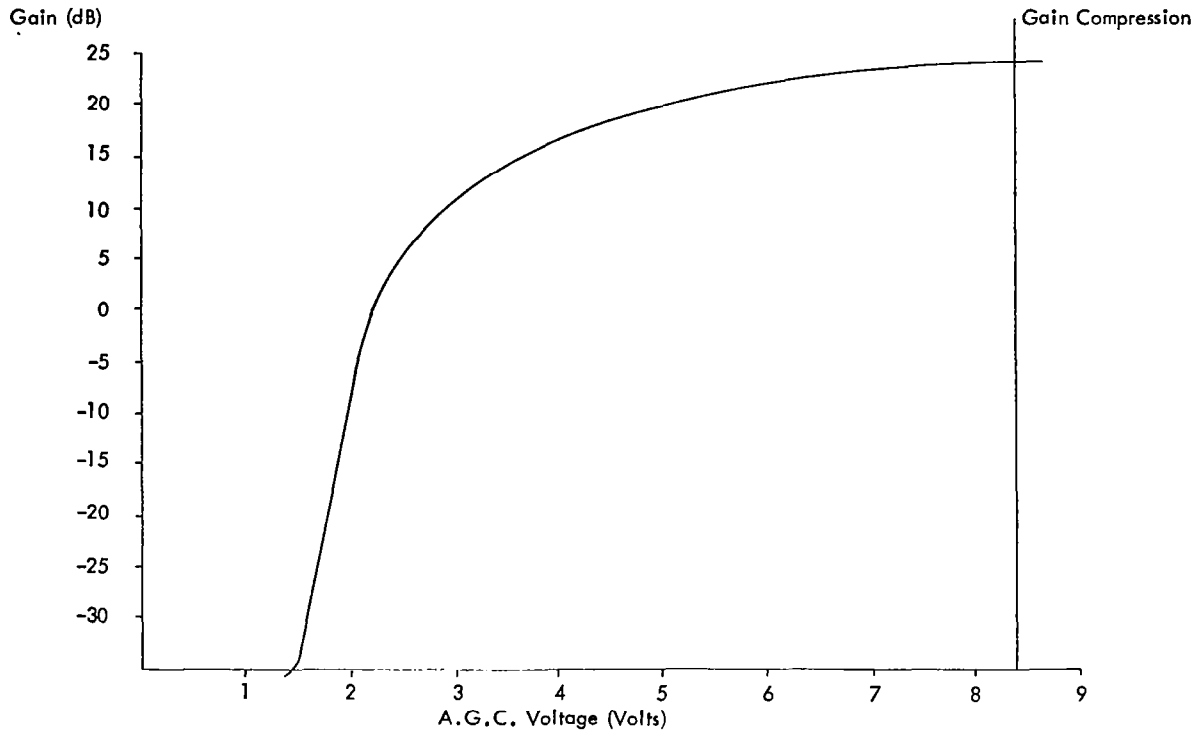
A.G.C. Voltage (Volts)

Figure 3. Gain Vs. A.G.C. Voltage.

Gain Vs. Signal Magnitude
f = 100 KHz

Gain (dB)

Gain Compression

Input Signal Voltage (mV)
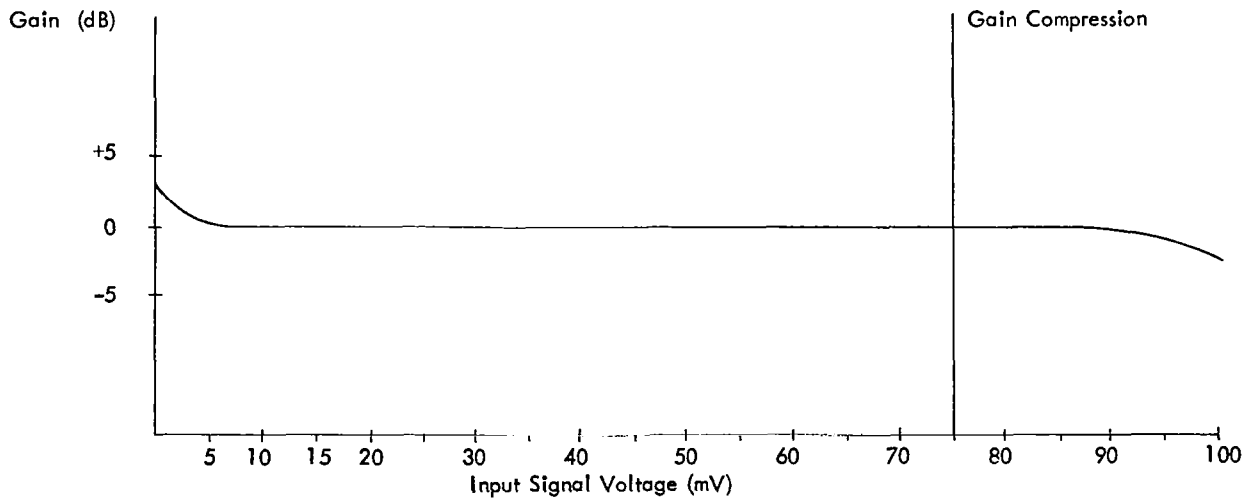
Figure 4. Gain Vs. Signal Voltage.

119

A LORAN-C PROTOTYPE NAVIGATION RECEIVER

FOR GENERAL AVIATION

The design, fabrication and evaluation of a proto-
type Loran-C receiver is described. Hardware is
complete, and microcomputer programming continues,
for addition of area-navigation capability. The
receiver is an envelope-processor, offering simpli-
city of RF processor circuitry.

Robert W. Lilley
Daryl L. McCall

Avionics Engineering Center
Department of Electrical Engineering
Ohio University
Athens, Ohio 45701

I. INTRODUCTION

The Avionics Engineering Center, Ohio University Department of
Electrical Engineering, has pursued the techniques required for
Loran-C navigation with application to the general-aviation pilot.
The goal has been to produce prototype equipment for flight evaluation
which will provide enroute navigation in both latitude-longitude and
rho-theta coordinates and to evaluate the non-precision approach capa-
bilities of such equipment.

For this prototype project, single-chain, master-dependent
operation was chosen as a demonstration mode, with three stations
tracked. The prototype hardware design will, however, permit cross-
chain, master-independent navigation. The number of stations tracked
simultaneously can be expanded. These extended operating modes are
implemented through programming utilizing existing shared tracking-
loop hardware as described below.

The prototype Loran-C receiver has been flight-tested using a
variety of flight paths, with and without simultaneous ground radar
position data collection. Results are presented later in this paper;
further flight evaluation is planned, and will be reported separately.

The following sections describe major receiver elements,
drawing upon the work and publications of project team members who
contributed to the design.

II. RECEIVER OVERVIEW

As configured for laboratory and flight evaluation (Figure 1),
the prototype Loran-C receiver utilizes an aircraft ADF sense antenna
or similar unit, connected directly to the wide-band preamplifier/
coupler. Signal levels for the linear RF processor are stabilized by
a commutated, sampled AGC element, under control of the receiver com-
puter.

The RF unit performs analog signal processing and conversion to
TTL-compatible output pulses corresponding to Loran-C envelope events.
For the prototype receiver, a commercially-available microcomputer is
utilized for both sensor and navigation processing, plus AGC control.
Computer control and data recording for experimentation are provided
by a hand-held ASCII terminal and either analog or digital cassette
units.

Pilot control of receiver functions is effected through the
panel-mounted keyboard and video display unit, supported by a video
processor board with independent memory. The receiver computer is, in
this prototype implementation, supported by a mathematical function
processor chip, aiding in the coordinate conversion from Loran-C to
geodetic coordinates, and for rho-theta conversions.

III.   ANTENNA PREAMPLIFIER/COUPLER

The Loran-C prototype utilizes the wide-band preamplifier of the type reported by Burhans [1, 2, 3] for connection to either a 1-meter (or larger) whip antenna for laboratory tests or to the existing ADF sense antenna aboard the test aircraft. This preamplifier, illustrated in Figure 2, provides -4.9 dB voltage gain at 100 kHz, matching a High-Z antenna to a 1000 ohm receiver input impedance, and a dynamic range from 0.2 to 10,000 microvolts rms at the input terminal. Preamplifier 3 db points occur at 10 Hz and 8 MHz.

The preamplifier schematic is shown as Figure 3. Input surge protection is provided by the NE-2 bulb at the input terminal. The low-noise JFET drives an open-collector output stage, the load resistor for which is contained in the receiver RF module. Both DC power and signal use the signal coaxial cable connecting the preamplifier to the receiver RF section, eliminating power-supply ground-loop problems.

IV.   LORAN-C RF PROCESSOR

The Loran-C receiver RF processor is based on an auto-correlation envelope detector. The unit is driven by the low-impedance output of the broadband, unity-gain antenna preamplifier. See Figures 4, 5 and 6.

The input circuit is a broad-tuned transformer with a 40kHz bandwidth, centered at 100kHz. The output of this transformer is placed across a 1K ohm potentiometer, the wiper of which controls the amount of signal provided to the trap circuitry. Note that this voltage-divider circuit has created a passive RF gain control, to which the operator has access in the prototype design.

To improve signal-to-noise ratio (with respect to interfering frequencies) of the Loran-C signal, it is desirable to eliminate strong signals close to the 100 kHz region before the RF is actively amplified. This is accomplished by passing the RF through a pair of notch filters. These narrowband filters are centered at 88 kHz and 119 kHz, to eliminate the 88 kHz, 116 kHz, and 122 kHz interfering frequencies affecting the 99600 U.S. Northeast Chain. These interfering frequencies are listed in the May 1980 edition of the Loran-C User Handbook by the U.S. Coast Guard [4].

Current work is underway to investigate distortion products from multiple RF signals and harmonic mixing or multiplying to produce new frequencies that interfere with Loran-C. Research results and documentation of this work will be available from the Avionics Engineering Center through the NASA Joint University Program.

Once the interfering frequencies are minimized, the RF signal is amplified by a tuned RF amplifier. This TL072 operational

amplifier circuit offers +30 dB gain with a 30 kHz bandwidth, centered at 100 kHz. The RF signal flow now branches into two separate paths, to be manipulated separately to create the RF signals required for the LM2111 FM Detector and Limiter. One path drives a T-notch filter tuned to 100 kHz which delays the RF signal and adds the delayed reproduction to the actual incoming RF (delay-and-add). The delayed-and-added signal is then amplified by a broadband, +30 dB gain TL072. This signal path is terminated at one of the RF inputs to the balanced demodulator of the LM2111. The second path drives the RF limiter of the LM2111 (the limiter has +60 dB gain), which in turn provides the signal for the second RF input of the balanced demodulator and the carrier zero-crossing detector.

The LM2111 IC provides a double-balanced active multiplier used as an envelope detector. The demodulated signal is fed to a lowpass RC filter (20 kHz bandwidth), creating the Loran-C envelope, from which the digital output is derived. An envelope level detector produces a digital pulse at the zero crossing of the rising edge of the Loran-C envelope. This pulse, correlated with the zero crossings of the RF carrier (from the output of the LM2111 limiter) produces the digital pulses to be used for signal processing. These pulses are stretched to 70 μsec. to permit the tracking loop search routines to operate efficiently.

V.   TRACKING LOOP HARDWARE

The Loran-C prototype receiver achieves time-difference measurement by use of a software-controlled, shared, digital loop. The block diagram for this loop circuit is shown in Figure 7, and its schematic in Figure 8. A 1 MHz clock drives the 6-digit BCD free-running counter portion of the MOSTEK 50395 integrated circuit, providing the receiver time base. The 6-digit comparator produces an EQ pulse each time the counter and the 6-digit register are identical.

In operation, the microcomputer loads the register with the count corresponding to the desired sample time for loop operation, while the counter continues to run. Equality of counter and register produces an EQ pulse, which is latched as an interrupt request (IRQ) for the microcomputer. At the time the EQ pulse is received, the Loran-C digital envelope signal is also latched, and its value made available to the microcomputer. The microcomputer may then reload the register for the next sample point, a process which has been measured to require 450 μsec. The loop, therefore, is able to detect each envelope pulse, at the 1 msec. Loran-C interval, with sufficient guard time to insure correct operation.

The schematic shows interconnection between the tracking loop and the Super-Jolt (TM) microcomputer, which is used in the prototype receiver for evaluation. Pinouts are detailed in Figure 9. This 8-bit microcomputer is based upon the MOS Technology 6502 CPU chip, running at a 1 MHz clock rate. In the prototype receiver, the computer and loop clocks are obtained from the same TCXO for convenience, but computer software is entirely asynchronous, interrupt-driven code.

The digital loop circuit board is shown in Figure 10. The MOS Technology 50395 is visible as the 40-pin chip, supported by a 7474 latch for IRQ and Loran-C input latching, and one monostable multivibrator, 74123, to stretch the Loran-C digital RF processor outputs to 70 μsec. for loop use. The remaining circuitry provides level shift services, to interface the MOS loop chip to TTL input/output lines for the microcomputer.

The entire loop circuit is operated by one 6520 PIA interface, which is an integral part of the Super-Jolt microcomputer.

VI.   TRACKING LOOP PROGRAMMING

Initially, tracking loop software has been developed to demonstrate correct hardware operation and to provide a basis from which coordinate-conversion and area-navigation routines could be developed. This sensor processor software consists of signal acquisition, tracking and time-difference generation segments, operating on a single Loran-C chain. In the current implementation, three stations are tracked, one of which must be the master station.

Loop routines are initiated at receiver start-up, by user choice of Loran-C chain. This selection, made by entering the group repetition interval (GRI), causes the loop routine to add the GRI, in microseconds, to the loop register upon receipt of each loop interrupt request (IRQ). The result is a series of interrupts, at the GRI rate, with samples of Loran-C input data occurring with each interrupt. Loop arithmetic is continuous; that is, the counter is allowed to overflow at 10^6 counts, with no resulting effect on sample rate.

Each IRQ causes loop software to read the state of the Loran-C latch and to clear the Loran-C and IRQ latches. While in this acquisition mode, the goal of the loop routines is to find correlated signals at the Loran-C latch, compared with the GRI samples. If no occurrence of five contiguous Loran-C ones in 32 GRI frames is found, the acquisition segment modifies the sample time by adding 6,500 μsec. to the register. This addition effectively delays the sample comb by 6,500 μsec., and the test for Loran-C signals is repeated. After an unsuccessful test at the 6,500 μsec. increment, the test is repeated for 36 mini-increments of 33 μsec. each.

With each Loran-C pulse stretched to 70 μsec., acquisition is generally accomplished in less than ten seconds. Once one Loran-C pulse is found, acquisition code passes control to station-track code, which immediately subtracts 2,000 μsec. from the original register contents and repeats the acquisition test. If no pulse is found, the register is increased by 1,000 μsec., and the test repeated. If a pulse is found, 2,000 μsec. is subtracted again. In this manner, the first pulse of each Loran-C station is acquired.

Fine tracking begins at this point, with the station-track routine subtracting one microsecond when the Loran-C data is high, and

adding one microsecond when the Loran-C data is low. A loop filter is inserted at this point, in the form of an up-down software counter, to provide for optimum loop characteristics. Filter parameters are taken from previous theoretical [5] and experimental [6] work, and were chosen as a 5-bit register. When this register overflows, one microsecond is added to the loop register. Upon filter register underflow, one microsecond is subtracted. The result is a low-pass loop filter, with time constant of 4 GRI time periods. Using the first-pulse position in the loop register, determined by the search/track process just described, the station-track segment then generates eight sample pulses, by 1,000 μsec. increments of the loop register, spaced one millisecond apart, and permits correction of the loop register value at each of the eight pulses.

After successful lock to the station, the loop register is incremented by 9035 μsec., and the master 9th pulse is sought by the acquisition test. If found, the current station is labeled as the master, for use by background routines in computing time differences. The register content, representing the time of occurrence of the station first-pulse, is stored for retrieval at the next occurrence of the station's signal.

The loop software then generates a search pulse immediately after the last pulse for the current station, and the search/track process is repeated. The third station is located in the same manner.

In addition to the basic pulse-tracking function, the loop routines also produce a signal-quality number, useful in generating user warnings and assessing receiver operation. A software counter is incremented by one, for each station, when the loop routines must subtract one microsecond to retain lock. This counter is then cleared by background routines after display. In the current implementation, the counter is active for ten GRIs, resulting in a total pulse count opportunity of 80. In ideal conditions, with no noise present on the Loran-C input, the counter should reach one-half the total pulse count, since alternate additions and subtractions of one microsecond would be required to retain lock on each of the station pulses. Significant deviations from this value indicate the potential for loss of lock, and may be used to trigger re-acquisition of the station.

The background routines, which operate with IRQ enabled, execute when the signal-processing software just described is completed for each Loran-C pulse. A BCD buffer for each Loran-C station contains the loop register value generated in the previous GRI; these values are averaged over ten GRI periods, and the slave values subtracted from the master after averaging. The results are displayed as the time differences. The signal quality numbers are displayed also. Time difference data is placed in buffers for use by the latitude-longitude conversion routines.

The initial implementation of tracking loop programs has met the desired objective. The receiver logic has been demonstrated, and

loop parameters measured. It has been determined that the single microprocessor receiver will be capable of five-station tracking plus coordinate conversion, and that ample guard time exists between Loran-C envelope pulses for signal processing to take place, with the microcomputer operating at 1 MHz.

A counter/comparator IC offering faster digit-strobe operation would be a definite aid, as the scan oscillator on this IC is the limiting factor in register loading by the microcomputer.

The software-controlled tracking loop implementation has demonstrated some interesting by-products, in that the loop has applications in time synchronization and navigation audio processing not contemplated at its inception. Use of the loop in IRIG-B time synchronization, for example, has been accomplished with complete success. [7]

VII. VIDEO OUTPUT

A prototype video interface [8], designed specifically for large-character output for cockpit use, has been used throughout the receiver development and evaluation program. Figure 11 shows this video circuit board. With the forthcoming addition of rho-theta area-navigation software, this video interface will be exchanged for a smaller circuit board, able to display both character and graphics data.

Two-page output permits display of Loran-C time-difference data, signal quality and housekeeping data on one video page, and the latitude-longitude and range-bearing waypoint data on the other. With the graphics interface available, CDI information will be displayed on both pages, driven by the bearing-distance coordinate conversion routines.

Figure 12 shows the receiver package, with video monitor and keyboard installed. The Loran-C RF processor will be enclosed under the chassis for isolation from the digital circuitry and the video monitor oscillator, and the digital circuit boards will surround the monitor chassis. The package is standard general-aviation width, for mounting in the vertical stack. The power transformer visible at the rear of the unit is installed for bench testing only, and is not part of the final prototype, which will operate on 14VDC.

VIII. LABORATORY AND FLIGHT EVALUATION

Receiver tests run with a Loran-C simulator have consistently provided receiver time differences within ± 1 μsec. of simulator outputs. These tests have also defined the need for receiver AGC applied station-by-station, due to TD offsets observed for variations in relative signal strength among stations. This AGC circuitry is currently under test.

Flight evaluations, made without AGC circuitry at Ohio University Airport, Athens, Ohio on March 9, 1981 are illustrated in Figures 13 and 14. These graphs are plots of receiver latitude/longitude outputs, converted to range and bearing from a waypoint.

For Figure 13, the waypoint is the calculated latitude and longitude of the runway center point. The flight path begins at point (1), on takeoff roll over the waypoint. The path proceeds on climbout, heading 240° and through pattern turns at 800 feet AGL to crosswind and downwind legs. Downwind is extended to seven miles northeast of the airport, where the aircraft is turned inbound, across the UNI non-directional beacon, 5.3 nautical miles from threshold. A normal low approach is then executed, heading 243, flying visually along the runway centerline.

Following the low approach, a tight turn is made to a close downwind leg, followed by an outbound segment (2) approximately 30° south of centerline. A perpendicular cut across the UNI beacon (3) is then executed, followed by a turn (4) back to the beacon, and a left 270° turn to the inbound approach course. A second low approach along runway centerline is then executed, followed by landing and taxi operations.

The data presented is averaged by the receiver over a ten-GRI time period; approximately one second on the 99600 chain. Positioning repeatability over the UNI NDB and along the approach track are observed to be excellent. Long-term variations along the approach course tend to be well-correlated, with a peak variation of less than 600 feet. Note, however, the offset to the north, resulting in a track parallel to the desired runway centerline track, of approximately one-half mile. This offset has been determined using the laboratory simulator to be due to signal-strength characteristics among Loran-C stations in the local area.

Figure 14 shows Loran-C data, with one-second TD averaging and subsequent latitude/longitude conversion, presented as distance and bearing from the runway. For this flight, a receiver waypoint was determined by placing the aircraft stationary at the runway center point, and entering the resulting receiver latitude and longitude value as the waypoint. The flight then consists of a takeoff and climbout to 1000 feet AGL, on runway heading. Variations noted on this plot are a maximum of 0.4 nmi south of course, and 0.3 nmi to the north.

It should be noted that these flight evaluations were local, short flights to assess basic receiver operation and raw data stability. Current plans call for documented flights, including ground radar tracking for position reference, as soon as AGC circuitry is fully tested.

IX.   CURRENT WORK IN PROGRESS

Tracking loop software changes are contemplated for five-station tracking with master independence. Decoded warning messages will be provided when the master 9th-pulse blink code is available. All valid time differences will be made available to the coordinate-conversion and area-navigation software, so that composite position fixes will be possible.

Initial flight evaluations have shown encouraging results, especially with regard to repeatability. Absolute accuracy in the first field tests suffered due to variations in signal strength among stations. A computer-controlled AGC, acting on each Loran-C envelope pulse and commutated among active stations, has been designed and is under test as of this writing. Initial results show marked improvement, with receiver bias reduced over 75% from operation without AGC, on the 9960 chain in southeastern Ohio.

The latitude/longitude and range/bearing coordinate conversion circuitry and software have been used routinely in receiver evaluation; the documentation for this portion of the receiver will appear [9] as a M.S. thesis in the near future.

Additional flight evaluations are planned, using ground-based radar for position reference data. Techniques and procedures for differential Loran-C are also under study, to determine whether receiver cost may be minimized by permitting a differential setting periodically during a flight, or prior to an approach.

X.   ACKNOWLEDGEMENTS

XI.   REFERENCES

[1]   Burhans, Ralph W., "Active Antenna for the VLF to HF Observer", OÜ NASA TM-65, Avionics Engineering Center, Department of Electrical Engineering, Ohio University, Athens, Ohio 45701, February 1979.

[2]   Burhans, Ralph W., "Active Antenna Coupler for VLF", OU NASA
        TM-70, Avionics Engineering Center, Department of Electrical
        Engineering, Ohio University, Athens, Ohio 45701, November
        1979.

[3]   Burhans, Ralph W.,"Wide-Band Active Antenna System", presented
        at NASA Joint University Program symposium, Ohio University,
        June 15, 1979.

[4]   U. S. Coast Guard, "Loran-C User Handbook", COMDTINST M165623,
        May 1980.

[5]   Blasche, P.R., "Analysis of First and Second Order Binary
        Quantized Digital Phase-Locked Loops for Ideal and White
        Gaussian Noise Inputs", M. S. Thesis, Ohio University,
        March 1980.

[6]   McCall, D.L., "Loran-C Digital Phase-Locked Loop and RF
        Front-End System Error Analysis", OU NASA TM-72, Avionics
        Engineering Center, Department of Electrical Engineering, Ohio
        University, Athens, Ohio 45701, December 1979.

[7]   Lilley, R. W., "Microprocessor-Controlled Precision Timing
        Applied to Microwave Landing System Data Collection",
        Technical Memorandum, FAA contract FA79NA-6030 in progress.

[8]   Fischer, J. P. and Lilley, R. W., "A Video Display Interface
        for the Loran-C Navigation Receiver Development System", OU NASA
        TM-58, Avionics Engineering Center, Department of Electrical
        Engineering, Ohio University, Athens, Ohio 45701, May 1978.

[9]   Fischer, J. P.,"A Microcomputer-based Position updating System
        for General Aviation Aircraft Using Loran-C", M.S. Thesis,
        Ohio University, in progress.

[10]   "Joint University Program for Air Transportation Research
        - 1980", NASA Conference Publication 2176, Langley Research
        Center, December 1980.
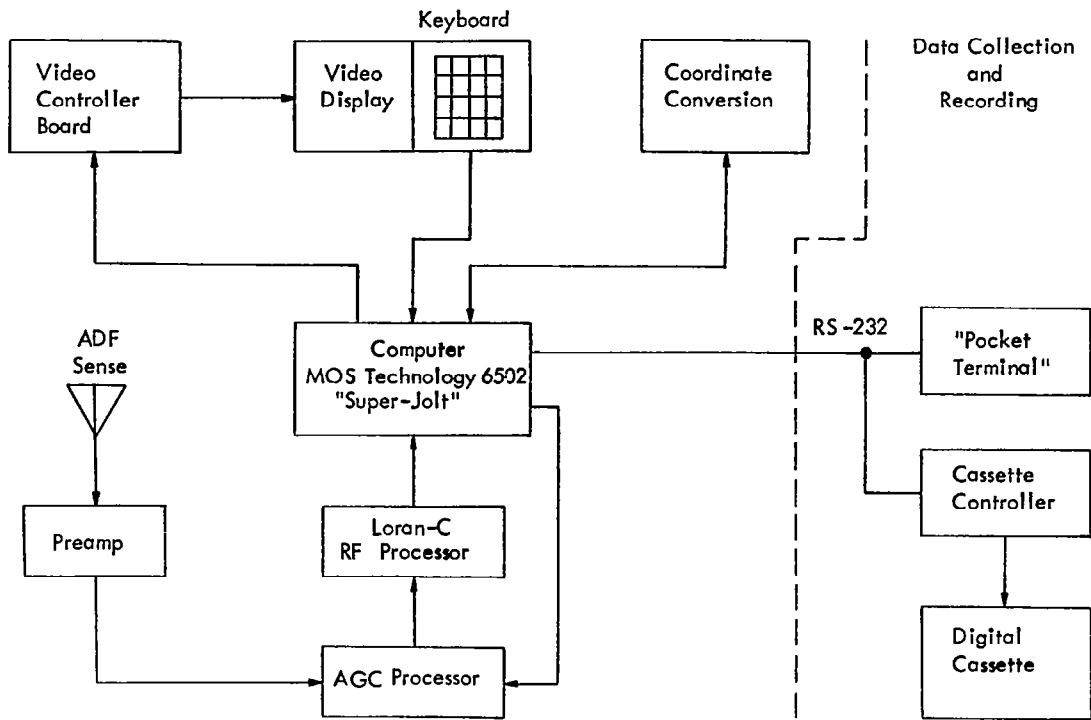
Figure 1. Prototype Loran-C receiver - block diagram.
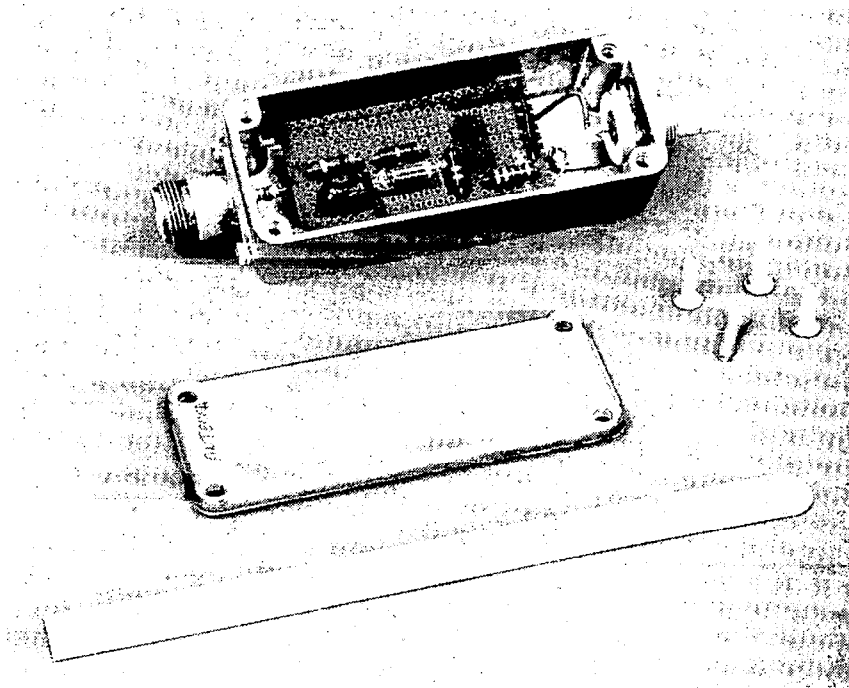
Figure 2. Wideband antenna preamplifier/coupler.
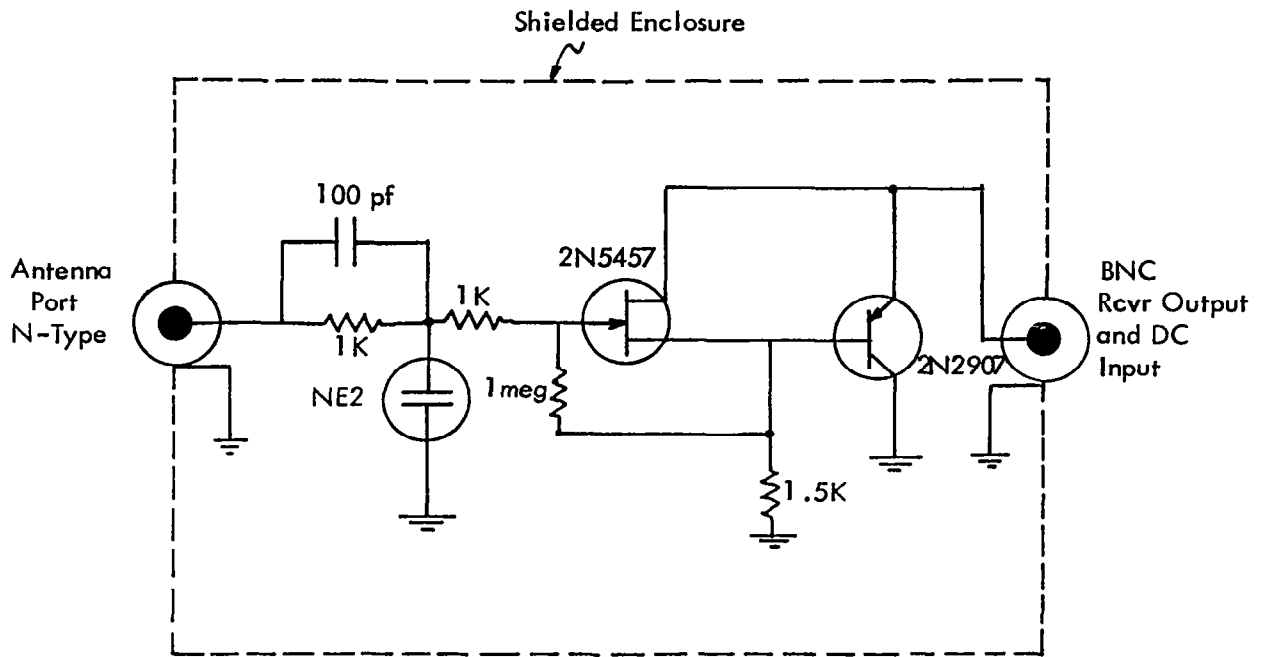
Figure 3.   Preamplifier schematic.

Z denotes a passive RCL Network
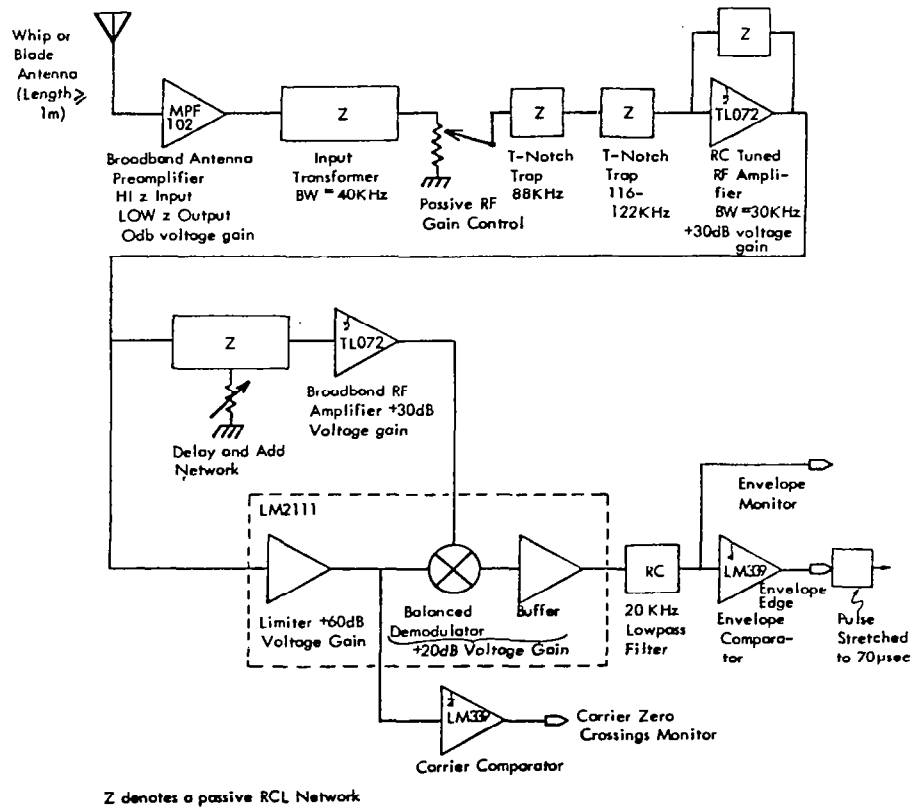
Figure 4.   Loran-C autocorrelation envelope detector.

T = Mouser 421F303
Transformer
5k to 20k, max. L=1mH

Input from ant. preamp.

.0033
RF Gain
1k
88KHz trap T
122KHz trap T
470pf 470pf
1k
33k

150
5k 5k
+8V

.01 .01
10k
trap Q adjust

.005 .005
10k

2
3
TL072
1
4
100kHz RF Amplifier

.0068 .0068
1k add adjust

Note: connect phase of this transformer for + envelope

Undelayed output A
B Delay output
C

All + marked bypass caps are 4.7 to 10mfd tantalum or low leakage electrolytics, 16V rating minimum.

+8V

C
5 8
+
TL072
6
7
1k 33k
Delay RF Amplifier

.005

1mH
+
2 12 13 +8V

.001
+

A
4
5
8 6

LM2111
Envelope Detector

1 D

3 7 8
10
14
E
.001

E 11
B 10
LM339
13 12
Carrier ZX out
External Pullup

Envelope Monitor

10m
External pullup

7808 +8V power supply regulator from +12volt input is not shown.

D
10k
.001
10k
9 3
10k
8
LM339
14
Envelope Edge

+8V

10k 2.7k
Edge threshold

Figure 5. Mini-L80 Loran-C detector circuit.

Figure 6. Prototype Loran-C RF processor.

133

Figure 7.   Tracking loop block diagram.
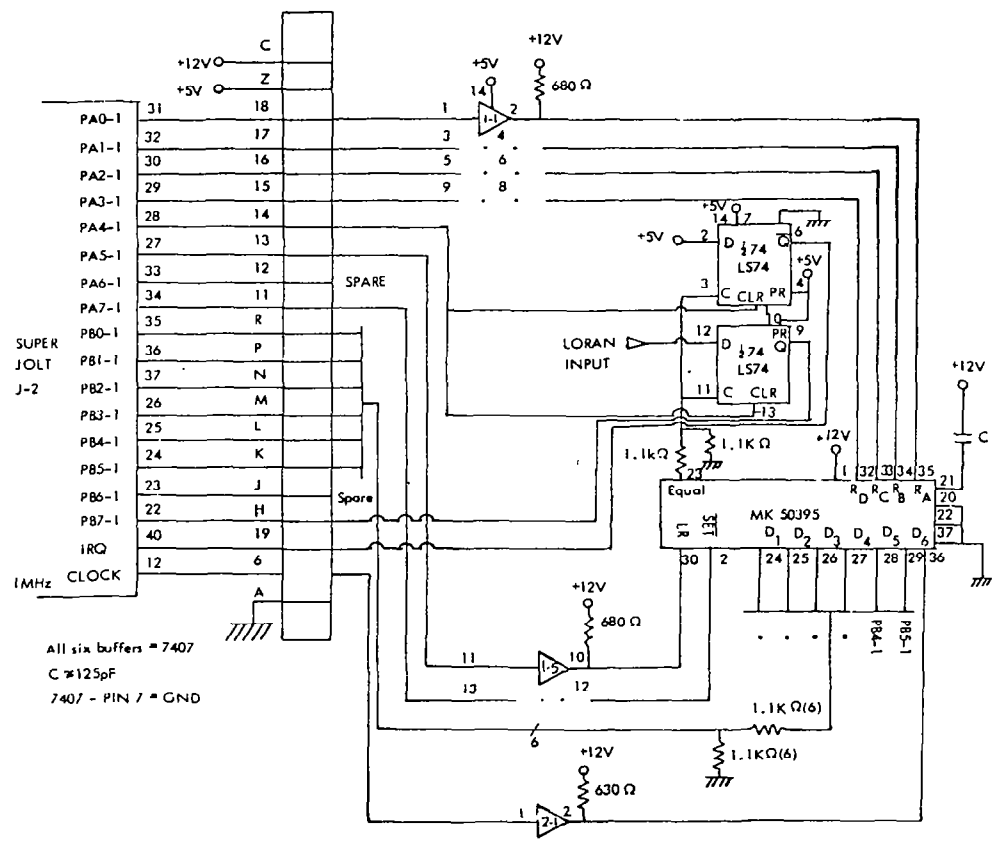
Figure 8.   Tracking loop schematic.
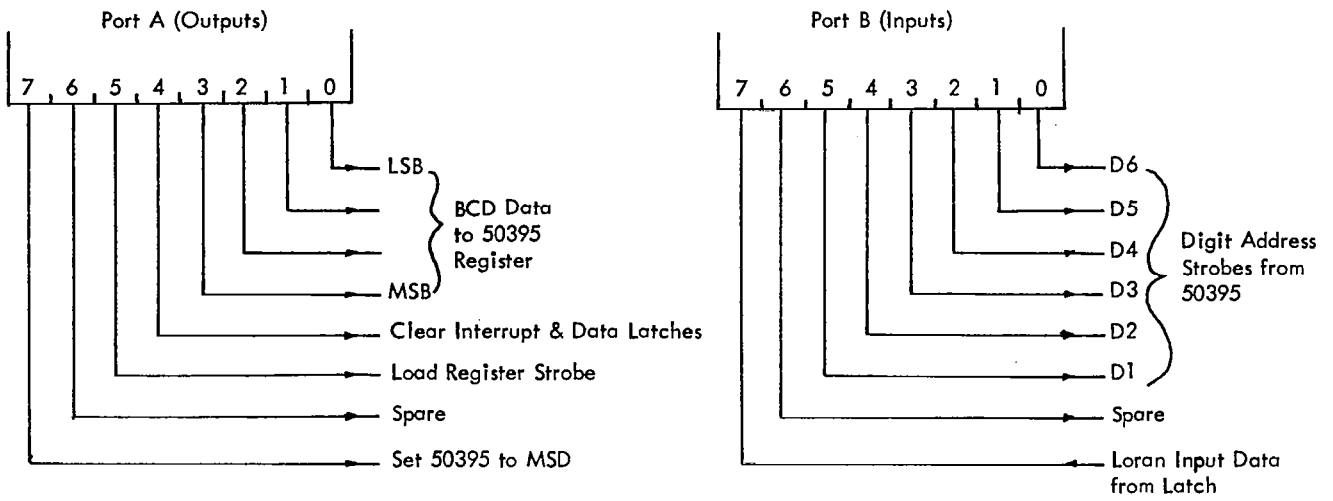
Figure 9. Tracking loop PIA assignment.
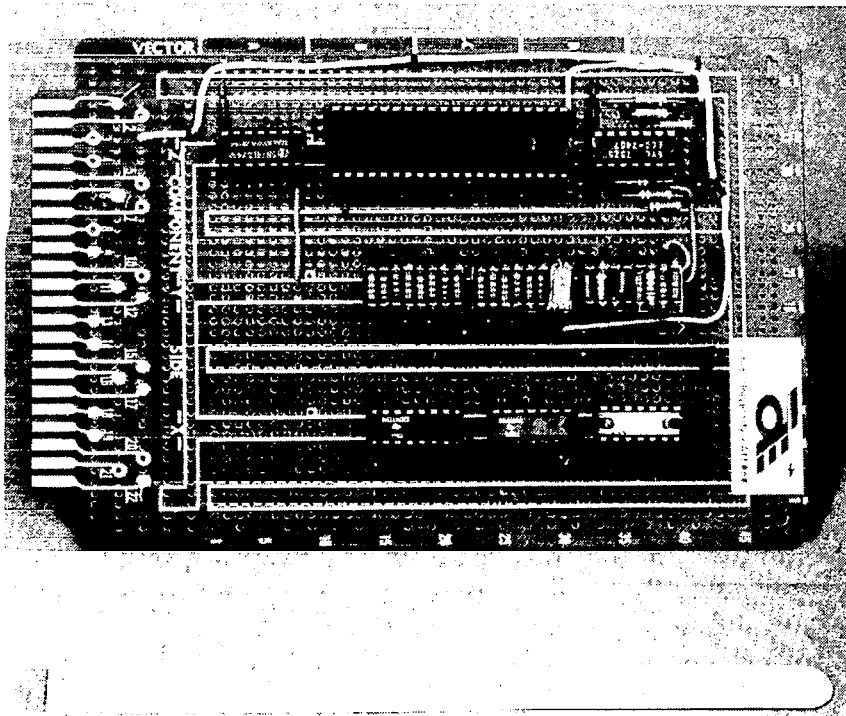
Figure 10. Tracking loop implementation.
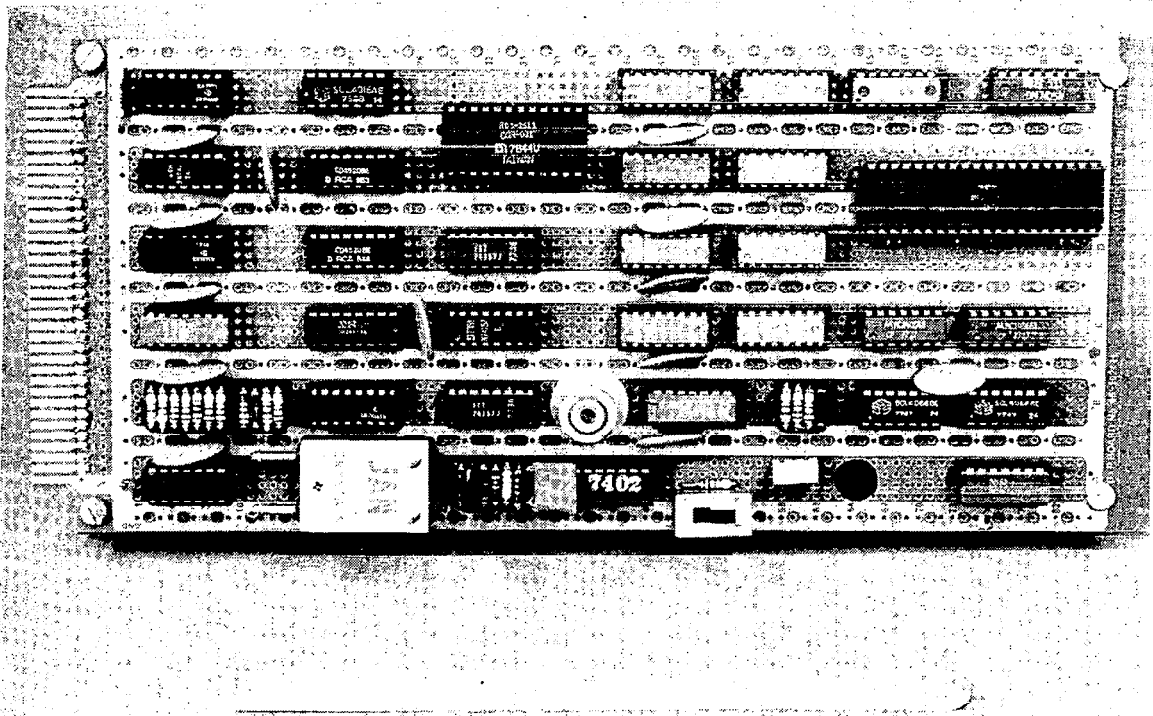
Figure 11. Video interface circuit board.
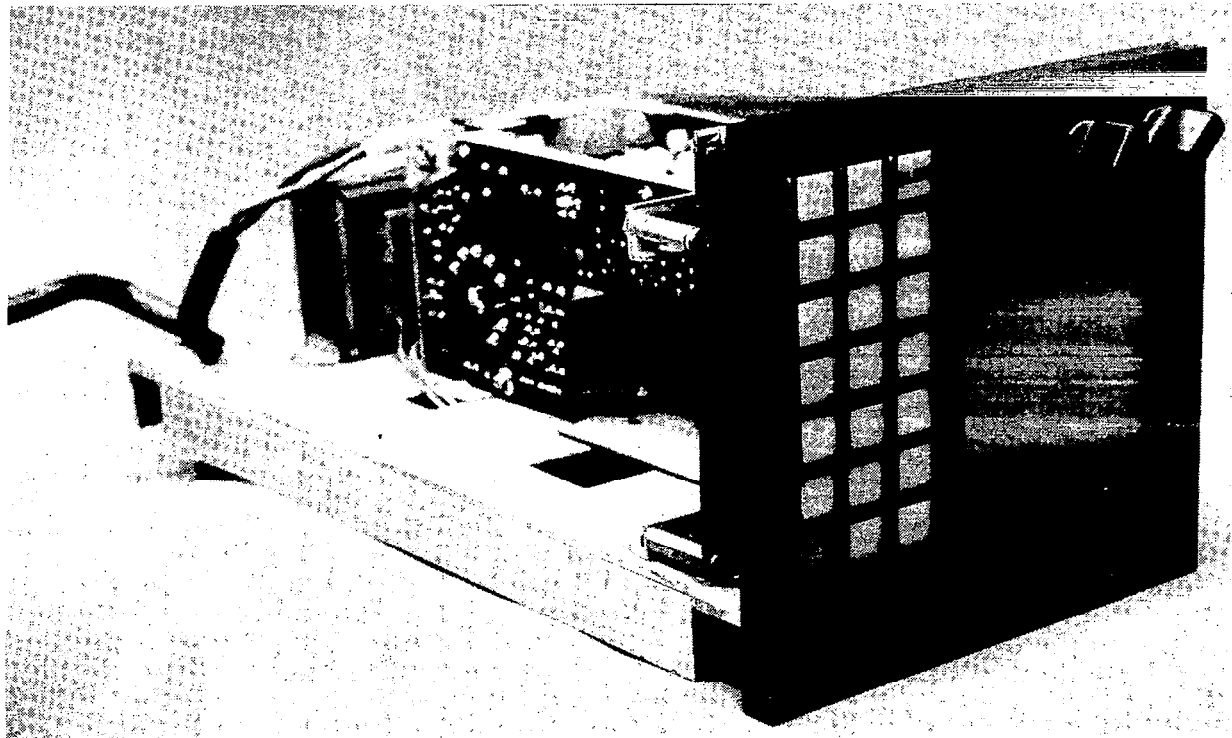
Figure 12. Receiver enclosure.
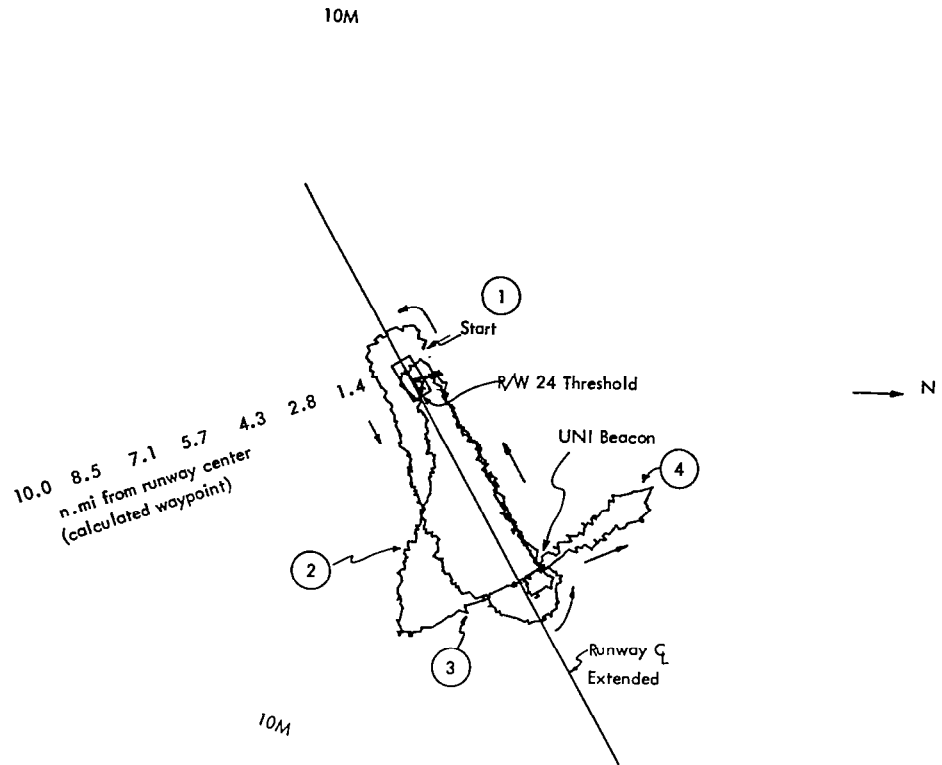
Figure 13. Flight test, Loran-C receiver prototype, March 9, 1981.
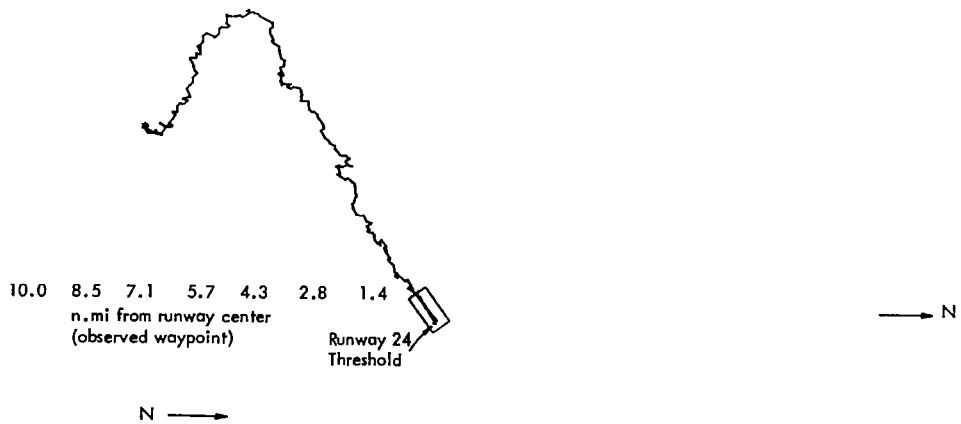
Figure 14. Flight test, Loran-C receiver prototype, March 9, 1981.
Ohio University Airport, PA-28-180, N56241, 99600 GRI.

COMMUTATED AUTOMATIC GAIN CONTROL SYSTEM

A commutated AGC system for the Ohio University prototype Loran-C receiver is described. The circuit design, fabrication, and test results are presented in this paper.

Stephen R. Yost

Avionics Engineering Center
Department of Electrical Engineering
Ohio University
Athens, Ohio 45701

I. INTRODUCTION

This technical memorandum deals with the commutated automatic gain control (AGC) system that has been designed and built for the Ohio University prototype Loran-C receiver (refer to Figure 1). The current version of the prototype receiver, the Mini L-80, was tested initially in the summer of 1980. The receiver uses a Microcomputer Associates™ Super Jolt microcomputer to control a memory-aided phase-locked loop (MAPLL). The microcomputer also controls the input/output, latitude/longitude conversion, and the recently added AGC system. (For a more detailed description of the receiver operation see ref. 1.)

The Ohio University receiver uses an envelope generator and zero crossing detector to produce a "Loran pulse" which is used by the MAPLL to track the Loran station. It was observed that significant errors in the time differences occurred when very strong or weak stations were included in the Loran chain being tracked (ref. 2). Experiments with a Loran simulator revealed that this error was caused by a phase shift and that this phase shift was due solely to the signal-to-signal ratio of the stations being tracked. For example, a 10 dB signal-to-signal difference produced approximately a 10 microsecond error while a 20 dB difference produced approximately a 25 microsecond error. (These results were obtained with an Epsco Loran simulator.)

To reduce or eliminate this error, a commutated AGC was proposed at the December 1980 NASA Joint University Program meeting (ref. 3). (See Figure 2.) The AGC samples the peak of the envelope for each station and stores the resulting voltage on a capacitor. This stored voltage is then used to control the gain of the input RF signal. The microcomputer switches the AGC sample from station to station. This paper describes the circuit designed for the AGC and will also present bench and flight test results. The AGC circuit described actually samples starting at a point 40 microseconds after a zero crossing determined by the software lock pulse ultimately generated by a 30 microsecond delay and add network in the receiver front-end envelope detector. Thus this sample point will be at about the peak of the ground wave signal and not necessarily at the peak of the envelope delayed by strong skywave contamination. Throughout this report the reference to "peak of the envelope" has this restricted meaning. The whole idea of AGC control is to adjust the level of each station signal such that the early portion of each envelope rise is about at the same amplitude in the receiver envelope detector.

The final design is an expansion of the original proposed design. (refer to block diagram Figure 3, as well as Figures 4, 5, and 6.) It consists of three major parts: A) The sample circuit, B) the DC gain circuit and, C) the AGC amplifier circuit.

II. SAMPLE CIRCUIT

The sample circuit is a two-stage sample-and-hold system with three separate channels; the switching of these channels is controlled by the

microcomputer. All integrated circuits are CMOS, and the supply voltage
is +12 volts. This supply voltage is necessary because the sample
voltage levels are in the range of 5 to 7 volts. It is important to note
that this design has not yet been optimized for minimum chip count.

The amplitude of a station's envelope varies with that station's
signal strength (refer to Figures 7 and 8). The two cascaded 4047
monostables create a delayed pulse to sample the peak of the envelope.
The first 4047 triggers on the equals pulse (zero crossing; refer to
Figure 9), and delays 40 microseconds. The second 4047 triggers on the
negative edge of the 40 microsecond delay output and produces a 20
microsecond sample pulse (refer to Figure 10). The delay and duration of
the sample pulse is optimized to sample the peak of the envelope for the
weak as well as the strong station.

The envelope from the RF front-end is passed through a voltage
follower, $1/2$LM353, and into the 4051 analog demultiplexer. The 4051 has
on-chip address decoding; therefore, the two control lines are decoded to:

0	0	search mode
0	1	channel one on
1	0	channel two on
1	1	channel three on

Note that the control lines are ANDed with the sample pulse so that each
channel samples the peak of only one station's envelope. Each Loran sta-
tion consists of eight pulses, and, therefore, the station is actually
sampled eight times (refer to Figure 11). These eight 20 microsecond
sample pulses are of sufficient duration to charge the 25 microfarad
capacitor to the desired final value (the voltage of the peak of the
envelope). Each station is sampled on a separate AGC channel every group
repetition interval (GRI). The 4016 analog switch is configured for the
negative of the logic of the 4051; therefore, the two- to three-line
decoder is needed. The 4016 controls the "hold" for each channel. When
a receiver channel is on, the corresponding switch for that channel in
the 4016 is off. This allows the first stage capacitor to be charged
while a constant voltage from the previous GRI charge is outputted from
the second stage capacitor to the AGC amplifier. The .68 microfarad
capacitor in the second stage of the sample-and-hold is large enough to
hold a constant voltage for .1 second, the maximum GRI value. The second
4051 is enabled in the same manner as the first 4051 except that it is
not pulsed. In addition, a +5 volt signal is applied to the 00 channel
on the second 4051 to serve as a receiver gain setting used during
Loran-C station search. The multiplexed output of the AGC sample voltage
is represented in Figure 12.

The software changes to implement the procedure outlined above are
minimal since the receiver operating software tracks each station indi-
vidually. When the microcomputer starts its search routine, the 00 chan-
nel is activated to output the constant +5 volt search voltage to the AGC
amplifier. When all three stations are being tracked, the commutated AGC

is activated and the envelopes for each station are sampled separately. It is not important to identify which Loran-C station is on a certain AGC channel since the microcomputer provides the necessary sychronization as a function of basic receiver operation.

III. DC GAIN CIRCUIT

The three AGC sample voltages are equal to the peak voltages of the envelopes of their respective stations. Therefore, a strong station stores a higher sample voltage than a weak station. The voltage-controlled amplifier designed for this AGC system requires a higher control voltage to amplify the weak stations; therefore, an inverter circuit was designed for this purpose. The circuit actually has a two-fold purpose, inverting and increasing the gain of the sample voltages. An LM 353 dual op-amp was chosen for this circuit. Referring to Figure 5, one can see that one-half of the chip is used for a voltage follower while the other half serves as the gain/inverter. The trimpot on the input to the second op-amp controls the gain of the AGC output voltage while the other trimpot controls the DC level of the output. The adjustment of these trimpots for proper AGC operation will be explained in Section V of this report.

IV. AGC AMPLIFIER

The AGC amplifier utilizes a CA3028A differential cascade amplifier (refer to Figure 6). The accompanying circuit has been optimized for this particular AGC application. (Refer to ref. 4 for a complete circuit description as well as test results.)

V. OPERATION

As stated previously, the gain and DC level trimpots of the DC gain circuit must be adjusted properly for optimum AGC performance (refer to Figure 13). As this graph indicates, the best AGC amplifier performance lies in approximately the three to eight volt range. The adjustment procedure is as follows:

1. Set the gain to unity (adjust the 10K ohm trimpot to its full value),

2. Set the DC level to +8 volts and allow the receiver to track all three stations and,

3. Increase the gain from unity until the lowest AGC voltage is equal to approximately 4 volts.

The properly functioning AGC will be similar to Figure 14. This adjustment procedure outlined above allows for the use of different antenna-preamp combinations which may possess different DC components in the input RF. It is important to note that once the DC gain circuit is properly adjusted to match a certain antenna-preamp combination, it need not be adjusted further.

VI   TEST RESULTS

The first test of the AGC system performance was the use of the Epsco Loran simulator to provide different signal-to-signal ratios and record the results. An example of such an experiment appears in Figures 15, 16, and 17. A 10-millivolt input signal was used, which is characteristic of the signal strengths encountered with "live" Loran signals. The GRI was set at 99,600 microseconds and the time differences (TD's) were set to resemble those received off the air at Clippinger Labs, Athens, Ohio (TDY=42,594.3 microseconds, TDZ=56,775.9 microseconds). These results are approximated, observed time differences:

Figure #	Attenuation	AGC	TDY	TDZ
15	none	on	42,594.5	56,776.0
17	20dB station Y	on	42,605	56,776
16	20dB station Y	off	42,622	56,776

CONCLUSION: The AGC has little or no effect on "perfect" Loran signals, meaning that there is no degradation of performance with the AGC in operation. Also, twenty dB of signal-to-signal difference is an extreme case which might be encountered only at the limit of a Loran coverage area.

Following a number of simulator tests, the receiver was tested with a live signal. The first step was to obtain an accurate value for the correct time differences as recorded at Clippinger Labs. The Loran chain used was the U.S. Northeast, GRI=99,600 microseconds. Four receivers were tested and the results are as follows:

Receiver	TDY	TDZ
Texas Instruments 9900	42,594.4	56,776.0
Trimble 10A	42,594.3	56,775.9
TDL 302	42,595	56,776
OU Mini L-80 (no AGC)	42,600	56,775

To obtain enough data points for a good statistical sample, sixty minutes of data was collected with the Ohio U. Loran receiver on October 20, 1981 from 4:00 to 5:00 p.m., thirty minutes without AGC, and thirty minutes with AGC. Each of these thirty-minute segments was broken into ten-minute blocks for a total of six blocks, 550 to 600 data points each. The atmospheric conditions were: light cloud cover with moderate spherics activity observed on an oscilloscope. A statistical analysis package available on Ohio University's IBM 370/158 was used to obtain the results shown in Figures 18 and 19. Most of the accuracy displayed is not significant but the trends are evident.

CONCLUSION: The addition of the AGC improved the value of TDY by approximately four microseconds. The overall accuracy of the receiver is approaching ±1 microsecond. One point of special interest is the greater variance of TDY with the AGC on. This is due to the occasional sampling of cross-rate interference.

The most important test of a prototype navigation receiver is a flight test. Ohio University's DC-3 flying laboratory made two Loran data collection flights on August 29th and 31st, 1981. The flights were centered around south-central Ohio and in areas of light thunderstorm activity. The operational Loran receivers were: TI 9900, Trimble 10A, and O. U. Mini L-80. The results of the August 29th Columbus to Albany via Zanesville leg are presented graphically in Figure 20. (August 31st data is omitted from this report because the results are essentially the same.) The O. U. receiver data was hand-collected and it appears with the flight path plotted by the TI 9900.

CONCLUSION: The plot shows a very close alignment of the two paths. Note the slight (less than .5 nautical miles) north bias of the O. U. receiver path. These plots were obtained with latitude/longitude data and not time difference data. The latitude/longitude conversion employed in the O. U. receiver does not use any overland propagation delay corrections in the calculations. This bias is due mainly to lack of propagation delay correction rather than large time difference errors.

VII. CONCLUSIONS

The addition of AGC to the O. U. Loran-C receiver has improved the accuracy of the time difference calculations to within approximately $\pm$ 1.5 microseconds of the observed time differences for a given position. This translates to an improvement of absolute accuracy of approximately 0.5 nautical mile. Tests of Ohio University's receiver with and without the AGC have indicated these results. The majority of error now present in the positional data supplied by the Ohio University receiver is due to the lack of propagation delay corrections.

Two additional refinements could improve the performance of the AGC system further: 1) a filter to reduce the effect of cross-rate interference on the sampling of the envelopes, and 2) an AGC amplifier with more dynamic range for an even greater signal-to-signal gain. Complete software control would eliminate the adjustments outlined in Section V, thus the receiver would require no manual gain adjustments. Other software development could allow for the tracking of all the Loran stations in a particular chain. The three most suitable signals would then be used to obtain positional data.

VIII. SUMMARY

A commutated automatic gain control system has been designed and constructed specifically for the Ohio University prototype Loran-C receiver. The AGC is designed to improve the signal-to-signal ratio of the received Loran signals. The AGC design does not require any analog to digital conversion and it utilizes commonly available components. The AGC system consists of three major parts: 1) the sample circuit, which samples the peak of the envelope of the Loran signal to obtain an AGC voltage for each of three Loran stations, 2) a DC gain circuit to control the overall gain of the AGC system, and 3) an AGC amplifier to amplify

the input RF signal. The performance of the AGC system has been observed in bench and flight tests and it has improved the overall accuracy of the Ohio University receiver considerably.

IX.   ACKNOWLEDGEMENTS

The design, construction and testing of the commutated AGC system has been funded by the NASA Joint University Program for Air Transportation Research as a part of the continuing development of Ohio University's prototype Loran-C receiver. The author would like to thank Dr. Robert Lilley and Mr. Ralph Burhans, both project engineers, for their help in the design of the AGC. James Nickum, Avionics Engineering Center engineer, helped with the data collection, especially the flight testing. He also took all of the photographs that appear in this paper. Research interns Stan Novacki, James Roman and David Bernard were also of assistance in various phases of this project.

X.   REFERENCES

1.   Lilley, Dr. R.W. and Daryl McCall, "A Loran-C Prototype Navigation Receiver for General Aviation", OU NASA TM-80, Avionics Engineering Center, Department of Electrical Engineering, Ohio University, Athens, Ohio 45701, August 1981. (Pages 121-137 of this compilation.)

2.   Fischer, Joseph P., "Results of a Loran-C Flight Test Using an Absolute Data Reference", OU NASA TM-74, Avionics Engineering Center, Department of Electrical Engineering, Ohio University, Athens, Ohio 45701, January 1980.

3.   "Joint University Program for Air Transportation Research - 1980", NASA CP-2176, Langley Research Center, December 1980.

4.   Roman, James P., "Automatic Gain Control", OU NASA TM-79, Avionics Engineering Center, Department of Electrical Engineering, Ohio University, Athens, Ohio 45701, March 1981. (Pages 115-119 of this compilation.
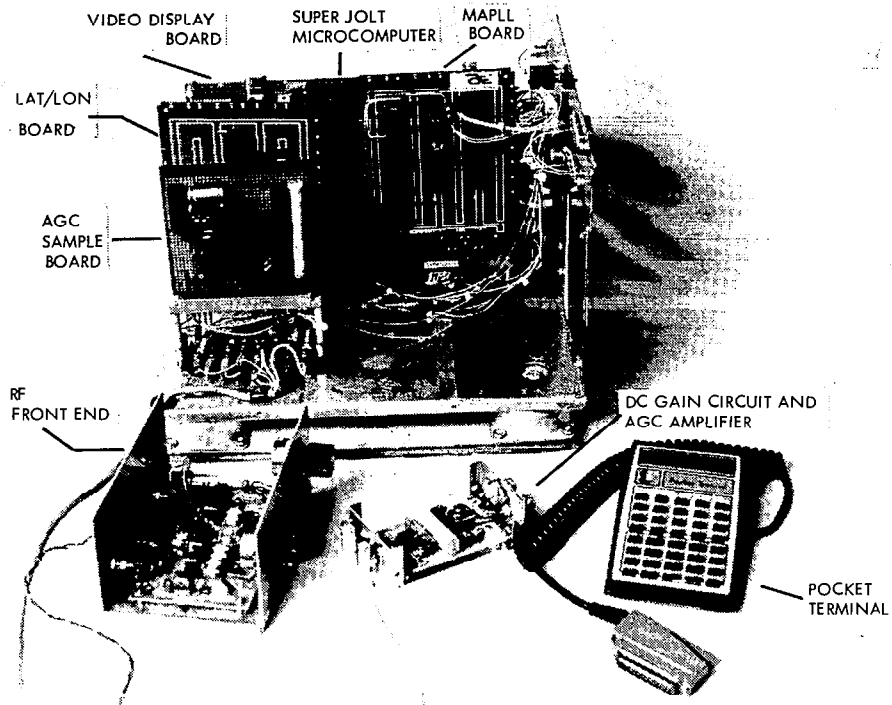
Figure 1.   Ohio University Loran-C receiver.
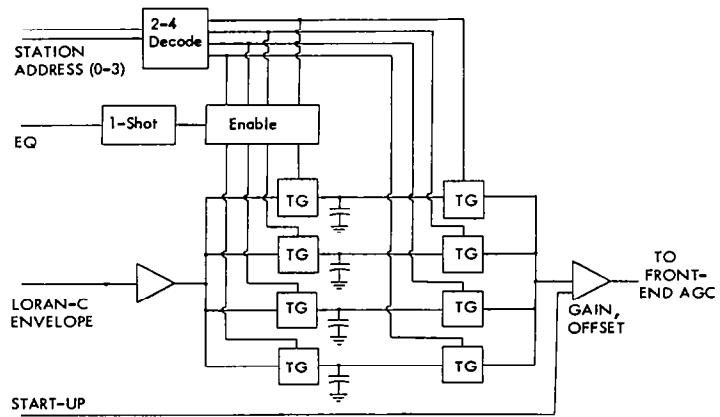
LORAN-C RECEIVER COMMUTATED AGC

- To be Added to Loran-C Low-Cost Prototype
- Commutated, Sampled AGC
- Avoids Front-End Phase Shift Problem
- Five Chips Required for Breadboard
- Permits Present AGC for Search Mode
- Minimum Load on Computer

Figure 2.   Proposed commutated AGC.
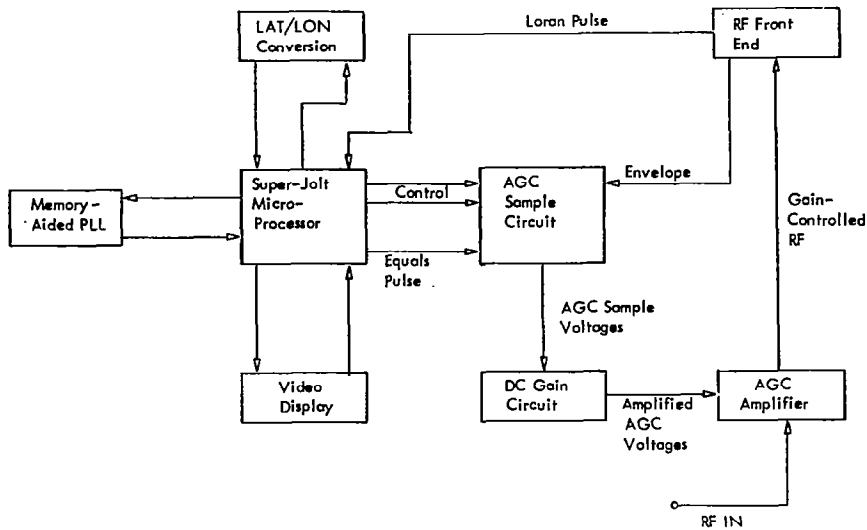
Figure 3. Ohio University Loran-C receiver block diagram with AGC.
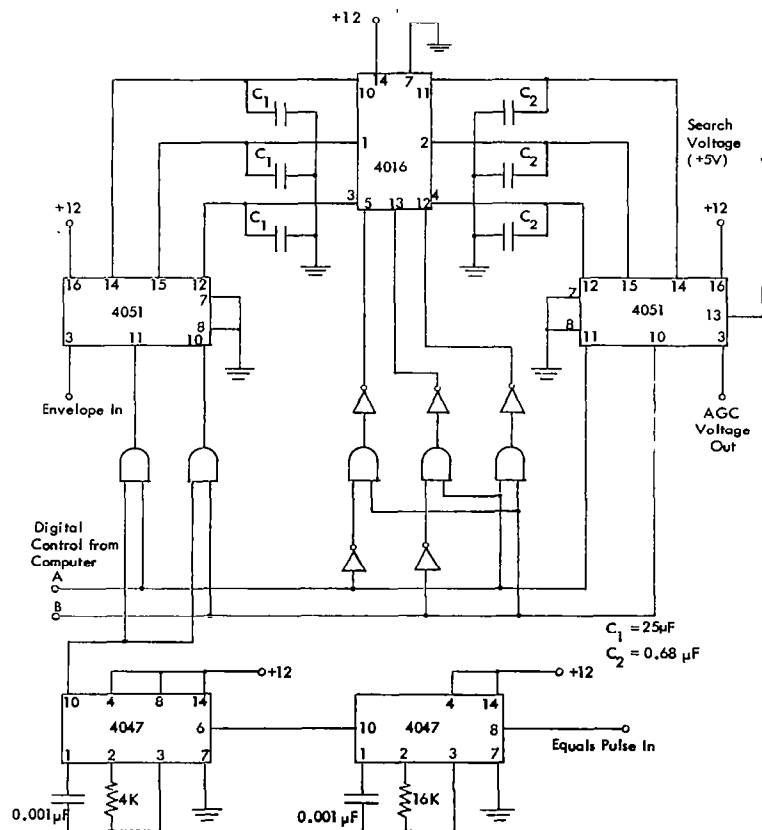
Figure 4. Schematic of the commutated AGC circuit designed for the Ohio University Loran-C receiver. All of the IC's are CMOS. This circuit is designed to sample the peak of the envelope of a Loran pulse to obtain an AGC voltage.
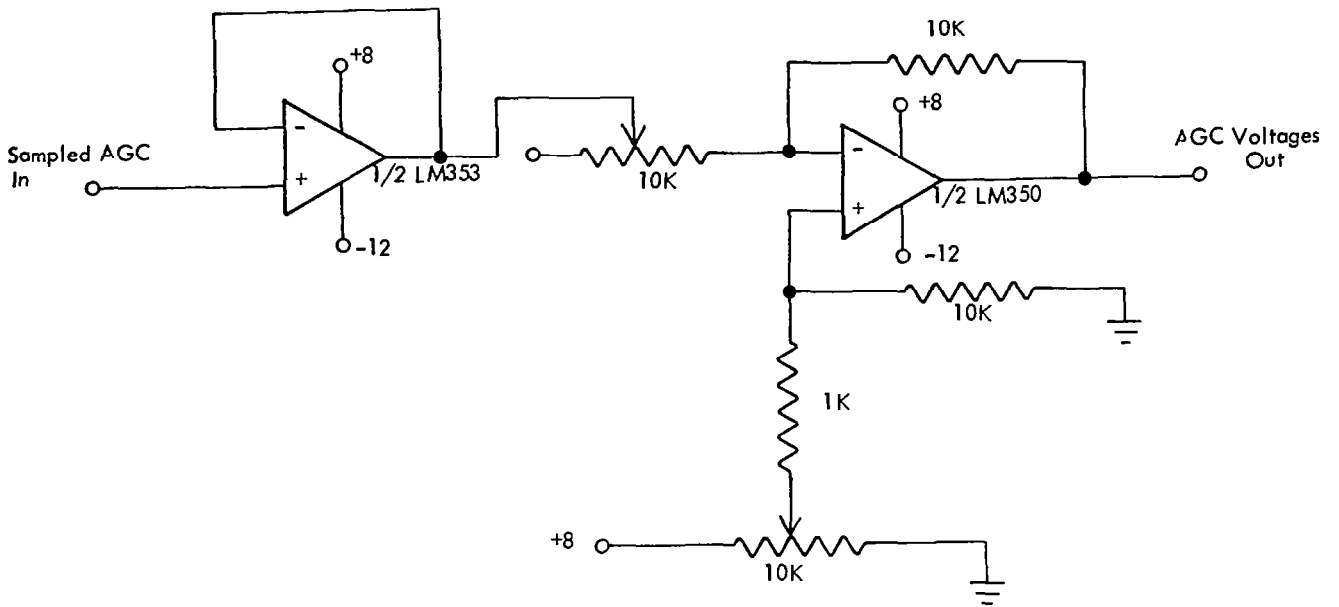
Figure 5. DC gain circuit.
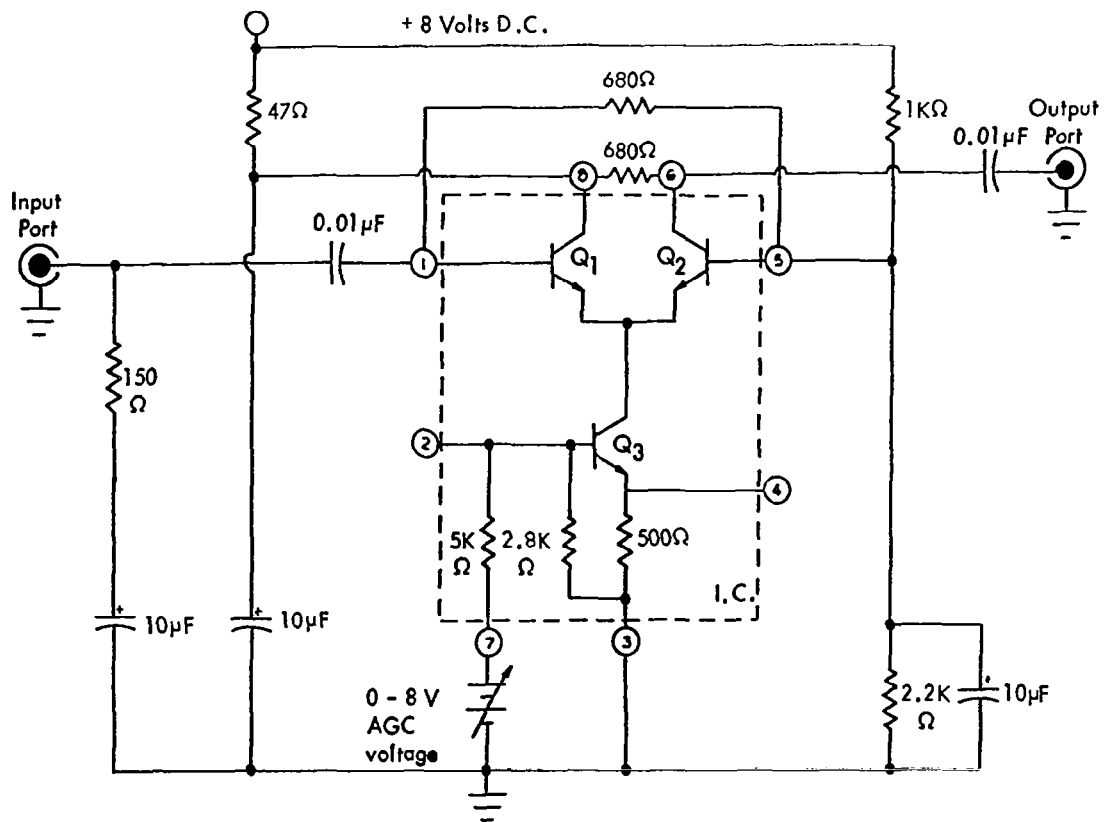
Figure 6. Automatic gain control circuit (amplifier only).
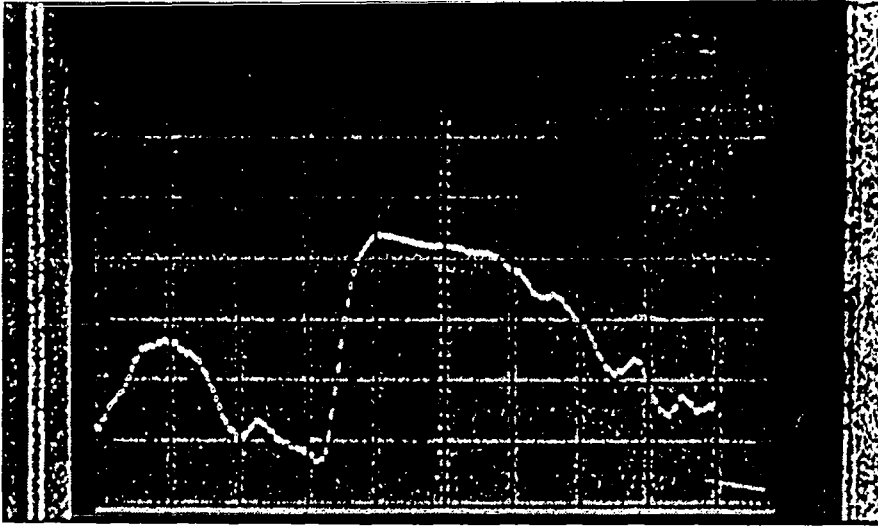
Figure 7. Strong station envelope. Live signal, M station (Seneca, NY).
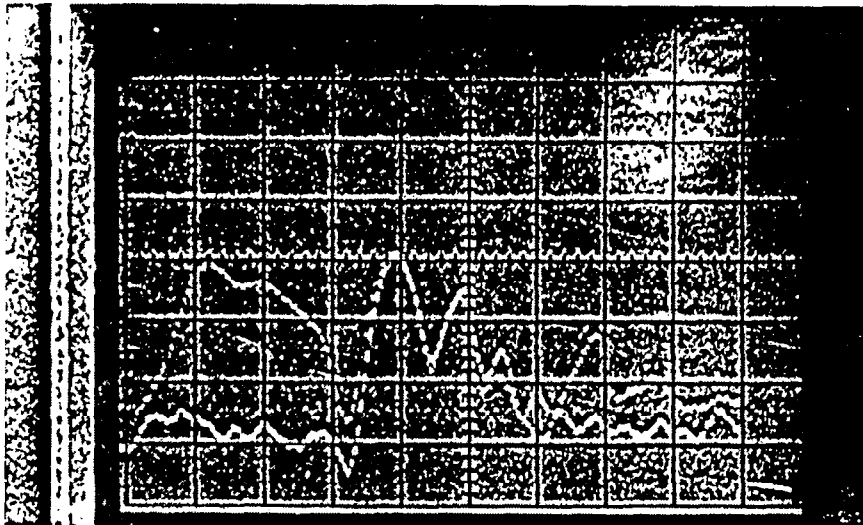
Figure 8. Weak station envelope. Live signal, Y station (Carolina Beach).
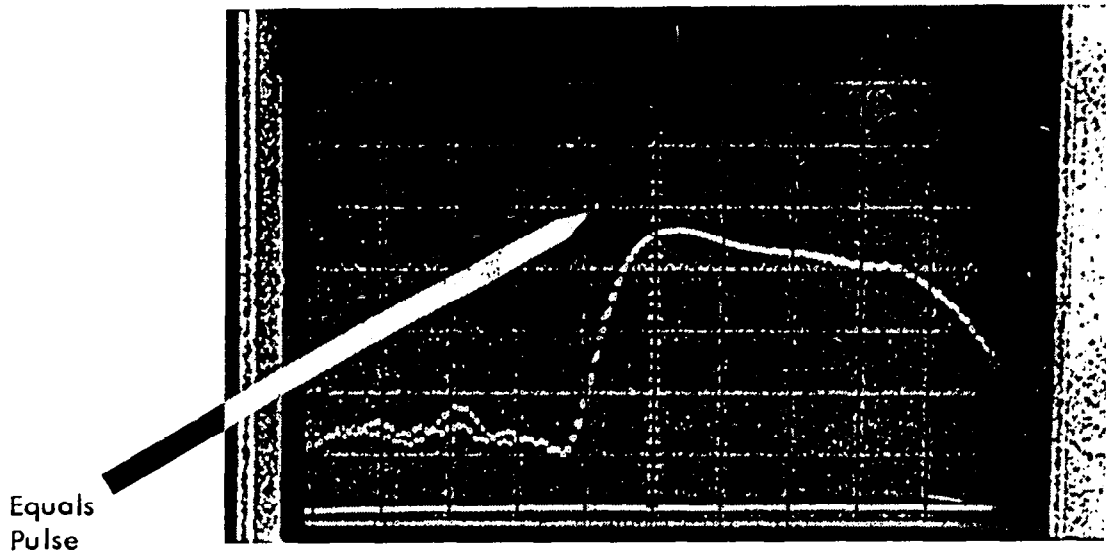
Equals
Pulse

Figure 9. One μsec equals pulse at zero crossing.
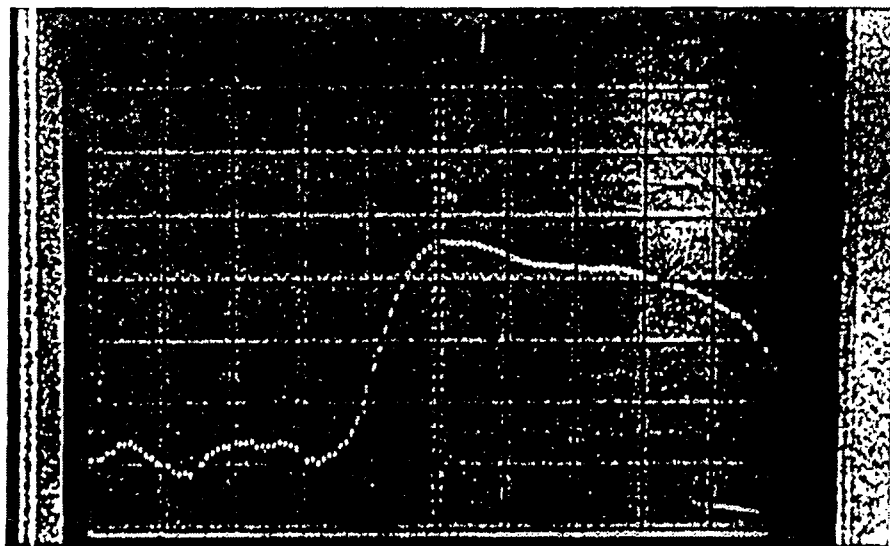
Figure 10. Twenty-μsec sample pulse at peak of envelope.
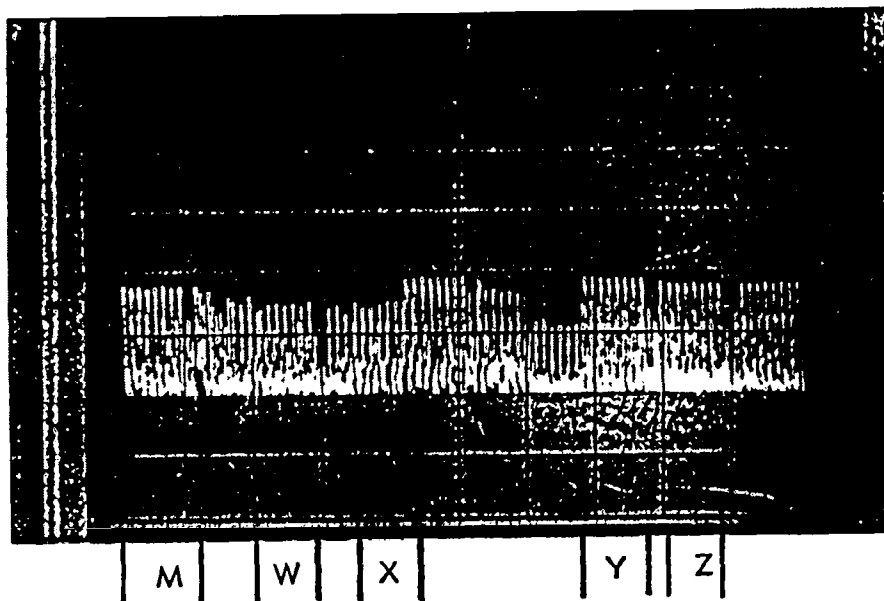
Figure 11.   Loran chain as received at Clippinger Labs.
GRI = 99600 μsec.   Note cross-rate interference.
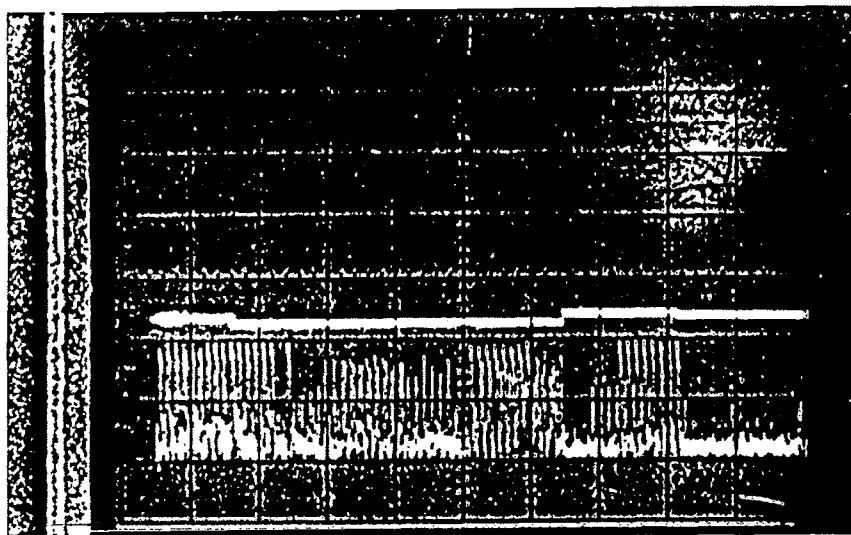
2 volts/Div.

GND. REF.

Figure 12.   AGC sample voltages.
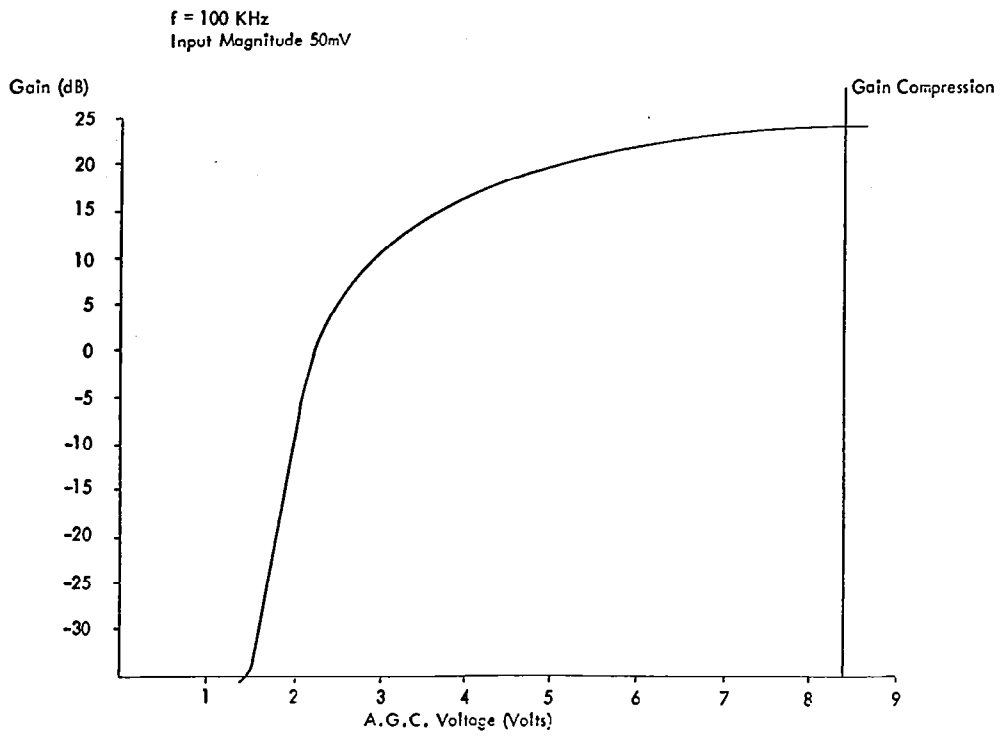
Figure 13. AGC amplifier performance curve.
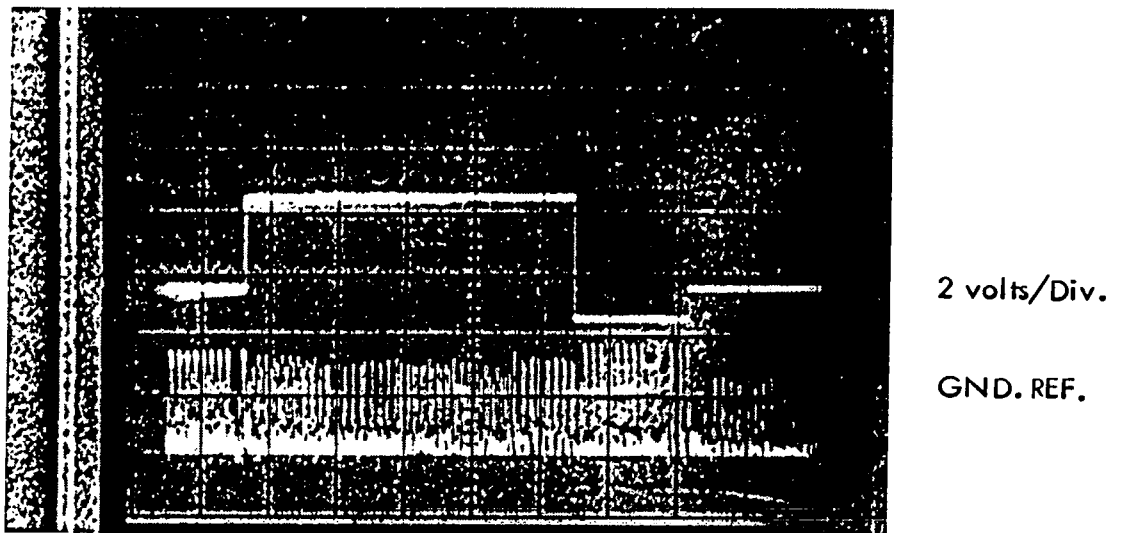
Figure 14. AGC voltages, live signal.
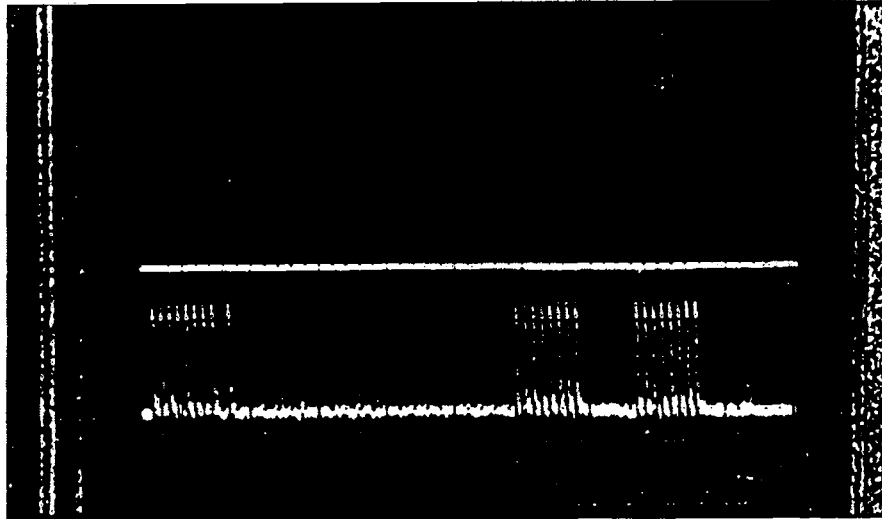
2 volts/Div.

GND REF.

Figure 15. Ten-mV signal on simulator, no station attenuation, AGC on.
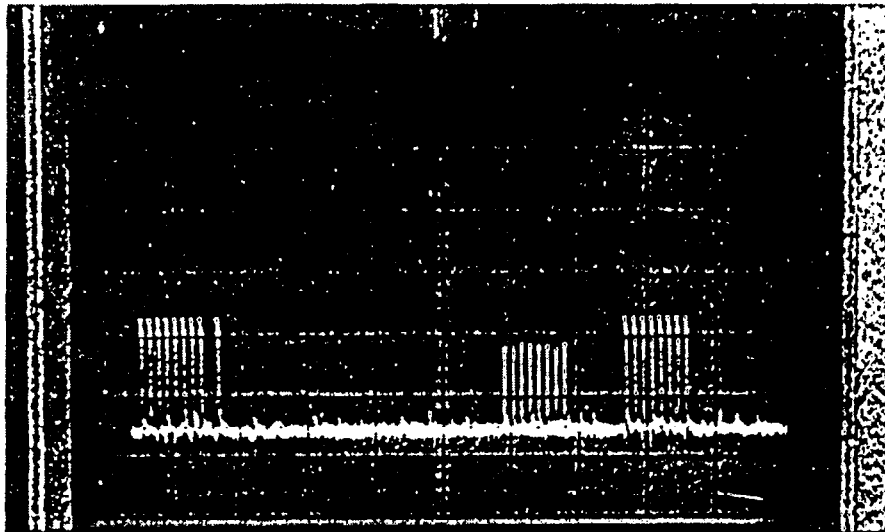
Figure 16. Ten-mV signal, 20 dB attenuation on station Y, AGC off.
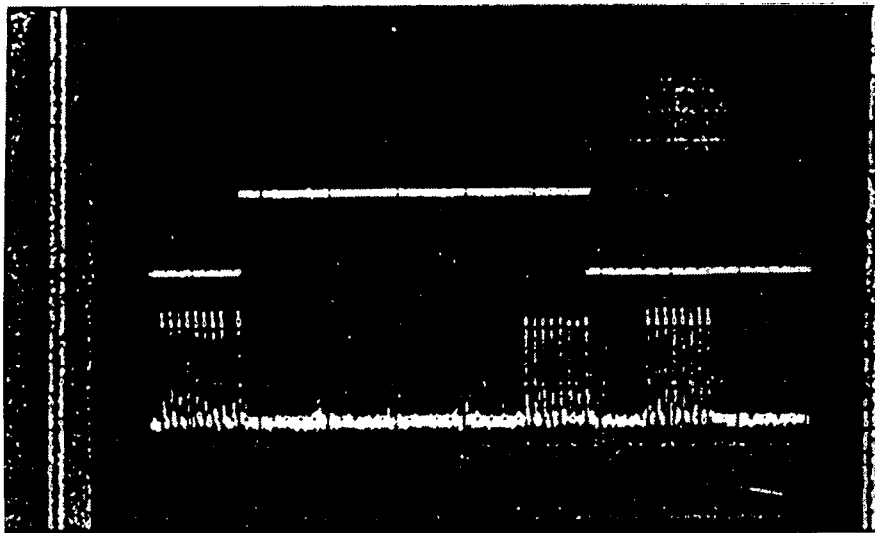
2 volts/Div

GND. REF.

Figure 17.   Ten-mV signal, 20 dB of attenuation on station Y, AGC on.
Note improvement from Figure 16.

                                    AGCTEST1   14:25 FRICAY, NOVEMBER

      MEAN   STANDARD   MINIMUM   MAXIMUM   STD ERROR   SUM   VARIANCE
                    DEVIATION   VALUE   VALUE   CF MEAN

   42599.4002347   0.51903853   42597.700000   42601.300000 0.02514750 18147344.500   0.26940039
   56775.3119718   0.52392441   56773.600000   56776.700000 0.02538422 24186282.900   0.27449678

                                    AGCTEST1   14:25 FRICAY, NOVEMBER
      MEAN   STANDARD   MINIMUM   MAXIMUM   STD ERROR   SUM   VARIANCE
                    DEVIATION   VALUE   VALUE   CF MEAN

   42599.4434109   0.45396906   42597.900000   42600.900000 0.02174578 21981312.800   0.24400543
   56775.3350775   0.44001746   56774.100000   56776.600000 0.01937069 29296072.900   0.19361537

                                    AGCTEST1   14:24 FRIDAY, NOVEMBER
      MEAN   STANDARD   MINIMUM   MAXIMUM   STD ERROR   SUM   VARIANCE
                    DEVIATION   VALUE   VALUE   CF MEAN

   42599.7463659   0.42819454   42598.500000   42601.000000 0.02143654 16997298.800   0.18335057
   56775.3644110   0.40127825   56774.200000   56776.500000 0.02008904 22653370.400   0.16102424

Figure 18.   Bench test results without AGC.

MEAN	STANDARD DEVIATION	MINIMUM VALUE	MAXIMUM VALUE	STD ERROR OF MEAN	SUM	VARIANCE
42596.2683342	0.61590858	42594.600000	42597.800000	0.02932898	18784354.600	0.37934338
56776.9375283	0.44090975	56775.700000	56778.100000	0.02099570	25038651.500	0.19440141

AGCTEST1   14:14 FRIDAY, NOVEMBER

MEAN	STANDARD DEVIATION	MINIMUM VALUE	MAXIMUM VALUE	STD ERROR OF MEAN	SUM	VARIANCE
42596.0725979	0.59603481	42594.600000	42597.400000	0.02514221	23938992.800	0.35525749
56776.9188612	0.43206040	56775.700000	56777.900000	0.01822537	31908628.400	0.18667619

AGCTEST1   14:13 FRIDAY, NOVEMBER

MEAN	STANDARD DEVIATION	MINIMUM VALUE	MAXIMUM VALUE	STD ERROR OF MEAN	SUM	VARIANCE
42595.5914894	0.87943572	42592.300000	42597.700000	0.03867754	22021920.800	0.77340719
56776.7504836	0.42543371	56775.400000	56777.900000	0.01871055	29353580.000	0.18099384

Figure 19.   Bench test results with AGC.
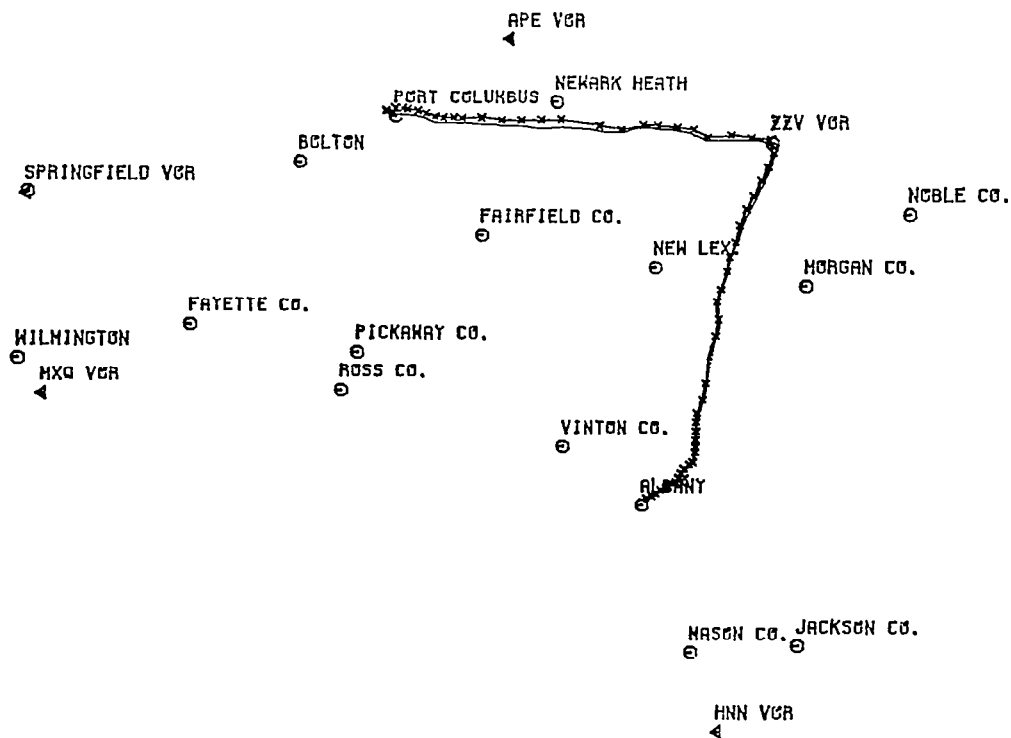
Figure 20.   DC-3 flight test, 29 August 1981. TI-9900 flight path is the solid
line. OU Loran-C is the line with X's. Note the slight north bias
of the OU Loran-C data.

A PROTOTYPE INTERFACE UNIT FOR

MICROPROCESSOR-BASED LORAN-C RECEIVER

A command entry and display device
designed to allow convenient operation
of the Loran-C receiver-processor is
described.

Stanley M. Novacki III

Avionics Engineering Center
Department of Electrical Engineering
Ohio University
Athens, Ohio 45701

I. INTRODUCTION

This paper documents an inexpensive data/command entry and display system being developed by the Ohio University Tri-University group. This system is designed to operate in place of a separate ASCII terminal. Also described is the software to interface this unit to the 6502-based navigation receiver currently under development at Ohio University.

II. HARDWARE IMPLEMENTATION

See Figure 1 for an overview of the command entry and display logic. In order to retain the use of some of the DEMON(TM) monitor facilities provided by the SuperJOLT(TM) microcomputer, an ASCII encoded keypad consisting of the decimal digits, decimal point, and nine letters has been designed as shown in Figure 2. A printed circuit board was prepared to produce the appropriate X-row Y-column code appropriate for each character (Figure 3). This X-Y code is input to a General Instruments AY-5-2376 keyboard encoder [1]. Figure 4 shows the encoder along with an NEC µ8212 octal latch, which stores the value of the pressed key until the microprocessor can poll the keyboard and read the data.

The latch holding the 7 bits of character data and a key-pressed strobe is made available to a 6530 Versatile Interface Adapter (VIA) on the J2 connector of the SuperJOLT microcomputer. Port A of the 6530 is configured as an input: lines 0 through 6 carry the ASCII value of the key, line 7 the key-pressed strobe which acts as a flag during the polling process to indicate that new data is present. Line 2 of the "B" port is set as an output line; after data has been read from the "A" port, line B2 is toggled to clear the latch so that new data can be read.

A Sony AVF-3250A 4-inch black-and-white monitor designed for 13 VDC operation was chosen for the display due to the ease with which it could be integrated into a standard avionics-size enclosure as shown in Figure 5. The monitor accepts standard NTSC composite video signals, requires 14 watts at 13 VDC and weighs approximately 1.9kg.

The VDM-1 Video Display Module [2] allows for the use of alphanumerics and graphic primitives in a 16x16 format along with a 256 x 256 coarse graphics mode and a 512 x 512 high resolution mode. This versatility allows for a variety of alphanumeric, graphic, or combined-mode displays. Such capabilities allow for receiver output to be displayed in CDI, HSI, or other analog data formats easily recognized and interpreted by the pilot.

III. SOFTWARE INTERFACE

A monitor routine is being written in 6502 assembly language to perform data input and output between the command/display unit and the

SuperJOLT microcomputer. The DEMON(TM) monitor routine can provide all services necessary for system initialization and data input; however, it also requires a full communications terminal and does not offer the range of display formats offered by the VDM graphics unit. The attendant reduction in size and weight coupled with the ease of operation made possible by tailoring the monitor to a specific application make the development of a custom software interface highly desirable.

There are four tasks currently envisioned for the interface monitor. They consist of:

1. Selecting the mode of operation; for example, direct-route or multi-waypoint navigation.

2. Provide user prompts for the data input needed for the specified mode of operation.

3. Provide data conversion from a user-oriented format to a microprocessor-oriented one.

4. Select the display mode of the processor output.

Tasks 1 and 2 are fairly obvious and no further elaboration will be given here. Data format conversion is required because the current versions of the time-difference to latitude-longitude and area navigation routines require information such as waypoint location to be given in a particular 32-bit floating-point format as used by the Advanced Micro Devices Am9511A arithmetic processor [3]. This format is illustrated in Figure 6. The format conversion typically consists of stripping the ASCII zone bits and performing a BCD-to-binary conversion and then "floating" the 8-bit integer number into the 32-bit format. This data format change is greatly simplified by the arithmetic facilities of the Am9511A: software multiply-and-add routines are replaced by presenting data to the math chip and giving it the appropriate operation codes. This decrease in the size of the interfacing software and attendant improvements in program legibility make software maintenance much easier, especially in terms of code optimization for faster execution as well as increased memory resources to allow for more sophisicated I/O routines.

Perhaps the most significant difference between the interface monitor and the terminal monitor is that the former cannot be interrupt driven. The processor's principal function is monitoring the LORAN-C pulse train and deriving time-differences from them to drive the navigation routines. An interrupt to service something as irrelevant to the pulse tracking and TD measurements as a change of display formats would force the receiver to retrack the pulse trains, reducing the total time the processor is devoting to actual navigation duties. As an extension of the data display currently used in the prototype receiver, the keyboard will be polled as part of the general housekeeping software. The information from the keypad is stored until the processor has the opportunity to implement the command.

IV.   SUMMARY

An ASCII keypad with a CRT display capable of alphanumeric and graphics-mode operation is being developed to provide specialized data entry and display for the Ohio University LORAN-C receiver/processor. This unit is being developed to replace conventional communications terminals so as to simplify receiver operations to a level typical of current avionics systems.

V.   REFERENCES

[1]   KBD-5 Keyboard and ASCII Encoder, Southwest Technical Products, San Antonio, Texas, 1978.

[2]   VDM-1 Video Display Module, Microcomputer Products Co.,Columbus, Ohio, 1980.

[3]   Am9511A MOS/LSI Arithmetic Processor, Advanced Micro Devices, Sunnyvale, California, 1979.
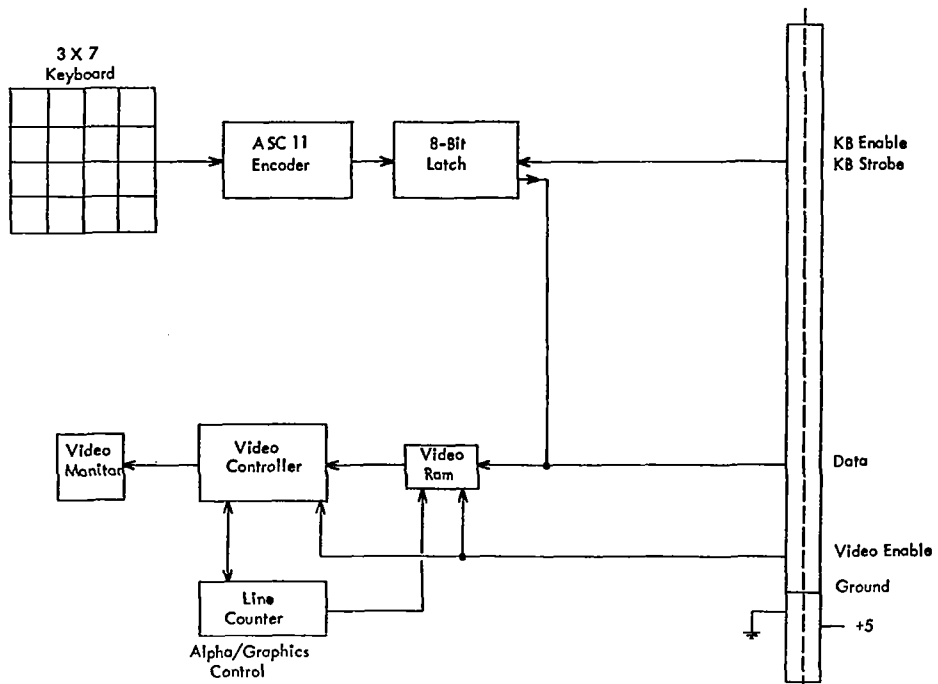
Figure 1. LORAN-C CONTROL/DISPLAY

Figure 2. Proposed ASCII Keypad Layout.

CONNECT → TO OBTAIN ↘		X_0	X_1	X_2	X_3	X_4	X_5	X_6	X_7
Y_0	NORMAL	NUL	DLE	-	Ø	;	I	o	9
	SHIFT	NUL	DLE	■·	NUL	+	L	O	)
	CONTROL	NUL	DLE	NUL	NUL	NUL	FF	SI	NUL
Y_1	NORMAL	SOH	K	FS	:	/	k	i	8
	SHIFT	SOH	C	FS	*	?	K	I	(
	CONTROL	SOH	VT	FS	NUL	NUL	VT	HT	NUL
Y_2	NORMAL	STX	L	GS	p	.	j	u	7
	SHIFT	STX	\	GS	P	>	J	U	'
	CONTROL	STX	FF	GS	DLE	NUL	LF	NAK	NUL
Y_3	NORMAL	ETX	N	RS	_	.	h	y	6
	SHIFT	ETX	^	RS	DEL	<	H	Y	8
	CONTROL	ETX	SO	RS	US	NUL	BS	EM	NUL
Y_4	NORMAL	EOT	M	US	@	m	g	t	5
	SHIFT	EOT	]	US	`	M	G	T	%
	CONTROL	EOT	CR	US	NUL	CR	BEL	DC_4	NUL
Y_5	NORMAL	ENQ	NAK	<	BS	n	f	r	4
	SHIFT	ENQ	NAK	<	BS	N	F	R	$
	CONTROL	ENQ	NAK	NUL	BS	SO	ACK	DC_2	NUL
Y_6	NORMAL	ACK	SYN	>	[	b	d	e	3
	SHIFT	ACK	SYN	>	{	B	D	E	#
	CONTROL	ACK	SYN	NUL	ESC	STX	EOT	ENQ	NUL
Y_7	NORMAL	BEL	ETB	.	]	v	s	w	2
	SHIFT	BEL	ETB	,	}	V	S	W	"
	CONTROL	BEL	ETB	NUL	GS	SYN	DC_3	ETB	NUL
Y_8	NORMAL	DC1	CAN	SP	CR	c	a	q	1
	SHIFT	DC1	CAN	SP	CR	C	A	Q	!
	CONTROL	DC1	CAN	SP	CR	ETX	SOH	DC1	NUL
Y_9	NORMAL	P	EM	.	LF	x	FF	HT	∧
	SHIFT	@	EM	.	LF	X	FF	HT	∼
	CONTROL	DLE	EM	NUL	LF	CAN	FF	HT	RS
Y_{10}	NORMAL	O	SUB	_	DEL	z	ESC	VT	\
	SHIFT	_	SUB	_	DEL	Z	ESC	VT	:
	CONTROL	SI	SUB	US	DEL	SUB	ESC	VT	FS

Figure 3.   Code Assignment Chart – AY-5-2376 Keyboard Encoder
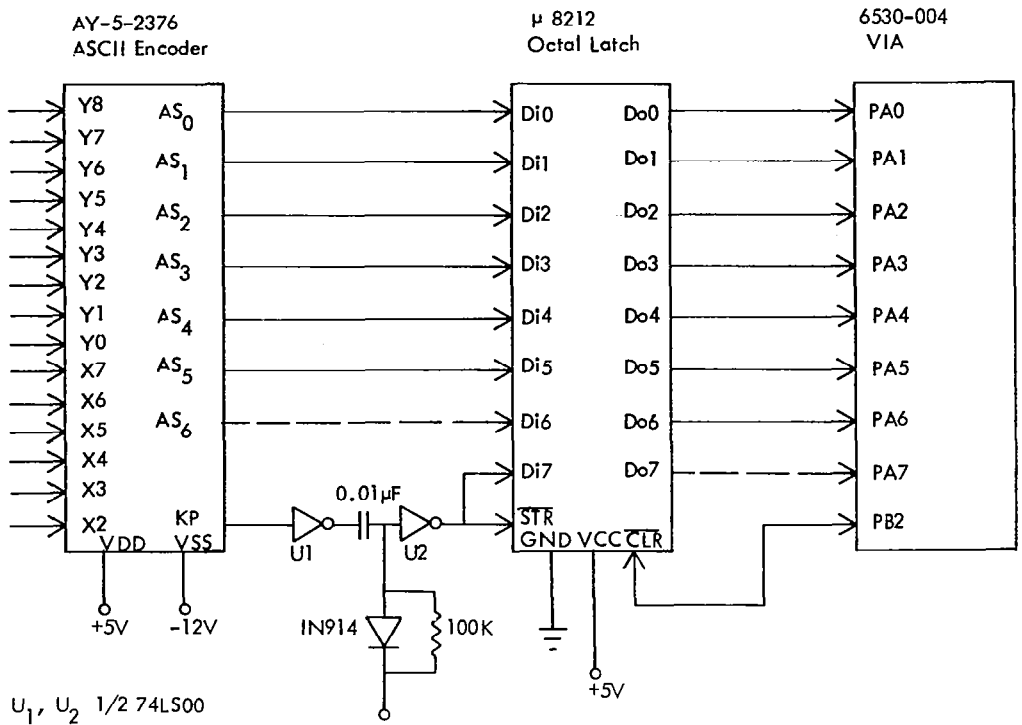
Figure 4. ASCII Keyboard Encoder Using AY-5-2376.
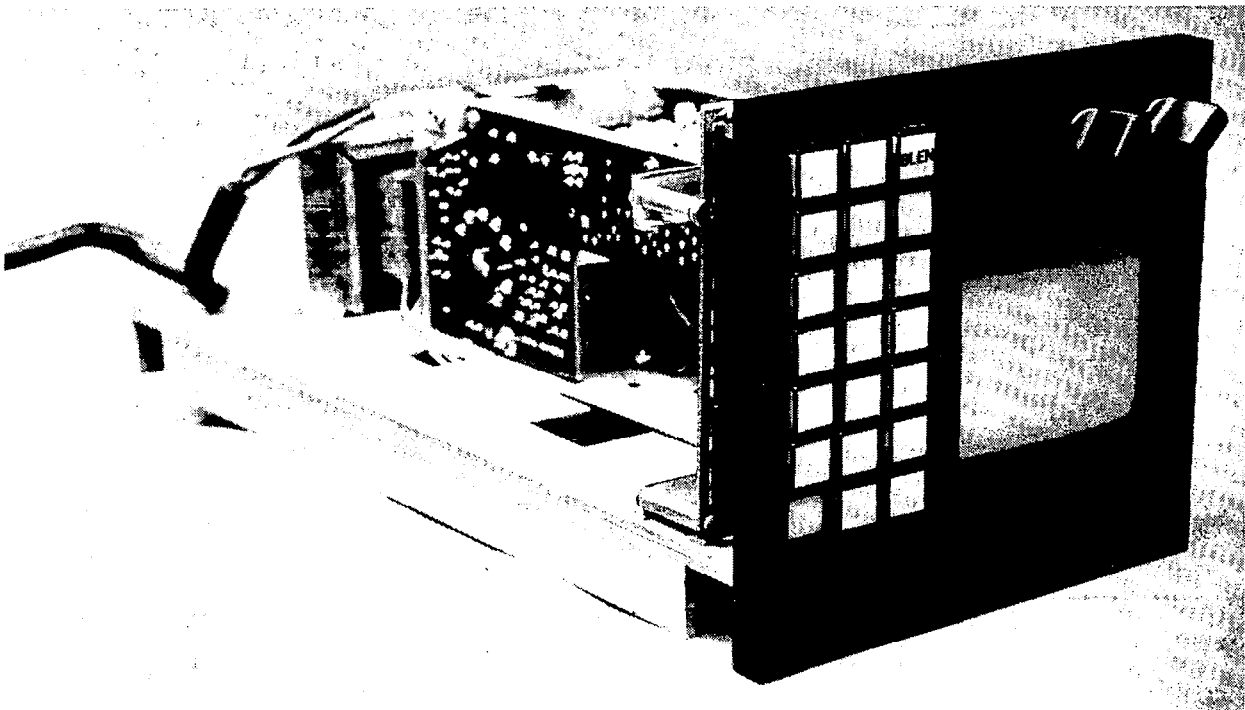
Figure 5. Proposed Display Unit.
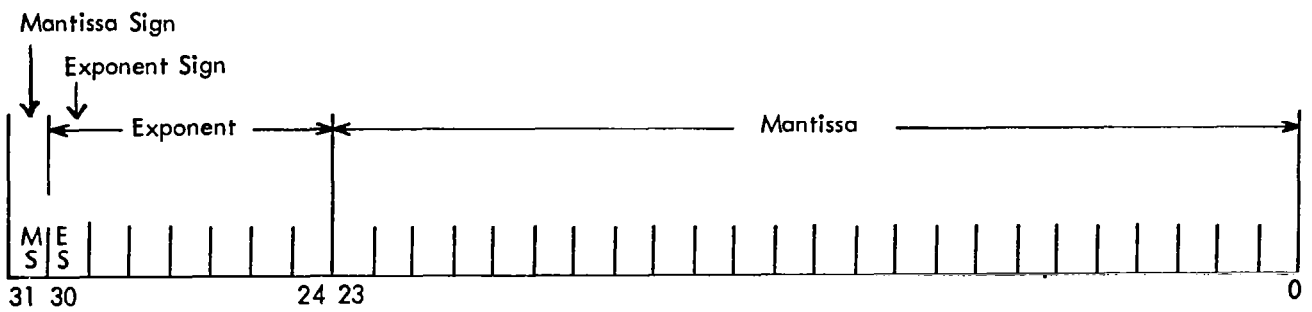
Figure 6. AM9511A 32-Bit Floating-Point Format.

164

R. F. PROCESSING

Ralph W. Burhans

Avionics Engineering Center
Department of Electrical Engineering
Ohio University
Athens, Ohio 45701

LORAN-C RF PROCESSING

ANTENNA   PREAMP   RF STATES   ENVELOPE GEN.

MINIMIZE   CONTROL   DELAY AND ADD
NOISE   GAIN AND   FOR 3RD CYCLE
AND   BANDWIDTH   ZERO CROSSING
INTERFERENCE

AGC
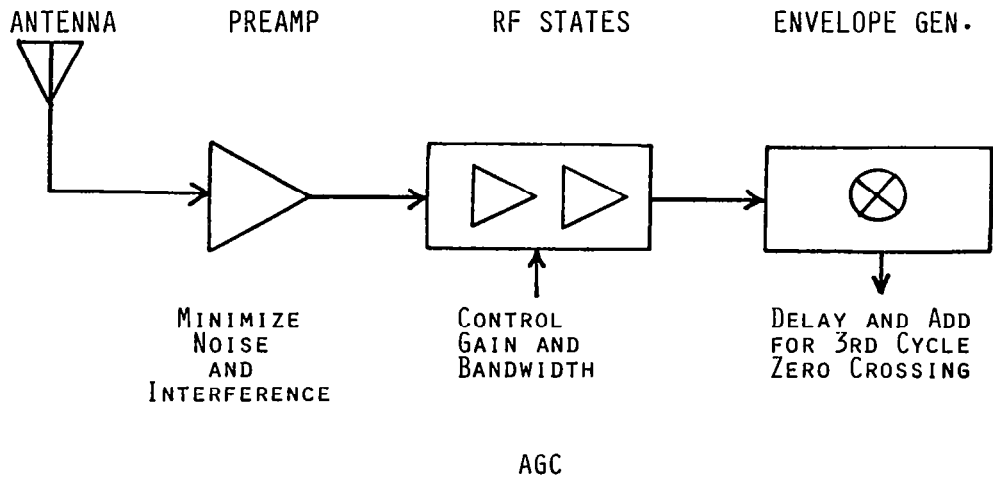
INTERFACE TO MICROPROCESSOR

RF SPECTRUM DATA

WEAK VLF SIGNALS

GBR 50 Hz SHIFT

PULSE SIGNALS

ADAPTER FOR STANDARD

COM RECEIVER

LORAN-C RESULTS

HF RADAR RESULTS

IONOSPHERE SCATTER FROM DISCOVERER II LAUNCH

"WOODPECKER" CHARACTER

PROPOSED   1982   DESIGN

| FROM ANTENNA | TRAPS | AGC AMPLIFIER | VIDEO DETECTORS | COMPARATOR |

PREAMP

MC1350   MC1330   LM311

88kHz | 116kHz

DELAY

ADD

AGC IN   ZERO CROSSINGS OUT

INTERFACE TO MICROPROCESSOR

whip
antenna

preamp   coupler

FRG 7700
receiver

XX.XXX MHz
slow AGC
12kHz AM
blanker off

audio record output

envelope
monitor

differential
monitor

CA81 amplifier   LM311 comparator

220k   10meg

.01   10k   +V   +V

10k
10k   zero crossing
                                          output

10k
delay adjust   .001
           200pf   220k   3mf   100k

2k   2k   +V   10k   threshold
                                adjust

AUGMENTED DIFFERENTIATOR FOR PULSE ENVELOPES

Circuit adapts conventional communications receiver with wideband AM capa-
bility to detection of pulse signals such as Loran-C. Also enhances reception
for surveillance and observation of HF over-the-horizon radar signals or others
where time difference estimates between pulse returns are of interest.
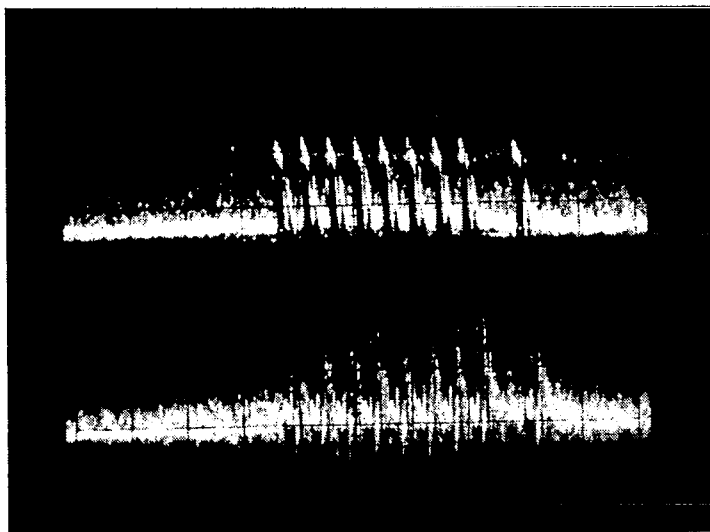
SWEEP   2.0ms/division

TOP   Direct Receiver Envelope

BOTTOM   Differentiated Envelope
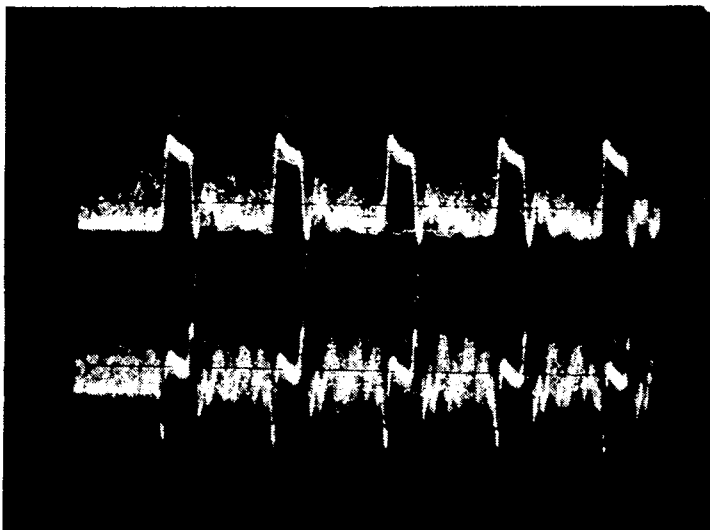
SWEEP   0.5ms/division

TOP   Direct Receiver Envelope

BOTTOM   Differentiated Envelope

20:00 EST 11/4/81   SENECA, N.Y., MASTER ON 99600   μsec. GRI

DIFFERENTIAL LORAN-C ENVELOPE SIGNALS

    As observed with YAESU FRG 7700 Communications Receiver, 12 kHz bandwidth, slow AGC, total input signal plus noise level = -66 DBM (20 DB over S9). Signal lag and subtraction circuit provides differential edge or zero crossings from a standard, unmodified communications receiver. Needed for driving external post detection microcomputer or digital tracking system for frequency standard or simple navigation experiments.

168
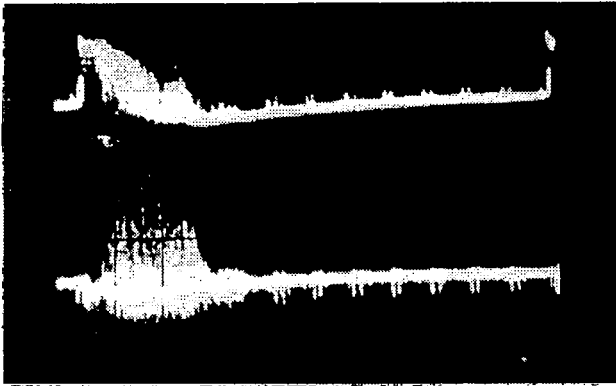
10:11AM 26.430MHz 1 minute
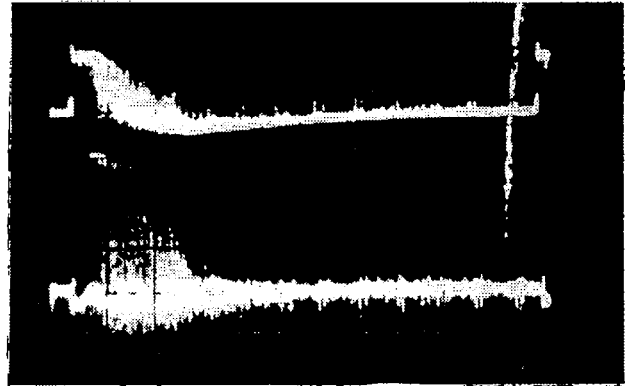
10:15AM 26.475MHz 5 minutes
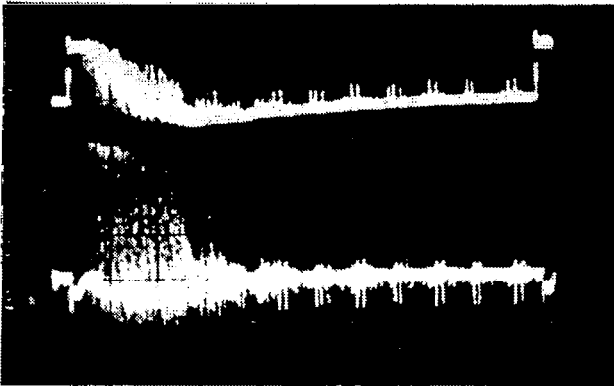
10:17AM 26.430MHz 7 minutes

10:19AM 26.320MHz 9 minutes
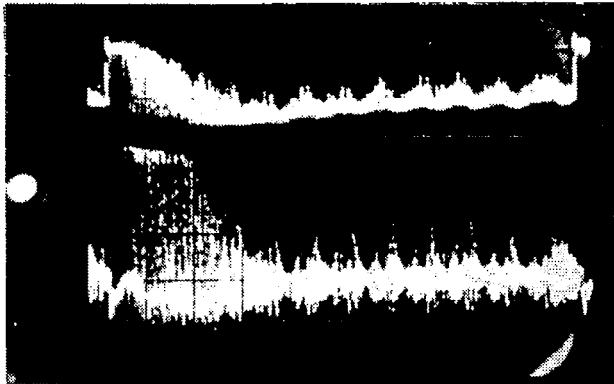
10:21AM 26.320MHz 11 minutes

10:24AM 26.320MHz 14 minutes

HF OTH RADAR RETURNS AT LAUNCH OF COLUMBIA, SHUTTLE II, November 12, 1981

Top trace is amplitude of received signal. Bottom is differentiated rise time
from scattered edges of ionosphere returns. Note, slight increase in amplitude
and intensity of scattered returns progressing to 14 minutes after launch.
Probable cause is ionized trail from main engine and booster exhaust.   The
pulse GRI was 100 milliseconds (10ms/division). Variable 120Hz interference
present. USSR "Woodpecker" changed channels and direction at about 10:25AM.

NORTH

USSR "Woodpecker"
HF RADAR

direct paths

observer

reflected
paths

ION CLOUD

(minutes)
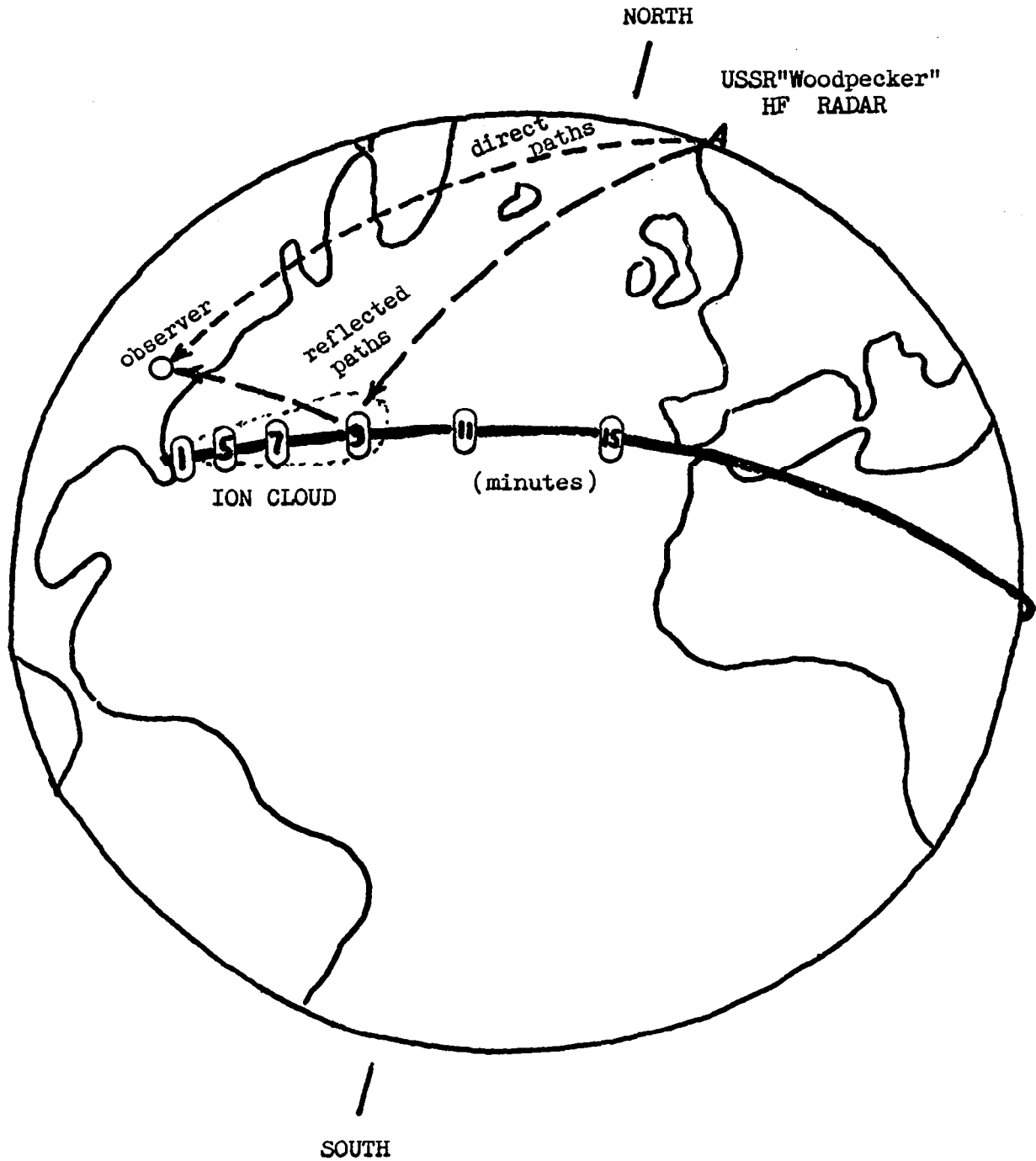
SOUTH

APPROXIMATE POSITIONS OF COLUMBIA SHUTTLE AT TIMES OF PHOTOS

Direct signal path is shorter, arrives at observer before southern
ionosphere scatter and much before any rocket exhaust ion enhancement.
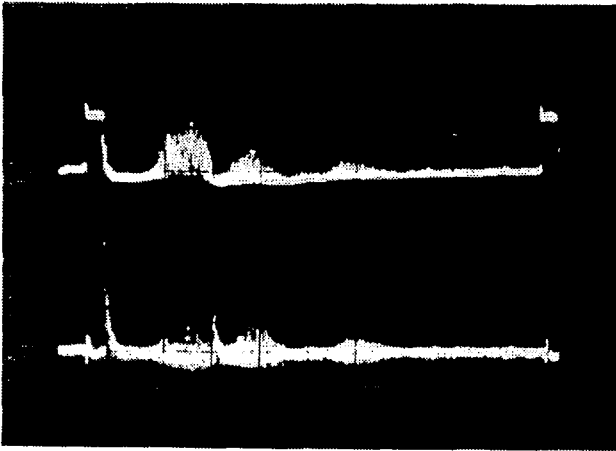
22:00 EST 11/4/81
23.800 MHz   GRI 100ms , 10ms/div.

4ms main bang with strong secondary
scatter at 15-25ms, 27-37ms, and 50-60ms
after start of main bang.

TOP   amplitude
BOTTOM   DE/DT
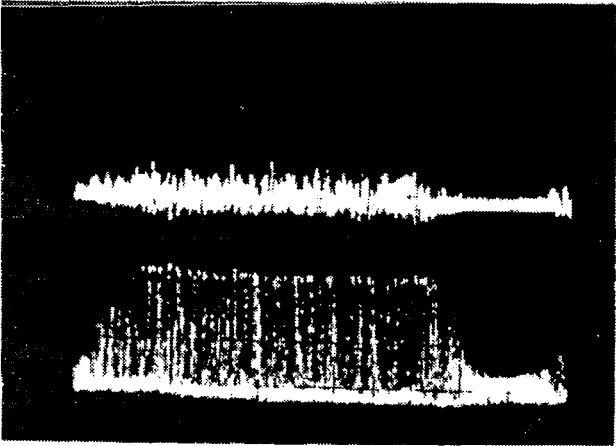
09:37 EST   11/2/81
27.900 MHz   GRI 100ms , 10ms/div.

Long PN code sequence, no FM

TOP   amplitude
BOTTOM   DE/DT
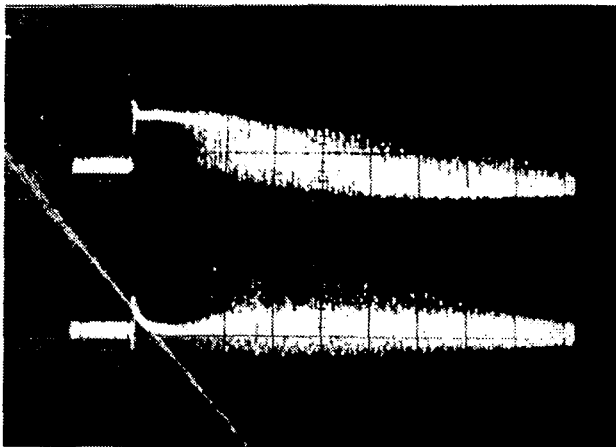
15:37 EST   11/4/81
18.575 MHz   GRI 100ms, 4ms/div.

Nominal 4 to 6ms single pulse with much
secondary scatter to 36 ms after main
bang starts.

TOP   amplitude
BOTTOM DE/DT

USSR HF "WOODPECKER" EXAMPLES WITH FRG 7700 RECEIVER
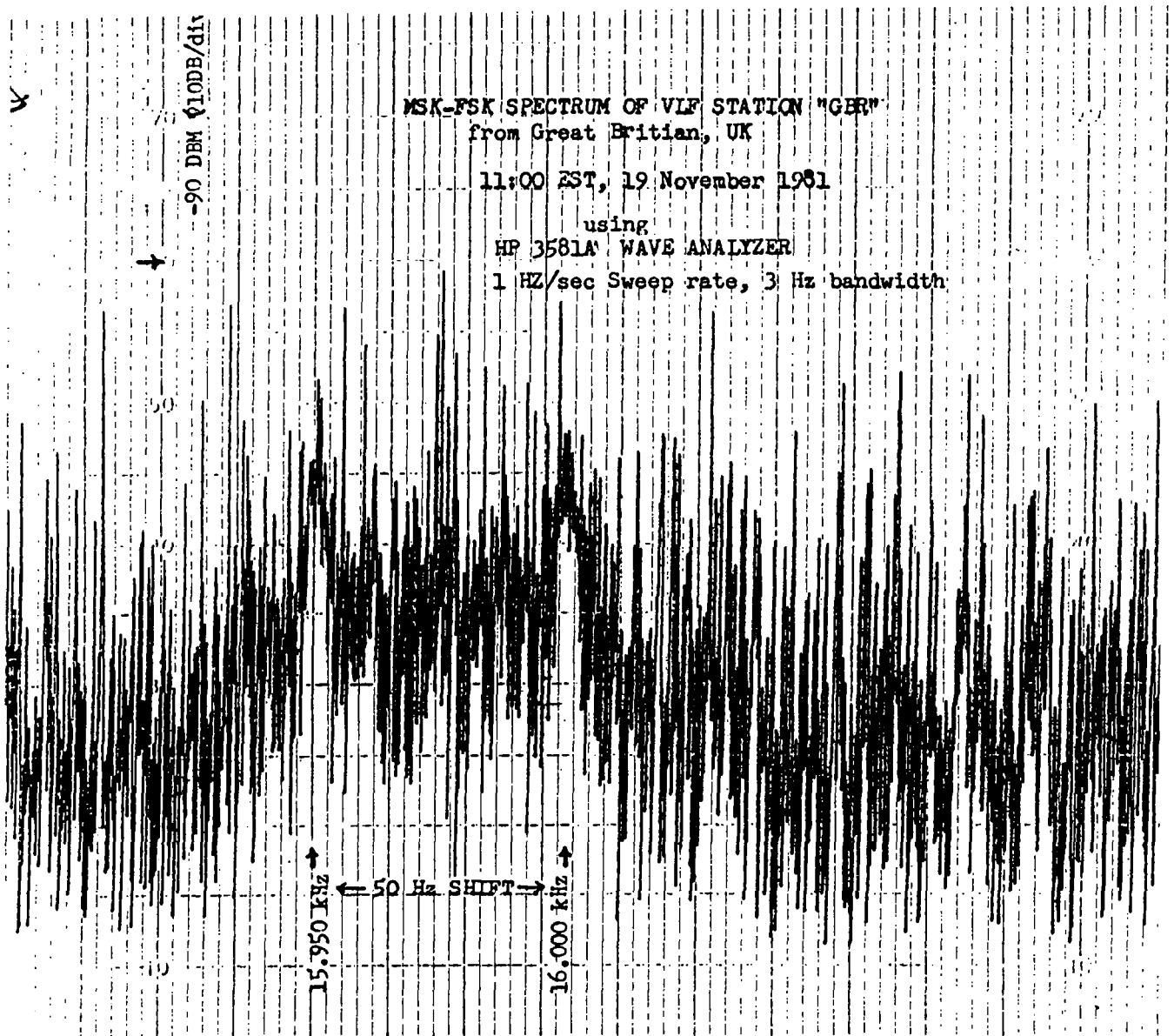
HIGH RESOLUTION VLF SPECTRUM

Example of reception of weak VLF signals using an HP 3581A Wave Analyzer which can detect signals with a very narrow bandwidth of only 3 Hz. The graph shows the 50 Hz frequency shift keying format transmitted by VLF station "GBR" on 16 kHz from Rugby, England as received in Athens, Ohio.

PROGRAMMING FOR LORAN-C RECEIVER PILOT DISPLAY

Fujiko Oguri

Avionics Engineering Center
Department of Electrical Engineering
Ohio University
Athens, Ohio 45701

PROGRAMMING FOR LORAN-C RECEIVER PILOT DISPLAY

PROBLEM

Compute: Range, Bearing, Ground Speed, & Cross Track Error

Given: Lat and Long of waypoints and receiver

Using: 6502 CPU and 9511A math chip

For: Final output & pilot display for OU Loran-C Receiver

Earth Model Chosen

Kayton & Fried "Avionics Navigation Systems",
John Wiley & Sons, NY 1969, p. 160.

PROGRESS

Basic equations used check with FORTRAN program for precision.

$$\text{Range} = a\Theta - \frac{af}{4}\left[(\sin\beta+\sin\beta_1)^2\left(\frac{1-\cos\Theta}{\sin\Theta}\right)\left(\frac{\Theta-\sin\Theta}{\sin\Theta}\right) + \left(\frac{\sin\beta-\sin\beta_1}{\sin\Theta}\right)^2(1+\cos\Theta)(\Theta+\sin\Theta)\right]$$

$$(\Theta) \text{ Bearing} = \tan^{-1}\left(\frac{\cos\beta_1\sin(\lambda-\lambda_1)}{\cos\beta\sin\beta_1 - \sin\beta\cos\beta_1\cos(\lambda-\lambda_1)}\right)$$

where:
- a = semimajor axis
- f = flattening of reference ellipsoid
- ϕ = geodetic latitude of the receiver
- ϕ_1 = geodetic latitude of the waypoint
- $\tan\beta$ = $(1-f)\tan\phi$
- $\tan\beta_1$ = $(1-f)\tan\phi_1$
- Θ = angle from receiver to waypoint
- λ = geodetic longitude of the receiver
- λ_1 = geodetic longitude of the waypoint

PLANNED WORK

Convert to assembly language program for 6502 and 9511 chips

Check precision
        anticipate 0.162° mean bearing error
                   0.0106 nm mean range error

Minimize Time Only 200,000 μsec.(0.2 sec.) available for these computations
        since lat-long and Loran-C receiver TDs take up remainder of
        computer time.

After computing range and bearing, other calculations are
relatively simple.

PROGRAMMING FOR LORAN-C

COMPUTE RANGE-BEARING-ETC.

FROM LORAN-C DATA

FOR MULTIPLE WAYPOINT POSITIONING

PROGRESS

EQUATIONS EVALUATED

PLANNED EFFORT

CONVERT TO MACHINE LANGUAGE

CHECK ACCURACY

MINIMIZE COMPUTER TIME

COMPREHENSIVE INVESTIGATION OF LORAN-C

FOR GA APPLICATION

Stephen R. Yost

Avionics Engineering Center
Department of Electrical Engineering
Ohio University
Athens, Ohio 45701

COMPREHENSIVE INVESTIGATION OF LORAN-C FOR GA APPLICATION

I. ESTABLISH PERFORMANCE CRITERIA
   A) FAA ENROUTE, TERMINAL, AND APPROACH ACCURACY
      REQUIREMENTS
   B) SUMMARIZE PREVIOUSLY COLLECTED O.U. LORAN-C DATA

II. DATA ANALYSIS TECHNIQUES
   A) INFORMATION SEARCH TO DETERMINE THE MOST CONCLUSIVE
      METHODS FOR STATISTICAL ANALYSIS
      1) DETERMINE OPTIMUM SIZE OF A STATISTICAL SAMPLE
   B) MULTIPLE, SIMULTANEOUS LORAN-C RECEIVER DATA COLLECTION
      1) UTILIZATION OF CASSETTE TAPE DATA RECORDERS
   C) USE OF OHIO U COMPUTER SYSTEM FOR DATA REDUCTION AND
      ANALYSIS

III. GROUND MONITORING
   A) LONG-TERM ON-SITE MONITORING OF LORAN-C POSITIONAL
      DATA
      1) EXAMINE DAILY AND POSSIBLY SEASONAL LORAN-C COVERAGE
         GRID WARPAGE
      2) DETERMINE LORAN-C WAYPOINT VALUES FOR RUNWAY
         THRESHOLDS
   B) SELECTION OF TEST SITES
      1) AREAS WHICH ARE COVERED BY MORE THAN ONE LORAN-C
         CHAIN PERMITTING CROSS-CHAIN POSITION COMPARISON
      2) EXAMINE LORAN-C PERFORMANCE IN FRINGE COVERAGE AREAS

IV. FLIGHT TESTING
   A) USE OF AN ABSOLUTE DATA REFERENCE TO SUBSTANTIATE LORAN-C
      DATA
   B) SIMULATE APPROACHES USING PREVIOUSLY DEFINED LORAN-C
      WAYPOINTS
   C) EXAMINE THE EFFECTS OF NON-GEOGRAPHIC IRREGULARITIES
      ON LORAN-C FLIGHT PATH DATA

V. CONCLUSIONS
   A) FORMULATE SPECIFIC HARDWARE AND SOFTWARE IMPROVEMENTS TO
      TO THE OHIO U LORAN-C RECEIVER
   B) COLLECTIVELY EXAMINE THE EFFECTS OF OVERLAND PROPAGATION
      DELAY TO LORAN-C SIGNALS
   C) ADDRESS THE POSSIBLE INTEGRATION OF LORAN-C NAVIGATION
      TO CURRENT ATC SYSTEM

Princeton
University

INVESTIGATION OF AIR TRANSPORTATION TECHNOLOGY

AT PRINCETON UNIVERSITY, 1981

Professor Robert F. Stengel
Department of Mechanical and Aerospace Engineering
Princeton University
Princeton, New Jersey 08544

SUMMARY OF RESEARCH

The Air Transportation Technology Program at Princeton University, a program emphasizing graduate and undergraduate student research, proceeded along seven avenues during the past year:

- Investigation of Fuel-Use Characteristics of General Aviation Aircraft

- Investigation of a Dead-Reckoning Concept Incorporating a Fluidic Rate Sensor

- Experimentation with an Ultrasonic Altimeter

- Development of Laser-Based Collision Avoidance Systems

- Flight Path Reconstruction from Sequential DME Data

- Application of Fiber Optics in Flight Control Systems

- Voice Recognition Inputs for Navigation/Communication Receiver Tuning

Principal investigators Robert Stengel and Larry Sweet have worked with Prof. H.C. Curtiss and Richard Miles in advising the students participating in this program.

Navigation research conducted during earlier years provided a logical stepping stone to consideration of flight management systems for general aviation aircraft, including fuel-minimizing guidance between origin and destination points. The effectiveness of such guidance logic is, of course, dependent on the accuracy of aircraft fuel-use models, and this, in turn, requires adequate mathematical description of engine characteristics. In his doctoral research, Richard Parkinson has developed a cruise performance model that can be developed from operating handbook data, and he has developed a detailed mathematical model of the fuel-use characteristics of general aviation reciprocating engines. Interim results are documented in a technical paper[1], and his thesis is near completion. Mr. Parkinson began his research under the guidance of Prof. Dunstan Graham, who retired from the university in 1980; he has continued with the supervision of Prof. Curtiss and Sweet. Graduate student Eugene Morelli is continuing this research.

A simple approach for dead reckoning navigation that is enhanced by the use of a fluidic angular rate sensor has been studied by M.S.E. candidate Robert Ellis. The fluidic sensor is used to correct the northerly turning error of conventional flux gate magnetic compasses. (The northerly turning error results from the effect of "dip angle" on sensed magnetic heading when the aircraft is banked to turn.) Limited flight tests were conducted during the year, and final results of experimental studies will be reported in Mr. Ellis's thesis. Mr. Ellis began his research with former principal investigator Dunstan Graham; Prof. Sweet is his current advisor.

Amy Snyder, a junior in mechanical and aerospace engineering, completed an investigation of the feasibility of using an ultrasonic transducer as an altimeter for the landing approach through touchdown. The transducer, initially developed for use in an automatic range-finding camera, demonstrated better than 1% accuracy for ranges of 0.27 to 10.67 m (0.9 to 35 ft) in laboratory and wind tunnel tests, with transverse air velocities of up to 45.7 m/sec (150 ft/sec) and with sensor angles of 0 to 25 deg[2]. Senior Philip Chu is continuing this research, with the objectives of doubling the sensor's range and conducting flight tests of the system. Prof. Stengel has been Ms. Snyder's and Mr. Chu's advisor.

The investigation of laser-based collision avoidance systems continued, resulting in several papers, reports, and theses[3-8]. This research is being conducted in parallel with a NASA Ames-sponsored study of short-range tracking between two cooperative aircraft using low-power lasers. Demonstration equipment has been assembled and will be tested in flight within the near future. This research has involved Prof. Richard Miles and Larry Sweet, graduate students Steven Webb, Edward Wong, and Gregory Russell, and undergraduates Leonard Blackburn and Maged Tomeh.

The Flight Research Laboratory is engaged in a continuing study of flying qualities criteria for single-pilot instrument flight operations with separate sponsorship from NASA Langley Research Center[9], and elements of the flight path reconstruction algorithms, which have common application for the study of air transportation technology, have been developed under this grant. Techniques for applying extended-optimal smoothing to sequential DME data and on-board inertial and air data have been developed and applied to flight test data by Ph.D. candidate Aharon Bar-Gill. In this approach, a single DME receiver is switched between alternate DME stations to update the state estimate, which is processed after the flight has been completed. Because all the measured data are applied to estimate the state at each point in the flight path, the result is somewhat more accurate than that which would be obtained from the extended-optimal filter. Mr. Bar-Gill is advised by Prof. Stengel.

Fiber optic data transmission promises to provide decreased weight, improved resistance to electro-magnetic interference, and increased reliability in future active flight control systems. Graduate student Kristin Farry is nearing completion of an application of fiber-optic technology in a multi-microprocessor system, with the combined sponsorship of this grant and the Office of Naval Research. Princeton's Variable-Response Research Aircraft (VRA) has dual angle-of-attack and sideslip angle vanes mounted at each wingtip, previously connected to the central analog and digital control logic by standard wiring. Dual microprocessors have been installed at the wingtips; the sensors are connected directly to these units, which in turn communicate with the central microprocessor via fiber-optic links. The local processors provide scaling and instrument-error correction, elimination of roll rate effects on sensed angles, and analog/digital conversion before sending the data to the flight control computer unit. The fiber-optic multiprocessor system will be tested in flight shortly, and the results will be presented in Ms. Farry's M.S.E. thesis. Ms. Farry is working with the guidance of Prof. Stengel.

Voice recognition of pilot inputs could play a major role in future air transportation, not only for commercial aircraft but for general aviation aircraft as well. This capability has particular significance for single-pilot instrument-flight operations, where one pilot is required to perform all the tasks normally carried out by two or three persons in the larger aircraft. The tasks that could be carried out using voice command are varied; as a generality, these are characterized as the jobs which a captain might ask the co-pilot to do, e.g., tuning radios, maintaining contact with air traffic control, holding altitude, and so on. Frances Koo, a senior in electrical engineering and computer science, is conducting a project in which voice recognition will be used to tune the navigation and communication receivers in Princeton's Avionics Research Aircraft (ARA). The ARA's receivers will be tuned by digital signals from a microprocessor, which will receive inputs from the pilot via the voice recognition board. Ms. Koo is being advised by Prof. Stengel.

In addition, the research on OMEGA-Dead Reckoning hybrid navigation completed earlier has been documented in the M.S.E. thesis of Ralph Nichols{10}, completed this year. Mr. Nichols began his research under the guidance of Prof. Graham and completed his thesis with Prof. Stengel as his advisor.

The NASA grant supporting student research in air transportation technology has inestimable value in helping educate a new generation of engineers for the aerospace industry, and it is producing research results that are relevant to the continued excellence of aeronautical development in this country.

REFERENCES AND ANNOTATED BIBLIOGRAPHY

1. R.C.H. Parkinson, "An Operational Model of Specific Range for Microprocessor Applications in Piston-Prop General Aviation Airplanes", AIAA Paper No. 81-2330, Nov 1981.

    The paper describes a cruise performance model for conventional general aviation airplanes of fixed design, powered by naturally aspirated spark ignition piston engines and constant-speed propellers. The model computes the airplane operating point which maximizes specific range and is suitable for airborne microprocessor implementation, with the assumptions that the engine ignition timing is optimized for maximum engine torque and that fuel-air mass ratio can be controlled. It appears that fuel savings of 20% to 26% could be achieved through use of this procedure.

2. Amy V. Snyder, "Ultrasonic Altimetry: Feasibility and Design Principles", Princeton M.A.E. Junior Independent Research Project Report, Princeton University, May 1981.

    The report examines the feasibility of using a Polaroid Ultrasonic Ranging System as an altimeter for aircraft on landing approach. The ranging device generates pulses in the 50 to 60 KHz band using an electrostatic transducer that functions as both an emitter and a receiver of the sound energy. Initial wind tunnel tests indicated that the flow of air over the unshielded transducer generated sounds in the operating band that precluded ranging; however, a megaphone-like baffle was found to restore ranging capability with air velocities up to 45.7 m/sec (150 ft/sec). This technique shows great promise for providing landing approach data at low cost, with high reliability, and for aircraft of all classes.

3. Richard B. Miles, "Laser Beacon System for Aircraft Collision Hazard Determination", Applied Optics, Vol. 19, No. 13, July 1, 1980, pp. 2098-2108.

    A laser beacon collision hazard determination system is capable of simultaneously determining range, bearing, and heading of threat aircraft. Calculations demonstrate that threat aircraft may be observed at >10 km under good visibility conditions, the conditions under which the overwhelming majority of mid-air collisions take place. A wide variety of detection systems may be chosen based on cost, detection range, and sophistication. Preliminary tests demonstrate that accurate range measurements are possible under daylight conditions.

4. Leonard A. Blackburn II, "A Display for a Laser Aircraft Position Locator System", Princeton M.A.E. Senior Independent Research Project Report, Princeton University, May 1981.

The purpose of this study was to develop a system that displays the relative (three-axis) position between a research aircraft and a following helicopter. Signals would be displayed in such a way that the helicopter pilot could hold position relative to the other aircraft to within one foot in distance and one degree in azimuth and elevation angles. The study included the selection and construction of a data acquisition system, the design of a suitable display, and the analysis of position control and pilot-helicopter dynamics using root-locus techniques. Helicopter dynamics were simulated using an eleventh-order, six-degree-of-freedom model; the pilot was modelled by a conventional compensatory transfer function. Particular attention was paid to the pilot gains and lead-lag compensation required for closed-loop stability. The analysis indicated that stabilizing the system would require substantial pilot effort at the data sampling intervals anticipated.

5. Maged Tomeh, "Non-Linear State Estimation Algorithms for the Development of an Air-Collision Avoidance System Using Laser Beacons", Princeton M.A.E. Senior Independent Research Project Report, Princeton University, May 1981.

An extended Kalman filtering algorithm based on a nonlinear dynamic system model was applied to the collision avoidance problem. The purpose was to assess the level of estimation accuracy that could be obtained in determining the flight path of threat aircraft and to evaluate on-board implementation using steady-state filter gains. Over 50 simulations of near-collision flight paths were computed. The filter was found to possess extreme sensitivity to initial conditions and an inherent instability in estimating one of the unmeasured state variables. Suggestions for improving the filter's characteristics centered on the use of a discrete linear Kalman filter.

6. Steven G. Webb, "Aircraft Position Measurement Using Laser Beacon Optics", Princeton M.S.E. Thesis, M.A.E. Report No. 1535-T, Princeton University, Sept. 1981.

The thesis investigates a system to precisely measure the relative position between two aircraft utilizing a laser beacon, an optical detector array, and on-board digital computation. The laser beacon consists of two orthogonal fan-shaped narrow-width beams with 166-deg coverage, each rotating at four revolutions per second. Each of the four detectors in the receiving array is composed of two compound parabolic concentrators which collect the incoming laser beams over a 150-deg field of view, collimate the light so that it can pass through an interference filter, and concentrate the beam on a photodiode. The diode converts the detected beams to pulses that are transmitted through a bandpass filter and processed for tracking purposes. Initial tests have demonstrated the system's potential for use as a position measuring system.

7. L.M. Sweet, R.B. Miles, S.G. Webb, and E.Y. Wong, "Wide Field of View Laser Beacon System for Three-Dimensional Aircraft Position Measurement", ASME Paper No. 81-WA/DSC-9, Nov 1981.

    This paper describes a new wide-field-of-view laser beacon system for measurement, in three dimensions, of aircraft or other remote objects. The system provides aircraft collision hazard warning independent of ground-based hardware, and it has applications in flight research, helicopter-assisted construction and rescue, and robotic manipulation. Accurate information describing the relative range, elevation, and azimuth of the aircraft is generated by the sweep of a low-power fan-shaped rotating laser beacon past an array of optical detectors. System reliability and performance are enhanced through bandpass filtering of the pulse signals, digital logic designed to mask spurious signals, and adaptive modulation of trigger threshold levels.

8. L.M. Sweet, R.B. Miles, G.F. Russell, M.G. Tomeh, S.G. Webb, and E.Y. Wong, "Digital Detection and Processing of Laser Beacon Signals for Aircraft Collision Hazard Warning", AIAA Paper No. 81-2328, Nov 1981.

    A low-cost collision hazard warning system suitable for implementation in both general and commercial aviation is presented. The laser beacon/photodetector system provides direct measurement of relative aircraft positions, using optimal nonlinear estimation theory. The measurements resulting from the current beacon sweep are combined with previous data to provide the best estimate of aircraft proximity, heading, minimum passing distance, and time to closest approach.

9. A. Bar-Gill, W.B. Nixon, and G.E. Miller, "Flying Qualities Criteria for Single-Pilot Instrument Flight Operations", Princeton M.A.E. Report No. 1528, Dec 1981.

    Preparations for flight test related to the development of flying qualities criteria for Single-Pilot Instrument Flight Rule (SPIFR) operations are described. The principal objective is to examine the effects of aircraft dynamic characteristics (representative of long period stability and ease of longitudinal trim variations) on pilot opinion, pilot workload, and flight technical error during simulated IFR missions in general aviation aircraft. The Avionics Research Aircraft (ARA) has been modified and adapted for SPIFR operations. Aircraft configurations to be tested using the ARA's variable-stability fly-by-wire system have been chosen and matched in flight. The mission matrix has been designed. Microprocessor software for the on-board data acquisition system has been flight tested. Flight path reconstruction procedures are in a final stage of computer program

development. Work has begun on algorithms associated with the statistical analysis of flight test results.

10. Ralph A. Nichols, Jr., "Implementation and Evaluation of an OMEGA-Dead Reckoning Hybrid Navigation System", Princeton M.S.E. Thesis, M.A.E. Report No. 1523-T, Princeton University, June 1981.

This thesis reports on the results of flight tests in which navigation is accomplished by combining data from an OMEGA radio receiver with heading and true air speed measurements. The implementation and evaluation of the system, which was installed in Princeton's LASA 60 utility aircraft, are discussed, including fabrication, hardware configuration, and software design. Flight test procedures are described, the theoretical basis for analysis is developed, and flight test results are presented. These flight tests showed 10% to 40% reductions in rms position errors over that obtained from OMEGA data alone. Raw OMEGA position errors typically ranged from 0.8 to 1.8 nm (rms). OMEGA signals were found to contain large amplitude, low frequency noise; flight test results were consistent with pre-flight predictions for noise of this type. The hybrid system improved navigation continuity with poor OMEGA signal reception. OMEGA lane count could be maintained during as much as an hour of signal loss. It was concluded that OMEGA navigation does not provide sufficient accuracy for general aviation operations over the continental United States, although improvements could be made in the navigation algorithm.

FLYING QUALITIES CRITERIA FOR GA
SINGLE PILOT IFR OPERATIONS

Aharon Bar-Gill
Princeton University

BACKGROUND

o Over 200,000 GA aircraft operational in U.S. only

o Over 40,000,000 flight hours per year

PROBLEM

GA accident statistics investigated by NASA (TM 78773) and attributed mostly to the SPIFR flight regime - due to coupling of the following effects:

o Low frequency aircraft dynamics deficiencies (no design criteria in FAR #23,181, wind shear)

o High workload environment

o IFR pilot experience

o Limited GA instrumentation (compared to airliners, e.g.)

DIRECTIONS FOR SOLUTION

o Autopilots (wing levelers, etc., e.g.,NASA CP 2170)

o Training (GA simulators, including IFR conditions, become available; e.g., Aviation Week and Space Tech.,11/30/81)

o Instrumentation improvements (advanced displays, DME sequencing, Loran C, etc.)

o Aircraft low frequency dynamic response improvement - to date little has been done in this area

MEANS

o Theoretical work

o Ground simulators - done a lot

o Actual flight testing plus extensive statistical analysis - much less

Modern control theory algorithms are employed to identify the most important - in the SPIFR context - aerodynamic configurations and to implement these configurations on the test vehicle.

The experimental vehicle is the Ryan Navion, which has been modified and instrumented to a level of a fly-by-wire system, capable of in-flight simulating a wide range of aerodynamic configurations.

The sensor package includes a strapdown IMU, and airspeed, altitude, and aerodynamic angles sensors. The navigational package provides VOR/DME measurements. Control manipulation time histories are recorded as well.

SPIFR RESEARCH - FRL, PRINCETON

o IDENTIFICATION OF KEY AERODYNAMIC CONFIGURATIONS

o IMPLEMENTATION ON THE ARA IN-FLIGHT SIMULATOR

o MISSION MATRIX DESIGN

o EXPERIMENTAL SYSTEM

o DATA REDUCTION

o OPTIMAL FLIGHT PATH RECONSTRUCTION

o REPRESENTATIVE RESULTS

LOGICAL FLOW CHART OF THE SPIFR RESEARCH

WORKLOAD
LEVEL

DYNAMIC RESPONSE
PARAMETER VARIATIONS

ACCURACY
BASED ON AN INEXPENSIVE
STRAPDOWN IMU AND ON THE
MULTIPLE DME CONCEPT.

FLIGHT PATH
RECONSTRUCTION

IN-FLIGHT MISSION
SIMULATION

IFR PILOT
EXPERIENCE

REGRESSION
ANALYSIS

PILOT OPINION
RATINGS

OBJECTIVE I

QUANTITATIVE AND
STATISTICALLY SIGNIFICANT
SPIFR FLYING QUALITIES
CRITERIA.
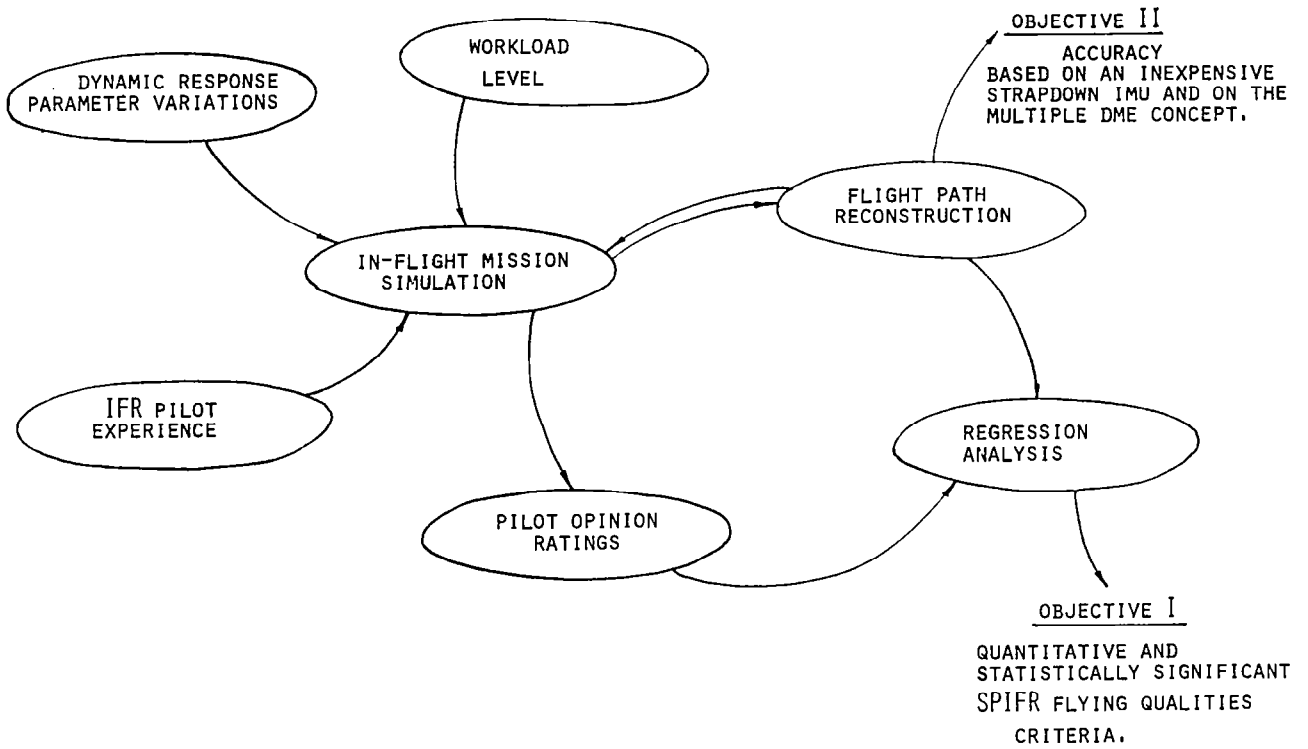
Formulation of the output command algorithm has been presented by Professor R. F. Stengel at the TRI-UNIV Conference in Boston, September 1980, and is discussed in the context of the SPIFR research in a report entitled Flying Qualities Criteria for Single-Pilot Instrument Flight Operations (M.A.E. Report No. 1528, Princeton University, December 1981). Implementation of the implicit model following algorithms may also be found in this report.

Ranges of variation in the aerodynamic parameters are intended to reflect possible trends in GA aircraft design.

IDENTIFICATION OF HIGHER-PRIORITY AERODYNAMIC CONFIGURATIONS

O OUTPUT COMMAND ALGORITHM

O COMPLETE DYNAMIC SIMULATION

CRITERIA FOR REPRESENTATION OF CHOSEN CONFIGURATIONS

O INPUT AND OUTPUT STEADY STATES

O TRANSIENT RESPONSE CHARACTERISTICS

IMPLEMENTATION OF CHOSEN CONFIGURATIONS ON ARA IN-FLIGHT SIMULATOR

O IMPLICIT MODEL FOLLOWING ALGORITHM

The experimental matrix is designed to provide a range of low-frequency aircraft flight characteristics. The numbers indicate how many replications will be made for each configuration and test subject. The pluses and minuses indicate whether the parameter variation will be positive or negative.

EXPERIMENTAL MATRIX DESIGN

TRADEOFF BETWEEN

- NUMBER OF CONFIGURATIONS,
- NUMBER OF REPLICATIONS,
- NUMBER OF EVALUATION PILOTS

(UNDER THE CONSTRAINT OF ~ 30 FLIGHT HOURS)

CONFIGURATION	PRINCETON TEST PILOT	NASA PILOT	GA PILOT	NO. OF MISSION RUNS
NOM.	2	2	2	6
X_U	2±	2±	3++	7
Z_U	2±	2±	4++	8
Z_W	2±	2±	3 ±	7
M_U	2±	2±	4++	8
$M_{\delta T}$	3 ±	3 ±	4++	10
$Z_{\delta E}$	2±	2±	4++	8
$Z_{\delta T}$	2±	2±	4++	8

$$\Sigma = 62$$

FLIGHT PLAN FOR EACH PILOT IS OF FOLLOWING STRUCTURE:

TAKEOFF NO.	MISSION NO.	CONFIGURATION NO.	TRACK NO.
1	1	1 (NOM)	1
	2	2	2
	3	6	3
2	4	1	2
	5	3	3
	6	6 (REPLIC.)	4

PILOT EXPERIENCE PARAMETER (PE):

PILOT NO.	PILOT	IFR LOGGED FLIGHT HOURS/TOTAL TIME	PE= $\dfrac{IFR\ TIME}{600}$
1	B. NIXON	600/5000	1.00
2	D. PEOPLES	270/2500	0.45
3	NASA	–	

o TRACK AND CONFIGURATION RANDOMIZATION

o LEARNING CURVE EFFECT

Navigational stations engaged during this flight test
series are Robbinsville, Colts Neck, Solberg and McGuire.

The semi-circles represent covariance contours along
which the flight technical error in the VOR/VOR or DME/DME
navigational modes is constant. GDOP effect (Geometrical
Dilution of Precision) and the covariance contour analysis
are discussed in M.A.E. Report No. 1528 (Princeton Univ.,
Dec. 1981).

SPIFR MISSION SIMULATION

Each variant has a different vertical profile in addition
to the horizontal projection differences. The evaluation
pilot is TAC - vectored on the McGuire AFB tower frequency.

SPIFR FLIGHT PATH VARIANTS
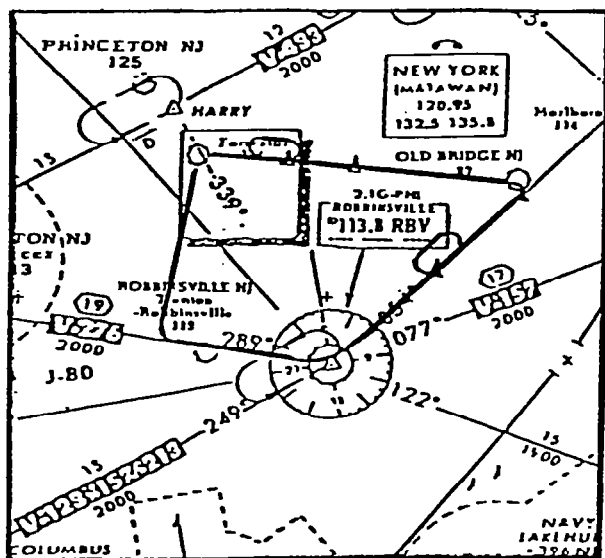
Variant I.
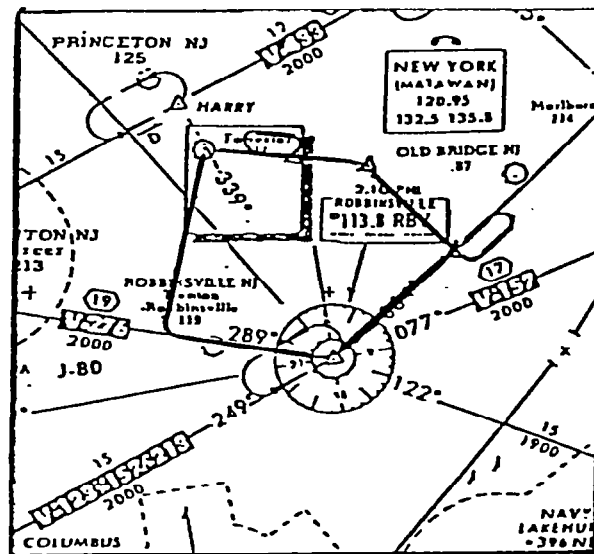
Variant II.
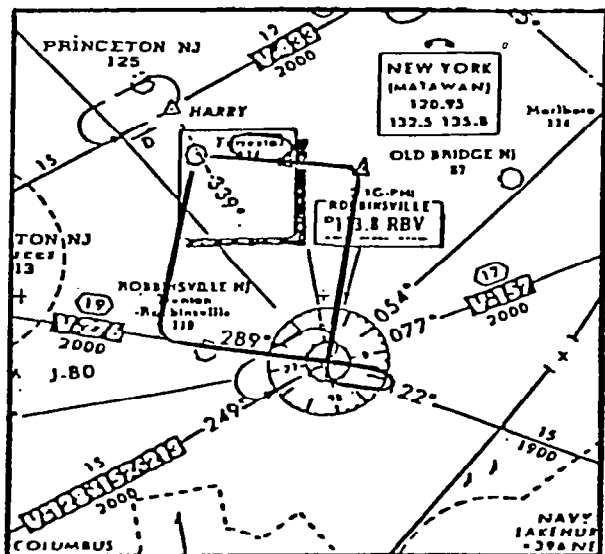
Variant III.
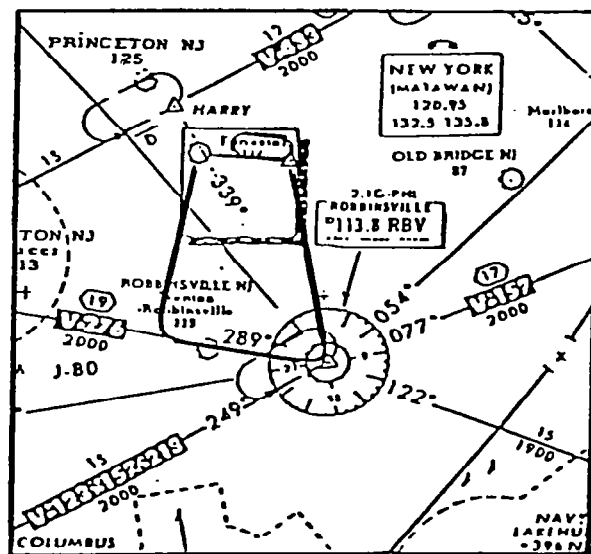
Variant IV.

SPIFR ON-BOARD DIGITAL DATA ACQUISITION SYSTEM

CONTROL/DISPLAY	SPIFR MICROCOMPUTER	RECORDING UNIT
• Termiflex HT/4 • Executive Control	• MSC 8004 Single Board Computer • iSBC 116 Memory • iSBC 732 Analog Input/Output • iSBC 724 Analog Output • FRL DME Distance & Frequency Converter	• Hewlett Packard 2644 Cartridge Drive • "3M" Tape Cartridge

ANALOG INPUTS		ANALOG OUTPUTS
• Air Data • Inertial Data • Navigation Data • Control/Trim	• TCU 410 Clock • Spare • Spare	• Workload Meters

DIGITAL INPUTS	NAVIGATION/COMMUNICA- TION (Bendix BX-2000)	DIGITAL OUTPUTS
• Navigation Data • Mode Switches • Workload Response	• DM-2030 DME • CN-2011 Dual VOR/ Comm • ADF, Transponder	• Workload Lights • Nav/Comm Frequencies

Subjective performance indicators are the Pilot Opinion
Ratings (PORs). CHR is the Cooper-Harper Performance scale
and the workload scale has been developed by the M.I.T. man-
machine laboratory.

We are examining both flight test segments characteristic
of the SPIFR regime and overall mission performance. This
provides additional insight and augments the statistical basis.

EVALUATION SHEET

MISSION VARIANT #

CONFIGURATION #

PILOT

DATE

SPEED RETRIMMING

CHR

WORKLOAD

COMMENTS

HOLDING PATTERN

CHR

WORKLOAD

COMMENTS

GLIDE SLOPE TRACKING

CHR

WORKLOAD

COMMENTS

OVERALL MISSION

CHR

WORKLOAD

COMMENTS

OBJECTIVE DATA PREPROCESSING

```
┌──────────────────────────────────────┐
│  SPIFR flight records on             │
│  DC100A digital data cartridges      │
└──────────────────────────────────────┘
                 │
                 ▼
┌──────────────────────────────────────┐
│  Transfer from cartridges to         │
│  9-track 1600 BPI magnetic tape      │
│     (HP 1000 digital computer)       │
└──────────────────────────────────────┘
        │                    │
        ▼                    ▼
┌─────────────────────┐  ┌─────────────────────┐
│ Data reduction &    │  │ Data reduction &    │
│ analysis            │  │ analysis            │
│ (IBM 4341 digital   │  │ (IBM 3033 digital   │
│  computer)          │  │  computer)          │
└─────────────────────┘  └─────────────────────┘
```
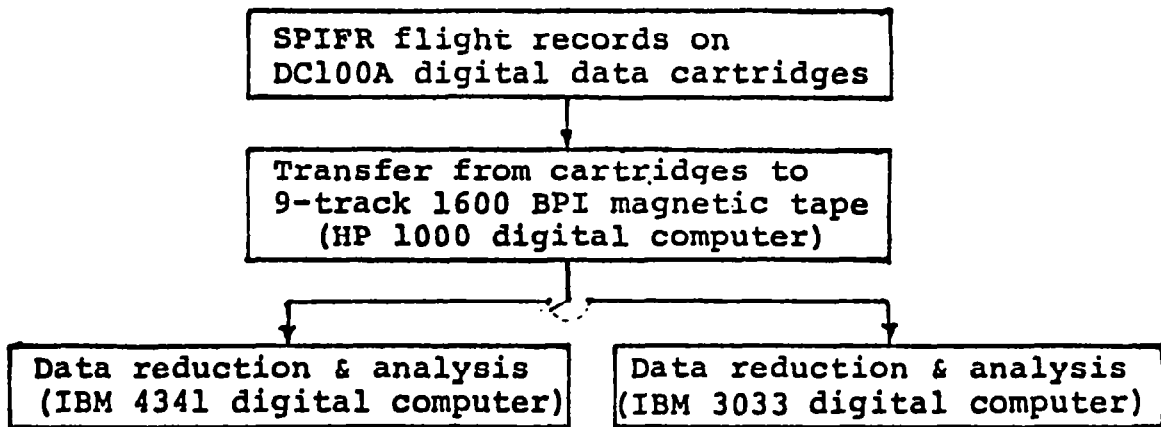
o   CONVERSION OF 16-BIT BINARY DATA INTO DECIMAL INTEGERS

o   PHYSICAL TIME VECTOR FORMATTING

o   CONVERSION INTO VOLTAGE

o   CONVERSION INTO ENGINEERING UNITS

200

As the mathematical model is nonlinear, the extended Kalman filter is employed. The stabilized Kalman filter formulation is implemented to provide numerical robustness.

Bias-type states account for directional gyro bias and drift, for the DME range error and for the low frequency wind gusts. The geoid geometry and Earth rotation effects are incorporated in the model.

The system model has been divided into angular and translational submodels, which may be addressed sequentially, thus augmenting the numerical robustness. The filter tuning methodology takes advantage of the model division. It applies theoretical considerations and interacts with the SPIFR generic simulation.

OPTIMAL FLIGHT PATH RECONSTRUCTION

o EXTENDED, STABILIZED KALMAN FILTER

o RAUCH-TUNG-STRIEBEL OPTIMAL SMOOTHER

o BIAS-TYPE STATES AND NAVIGATIONAL ASPECTS
    (MATHEMATICAL MODEL EXTENSION)

o ANALYTICAL DERIVATION OF STATE AND OBSERVATION JACOBIAN MATRICES

o DIVISION INTO LOWER-ORDER SUBMODELS

o SEQUENTIAL COMPLEMENTARY FILTER TUNING

The optimal smoother algorithm improves both the state estimates and the associated covariances. Bias-type states may cause significant estimation errors if their wide-range variations are not accounted for.

DESIGN AND ANALYSIS OF THE OPTIMAL SMOOTHER

o FILTER SENSITIVITY ANALYSIS

o IMPLEMENTATION ISSUES (DATA COMPRESSION, NONSIMULTANEOUS
                    DME LOCK-ON, OUTLIERS)

o INTERACTION WITH PREFLIGHT AND FLIGHT-TESTING PROCEDURE
   (BIASES EXTRACTION, MISSION STARTING POINT)

FORWARD FILTERING PROGRAM
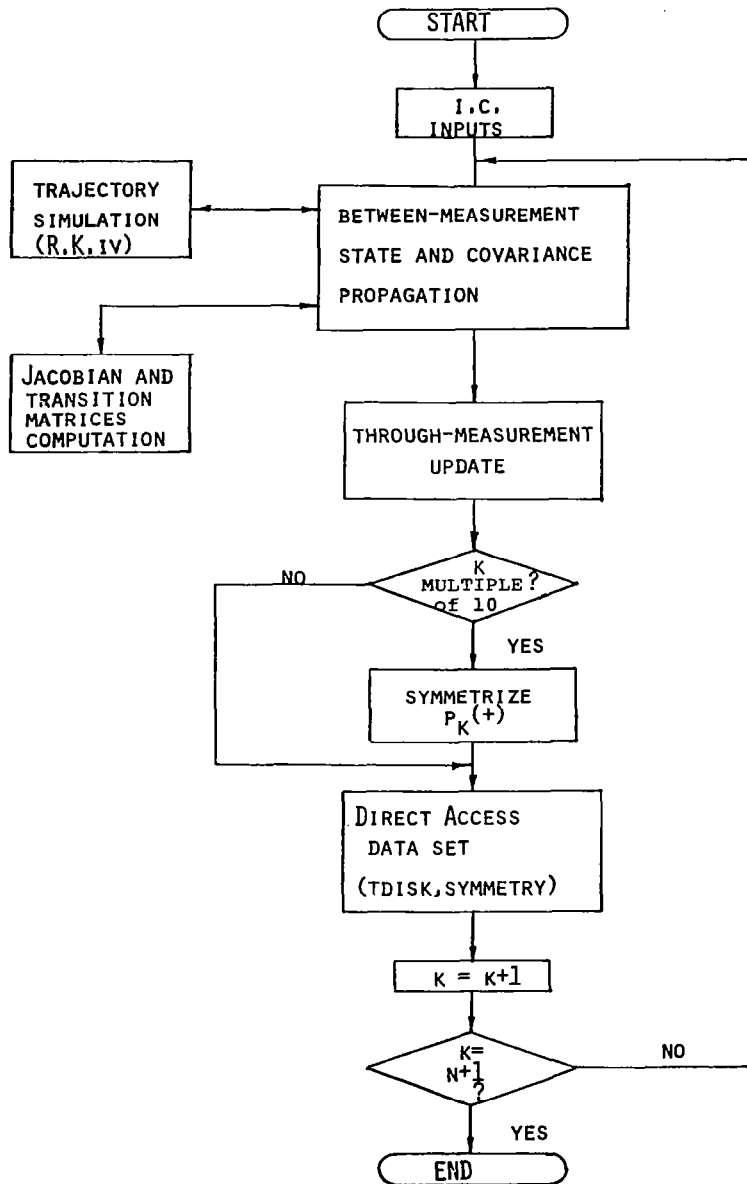
BACKWARD SMOOTHING PROGRAM

```
                        ( START )
                            │
                            ▼
                    ┌─────────────────┐
                    │      READ       │
                    │ X̂_K(+), X̂_K(-); │
                    │   P_K(+), P_K(-) │
                    └─────────────────┘
                            │
                            ▼
┌─────────────────┐   ┌─────────────────┐
│ JACOBIAN AND    │   │ COMPUTATION OF  │
│ TRANSITION      │◄──│ SMOOTHED ESTIMATES │
│ MATRICES        │   │ OF STATES AND   │
│ COMPUTATION     │   │ ASSOCIATED      │
└─────────────────┘   │   COVARIANCES   │
                      └─────────────────┘
                            │
                NO          ▼
        ◄───────────  ╱ K        ╲
                      ╱ MULTIPLE OF ╲
                      ╲   10 ?     ╱
                       ╲          ╱
                            │ YES
                            ▼
                    ┌─────────────────┐
                    │ SYMMETRIZE P_K/N │
                    └─────────────────┘
                            │
                            ▼
                    ┌─────────────────┐
                    │  ^   WRITE      │
                    │ X_K/N, P_K/N,   │
                    └─────────────────┘
                            │
                            ▼
                    ┌─────────────────┐
                    │   K = K-1       │
                    └─────────────────┘
                            │
                            ▼
                      ╱          ╲      NO
                      ╲  K = 0   ╱ ─────────►
                      ╲    ?    ╱
                       ╲      ╱
                            │ YES
                            ▼
                        ( END )
```
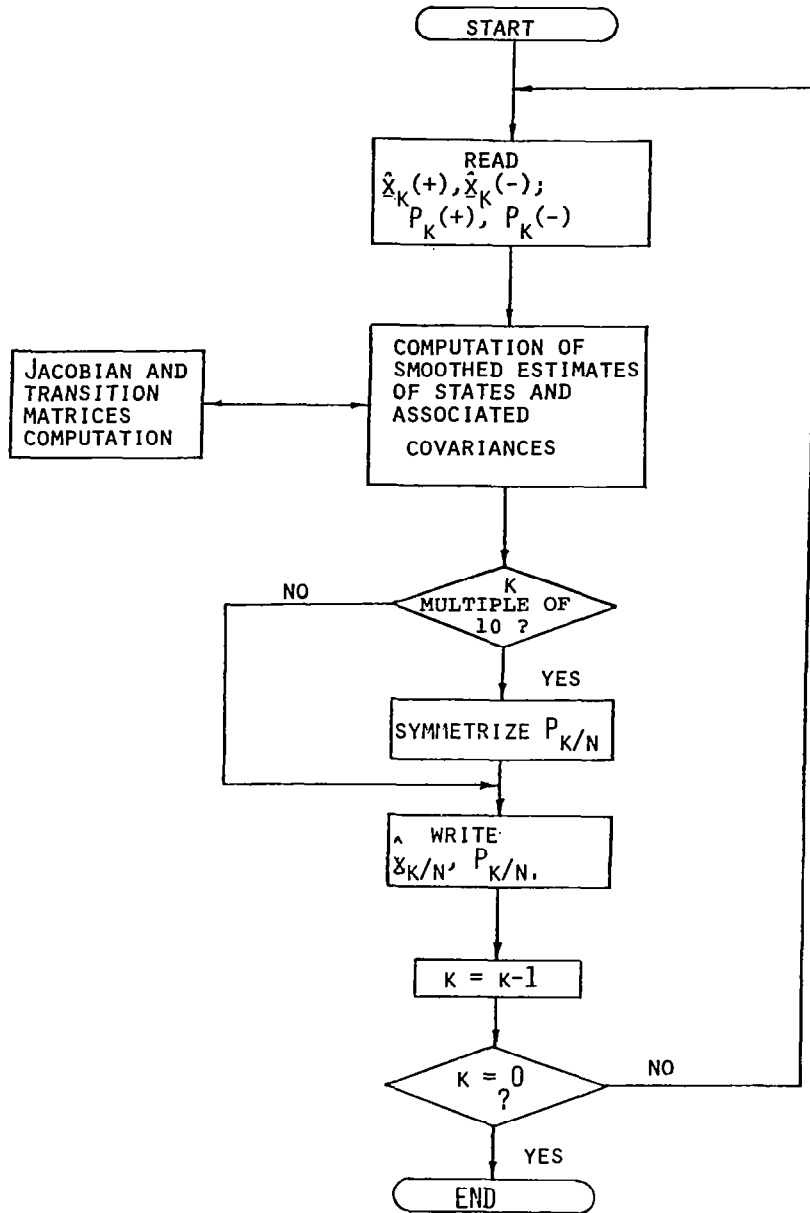
With regard to the pitch angle and yaw rate time histories, "derivative" states are noisier than "integral" states, as may have been expected.

OPTIMAL FLIGHT PATH RECONSTRUCTION - INPUTS

- Data record length
- Time vectors of codes identifying the ground stations

STATION CODE	STATION	λ N 40° X'	μ W 074° Y'	Z_I (FT)
1	RBV	12.1	29.7	-250.
2	COL	18.7	09.6	-120.
3	GXU	00.6	35.8	-120.
4	SBJ	35.0	44.5	-190.
0	FORR.	20.8	36.6	-109.

Channel dedicated to station switching timing

NAV2 \ NAV1	RBV	COL	GXU	SBJ
RBV	EE	ED	EB	E7
COL	DE	DD	DB	D7
GXU	BE	BD	BB	B7
SBJ	7E	7D	7B	77

- Approximate initial conditions

APPLICATION OF OPTIMAL FLIGHT PATH RECONSTRUCTION
ALGORITHM TO ACTUAL FLIGHT-TEST DATA

PITCH ANGLE SMOOTHING (SEPT.17, 1981)
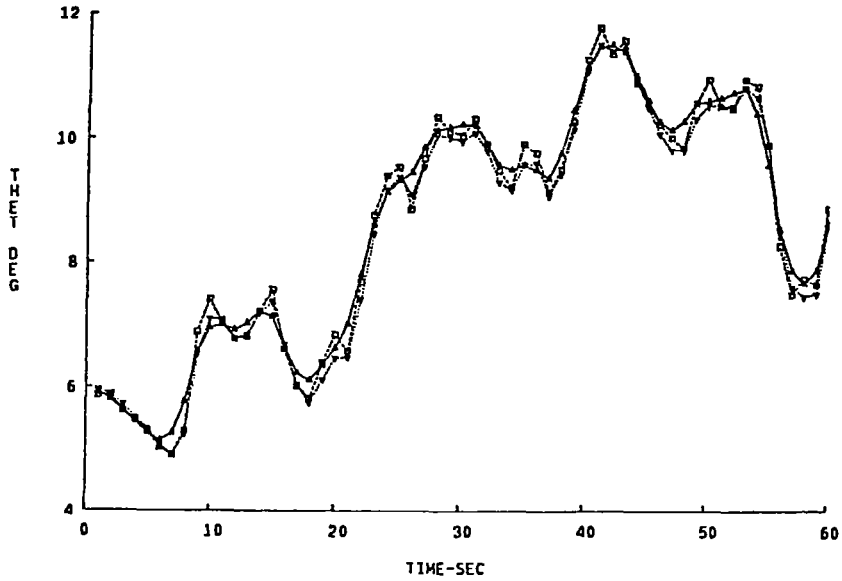
YAW RATE SMOOTHING (SEPT. 17, 1981)
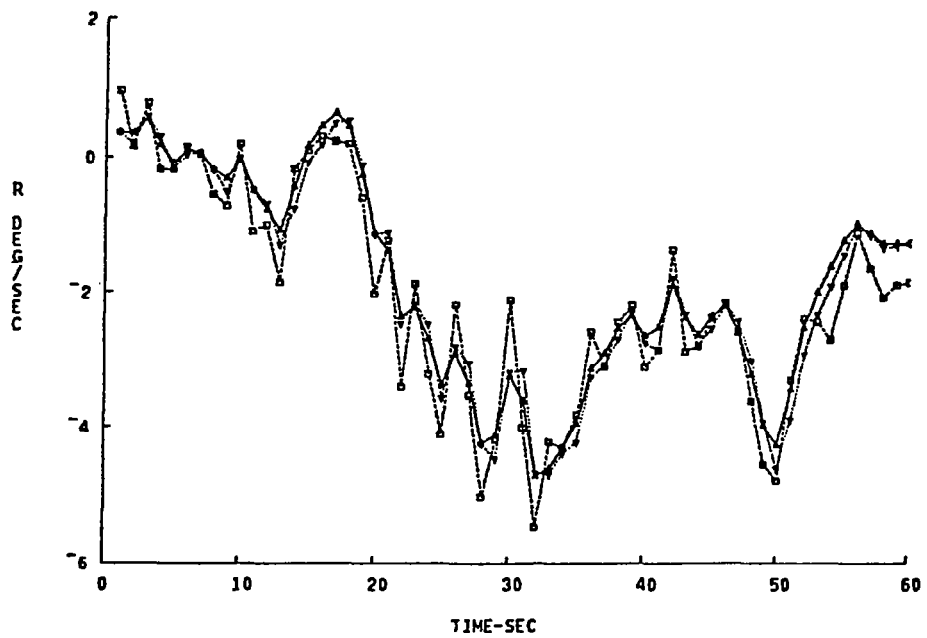
With regard to the true airspeed time history, note demonstration of characteristic filter lag, which is corrected by the smoother. This is a reconstructed measurement from the $[u,v,w]^T$ states.

TRUE AIRSPEED RECONSTRUCTION (SEPT. 17, 1981)
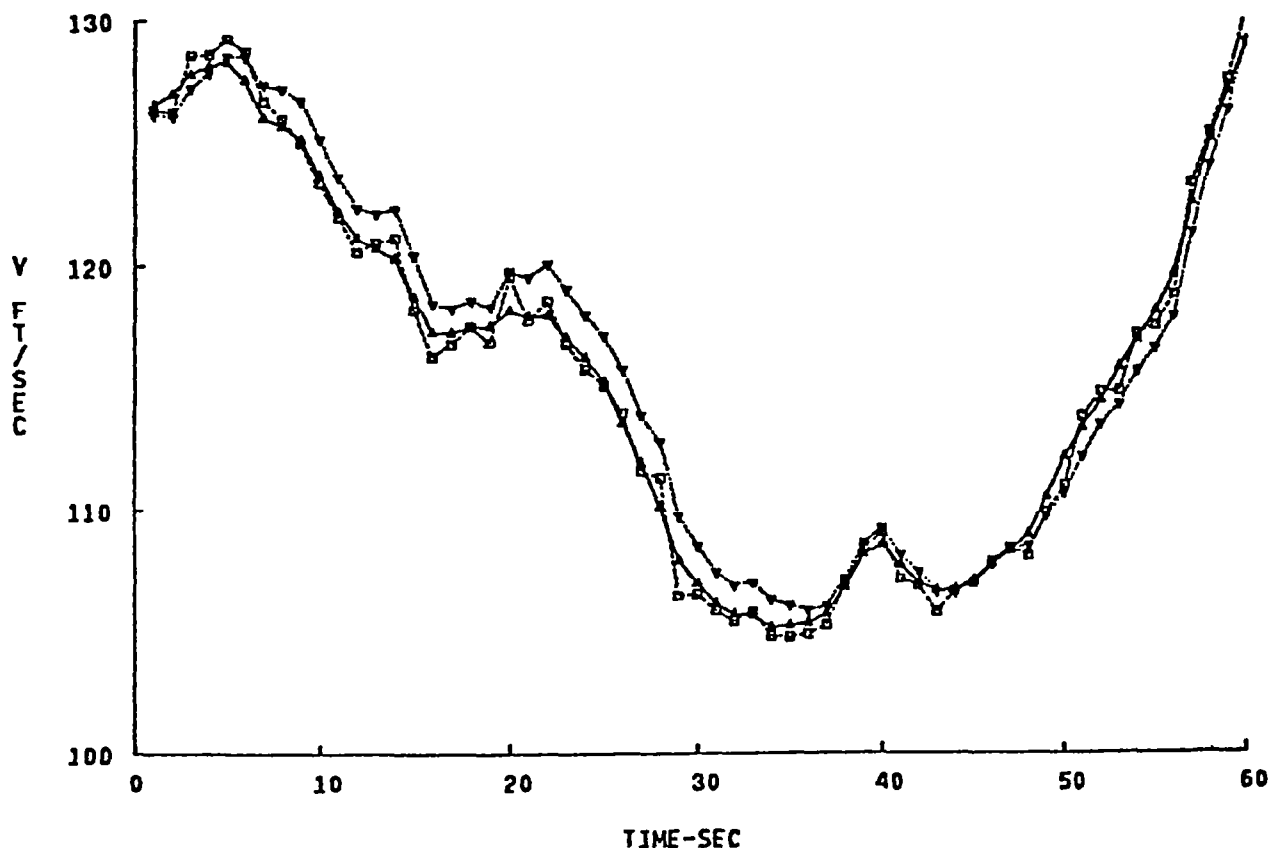
With regard to the trajectory reconstruction,
note that optimal smoothing improves the state estimates
and at the same time also shrinks the statistical
uncertainty ellipsoid.

Note: Line segments are used to link results but not to
        suggest a functional relationship.

TRAJECTORY RECONSTRUCTION (SEPT. 17, 1981)
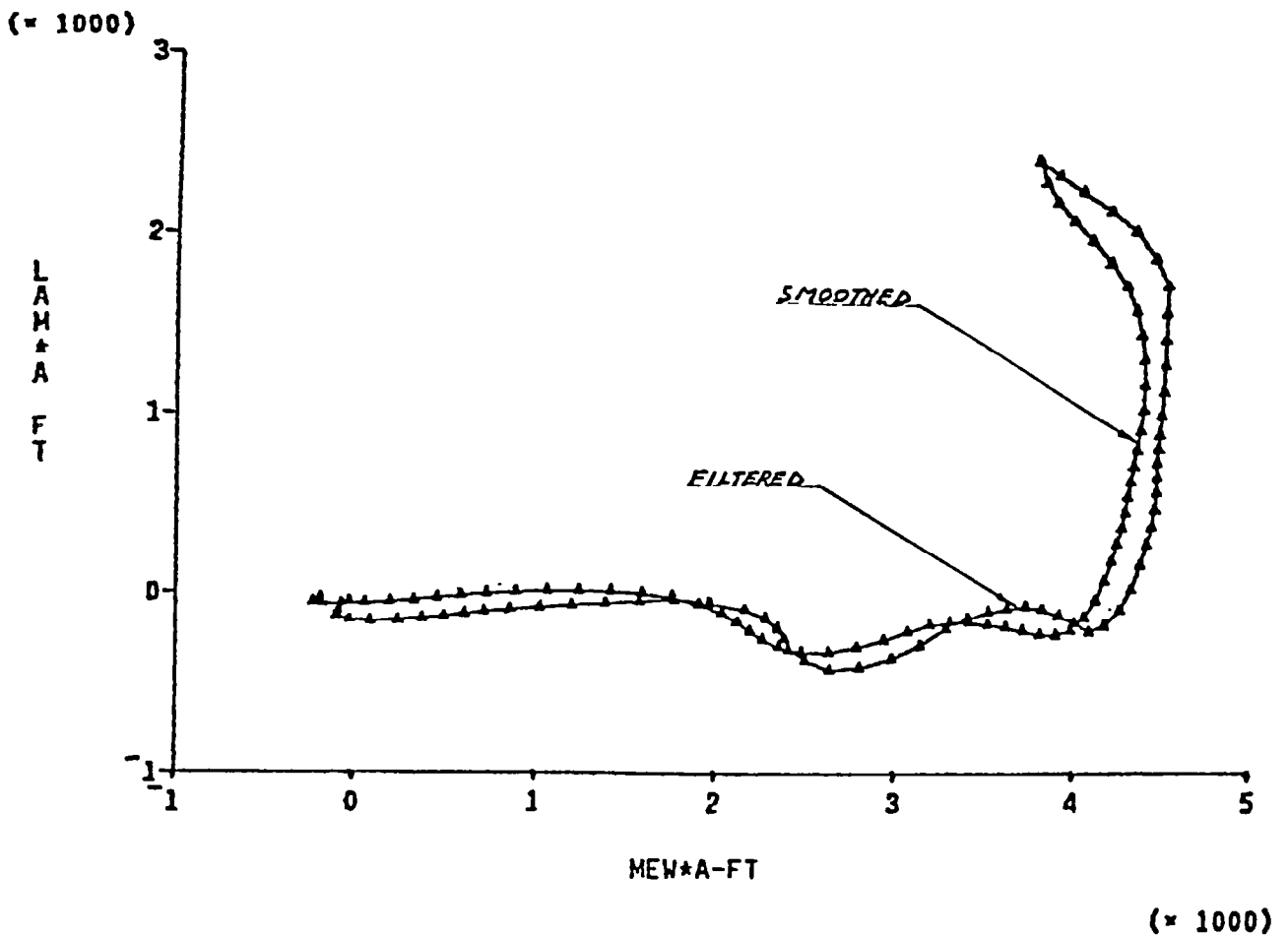
This post-flight flight path reconstruction approach may be useful in evaluating navigational system performance (on board the TCV, e.g.) or to investigate statistically causes of flight path deviations if recording altitude, airspeed, and DME data in the "black box".

SPIFR MULTIPLE REGRESSION ANALYSIS (PHASE I)

SUBJECTIVE INDICATORS (PORS)
OBJECTIVE INDICATORS (GS-,H-,V-TRACKING DEVIATIONS
                            CONTROL MANIPULATIONS
OVER
FLIGHT SEGMENT
OR WHOLE MISSION

1 2 3 4 5 6 7 8   A/C DYNAMIC
                              CONFIGURATION

.25
.50
.75
1.00

PILOT EXPERIENCE
(PE)

INTERACTION
?
WORKLOAD
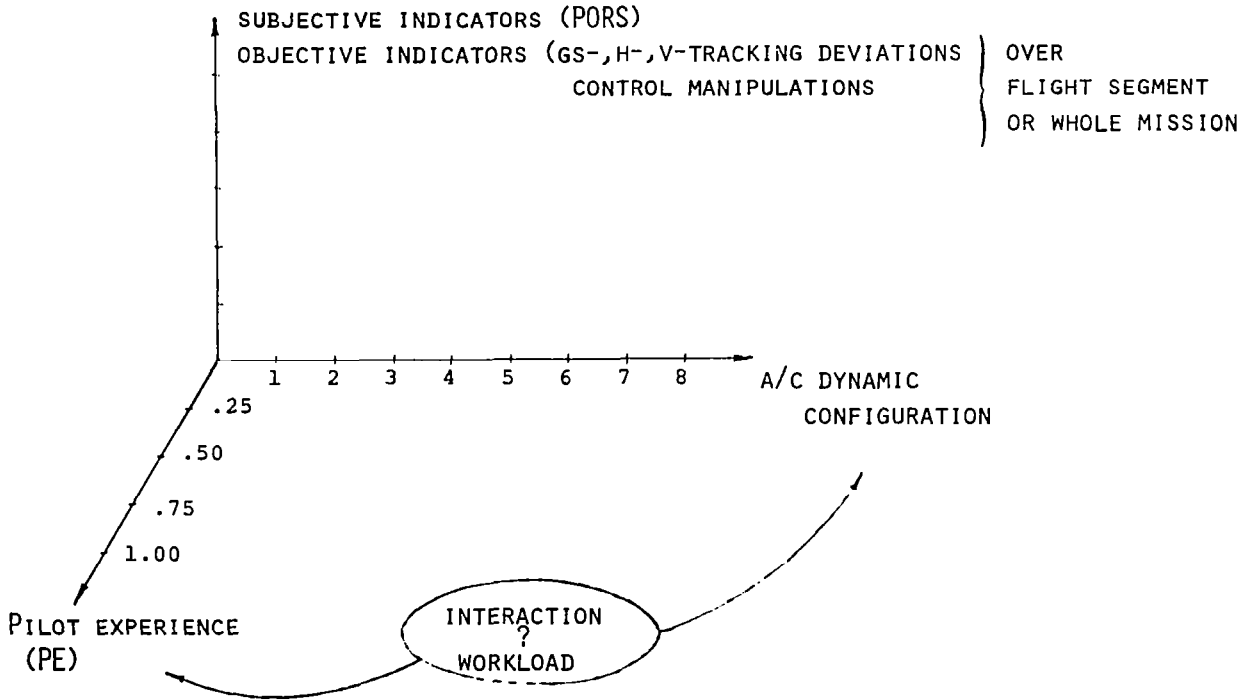
WORK ACCOMPLISHED TO DATE

o INTEGRATED FLIGHT TESTING AND FLIGHT PATH RECONSTRUCTION
  METHODOLOGY DEVELOPED

o HIGH ACCURACY IN TRAJECTORY ESTIMATION ACHIEVED WITH AN
  INEXPENSIVE EXPERIMENTAL SETUP

o PART OF FLIGHT TEST SERIES FLOWN

AIR DATA MEASUREMENT USING
DISTRIBUTED PROCESSING AND
FIBER OPTICS DATA TRANSMISSION

Kristin A. Farry
Princeton University

A DUAL REDUNDANT AIR DATA MEASUREMENT SYSTEM INCORPORATING DISTRIBUTED PROCESSING AND FIBER OPTIC DATA BUSES

OVERALL RESEARCH GOAL:

GAIN EXPERIENCE WITH --DISTRIBUTED PROCESSING
                      --FIBER OPTIC TECHNOLOGY AND
                      --REDUNDANCY MANAGEMENT
  IN THE AIRCRAFT ENVIRONMENT.

THIS PROJECT:

DEVELOPMENT OF AN ANGLE OF ATTACK AND SIDESLIP DATA COLLECTION SYSTEM WHICH FEATURES:

      --TWO INDEPENDENT MICROPROCESSOR-CONTROLLED DATA
        COLLECTION AND CALIBRATION UNITS
      --TRANSMISSION OF DATA TO THE CONTROL SYSTEM ON A
        FIBER OPTIC DATA BUS
      --SOFTWARE-IMPLEMENTED ERROR DETECTION AND RECOVERY

AIR DATA MEASUREMENT SYSTEM

   This figure shows a functional breakdown of the entire system.

   Two air data sensor vanes -- measuring angle of attack and sideslip angle -- are mounted at each wingtip of the aircraft. Their analog output signal is converted to digital format by a multiplexed A/D converter. Next, any signal noise and other unwanted contributions such as upwash and roll are eliminated from the raw data by software-implemented filtering and calibration, so that each wingtip sensor unit's data is independent of the other's, thus giving the system dual redundancy. Finally, the data are transferred via a fiber optic data link to the aircraft's digital flight control system, which uses the system's dual redundancy to determine the data's validity before using it as inputs to the flight control system.
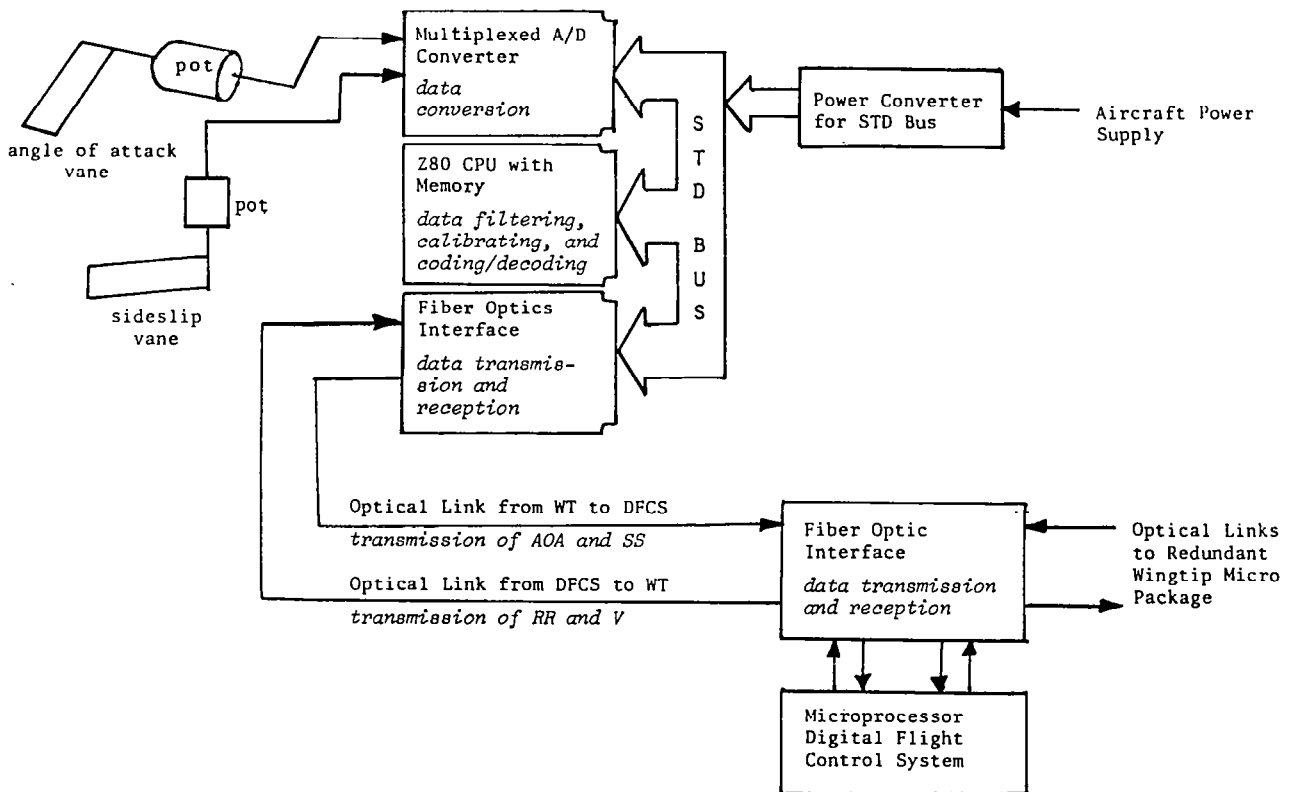
EQUIPMENT INSTALLED IN AIRCRAFT

This figure shows the location of the equipment in the aircraft.

WINGTIP MICROPROCESSOR PACKAGE:

Card cage and microprocessor bus --
    Prolog STD (56-pin, tightly structured bus).
CPU and memory --
    Mostek MDX-CPU2 (4 MHz Z80 CPU with byte-wide
    interchangeable RAM, PROM, and ROM).
A/D converters --
    Data Translation DT2742 (12-bit converter with 8 differ-
    ential input channel multiplexing capability).
Fiber optic interface --
    Optelecom 2100 series fiber optic transmitter and
    receiver mounted on a Prolog Utility I/O card.
Power supply --
    Power Products DC-DC converters (28 vdc to 5 vdc and ±
    12 vdc).

FIBER OPTIC LINKS:

Cables --
    Siecor 155 (200 micron core all-glass fiber in rugged
    sheathing).
Connectors --
    Epoxy Technology SMA (all-metal epoxy-bonded connectors).

MICROPROCESSOR DIGITAL FLIGHT CONTROL SYSTEM WITH TWO FIBER OPTIC TRANSMITTERS AND RECEIVERS

NAVION N9I566

REDUNDANT SENSORS AND WTMP PACKAGE

FIBER OPTIC CABLES

AIR DATA SENSORS

WINGTIP MICROPROCESSOR PACKAGE WITH
    --CPU AND MEMORY
    --A/D CONVERTERS
    --FIBER OPTIC TRANSMITTER
        AND RECEIVER
    --POWER CONVERTERS
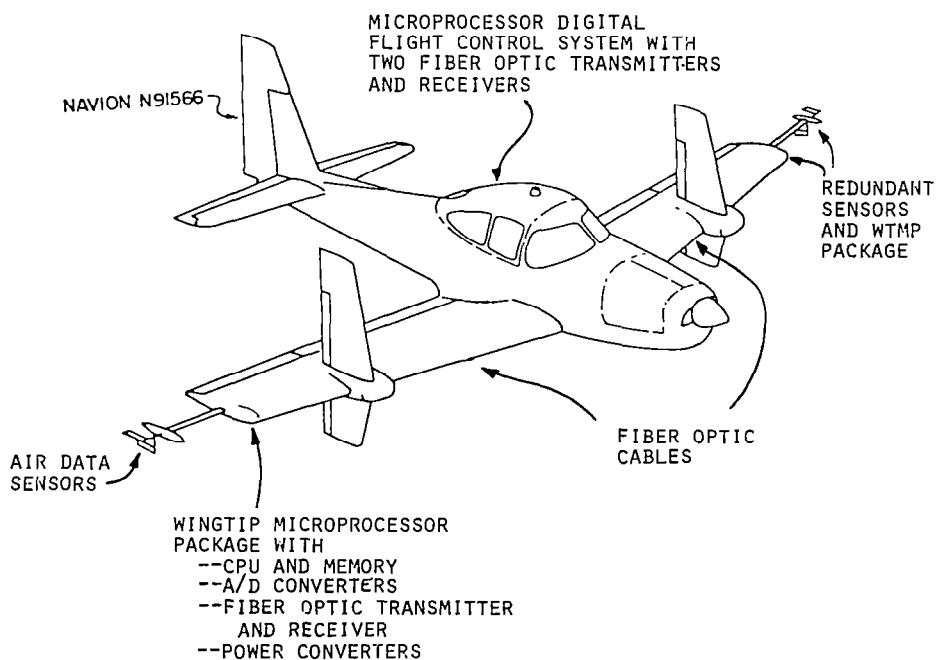
DATA COMMUNICATIONS STRUCTURE

This air data measurement system uses two microprocessors loosely coupled to a third, the micro-DFCS, which is the executive processor of the system.

The traffic management scheme chosen for data exchanges between the microprocessors is a modified polling system. The micro-DFCS interrupts the wingtip microprocessors whenever angle-of-attack or sideslip data is needed and whenever roll rate and velocity data is available. The wingtip microprocessors cannnot interrupt the micro-DFCS, however, since uncontrolled delays in some flight control routines might be undesirable. This bus protocol minimizes the data communications overhead for all processors, the timing sensitivity, and the propagation of wingtip microprocessor problems to the micro-DFCS.

To further simplify timing, each data point transmitted is accompanied by a name. Transmission of a parity bit enables the receiving processor to identify most transmission errors.

The code used in transmitting data is Manchester Bi-Phase, also known as self-clocking return-to-zero (RZ) code. The beginning of each bit interval is marked by a transition. If the bit is a one, a second transition will occur in the middle of the interval; for a zero bit, the signal will remain at the same level throughout the interval. This code requires twice the bandwidth of more commonly used non-return-to-zero code schemes, but eliminates many of their timing problems and lengthens transmitter life.

TRAFFIC MANAGEMENT -- POLLING

µDFCS INTERRUPTS THE WINGTIP MICROPROCESSORS WHENEVER DATA IS NEEDED OR AVAILABLE.

DATA COMMUNICATIONS FORMAT --
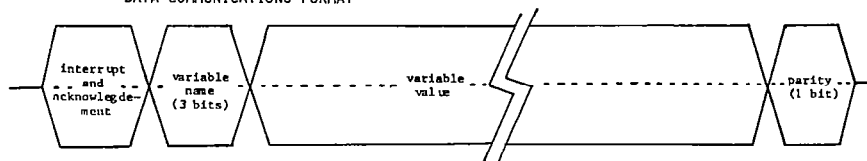
CODE TYPE --

BI-PHASE SELF-CLOCKING

FLIGHT TESTING

Flight testing of this system will be divided into two phases: hardware evaluation and total system evaluation.

The primary goal of the first phase is verifying that all the sytem hardware performs satisfactorily in flight. These tests will be done with a minimum of software so that hardware faults can be easily separated from software bugs. Of course, the communications hardware cannot be adequately tested without the data communications software, so the data communications techniques just described will be tested simultaneously. A secondary task scheduled in this part of the testing is collecting some data to check the analytically estimated calibration coefficients to be used in the system later.

The second phase of the tests, total system evaluation, will focus on verifying the data filtering and calibration software as well as the system's fault tolerance. Performance criteria for this phase include the accuracy of the calibration and the degree of isolation of each sensor unit.

OBJECTIVES

1) HARDWARE TECHNOLOGY EVALUATION

--TEST OF HARDWARE AND DATA TRANSMISSION TECHNIQUE

--COLLECTION OF DATA TO CHECK CALIBRATION COEFFICIENT ESTIMATES

2) TOTAL SYSTEM EVALUATION

--TEST OF DATA FILTERING AND CALIBRATION SOFTWARE

--TEST OF SOFTWARE-IMPLEMENTED FAULT TOLERANCE

PROGRESS SUMMARY

PREVIOUS--

--FIBER OPTIC LINKS DESIGNED, ASSEMBLED, AND GROUND TESTED
--MICROPROCESSOR, A/D, AND POWER HARDWARE ACQUIRED
--SOFTWARE PARTIALLY COMPLETE

THIS PERIOD--

--FIBER OPTIC/ MICROPROCESSOR INTERFACES DESIGNED, ASSEMBLED, AND
GROUND TESTED
--MICROPROCESSOR, A/D, AND POWER HARDWARE GROUND-TESTED OUTSIDE
THE AIRCRAFT
--ALL HARDWARE INSTALLED IN THE AIRCRAFT AND GROUND-TESTED IN POSITION
--TRANSMISSION SOFTWARE GROUND TESTING IN PROGRESS
--CALIBRATION AND FILTERING SOFTWARE STILL IN DEVELOPMENT

FUTURE WORK--

--EVALUATE ALL HARDWARE AND DATA TRANSMISSION IN FLIGHT
--FINISH DATA FILTERING AND CALIBRATION SOFTWARE
--GROUND TEST SYSTEM WITH FILTERING AND CALIBRATION SOFTWARE ADDED
--FLIGHT TEST COMPLETE SYSTEM

INPUT/OUTPUT MODELS FOR GENERAL
AVIATION PISTON-PROP AIRCRAFT FUEL ECONOMY

L. M. SWEET

PRINCETON UNIVERSITY

A FUEL-EFFICIENT CRUISE PERFORMANCE MODEL
FOR GENERAL AVIATION PISTON ENGINE AIRPLANES

SPECIFIC RANGE   =   R*

                      =   GROUND MILES/LB FUEL

                      =   INSTANTANEOUS FUEL ECONOMY

FIXED WING GA AIRPLANES

- FIXED DESIGN
- NATURALLY ASPIRATED SI PISTON ENGINES
- CONSTANT SPEED PROPELLERS
- MAXIMIZE R* USING AVIONICS AND CONTROLS
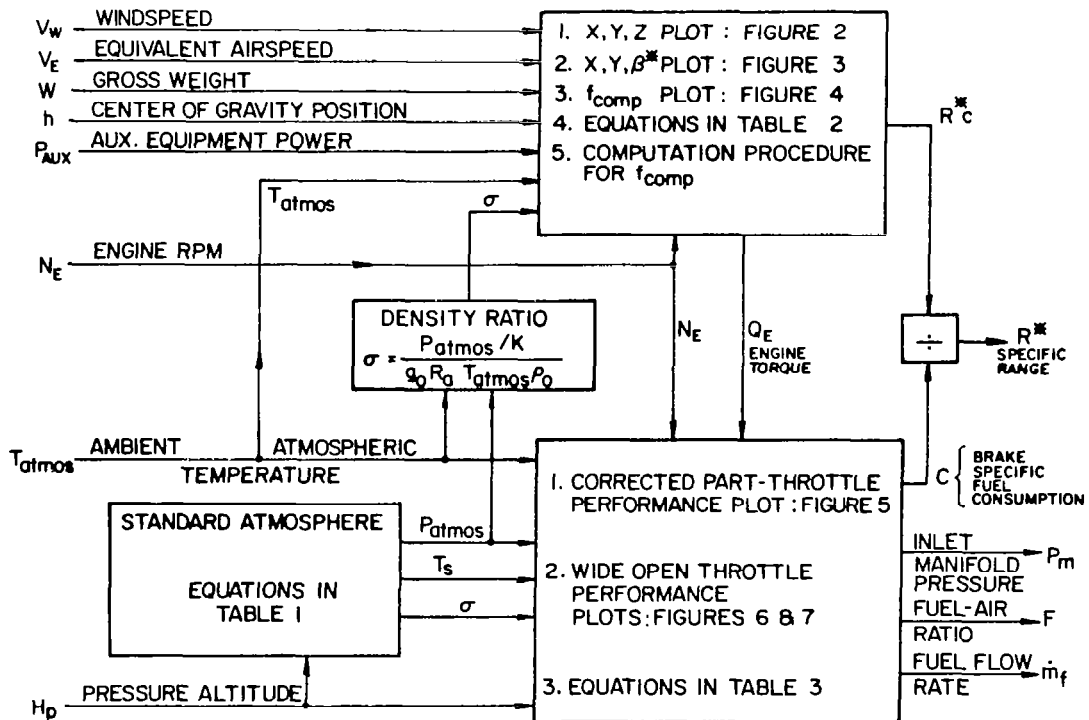
Figure 1.   Block diagram: Cruise performance model
(standard and nonstandard atmospheres).
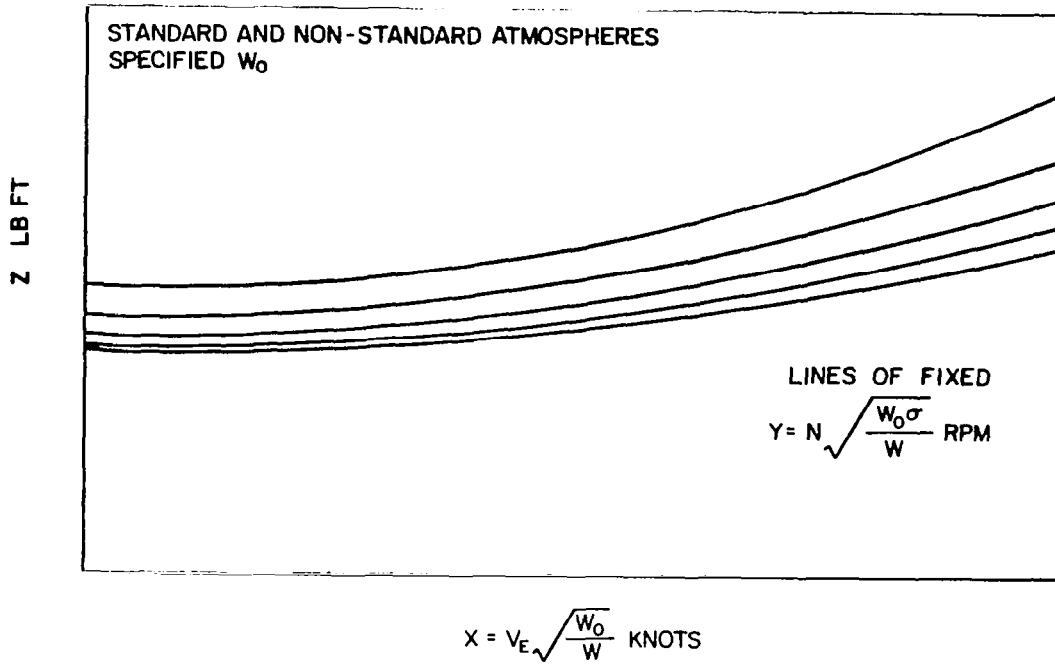
Figure 2. X,Y,Z plot: Airframe-propeller performance.
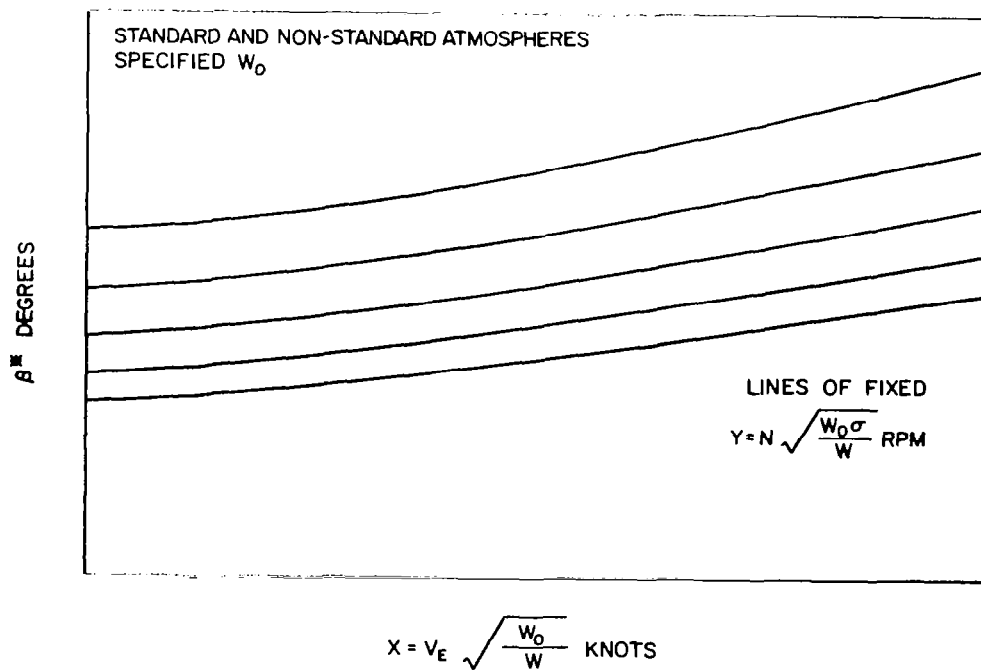
Figure 3. X,Y,β* plot: Airframe-propeller performance.
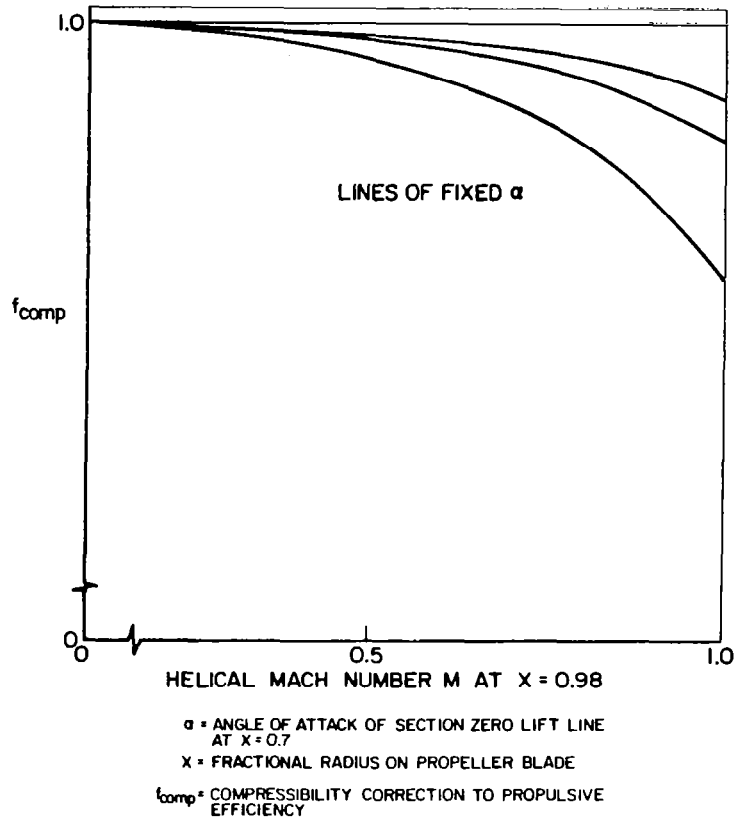
Figure 4. Propeller performance: Compressibility correction f_{comp} plot.

TABLE 1.

EQUATIONS FOR THE STANDARD ATMOSPHERE

These equations approximate the characteristics of
the U.S. Standard Atmosphere 1962 in the troposphere.

$$H = H_p \tag{1.1}$$

$$\theta = 1 - 6.87239 \times 10^{-6} \, H \tag{1.2}$$

$$\delta = \theta^{5.25581} \tag{1.3}$$

$$\sigma = \frac{\rho}{\rho_o} = \frac{\delta}{\theta} \tag{1.4}$$

$$T_s = 288.15 \, \theta \tag{1.5}$$

$$P_{atmos} = 29.92 \, \delta \tag{1.6}$$

TABLE 2

EQUATIONS FOR AIRFRAME-PROPELLER-ATMOSPHERE CRUISE PERFORMANCE

$$V_e = 1.6889 \, V_E \qquad (2.1)$$

$$C_L = 2W/\rho_o \, V_e^2 \, S \qquad (2.2)$$

$$P_{AUX_c} = P_{AUX} \sqrt{W_o^3 \sigma / W^3} \qquad (2.3)$$

$$V_{w_c} = V_w \sqrt{W_o \sigma / W} \qquad (2.4)$$

$$X = V_E \sqrt{W_o / W} \qquad (2.5)$$

$$Y = N \sqrt{W_o \sigma / W} \qquad (2.6)$$

$$S^* = \frac{5252.1}{E} \frac{X}{YZ} \frac{W_o}{W} \qquad (2.7)$$

$$\psi = A\beta^* - B \qquad (2.8)$$

$$\Delta\beta = C \cos\psi \sin\left(\psi - \frac{D \, dh}{|dh|}\right)\left[(1 + \xi C_L dh)^{\frac{1}{2}} - 1\right] \qquad (2.9)$$

$$\beta = \beta^* + \Delta\beta \qquad (2.10)$$

$$Q_a = \frac{WZ}{W_o (1 + \xi C_L \, dh) \, f_{comp}} \qquad (2.11)$$

$$\Lambda = 1 + 5252.1 \, (1 + \xi C_L \, dh) f_{comp}\left[\frac{P_{AUX_c}}{YZ}\right] \qquad (2.12)$$

$$N_E = G \, N \qquad (2.13)$$

$$[Q_E]_{APA} = Q_a \, \Lambda/G \qquad (2.14)$$

$$R^*_c = \left[1 + \frac{V_{w_c}}{X}\right] \frac{(1 + \xi C_L \, dh) \, f_{comp} \, S^*}{\Lambda} \qquad (2.15)$$

Note: β is required for computing f_{comp}.

NATURALLY ASPIRATED SI ENGINE
MBT IGNITION TIMING
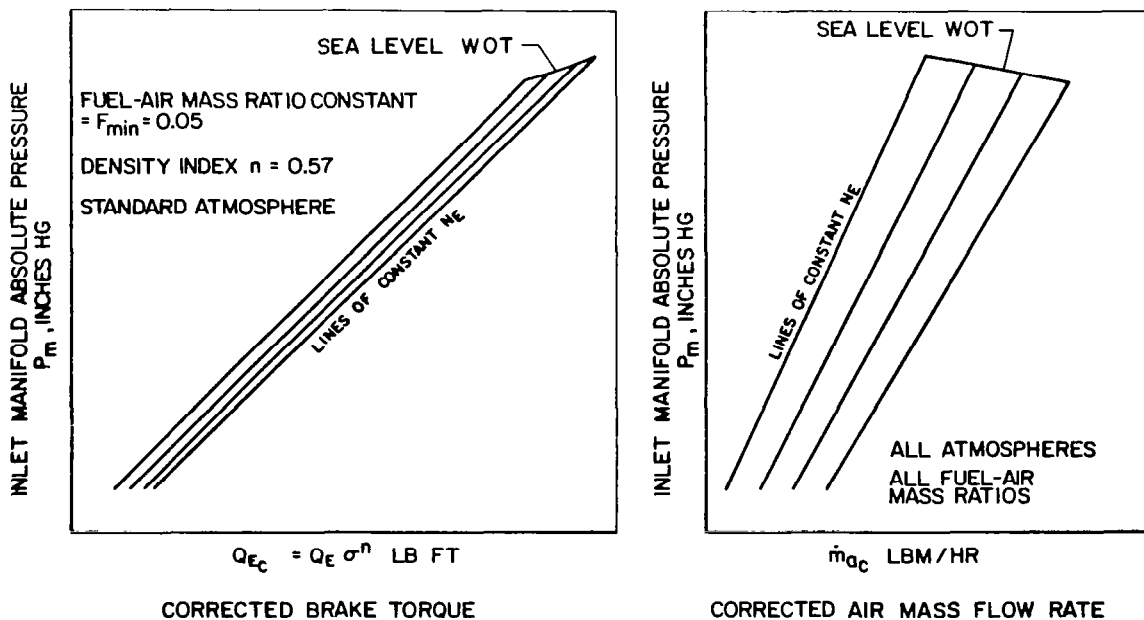
Figure 5.   Corrected part-throttle engine performance.

NATURALLY ASPIRATED SI ENGINE WITH MBT IGNITION TIMING
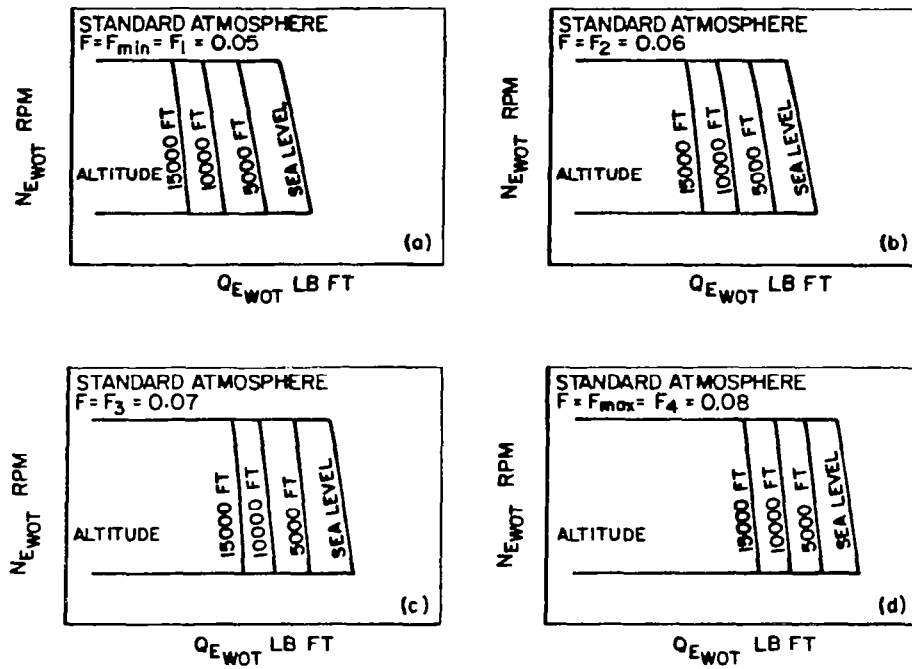
Figure 6. Wide open throttle performance: Engine shaft speed $N_{E_{WOT}}$ versus engine brake torque $Q_{E_{WOT}}$.
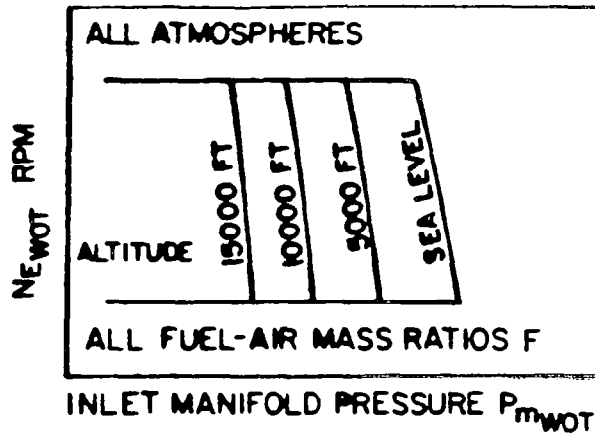
Figure 7. Wide open throttle performance: Engine shaft speed $N_{E_{WOT}}$ versus inlet manifold absolute pressure.

TABLE 3.

EQUATIONS FOR NATURALLY ASPIRATED ENGINE CRUISE PERFORMANCE

$$\Delta T_{atmos} = T_{atmos} - T_s \qquad (3.1)$$

$$Q_E = [Q_E]_{APA} - \left[\frac{\partial Q_E}{\partial T_{atmos}}\right] \Delta T_{atmos} \qquad (3.2)$$

$$Q_{E_c} = Q_E \, \sigma^n \qquad (3.3)$$

$$\dot{m}_{a_c} = \dot{m}_a \left[\frac{T_{atmos}}{288.15}\right]^{(1-\epsilon_t)} \left[\frac{P_{atmos}}{29.92}\right]^{\epsilon_p} \qquad (3.4)$$

$$\dot{m}_f = F \, \dot{m}_a \qquad (3.5)$$

$$P_E = 2\pi \, [Q_E]_{APA} \, N_E / 33{,}000 \qquad (3.6)$$

$$c = \dot{m}_f / P_E \qquad (3.7)$$

SUMMARY

1. COMPACT CRUISE PERFORMANCE MODEL
   - CORRECTED QUANTITIES
   - CORRECTED PERFORMANCE PLOTS
   - ALGEBRAIC EQUATIONS
   - MAXIMIZE R* WITH OR WITHOUT CONSTRAINTS
   - APPEARS SUITABLE FOR AIRBORNE MICROPROCESSOR IMPLEMENTATION

2. HARDWARE REQUIREMENTS
   - IGNITION TIMING REGULATOR
   - FUEL-AIR MASS RATIO CONTROLLER
   - MICROPROCESSOR
   - SENSORS AND DISPLAYS

3. TYPICAL R* INCREASE = 20% TO 26% ABOVE CURRENTLY ACHIEVED R* VALUES.
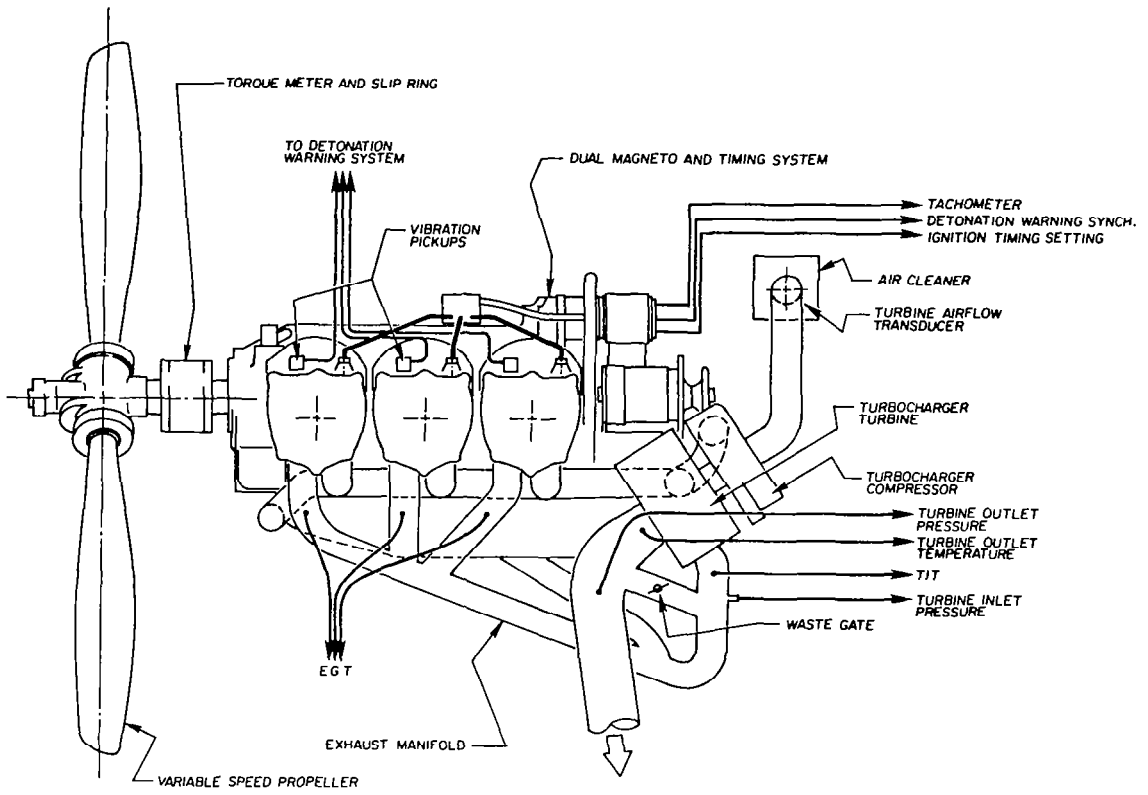
LEFT ELEVATION VIEW
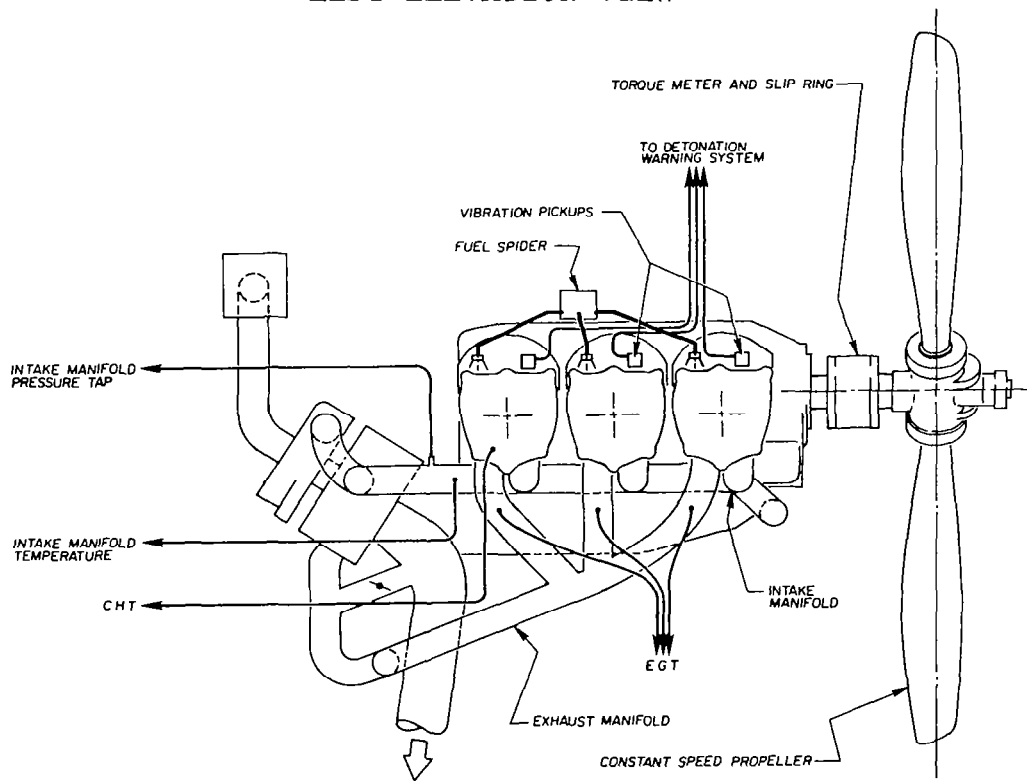
RIGHT ELEVATION VIEW

226

TORQUE METER AND SLIP RING

DUAL MAGNETO WITH ADJUSTABLE TIMING

FLOSCAN FUEL METER

FUEL SPIDER

INTAKE MANIFOLD PRESSURE

COMPRESSOR OUTLET PRESSURE

INTAKE MANIFOLD TEMPERATURE

INTAKE MANIFOLD

THROTTLE

FUEL TEMPERATURE

COMPRESSOR OUTLET TEMPERATURE

AIR CLEANER

INLET PRESSURE

INLET TEMPERATURE

TURBINE AIRFLOW TRANSDUCER

COMPRESSOR AIR SUPPLY TUBES

TURBOCHARGER COMPRESSOR

TURBOCHARGER TURBINE

CONSTANT SPEED PROPELLER

PLAN VIEW

227

WIDE FIELD OF VIEW LASER BEACON SYSTEM
FOR THREE DIMENSIONAL AIRCRAFT RANGE MEASUREMENTS

E. Y. WONG
PRINCETON UNIVERSITY

OBJECTIVE

This is a project for NASA Ames Research Center to develop
a system that can measure accurately the distance from an air-
craft to a helicopter for rotor noise flight testing. This
system will be able to measure the range and angles between
these two aircraft using laser optics. This system could be
applied in areas such as collision avoidance, robotics, and
other measurement-critical tasks.

PRINCIPLES OF OPERATION

A laser beacon is mounted on the front of a helicopter which has a pair of sweeping orthogonal fan-shaped beams of laser light. This light passes a set of detectors that are mounted on the back of another aircraft, which receives a set of pulses on each sweep. These pulses determine the vector orientation of each rotating beam; using this pair of vectors the vector pointing from the array to the beacon can be found. True range measurements can be calculated once the sweep rate and array geometry are known. This position data is then displayed to the test engineer in the aircraft,and error signals are sent to the helicopter pilot.

HUB-TO-TAIL
MICROPHONE
DISTANCE

75 ft
(22.86 m)

30°

UH-1H

γ

CONSTANT FORWARD VELOCITIES
AND RATES OF DESCENT

YO-3A   V
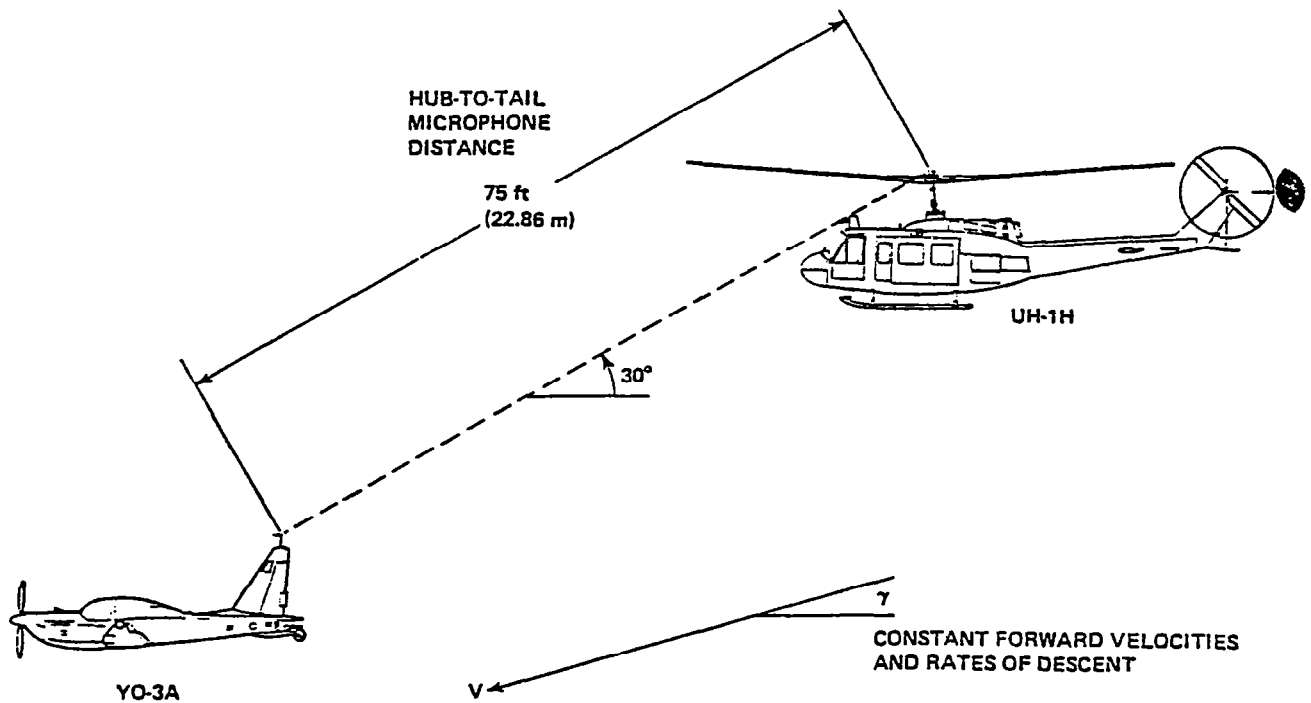
LASER BEACON SUBSYSTEM

The laser beacon consists of two 5 mW He-Ne lasers, optics, and motor drive. The two lasers are placed underneath the beacon and brought to the top by means of prisms. Beam expansion optics are used to expand the beams for the cylindrical mirrors. These mirrors are used to reflect the expanded beams into the fan-shaped light beacon. The motor drive unit powers two orthogonal shafts in which these mirrors are mounted. The drive will rotate the mirrors giving sweep rate from two to four revolutions per second. A belt drive and flywheel are added for increased noise reduction from the motor.

ROTATING
MIRROR

BEACON

DETECTOR
ARRAY

LOW POWER
HE - NE LASER

| DIGITAL PULSE TIMING CIRCUIT | POSITION ESTIMATION COMPUTER | HAZARD WARNING SYSTEM/ DISPLAY |

TO 28 VOLTS DC

TO AC MOTOR

SWITCH

LASER

LASER POWER SUPPLY

DC TO AC CONVERTED

PRISM

PRISM

LASER

BOTTOM

AC MOTOR

MOUNT

PLANO-CONVEX LENSE

CYLINDRICAL MIRROR

DIFFRACTING LENSE

PRISM

TOP
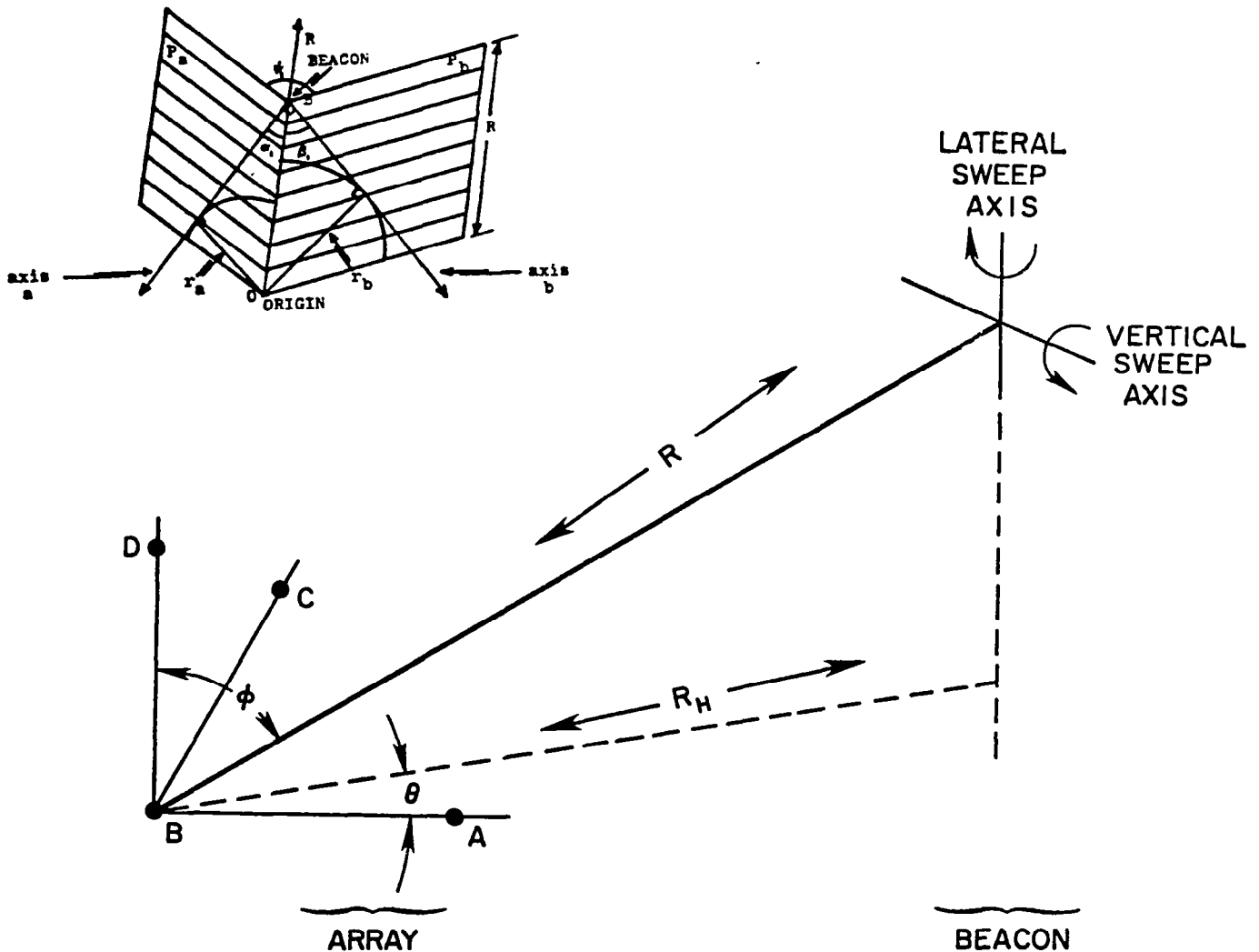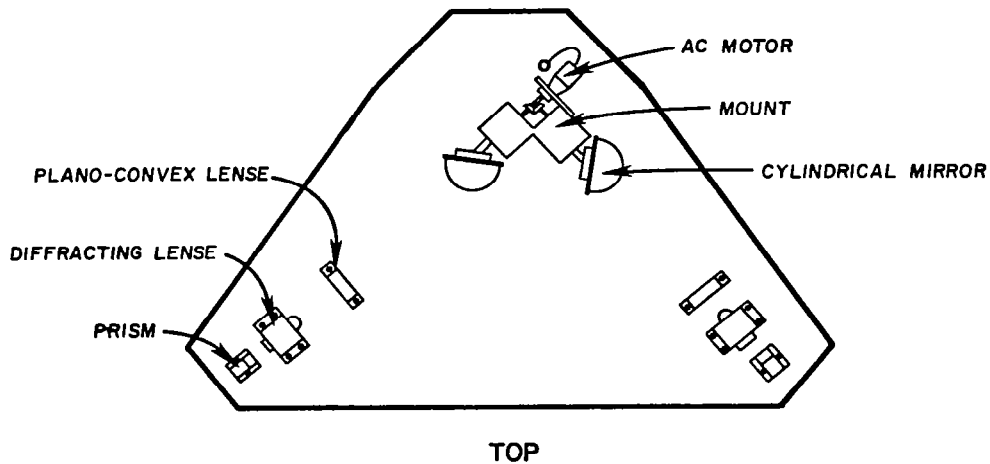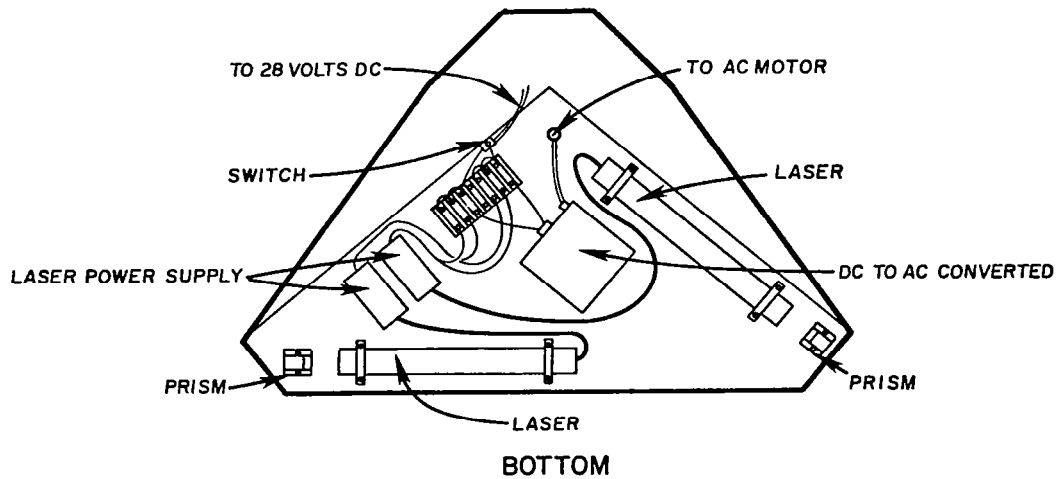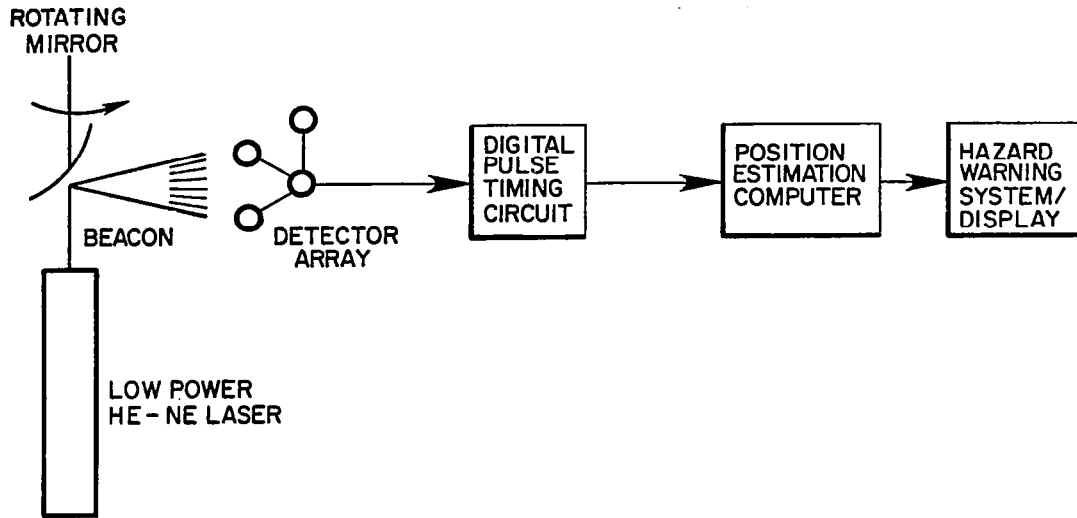
DETECTOR AND ARRAY SUBSYSTEM

The detectors are a pair of compound parabolic
concentrators mounted end to end. This configuration results
in a non-imaging wide-angle lens. A narrow-band interference
filter is placed between the concentrators to reduce solar
interference. A photodetector is placed at one end to
collect the resulting light from a beam sweep. Further
electronic filtering is done and is made compatible with our
timing circuitry. The detector array that we are testing is
a right tetrahedron of four detectors. This gives a simpler
mathematical relation between the rotation axes of the beacon
and the detector array.

COMPOUND PARABOLIC CONCENTRATORS   DETECTOR

INTERFEROMETRIC FILTER   CASE

DETECTOR

TIME ➡

LATERAL
SWEEP

VERTICAL
SWEEP

LATERAL
SWEEP

D

B

A   C

⟷ DETECTOR
ARRAY ⟷

D

B

A   C

LATERAL
BEACON
SWEEP

VERTICAL
BEACON
SWEEP

D

C

90°

B

90°

ℓ

A
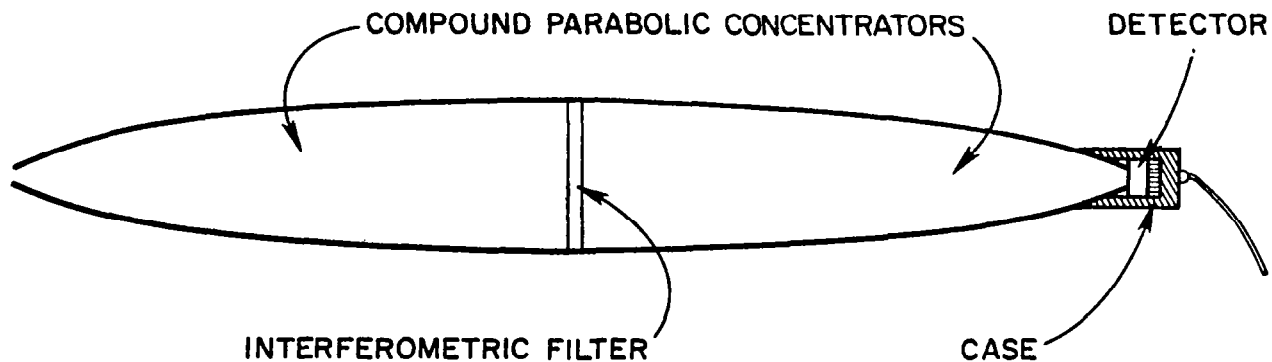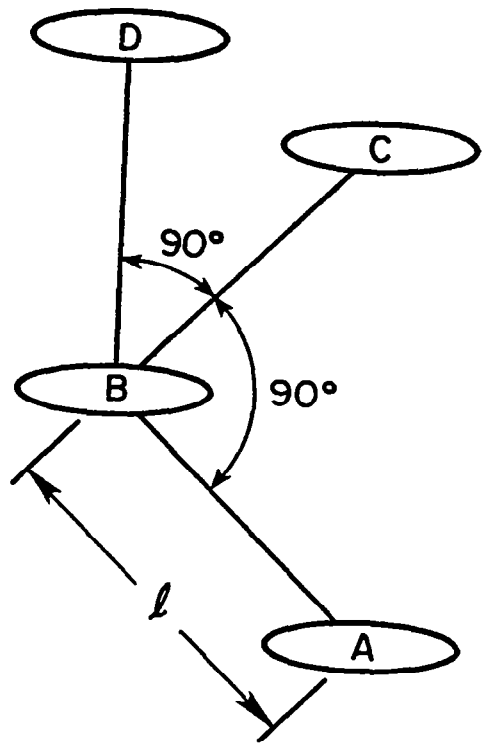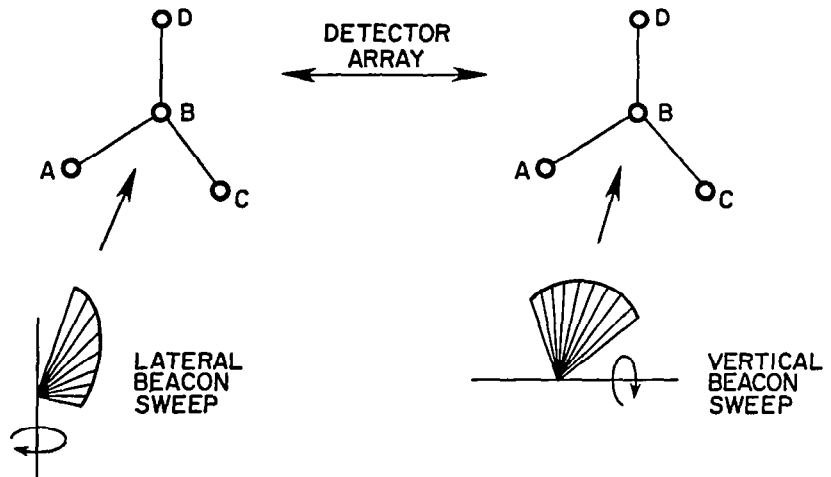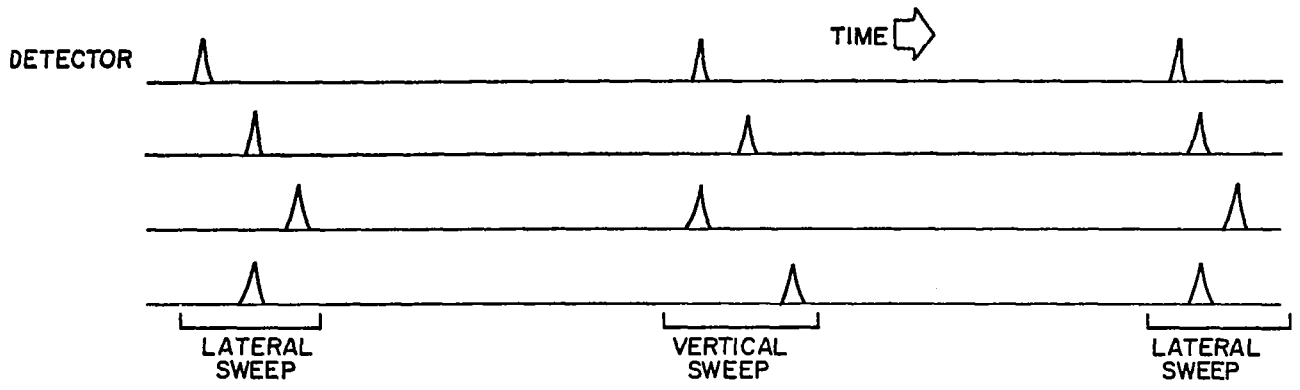
MICROPROCESSOR SUBSYSTEMS

A microprocessor is used to implement the vector
relations and to do further signal conditioning on board
the detector-carrying aircraft. This computer is also
transmitting the error signals to the helicopter, driving
the I/0 interface with the test engineer, and outputting
the measurements to a data recording device. This system
consists of a 4 MHz Z-80 microprocessor, a 9511 math chip
for high speed floating point arithmetic, an 8253 counter/
timer board for 0.5 microsecond timing resolution, and
other peripheral drivers. A radio link is put into the
system to transmit serial data from the aircraft to the
helicopter. Another microprocessor is used in the helicopter
for driving the displays. A glide slope indicator displays
the Y-Z error measurement and a LED panel meter displays the
X error measurement. This microprocessor will also have
other warning lights and error checking functions.

TESTING

Static tests were run to examine system performance
without aircraft dynamics. These tests were used to determine
the current noise levels in the complete system. The follow-
ing test results have been obtained:

1) A 1-foot standard deviation with approximately
   100 feet beacon to detector array distance

2) A 1/2 degree standard deviation in angular
   measurements.

In these tests there was no signal conditioning done by the
microprocessor.
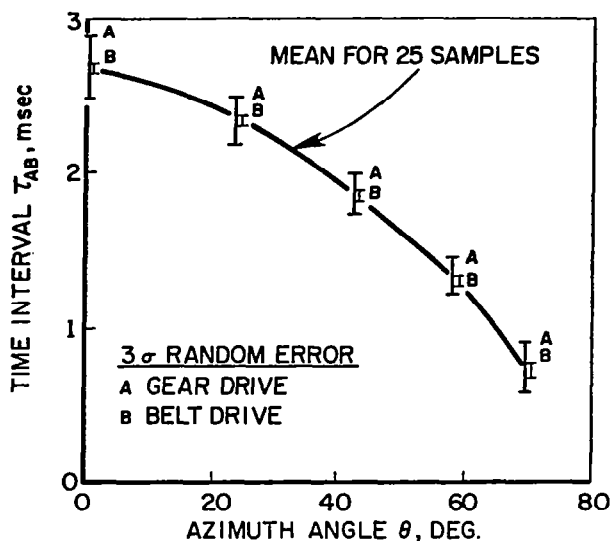
FUTURE PLANS

With the conclusion of the static tests, a digital
filter can be introduced into the software to improve system
performance. Flight tests then will be run at NASA Ames
Research Center for actual measurement capabilities. Further
modifications then can be made to the hardware and software to
meet or exceed the design specifications.

1. Report No. NASA CP-2224	2. Government Accession No.	3. Recipient's Catalog No.
4. Title and Subtitle JOINT UNIVERSITY PROGRAM FOR AIR TRANSPORTATION RESEARCH - 1981		5. Report Date June 1982
		6. Performing Organization Code 505-34-13-01
7. Author(s)		8. Performing Organization Report No. L-15346
		10. Work Unit No.
9. Performing Organization Name and Address NASA Langley Research Center Hampton, VA 23665		11. Contract or Grant No.
		13. Type of Report and Period Covered Conference Publication
12. Sponsoring Agency Name and Address National Aeronautics & Space Administration Washington, DC 20546		14. Sponsoring Agency Code

15. Supplementary Notes

16. Abstract

This report summarizes the research conducted during 1981 under the NASA-sponsored Joint University Program for Air Transportation Research. This material was presented at a meeting held at NASA Headquarters, December 11, 1981. The Joint University Program is a coordinated set of three grants sponsored by Langley Research Center, one each with the Massachusetts Institute of Technology, Ohio University, and Princeton University. Research topics include navigation, guidance, control and display concepts, and hardware, with special emphasis on applications to general aviation aircraft. Completed works and status reports are presented. Also included are annotated bibliographies of all published research sponsored on these grants since 1972.

17. Key Words (Suggested by Author(s)) Air transportation Avionics General aviation Low-frequency terrestrial navigation Aircraft displays Aircraft stability and control	18. Distribution Statement Unclassified - Unlimited Subject Category 01	
19. Security Classif. (of this report) Unclassified	20. Security Classif. (of this page) Unclassified	21. No. of Pages 241
		22. Price A11

National Aeronautics and
Space Administration

Washington, D.C.
20546

Official Business
Penalty for Private Use, $300

NASA